Dept.

Food Acquisition, Ingestion and Digestion in the Slipper Lobster, *Thenus orientalis* Lund (Decapoda: Scyllaridae)

Thesis submitted by
DANIELLE JANE JOHNSTON BSc. Hons (*J.C.U.N.Q.*)
in December 1995

for the degree of Doctor of Philosophy
in the Departments of Marine Biology and Biochemistry and Molecular Biology
at James Cook University of North Queensland

Frontispiece

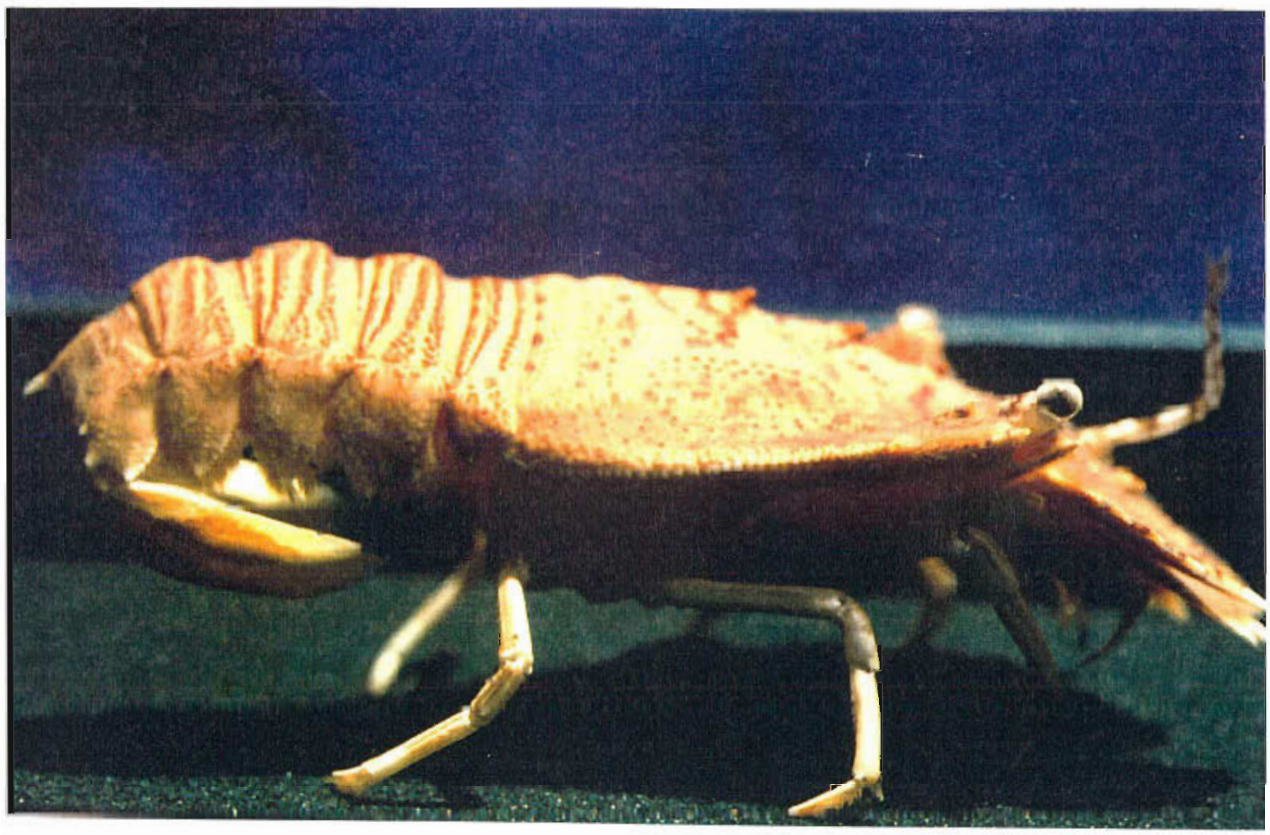

.....The Slipper Lobster - ***Thenus orientalis***.....

Abstract

This study examines food acquisition, ingestion and digestion in the most economically significant scyllarid for Australian fisheries, *Thenus orientalis* (Lund, 1793). It is a carnivorous scavenger which uses two foraging modes, probing or digging, to locate prey. Bivalves are the preferred food source and are opened efficiently by "wedging". Structural characteristics of the mouthparts and proventriculus are consistent with a predominantly soft flesh diet, with mechanical degradation primarily carried out by the gastric mill, the teeth of which are adapted for tearing and cutting flesh.

Two distinct modes of ingestion are used: The first, for small flesh items <10 mm^3, is characterised by alternating action of the second maxillipeds and first maxillae. The second, for large and/or hard items >10 mm^3, involves a tearing action between the third maxillipeds and mandibles. Ingestion is rapid, less than 5 s for a 10 mm^3 piece of flesh and is facilitated by lubrication with mucus produced by tegumental glands in the paragnaths, membranous lobe and oesophagus. During ingestion, food is passed over the membranous lobe while its anterior lip retracts ventro-posteriorly, thus dilating the preoral cavity to allow quick and efficient swallowing of large food items.

Alimentary tract structure conforms to the general plan exhibited by all decapods, although a posterior pyloric sector appears to be unique to this scyllarid. The digestive gland primary ducts possess extensive musculature, suggesting they have an active role in fluid movement into and out of the glands. Tubule epithelia are differentiated into E-, R-, B- and F-cells, the structural characteristics of which are similar with those of other decapods. R-cells are involved in the storage of lipids and detoxification of metals (Ca, Mg, Al, K, Cr) by their accumulation in residual bodies. An absorptive role of B-cells is evident and immunohistochemical localisation of *T. orientalis* trypsin conclusively verified that F-cells are responsible for the production and secretion of digestive enzymes. Absence of trypsin from tissues in the oral region, proventriculus and hindgut, revealed that the digestive glands are the primary site of enzyme synthesis and secretion in the alimentary tract of *T. orientalis*.

The range and concentration of digestive enzymes produced by *T. orientalis* reflects its carnivorous diet, with the proteases trypsin and chymotrypsin produced in high concentrations. Detection of α-amylase and α-glucosidase indicate potential to hydrolyse glycogen, while N-acetyl-glucosaminidase suggests chitin is also a dietary component. Digestive fluid pH (5.9) is consistent with the acid pH optima of carbohydrases, verifying they are well adapted for extracellular digestion.

Trypsin was purified and shown to be a glycoprotein (35 kDa). The N-terminal amino acid sequence has strong homology to crustacean trypsins revealing their structure is highly conserved. This is confirmed by the cross-reaction of crustacean trypsins to the *T. orientalis* enzyme. The optimal k_{cat} and k_{cat}/K_m values for N-α-benzoylarginine-ρ-nitroanalide were 0.91 s^{-1} and 9.7 x 10^3 $M^{-1}s^{-1}$, respectively, with this specificity constant being lower than those reported for other crustacean trypsins. Inhibition studies indicated the presence of serine and histidine at the active site, which implicates a similar catalytic mechanism with all other serine proteases.

DECLARATION OF SOURCES

I declare that this thesis is my own work and has not been submitted in any form for another degree or diploma at any university or other institution of tertiary education. Information derived from the published or unpublished work of others has been acknowledged in the text and a list of references is given.

5.12.95

D.J. Johnston Date

STATEMENT ON ACCESS TO THE THESIS

I, the undersigned, the author of this thesis, understand that James Cook University of North Queensland will make it available for use within the university library and, by microfilm or other photographic means, allow access to users in other approved libraries. All users consulting this thesis will have to sign the following statement:

" In consulting this thesis I agree not to copy or closely paraphrase it in whole or in part without the written consent of the author; and to make proper written acknowledgement for any assistance which I have obtained from it."

Beyond this, I do not wish to place any restriction on access to this thesis.

5.12.95

D.J. Johnston Date

Acknowledgements

Many people contributed in a myriad of ways to make this project possible. First and foremost I wish to thank my supervisors, Chris Alexander and Dave Yellowlees for their guidance, advice and encouragement over the last few years. Their belief in my ability to combine the fields of biology and biochemistry enabled me to pursue a variety of avenues which would otherwise have been impossible.

Sincere thanks to Chris for initially fostering my interest in crustaceans and his enormous enthusiasm and intuition for things that will "tell a good story". His gentle guidance helped me avoid the pitfalls of research and his endless patience with teaching me the art of concise writing was greatly appreciated during the thesis write-up. Thanks also for the stimulating (and perhaps unintelligible) conversations over a moselle and vodka and lemonade on a Friday afternoon at the Club. These helped keep my sanity on countless occasions. Special thanks to Dave Yellowlees for his logical advice and support on all the biochemical aspects of this project. His ability to explain concepts and "get back to basics" was invaluable, particularly in the early stages of this work. His practical approach to science has been an important influence on my research.

Leigh Winsor provided many hours expanding my knowledge on the intricacies of histology and histochemistry and his many tricks to overcome logistical problems in sectioning always proved fruitful. His help in interpreting tissue and cell structure and his willingness to advise and contribute many discussions were greatly appreciated. Zolly Florian always went that much further to get the best results in macrophotography, photomicroscopy and video recording. Thanks for all the lessons imparted, the most important being patience.

Thanks to Heather Winsor and Jim Darley for their expert guidance in scanning and transmission electron microscopy. Heather also helped in the final production of thesis prints and her extensive knowledge of photo presentation was invaluable. Thanks also to Roger, Brian and Shirley in the photography department who managed to produce excellent colour prints despite my often confusing instructions. A big thanks to John Collins who gave me a crash course on the computor software for presentation of illustrations. Thanks also for all the friendly advice over the years.

Thanks to Fedi and all the people who helped collect bugs on the James Kirby. Thanks to the crew who were always prepared to go out in rough conditions, even though we were the ones who normally suffered! Don Booth and Dave Welch assisted in the maintenance of optimal aquarium conditions. Thanks for fending off the many people who had aspirations of bugs for dinner.

Brett Baillie and Spencer Whitney helped me tackle many of the procedures and day to day tasks in the biochem lab. Thanks for the friendship over the years as well as companionship and good humour during the long hours. Thanks also to my labmates Bill, Jack, Darren, Amanda, Angie and Carmen, who made the lab an enjoyable place to work. Special thanks to Bill for reading the final draft of the thesis. Jo Hermans provided many hours teaching me the often delicate techniques of enzyme kinetics and introduced me to the world of serine proteases. Thanks for understanding my frustrations and for not only being a teacher, but a friend. Thanks also to Dr Dennis Shaw for providing the N-terminal amino acid sequence of *T. orientalis* trypsin.

Howard Choat strongly supported this research and I am indebted to his financial provision to attend the Crustacean Society Meeting in America. His fostering of "more unusual" projects was greatly appreciated.

Many people have maintained my sanity and perspective on life by their friendship. Special thanks to: Ilona, Jess, Jacqy, Heather, Vicki, Judy, Larn, Dave and Eliza. Thanks Loni and Jess for dragging me away from my computor during the write-up and forcing me to be sociable. Thanks also to my big sis, Kay, for putting up with me at home and encouraging me when the going got tough.

Most importantly, my heartfelt thanks to my parents, Iris and Eddie, who have supported me emotionally and financially throughout this project and have sacrificed everything over the years to provide me with the best education possible. Their complete understanding and calm advice in the frequent periods of stress and worry have kept me strong. Thanks to them, I have finally made it and I dedicate this work to you both. Finally, I wish to thank Troy for his unfailing love and encouragement every step of the way. His devotion and ability to take me away from it all is most surely cherished.

List of Contents

List of Figures

List of Tables

Publications Resulting from this Thesis

Johnston, D. J., 1994. Functional morphology of the membranous lobe within the preoral cavity of *Thenus orientalis* (Crustacea: Scyllaridae). *J. Mar. Biol. Ass. (U.K.).*, **74**, 787-800.

** Refer to Appendix 3 for reprint.

Johnston, D. J, Hermans, J. M. and Yellowlees, D., 1995. Isolation and characterisation of a trypsin from the slipper lobster *Thenus orientalis* Lund. *Archiv. Biochem. Biophys.*, **323**,

** Reprints not yet available.

Chapter 1. General Introduction

Thenus orientalis (Lund, 1793) belongs to the Family Scyllaridae, commonly referred to as slipper, shovel-nosed, Spanish or bay lobsters. They are closely related to the three other families of decapod lobsters which include the clawed lobsters (Family Nephropidae), spiny lobsters (Family Palinuridae) and coral lobsters (Family Synaxidae). They are characterised by a flattened carapace that has no anterior horns or spines, short broad antennae and non-chelate pereiopods (Phillips *et al.*, 1980). Although there is an extensive body of research on the palinurid and nephropid lobsters, the scyllarids, despite their commercial importance, have been relatively ignored.

Research on scyllarids has concentrated on taxonomy (Harada, 1962; Holthuis, 1968; 1977; 1985; Lyons, 1970; George and Griffen; 1972; 1973; Chan and Yu, 1992), general morphology (Branford, 1980; Jones, 1990), and the description of larval stages (Lyons, 1980; Barnett *et al.*, 1984; 1986; Phillips and McWilliam, 1986; Barnett, 1989; Ito and Lucas, 1990). Biological and ecological knowledge is limited and the few reports have dealt with species of economic significance. Aspects include seasonality and shelter selection (Spanier *et al.*, 1988; Spanier and Almog-Shtayer, 1992), reproduction and fecundity (Hossain, 1979; Martins, 1985), moulting (Kaleemur Rahman and Subramoniam, 1989), swimming technique (Jacklyn and Ritz, 1986; Spanier *et al.*, 1991) and population structure (Jones, 1993). This patchy literature has contributed to a poor general understanding of scyllarids.

Thenus is the most economically significant of the seven scyllarid genera (Jones, 1990). Species of this genus contribute to many of the demersal trawl fisheries which operate along the tropical coasts of the Indian Ocean and the Western Pacific (Jones, 1993). In Australian waters, *Thenus* is distributed along the tropical and sub-tropical coast (10°S-30°S) from northern New South Wales to Shark Bay in Western Australia (George and Griffen, 1972) and contributes significantly to the incidental catch of otter trawlers which fish for penaeid prawns and scallops (Jones, 1984; 1988; 1993). Catches from eastern Queensland, particularly from Townsville to Mackay and Yepoon to Gladstone, are the most significant (Jones, 1984; 1988).

Despite the importance of *Thenus* to Australian fisheries, little attention has focused on its biology. Jones (1988) conducted a PhD project on the biology and behaviour of *Thenus* spp., although most emphasis, both in the thesis and subsequent publications (Jones, 1990; 1993) was on population structure and morphology. General aspects including reproduction, moulting, growth and behaviour (feeding, burying, sediment preference) were also covered but not published.

Until recently, *Thenus* had been considered monospecific since the original description of *T. orientalis* was made by Lund in 1793. *T. indicus*, identified by Leach in 1817, was not considered a valid species and has been synonomised with *T. orientalis*. However, Jones (1988) differentiated two distinct morphs which he termed *T. orientalis* and *Thenus* sp. A, and later re-classified as *T. orientalis* Type A and *T. orientalis* Type B, respectively (Jones, 1990). The species investigated in the present study is consistent with his description of *T. orientalis* (Jones, 1988) and *T. orientalis* Type A (Jones, 1990). Based on the lack of taxonomic clarification of species in the literature upon commencement of this project, it was assumed that the species collected was indeed *T. orientalis*. Investigation of type material and published manuscripts have since led to the conclusion that *T. indicus* is a valid species. Jones (1993) now states that *T. orientalis* (Jones, 1988) and *T. orientalis* Type A (Jones, 1990) are *T. indicus*, whereas *Thenus* sp. A (Jones, 1988) and *T. orientalis* Type B (Jones, 1990) are *T. orientalis*. However, until taxonomic evidence verifying the classification of two species is published (Davie and Jones, unpubl.), species identification in this study remains based on Lund (1793) and Jones (1988; 1990).

To maintain an effective and viable fishery it is essential that the biology of the animal is comprehensively understood. Jones (1988) provided an overview of selected aspects, none of which were closely linked to provide a coherent picture of any one system. The present study addresses three integrated aspects of *T. orientalis* biology, namely food acquisition, ingestion and digestion. All three are of importance to fisheries and aquaculture industries as a knowledge of food consumption and digestive capabilities is fundamental to growth and production of both wild and cultivated populations. This is especially so in husbandry systems as an understanding of digestive capabilities aids the formulation of commercial diets, one of the principal costs in aquaculture, for maximal efficiency in digestive assimilation. At present such information is non existent for

scyllarids.

To survive in a wide range of habitats, decapod crustaceans have developed an extensive repertoire of feeding strategies which, depending on the food available, they exercise selectively. These strategies may be categorised as filter and suspension feeding, scavenging, predation and parasitism (McLaughlin, 1982), and involve a highly proficient system of food acquisition and ingestion. Scyllarids are primarily carnivorous scavengers preferring small benthic invertebrates including molluscs, polychaetes and crustaceans (Suthers and Anderson, 1981; Lau, 1988). The genera *Scyllarides, Parribacus* and *Arctides* specialise in molluscs of which the bivalves *Glycymeris pilosus* (Linnaeus), *Ostrea sandvicensis* (Linnaeus), *Isognomon incisum* (Linnaeus) and *Venus verrucosa* Linnaeus are preferentially selected (Lau, 1987; Spanier *et al.*, 1988). Jones (1988) found that scallops (*Amusium* spp.) were preferentially selected by *T. orientalis* when presented with a variety of species from the most abundant macrofaunal groups associated with this scyllarid. He did not, however, specify whether they were presented dead or alive (see Ch 2).

Food acquisition by scavengers like scyllarids involves the location of food by foraging. This entails orientation toward a food source using distance chemoreceptors on the antennules and co-ordinated probing of the substratum by the pereiopod dactyls which act as contact chemoreceptors (Hazlett, 1971). Although foraging behaviour is exhibited by all scavengers, few detailed studies exist, with descriptions of penaeids by Hindley and Alexander (1978) and lobsters by Derby and Atema (1982). Decapods which preferentially feed on molluscs, principally bivalves, manipulate their prey extensively to remove the flesh prior to ingestion. Complex attack behaviours have evolved and are derived from a combination of chela morphology and the nature of molluscan prey. Lau (1987) described a wedging technique used by *Scyllarides squamosus* (Milne-Edwards) to open bivalves. He noted that the non-chelate scleritised pereiopods of all scyllarids are a specific adaptation for opening bivalves in this way.

Food ingestion in decapods involves a complex functionally integrated action of the mouthparts (maxillipeds, maxillae, mandibles) and can be summarised into four phases: i) introduction to the preoral cavity, ii) passage of food up the preoral cavity, iii) insertion between the mandibles and iv) trituration and swallowing (Alexander and

Hindley, 1985). Ingestion may be macrophagous or microphagous, depending on the nature of food to be consumed. Macrophagous ingestion is used by the majority of carnivores which prey on relatively large food items and is characterised by a tearing action between the third maxillipeds and mandibles (Caine, 1975a,b; Kunze and Anderson, 1979). Microphagous ingestion is adopted for small pieces of flesh and particulate material but the role and involvement of mouthparts is more variable (Caine, 1975b; Alexander and Hindley, 1985). By examining the action of mouthparts manipulating a range of food types, the ability of a species to adopt more than one ingestion mode can be determined. If more than one mode is used a greater range of food size and textures would be available, which is important for the survival of slow moving benthic crustaceans like scyllarids.

As decapods evolved a feeding preference or feeding mechanism the appendages evolved specialisations to maximise their functional efficiency. Consequently, examination of the structural characteristics of each mouthpart is essential to understand their role in ingestion. One of the most important adaptations is setation, the morphology, position and innervation of which provides an indication of their roles in feeding and grooming (Pohle and Telford, 1981; Derby, 1982; Felgenhauer and Abele, 1983; 1985; Lavalli and Factor, 1992). In addition, the overall morphology of mouthparts is closely related to diet and can therefore be used as a general indicator of dietary preferences. For example, the development of crista dentata on the third maxillipeds and robustness of the mandibles is positively correlated with macrophagy (Kunze and Anderson, 1979; Skilleter and Anderson, 1986).

Ingestion mechanisms and mouthpart functional morphology have been thoroughly investigated in a number of decapods including the macrurans (lobsters and crayfish) (Yonge, 1924; Farmer, 1974; Caine, 1975b; Barker and Gibson, 1977; Factor, 1978), crabs (Nicol, 1932; Greenwood, 1972; Caine, 1975a; Kunze and Anderson, 1979; Skilleter and Anderson, 1986; Creswell and Marsden, 1990; Manjulatha and Babu, 1991) and penaeid prawns (Alexander *et al.*, 1980; Suthers, 1984; Hunt *et al.*, 1992). There is only one example describing mouthpart structure and ingestion in the scyllarid *Ibacus peronii* Leach (Suthers and Anderson, 1981).

Digestion involves the mechanical and chemical degradation of ingested food into its constituents for subsequent absorption and removal as wastes. In decapod crustaceans, mechanical degradation is initiated by the mouthparts which cut and macerate food into smaller ingestible pieces. Most occurs internally in the gastric mill in the cardiac stomach, the teeth of which are adapted for grinding, tearing and cutting (Kunze and Anderson, 1979). At the same time, chemical hydrolysis is initiated by digestive enzymes secreted by the digestive glands. Fluid and small particles are then filtered by a complex system of setae in the cardiac stomach and pyloric stomach filter press prior to entry into the digestive gland. Here, final chemical hydrolysis into constituent amino acids, glucose and fatty acids takes place for storage or mobilisation. Waste products of digestion pass from the stomach and digestive gland into the hindgut where they are expelled as faeces.

A description of the entire alimentary tract provides a structural basis upon which to understand the mechanical aspects of digestion. Past studies on decapod digestion have used this approach, although the majority concentrated on specific regions of the tract providing limited information on the digestive process *in toto* (Powell, 1974; Felder and Felgenhauer, 1993; King and Alexander, 1994). The few studies that have detailed the entire tract have been primarily histological and histochemical providing basic information on the nature of, and region in which, digestive processes take place (Barker and Gibson, 1977; 1978; Babu *et al.*, 1982).

The most significant regions of the tract involved in digestion are the proventriculus (cardiac and pyloric stomach) and digestive gland, the former because of its role in mechanical degradation and initial chemical hydrolysis and the latter because it is central to all digestive processes in decapods (Icely and Nott, 1992; Brunet *et al.*, 1994). Although both have received considerable attention in a number of decapod groups, the Scyllaridae have been relatively ignored with only one notable study on the external morphology of the proventriculus and gastric mill structure and function in *I. peronii* (Suthers and Anderson, 1981).

The digestive gland has a number of roles in digestion including final chemical hydrolysis, the processing of food constituents for storage or mobilisation, synthesis and secretion of digestive enzymes, detoxification of metals and the elimination of wastes

(Icely and Nott, 1992). Despite extensive research, considerable confusion remains over the appointment of these functions to the cell types of the gland. This is primarily attributable to its fragility forcing workers to rely on histological and cytological techniques as well as histochemical identification of digestive enzymes, all of which, as a result of cell fixation, have limitations (Gibson and Barker, 1979; Hopkin and Nott, 1980; Caceci *et al.* 1988). To clarify cell function, it is necessary to complement these techniques with specialised ones such as x-ray microanalysis and immunohistochemistry.

To understand the process of chemical degradation, biochemical determination of the types and relative concentration of digestive enzymes produced by the digestive glands is essential. Based on the close relationship between diet and the range of digestive enzymes produced (Lee *et al.*, 1984; McClintock *et al.*, 1991; Rodriguez *et al.*, 1994), this information enables assessment of which dietary components a crustacean is able to digest and utilise for metabolic purposes, that is, its digestive capabilities (Galgani *et al.*, 1984; Galgani and Nagayama 1987). Information of this type has been used by aquaculturalists to formulate commercially produced diets to maximise production and growth (Lee *et al.*, 1984; Glass and Stark, 1995). Although the number of studies quantifying digestive enzymes is increasing, no such work has been conducted on scyllarids.

There is little information on the purification and characterisation of a particular enzyme. Proteases play an important role in the digestion process of carnivores, as they ingest large quantities of dietary protein. The serine protease, trypsin, has been detected in almost all crustaceans studied and is considered to be one of the most important enzymes in crustacean proteolysis (Dendinger, 1987; Lu *et al.*, 1990). Recent characterisation of its structural properties has enabled the relationship with mammalian trypsins to be assessed (Dendinger and O'Conner, 1990; Honjo *et al.*, 1990; Guizani *et al.*, 1992). However, functional aspects of this enzyme have not been determined so that information on crustacean proteolysis remains limited. This can be achieved by kinetic analysis which provides detailed information on the catalytic mechanism. Comparisons with mammalian trypsins can then be made to ascertain whether evolutionary divergence in catalytic mechanism has occurred.

Purification of an enzyme is also important in the production of antibodies for the application of immunohistochemical techniques to identify the site of digestive enzyme synthesis in the alimentary tract (see Ch 5). In particular, immunolocalisation of trypsin can be used to verify whether F-cells of the digestive gland are the site of enzyme synthesis, as was found by Vogt *et al.* (1989) in *Astacus astacus* Linnaeus. Hence biochemical techniques are an integral part in linking structural characteristics of cells and tissues with function.

Objectives of this Study

The purpose of this study was to better understand the processes of food acquisition, ingestion and digestion in the scyllarid *T. orientalis*. Research was divided into three integrated sections, with the following aims:

Food Acquisition:

⋆ to describe foraging behaviour and the mechanism by which a preferred food source, bivalve molluscs, are manipulated and opened (Ch 2).

Food Ingestion:

⋆ to determine the role of mouthparts during ingestion and ascertain whether more than one mode is adopted with food type.

⋆ to identify structural characteristics of mouthparts, including the paragnaths and membranous lobe, a structure unique to scyllarids, in relation to their function (Ch 3).

Food Digestion:

⋆ to detail the functional morphology of the entire alimentary tract (Ch 4).

⋆ to determine the structure and function of the digestive glands (Ch 5).

⋆ to identify the range and concentration of some digestive enzymes (proteases and carbohydrases) produced by the digestive glands (Ch 6).

⋆ to purify and characterise trypsin, an important serine protease in crustacean digestion (Ch 7).

Although information derived from this study has applications for the promotion and assessment of commercial viability of *T. orientalis*, it was essentially used to provide a scientific basis for understanding these important biological processes in a little researched decapod family. This study is significant as it combines specialised biological and biochemical techniques to give a comprehensive account of scyllarid digestion. This enabled both mechanical and chemical degradation to be extensively investigated. By combining digestion with food acquisition and ingestion an overall picture of food procurement and processing was achieved.

Chapter 2. Foraging Behaviour and Prey Manipulation

2.1 INTRODUCTION

Food acquisition by scavengers, such as scyllarids, involves the initial location of food by foraging. In contrast, filter feeders and deposit feeders acquire their food directly from the water column or substratum using highly modified setose appendages, such as the pereiopods (Atyid shrimps - Felgenhauer and Abele, 1983; 1985), or third maxillipeds (Anomura - Caine, 1975a; Galatheidea - Nicol, 1932).

Foraging principally involves chemoreception and other sensory modalities to a lesser degree. The principal appendages implicated are the antennules and pereiopods, the chemoreceptors of which control different subsets of behaviour in the sequence of actions leading to food location and ingestion (Derby and Atema, 1982). The antennules of decapods function as low threshold distance chemoreceptors (Hazlett, 1971), via the tufts of thin-walled aesthetascs borne on the lateral antennular filament (Ghiradella *et al.*, 1968; Shelton and Laverack, 1970). Antennular flicking is common and temporarily enhances the response of olfactory receptors to changes in stimulus concentration (Schmitt and Ache, 1979). Detection of extremely low concentrations (10^{-6} - 10^{-5} M) of chemicals by the aesthetascs can elicit foraging behaviour in the prawn *Penaeus merguiensis* de Man (Hindley, 1975). Foraging is a true rheotaxis whereby the animal orientates toward the food source and begins extensive probing of the substratum using dactyls of the anterior pereiopods. This allows the animal to search an area considerably larger than its body size and therefore maximises foraging efficiency.

The pattern of pereiopod movement appears to be distinctive for a species or group but is generally a slow methodical searching for food either on the surface or directly beneath the substratum (Hindley and Alexander, 1978). During this process, mechanoreceptors on the dactylus and/or propus can also be used to detect the depth to which the limb has been inserted into the substratum.

Once food is located, the shift from searching to grasping is dependant on the stimulation of low threshold contact chemoreceptors located on the pereiopod dactyls, which are reportedly 10 times less sensitive than the aesthetascs (Hazlett, 1971). Food is

probed and manipulated by the dactyls of the anterior pairs of pereiopods during which time the chemoreceptors assess its palatability. If palatable, food is passed to the third maxillipeds and ingestion is initiated (Hindley and Alexander, 1978; Derby and Atema, 1982).

Decapods that preferentially feed on molluscs, principally bivalves, have to manipulate their prey extensively to remove the edible flesh. To compensate for additional manipulation time, most have complex attack behaviours which are often associated with specialised structures. Attack behaviour patterns are derived from a combination of chela morphology and the nature of the molluscan prey.

The techniques employed by chelate predators to open bivalves usually involve crushing of the shell (Du Preez, 1984; Skilleter and Anderson, 1986), or depending on the strength of the claw relative to shell thickness, chipping the outer edge of the bivalve until the soft bodied parts can be reached (Hughes and Seed, 1981; Davidson, 1986). Specialisations in chela morphology and shell-opening behaviour are often apparent. For example, dactylar teeth or tubercles are common on the cutting edge of the claw in many crabs (Du Preez, 1984; Creswell and Marsden, 1990).

Non-chelate decapods which prey on bivalves have adopted alternative tactics for opening the shell. The rock lobster *Jasus lalandii* Milne-Edwards uses its mandibles rather than the claw to chip open the mussel *Aulacomya ater* Molina (Pollock, 1979). The wedging open of bivalves is also common and has been reported for the scyllarid *S. squamosus* (Lau, 1987). In general, insertion of the dactyl tips of the anterior pereiopods widen the gap between the valves progressively, so that the flesh can be devoured. The effectiveness of this tactic depends to some extent upon the degree of tapering of the dactyli of the pereiopods. Variations in attack are in part, dependant on the morphology of the bivalve species and its attachment to the substratum.

The primary objective of this study was to investigate food acquisition by *T. orientalis*. This involved documentation of foraging behaviour, during which its preference for scallops (*Amusium balloti* (Bernadi)) was verified (Jones, 1988). Consequently, the mechanism by which *T. orientalis* manipulated and opened scallops was detailed. As *T. orientalis* found it difficult to open live scallops, a range of benthos

common in their native habitat (Cleveland Bay) was offered to determine whether *T. orientalis* preferentially selected bivalves, and was able to open live bivalves using a similar technique to that used on scallops.

2.2 MATERIALS AND METHODS

2.2.1 Collection and Maintenance

Thenus orientalis specimens were collected by otter trawling in Cleveland Bay, Townsville, Australia (19° 15'S 146° 50'E). They were most abundant on sandy substrata at depths of 15-20 m between Cape Cleveland and Magnetic Island (Fig. 2.1). They were transferred to and maintained in recirculating sea water circular holding tanks (1.5 m x 1 m) and fed every second day on a mixed diet of scallops (*Amusium balloti*), marine fish (goatfish, lizardfish, trevally) and prawns (*Penaeus merguiensis*). A 5 cm sand substratum allowed the lobsters to bury and forage without restriction. This was replaced every 2 months to minimise fouling.

2.2.2 Foraging Behaviour

T. orientalis were starved for 5 days to enhance foraging activity and then placed in a well aerated 60 cm x 60 cm flow through sea water tank, with a 5 cm substratum of sand. They were acclimated for 24 h and then offered whole scallops (*A. balloti*), fish and prawn flesh. Behaviour was recorded with a Javelin low light, infra-red sensitive video camera with an F2 lens operating to 1 lux intensity. As decapods are sensitive to white light (Hindley, 1975), a Panasonic WV-CD810 infra-red camera with near infra-red LED (950 nm) lighting was used to illuminate the tank. As this wavelength is absorbed rapidly in water, additional illumination was provided by two Volpi 6000 fibre-optic units fitted with red filters. The experiment was run at night as scyllarids are nocturnally active (Jones, 1988). Camera output was recorded on a National 6010 time lapse recorder operating at both 25 and 50 frames s^{-1}. Recordings were analysed at normal speed (50 frames s^{-1}).

A range of benthic organisms common to Cleveland Bay, including crabs, bivalves and polychaetes was also offered to a number of scyllarids to determine whether *T. orientalis* preferentially selects bivalves. This was based upon observations of consistent selection and highly efficient manipulation of scallops by *T. orientalis*.

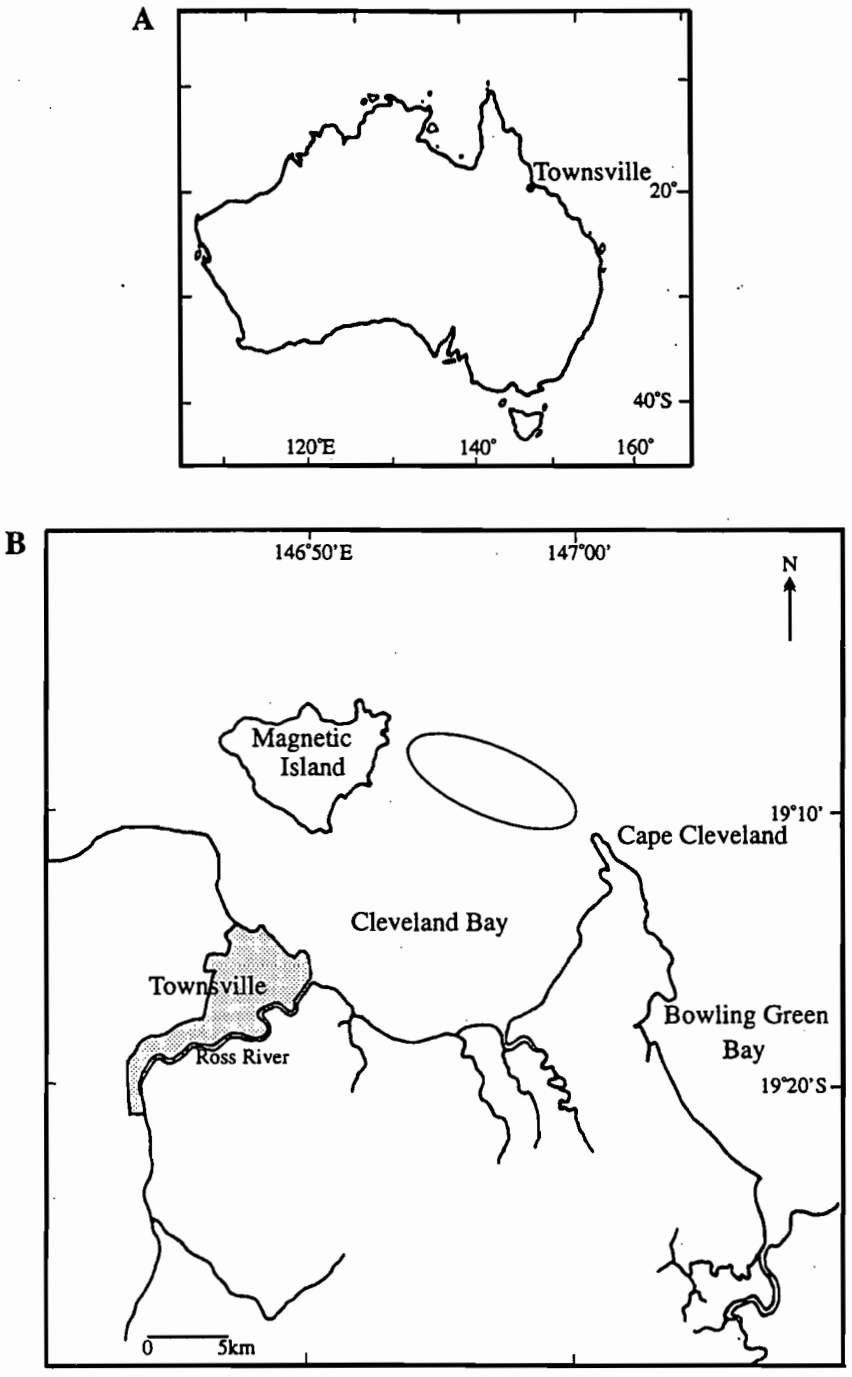

Figure 2.1. Location map of **A.** Townsville; **B.** the position of *T. orientalis* trawling sites in Cleveland Bay (area enclosed within the oval).

2.3 RESULTS

2.3.1 Foraging Behaviour

T. orientalis is a nocturnal slow moving benthic crustacean which spends a large proportion of daylight hours buried beneath the surface of the substratum with only its antennules and eyestalks exposed. During the night it forages for food, these periods being interspersed with bursts of swimming or quiescence.

When quiescent, the body is raised above the substratum on the dactyls of the third, fourth and fifth pereiopods (Fig. 2.2). The first and second pereiopods are raised anteriorly under the antennae, the dactyls directed inwards and ventrally. Antennules are flexed above the antennae with the distal segment and flagella projected posterially. The uropods and telson are curled under the three posterior abdominal somites. The third maxilliped endites often extend ventrally and are raised and lowered as the first and second pereiopods move latero-medially. The third pereiopods are often raised anteriorly above the eyestalk and the dactyl setae brushed over the eye to remove particulate matter.

Two modes of foraging are used by *T. orientalis* and are described as follows.

Probing

The first and second pereiopods are the principal appendages used in probing the substratum, although the third and fourth may also be used. A probing sequence may last between 1-5 minutes. The dactyls of pereiopods 1 and 2 are sharp and hardened by a keratinised cap and those of pereiopods 3, 4 and 5 have two rows of setae.

The third, fourth and fifth pereiopods extend laterally to lower the body and the third maxilliped dactyls brush the sand surface. The first three pairs of pereiopods extend anteriorly and the dactyl tips are inserted into the substratum. They probe in a posterior direction towards the mouth while the animal walks slowly over the substratum using the fourth and fifth pereiopods. When food is encountered, the body is lowered further and the antennae are placed on the substratum. The third maxilliped endites are lowered and the first and second pereiopods probe the item. If it is rejected, the scyllarid re-orientates and moves away. If accepted, it is picked up and held to the oral region in the propus-dactylus articulation of the second and third pereiopods, while the first pereiopods insert portions between the third maxilliped endites. During ingestion, pereiopods remain in the

oral region to secure food as well as helping to manipulate large or hard items. If food has not been found after approximately 5 minutes, it swims away to another location.

Digging

The body is lowered and the third, fourth and fifth pereiopods are inserted, up to the propus/carpus articulation, into the substratum. While buried, they move slowly inwards and then dorsally under the body, turning over the substratum. On completion of the inward motion, the body jerks upward and sideways and the pereiopods are re-inserted. Material found is probed and manipulated as described above.

2.3.2 Bivalve Manipulation and Opening

During foraging experiments, *T. orientalis* preferentially selected the scallop *A. balloti* over fish and prawn flesh and are adept at removing the flesh from thawed scallops. They could not do this with live scallops as they closed the shell valves and swam away.

When presented with a scallop, the antennules are lowered and continually flicked up and down. The scyllarid positioned itself over the scallop and the third pereiopods are inserted between the shell valves to prise them apart (Fig. 2.3). The sharp dactyls of the first and second pereiopods are inserted to sever the adductor muscle and remove the soft bodied parts of the bivalve. This process is often completed in less than 1 minute. Once the tissue has been removed, the adductor muscle is separated from the mantle by the first, second and third pereiopods and ingested.

Preferential Selection of Bivalves

Although *T. orientalis* was unable to open live scallops, it preferentially selected and successfully opened small live bivalves (*Drosinia* spp. and *Mactra* spp.) from a range of benthos common to its Cleveland Bay habitat, including: polychaetes, enteropneust worms, bivalves, hermit crabs and a range of brachyuran crabs. The opening sequences were the same as above but took slightly longer (1-2 minutes) with the shell periphery often chipped by the pereiopod dactyls and the hinge broken.

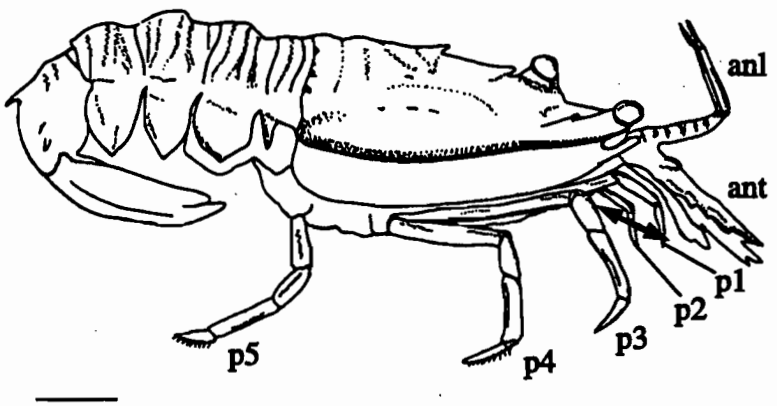

Figure 2.2. Orientation of the body, pereiopods, antennae and antennules of *T. orientalis*, when quiescent. Arrow indicates the latero-medial movement of the first and second pereiopods. The third maxillipeds are obscured from view. Scale, 1 cm.
anl, antennules; ant, antennae; p1,2,3,4,5, pereiopod 1,2,3,4,5.

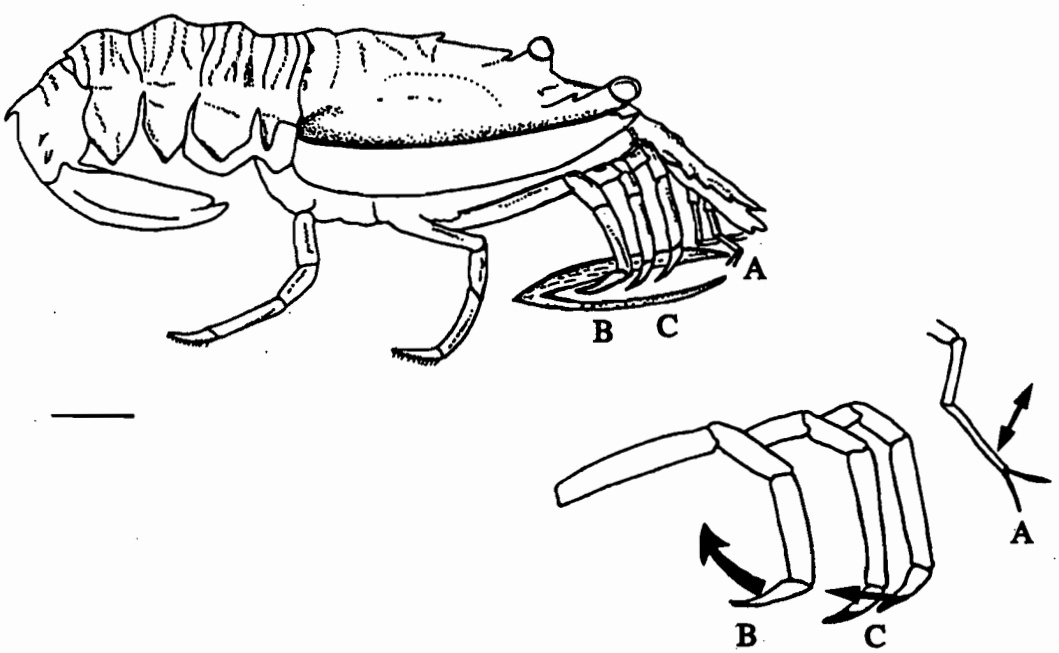

Figure 2.3. The orientation and direction of movement of the pereiopods (right side) during the opening of the scallop *A. balloti* by *T. orientalis*. **A.** antennules are continually flicked up and down; **B.** the dactyl of the third pereiopod is forced inwards as the upper shell is pushed upwards; **C.** the first and second pereiopods are inserted and the dactyli sever the adductor muscle. Scale, 1 cm.

2.4 DISCUSSION

Exhibition of two foraging modes indicates that *T. orientalis* has a flexible search pattern, the adoption of each mode dependant on the distribution, density and type of prey. According to optimal foraging theory (Hughes, 1980), digging would be employed in areas of high prey density as it is only in these areas where this time and energy costly, but highly effective foraging mode, would be profitable. Similarly, it would be advantageous to switch to the less costly search method of probing in areas of low prey density. This flexible foraging behaviour enables *T. orientalis* to feed on patchily distributed prey types while simultaneously maximising energy intake and minimising time expenditure (Davidson, 1986).

Digging is particularly suited for locating sub-surface fauna, like bivalves, that would be successfully overturned and exposed by the digging action. The third, fourth and fifth pereiopods are morphologically adapted for digging as their dactyls are more robust than the first and second pereiopods used in contact chemoreception. Similar digging by the pagurid *Petrochirus diogenes* Linnaeus was used to expose benthic prey such as polychaetes and ophiuroids (Caine, 1975a).

Intermittent bursts of swimming between foraging serve to re-position the scyllarid. This is consistent with optimal foraging theory which states that when net rate of energy intake drops below the average for a habitat the animal moves to another more profitable patch (Hughes, 1980).

Periodic flicking of the antennules increases in frequency during foraging. Flicking splays out the tightly packed aesthetascs allowing increased exposure to the chemical environment (Snow, 1973; Schmitt and Ache, 1979). This enhances the ability of the antennules to distinguish between near threshold changes in stimulus concentration which is advantageous for effective orientation towards the food source. This response has also been demonstrated in several other decapods where flicking becomes maximal at the onset of stimulation (Price and Ache, 1977; Schmitt and Ache, 1979). The lowering of antennules upon finding food, together with probing by the chemoreceptive first and second pereiopods, determines its palatability. If palatable, the anterior pereiopods transfer food to the third maxillipeds initiating ingestion (refer Ch 3). This manipulation by the pereiopods is common among scavenging decapods such as penaeid prawns

(Hindley and Alexander, 1978).

T. orientalis is a specialised predator of bivalves and preferentially selects them from a range of common benthic fauna. It is also adapted for efficient bivalve manipulation and opening. This is consistent with other scyllarid genera which prey on bivalves and have similarly efficient manipulation and opening behaviours (Lau, 1987; 1988; Spanier *et al.*, 1988).

T. orientalis is proficient at manipulating and removing the flesh from dead scallops (*A. balloti*) and live bivalves (*Drosinia* spp., *Mactra* spp.). The technique adopted is similar to that of wedging used by the scyllarid, *S. squamosus* on the oyster *O. sandvicensis* and toothed pearl shells *I. incisum* and *I. perna* (Lau, 1987). However, the role of the pereiopods differs between the two species and the patience attack, involving a waiting period while poised over the bivalve, was not exhibited by *T. orientalis*. The more robust third pereiopods of *T. orientalis* are adapted to prise the shell open, and the slender and sharply tapered dactyls of the first and second pereiopods for insertion and severing the adductor muscle.

In contrast to *S. squamosus*, *T. orientalis* was unable to open the shell valves of large live bivalves like the scallop *A. balloti*. However, the smaller live bivalves, *Drosinia* and *Mactra* were easily opened. This indicates that *T. orientalis* either does not feed on live scallops in the wild, or it only preys on dead or dying ones. This is because, based on the strength of their adductor muscle compared with smaller bivalves, live scallops are probably above the optimal prey size for *T. orientalis* . The pereiopod dactyli of *T. orientalis* are slender and tapered, whereas they are robust and flared in *S. squamosus*. Hence, the effectiveness of the wedging tactic is related to the degree of tapering of the dactyli and the force they can generate. This is verified by Lau (1987) who observed that *Arctides regalis* Holthuis and *Parribacus antarcticus* Lund, which possess tapered dactyli, took considerably longer to open the toothed pearl shell *I. perna* than in *S. squamosus*.

Based on these behavioural and structural observations it is evident that *T. orientalis* is adapted for locating and opening bivalve molluscs. Hence soft flesh and muscle are important dietary components of this scyllarid. A comprehensive dietary analysis is required to verify these findings and identify other items preyed upon.

Chapter 3. Structure and Function of the Mouthparts During Ingestion

3.1 INTRODUCTION

3.1.1 Ingestion

Ingestion involves the closely co-ordinated action of the six pairs of mouthparts: third, second and first maxillipeds, second and first maxillae and the mandibles (McLaughlin, 1982). Accessory roles have also been reported for the paragnaths and labrum (Robertson and Laverack, 1979; Alexander and Hindley, 1985; Hunt *et al.*, 1992) (see Ch 3.1.3). The degree of involvement and role of each mouthpart varies between species and is primarily dependant on the nature of food being ingested. More than one ingestion mode may also be adopted depending on the item to be consumed. This enables a species to maximise feeding potential in a given habitat by its capacity to ingest a wider range of items, some of which would have otherwise been unavailable (Maitland, 1990).

Previous interpretations of mouthpart function during ingestion have relied entirely on the morphology and musculature of each appendage. Although these analyses were essentially correct, recent application of high-speed cinematography, video-recording and macrophotography has revealed a greater variation in movements (Alexander and Hindley, 1985; Hunt *et al.*, 1992). In particular, the use of an endoscope by Hunt *et al.* (1992) enabled detailed observations on the role of the anterior mouthparts (maxillae, paragnaths and labrum) of *P. merguiensis*, which are obscured when using conventional video techniques.

Ingestion in decapods can be macrophagous or microphagous, one or both being exhibited by a given species. Macrophagous ingestion is used by the majority of carnivores and predators which prey upon relatively large food items. It is quite consistent throughout the Decapoda and is characterised by a co-ordinated tearing action between the third maxillipeds and mandibles (Greenwood, 1972; Farmer, 1974; Caine, 1975a,b; Kunze and Anderson, 1979; Alexander *et al.*, 1980; Suthers, 1984). Food received from the anterior pereiopods, is gripped between crista dentata on the ischium of the third maxillipeds and presented to the mandibles. These clamp on the food while the third maxillipeds are pulled ventrally to tear the food. The second maxilliped endopods may also macerate the food and together with the maxillae, push the torn piece

between the mandibles and into the mouth. As this occurs the paragnaths and labrum rotate out of the way and then resume their original position once food has been inserted (Robertson and Laverack, 1979; Alexander and Hindley, 1985). This process is repeated until the food is completely ingested.

Greater variability in mouthpart function occurs in microphagous ingestion, attributable to the wide range of food types ingested from small pieces of flesh to particulate matter. A mouthpart may also be highly specialised which consequently affects the respective roles of the remaining mouthparts. For example, the third maxillipeds are modified into setose "nets" to filter suspended detritus or plankton from the water column in the Anomura (Caine 1975a) and as "brooms" to sweep the substratum for algae and small animals in the Galatheidea (Nicol, 1932).

In general, once food has been collected or received by the third maxillipeds it is removed by alternating movements of the second maxilliped endopods and transferred progressively to the first maxillipeds and second and first maxillae where it is sorted and/or macerated prior to insertion between the mandibles (Caine, 1975b; Kunze and Anderson, 1979; Alexander and Hindley, 1985). A feeding current, created by beating of the maxilliped exopods, aids the passage of food, especially particulate material, toward the mouth.

3.1.2 Mouthpart Structure

To function efficiently, mouthparts have evolved structural adaptations, of which the setae are the most important. Setae are highly variable in structure; their morphology, position and innervation providing clues about their function in feeding and grooming. The classification of crustacean setae is, at present, defined on their morphology and state of development because there is insufficient physiological information as a basis for definition (Jacques, 1989). The principal schemes were proposed by Thomas (1970), Farmer (1974) and Jacques (1989) and vary in complexity and the degree to which they agree. Thomas (1970) offered the earliest comprehensive setal classificatory system which was modified by Factor (1978) and Lavalli and Factor (1992). Jacques (1989) substituted descriptions and illustrations with a shortened notation system where characters with functional significance were expressed by an analytical formula denoting presence or absence (+, -). In contrast, Watling (1989) proposed a classification based

on the homology concept so that setae could be used to assess taxonomic status. All systems stress the need for careful definition and application of terminology.

Although there are several studies documenting the setation of mouthparts, the majority have concentrated on light microscopy which has limitations in discerning diagnostic morphological details such as the presence or absence and position of pores (Nicol, 1932; Thomas, 1970; Coombs and Allen, 1978; Kunze and Anderson, 1979). Consequently, inappropriate terminology has often been applied creating confusion when comparisons between studies are attempted. More recently, scanning electron microscopy has enabled detailed examination of external morphology (Pohle and Telford, 1981; Derby, 1982; Felgenhauer and Abele, 1983; 1985; Maitland, 1990; Lavalli and Factor, 1992).

Identification of setal function has generally been based on examination of morphology, location and behaviour, but electrophysiological evidence is necessary to define their sensory capabilities. Based on combined evidence from these techniques three broad function categories associated with feeding and grooming have been proposed: i) mechanoeffectors, ii) mechanoreceptors and iii) chemoreceptors (Jacques, 1989). Mechanoeffectors lack innervation and are morphologically adapted for their particular role. For example, plumose setae on the scaphognathites of the second maxillae have interlocking setules which form a palisade to screen particles from entering the branchial chamber and damaging the delicate gills (Farmer, 1974; Pohle and Telford, 1981). Simple stout setae on the dactyls of the second and third maxillipeds are well adapted to grip food and aid in maceration (Suthers and Anderson, 1981; Skilleter and Anderson, 1986). Setobranchs on the third maxillipeds and pereiopods have digitate scales used to inhibit fouling from parasites and foreign matter on the gills (Felgenhauer and Abele, 1983; Bauer, 1989).

Mechanoreceptors are innervated by similar neurones to those of chemoreceptors except that the mechanosensitive dendrite attaches to the side of the setal base whereas the chemosensitive dendrite extends the length of the seta (McIver, 1975). They have many forms of external morphology and function in: current detection, proprioreception and directional sensitivity (McIver, 1975; Felgenhauer and Abele, 1983). For example, peg sensilla on the surface of the maxillipeds and carapace of *Homarus americanus*

Milne-Edwards respond to water vibrations and touch (Derby, 1982). Chemoreceptors may possess a terminal or subterminal pore (Thomas, 1970), or have a thin porous cuticle (Pohle and Telford, 1981), through which the chemical properties of food are received. Based on the nature of these chemicals these setae may either elicit a gustatory response, or if unpalatable, they initiate rejection of the item performed by a reversal of movement of the mouthparts and current flow (Kunze and Anderson, 1979).

Although many setal types are specialised for only one of these roles, many are bimodal serving both mechano- and chemosensory functions. For example, smooth (simple) and squamose (serrulate) setae (Shelton and Laverack, 1968; Derby, 1982). Trimodal setae which perform all three mechanical, mechanosensory and chemosensory functions, are also common. The most notable of these are serrate setae present on the third and second maxilliped endopods of the majority of decapods (Bauer, 1989; Lavalli and Factor, 1992). These setae have two rows of serrations distally which are used to scrape clean the antennules and other mouthparts.

In addition to the array of setae, the overall morphology of mouthparts varies considerably between groups and is closely related to diet. In general, macrophagy has been associated with robust mouthparts and a reduced development of these structures has been established for detritivory (Caine, 1975a; Coombs and Allen, 1978). More specifically, the development of crista dentata on the third maxillipeds and robustness of the mandibles was found to be positively correlated with macrophagy whereas the mouthparts of filter feeding decapods were more delicate and setose (Kunze and Anderson, 1979; Skilleter and Anderson, 1986).

3.1.3 The Paragnaths

The paragnaths are often conspicuous structures located in the preoral cavity of the majority of decapod Crustacea. They are not true appendages but are soft outgrowths of the exoskeleton which lie on the aboral side of the mandibular gnathobase. Here they form the lateral margins of the oral cavity.

Despite the obvious size of paragnaths, most publications on feeding appendages either fail to mention them (Greenwood, 1972; Kunze and Anderson, 1979; Suthers and Anderson, 1981; Skilleter and Anderson, 1986), or give only a brief description of their

external morphology (Farmer, 1974, Felgenhauer and Abele, 1985). Only recently has a detailed description of their external morphology in a range of crustaceans been provided by Alexander (1988), with particular attention focussed upon penaeid prawns (Alexander and Hindley, 1985; Alexander, 1989; Hunt *et al.*, 1992).

All reports established that paragnaths have numerous pores on the integument surface, which overlie numerous tegumental glands in the tissue. Thomas (1984) noted this in *Austropotamobius pallipes* Lereboullet and suggested they may be involved in mucus production and secretion. Using transmission electron microscopy, Alexander and Hindley (1985) verified their secretory nature and demonstrated an extensive system of canals used to carry secretions to the surface.

Tegumental glands are small spherical exocrine glands located beneath the crustacean integument and have been reported in a wide range of Crustacea including isopods, amphipods, copepods, cirripedes and decapods. Their distribution in the body is widespread; for example, the mouthparts (Gorvett, 1946; Stevenson and Murphy, 1967), oesophagus (Barker and Gibson, 1977; 1978), eyestalk (Arsenault *et al.* 1979) and pleopods (Johnson and Talbot, 1987; Talbot and Zao, 1991). A comprehensive list of their location and presumed function was given by Alexander (1989).

The structure of tegumental glands appears to be remarkably conservative. Each gland is organised into a rosette of conical-shaped secretory cells which are arranged around a central or duct cell (Gorvett, 1946; Arsenault *et al.*, 1979; Aiken and Waddy, 1982). It is because of this anatomical configuration that they are often referred to as rosette glands. A canal cell has been identified in *Palaemonetes pugio* Holthuis through which the duct passes from the gland centre to the outer periphery (Doughtie and Rao, 1982). This cell appears analogous to the duct cell described by Arsenault *et al.* (1979) in *H. americanus*.

Ultrastructural characteristics of the tegumental gland cells, namely the large quantities of rough endoplasmic reticulum, Golgi apparatus and densely staining granular vesicles confirm that they are secretory (Arsenault *et al.*, 1979; Felgenhauer and Abele, 1983). This secretory function was verified by Johnson and Talbot (1987) who reported that the cisternae of rough endoplasmic reticulum were swollen with secreted material

and that the Golgi apparatus released spheroid secretory vesicles at their trans face in the pleopod gland cells of *H. americanus*.

Transmission electron microscopy has revealed subtle cytological differences between secretory cells. This has led authors to define more than one type of secretory cell and, in some cases, more than one type of tegumental gland. Eloffson *et al.* (1978) defined two types of cells in the glands of *Gammarus pulex* Linnaeus, one of which contained rough endoplasmic reticulum and large electron lucent vacuoles, and the other containing smooth endoplasmic reticulum and electron dense vesicles. Johnson and Talbot (1987) also defined two types of secretory cell; one containing homogenous granules and the other honeycombed granules. From this they concluded the glands have multiple functions. Thus although their anatomical configuration is conservative, cellular differences are becoming increasingly apparent.

Despite this structural information, the role of tegumental gland secretions is far from clear. Based upon their presence in the mouthparts and oesophagus of decapods (Yonge, 1932; Barker and Gibson, 1977, 1978), isopods (Gorvett, 1946), copepods (Boxshall, 1982), amphipods (Shyamasundari and Hanumantha Rao, 1977, Eloffsson *et al.*, 1978) and cirripedes (Rainbow and Walker, 1977), it was assumed they had a salivary function, their secretions contributing in some way to the initial breakdown of food. However, Yonge (1932) and Gorvett (1946) both discounted this idea believing they had a role in cuticle formation. The only biochemical evidence for their digestive role was provided by Tyagi and Kaushik (1970) who detected the enzymes: maltase, lactase, salicinase, amylase, invertase and glycogenase in the mandibular secretions of *Potamon martensi*, but no methodolgy or quantitative data were given.

Histochemical analyses revealed gland cells in the mouthparts of various crustaceans contained acid and neutral mucopolysaccharides (Stevenson and Murphy, 1967; Shyamasundari and Hanumantha Rao, 1977, 1978; Kumari *et al.*, 1983). Mucopolysaccharides are glycoprotein complexes consisting of hexosamine sugars covalently bound to varying amounts of protein (Cook, 1972). Neutral mucins carry no free group, whereas acid mucins are associated with glucuronic, hyaluronic, iduronic and sialic acids. The prefix muco- was chosen to denote the relationship of this substance with mucus, the physiological term for a viscous secretion (Brimacombe and Webber,

1964). Hence, they concluded tegumental glands play an important role in lubrication and food entanglement during ingestion.

The only comprehensive histochemical examination of gland secretions in the paragnaths is that of McKenzie and Alexander (1989) on *P. merguiensis*. Based on their staining characteristics seven gland types were described, the secretions of which were differentiated into acidic sulphated and carboxylated mucopolysaccharides (denoting the active group). Based on physical and chemical properties, McKenzie and Alexander (1989) concluded the paragnaths have a role in lubricating large particles and entangling particulate matter.

Despite the obvious importance of paragnaths within the preoral cavity, their role in the ingestion mechanism of crustaceans is poorly known. Borradaile (1917) commented that their role was a passive one, whereas Cannon and Manton (1927) suggested they aid in pushing food toward the mouth in the mysid *Hemimysis lamornae* Couch. Fryer (1977), on the other hand, proposed a role in the retention of food in the mouth region of Atyid prawns. In contrast, Felgenhauer and Abele (1985) assigned the assymetrical paragnaths of *Atya innocous* (Herbst) a minor role in particle collection. It is evident from these conflicting viewpoints that interpretations of paragnathal (and other mouthparts) movements from their morphology and musculature, are at best, difficult.

Using photomicroscopic equipment, Alexander and Hindley (1975) and Hunt *et al.* (1992) reported that the paragnaths of *P. merguiensis* open laterally to allow food to enter the mouth and close to prevent food loss from the oral cavity. Statistical analysis revealed a highly significant correlation between paragnathal opening and the movements of the labrum and first maxillae, the appendage principally involved in directing particulate food toward the mouth.

3.1.4 The Metastome - Possession of a Posterior Membranous Lobe

All crustaceans possess a metastome which is supported on a metastomal sclerite located between the first maxillae (Snodgrass, 1951). It consists of either a single lobe, a pair of lobes (paragnaths) or three lobes (lingua, paragnaths or superlinguae). Hence, the paragnaths have often been referred to as the metastome (metastoma) by a number of authors including Yonge (1924) and Erri Babu *et al.* (1979). Snodgrass (1951) notes

that the labrum is supported by the posterior margin of the epistome, a preoral segment, and is not considered part of the metastome.

Although the paired lobes or paragnaths have been reported in a number of crustaceans (Boxshall, 1985: Felgenhauer and Abele, 1985; Alexander, 1988, 1989; Hunt *et al.*, 1992), an additional lobe (lingua) has not been found in any decapod. Suthers and Anderson (1981) reported a muscular protuberance arising midventrally between the second maxillipeds which projected forwards below the mandibles of the scyllarid *I. peronii*. They referred to this structure as the metastome but excluded the paragnaths from this terminology. They did not describe either its structure or role in the preoral cavity, stating only that it is drawn back during ingestion. Another brief mention of a metastome was made by McKenzie and Alexander (1989) in the prawn *P. merguiensis*. They illustrated the metastome as a small structure at the base of the paragnaths and reported the presence of tegumental glands that contained acidic sulphated mucopolysaccharides. They did not detail its structure, or its relationship with other mouthparts in the preoral cavity.

Status of Knowledge on Scyllarids and Objectives

Ingestion and mouthpart functional morphology is little known in scyllarids. Mouthpart structure and function was outlined by Suthers and Anderson (1981) for *I. peronii*. However, only light microscopy was used and observations of ingestion were based on only one food type. They acknowledged that other ingestion modes may be adopted for other food types and sizes and suggested further studies were needed to confirm this. Detailed analysis of setal types were not performed.

The major objective of the present study was to investigate the process of food ingestion in *T. orientalis*. This involved determination of the role of each mouthpart by documentation of ingestion sequences and detailed descriptions of mouthpart structure. Ingestion sequences were examined using microscope and endoscope video analysis. A range of food types were offered at various sizes to determine whether different ingestion modes (mouthpart sequences) were adopted. The rate of food ingestion was measured to assess the ingestive efficiency of *T. orientalis*. Correlations between the role of mouthparts were analysed statistically to determine whether any functional relationships exist. Structural characteristics of the mouthparts, including the types and

distribution of setae, were described using dissections and scanning electron microscopy.

The morphology and internal structure of the paragnaths of *T. orientalis* were described with emphasis on the tegumental rosette glands and the nature of their secretions. Combined with their action during ingestion, the role of the paragnaths in the preoral cavity was determined.

A large and conspicuous membranous lobe lies posterior to the mandibles and paragnaths of *T. orientalis*. Other scyllarid genera: *Scyllarides, Scyllarus, Parribacus, Evibacus* and *Ibacus* were also examined to determine whether its presence and position are consistent throughout the Scyllaridae. This study clarifies whether it is a part of the metastome, as defined by Snodgrass (1951). Its morphology and internal structure are detailed and its role is discussed.

3.2 MATERIALS AND METHODS

3.2.1 Mouthpart Structure

3.2.1.1 Dissection

Mouthparts were removed and fixed in 10% seawater formalin or formal calcium acetate (4% formaldehyde, 2% calcium acetate) and their gross morphology examined using a stereo microscope. Accurate illustrations of individual mouthparts and their *in situ* positions were made with the aid of a camera lucida.

The position of the membranous lobe and its relationship with the sternal skeleton was examined by dissection. The cephalothorax was digested in 10% NaOH for 24 h to remove adhering musculature from the mouthparts and gnathal segments. The position of the lobe and its relationship with the sternal skeleton were photographed and drawn.

3.2.1.2 Scanning Electron Microscopy

Freshly dissected mouthparts were fixed in 10% seawater formalin for 24 h, washed in distilled water and sonicated for 4 x 30 s bursts. A method of cleaning derived from Felgenhauer (1987) and Alexander (1988) was applied to the paragnaths and membranous lobe as their surfaces were consistently obscured by mucus and particulate matter. They were fixed for 4 h in 2.5% glutaraldehyde in filtered seawater, post-fixed in 2.5% osmium tetroxide for 4 h at 20°C (to ensure minimal shrinkage of soft structures) and then transferred to a freshly prepared saturated solution (2%) of thiocarbohydrazide, an osmium binding agent, for 45 min. This was removed by numerous of washes in distilled water over a period of 1 h. Particulate matter was removed by agitating the specimens on a rotator in a 5% solution of anionic surfactant (Decon 90) for 2 h and further cleaned by 5 x 40 s bursts in an ultrasonicator. Several washes in distilled water preceeded mucus removal, which was achieved by placing the specimen in 40% glycerol on a rotator for 20 h. The glycerol was removed by rotating in at least 5 changes of 40% ethanol for 6 h. Despite this, only in recently moulted specimens was the surface totally free from contamination.

All mouthparts were then dehydrated to 100% ethanol, critical point dried, mounted on stubs, gold coated in a Hummer V sputter coater and examined on a Philips XL 20 scanning electron microscope at 10 kV.

Table 3.1. Histochemical tests for the identification of carbohydrates, proteins and glycoprotein in the membranous lobe, paragnaths and labrum of *T. orientalis*. PAS, periodic acid Schiff. Puchtler *et al.* (1962) cited in Bancroft and Stevens (1982).

Stain	To Demonstrate	Control	Reference
diastase-PAS	glycogen	*Bufo marinus* liver	Cook (1974)
PAS-alcian blue (pH 2.5)	acid/neutral/mixed mucopolysaccharides	cat pyloro-duodenal junction	Cook (1974)
aldehyde fuchsin-alcian blue (pH 2.5)	sulphated/carboxylated mucopolysaccharides	guinea pig trachea, cat stomach, *Bufo marinus* liver	Cook (1974)
alcian blue (pH 0.2)	strongly/weakly sulphated mucopolysaccharides	as above	Winsor (1984)
mercuric bromophenol blue	general protein (NH_2 groups)	*Bipalium kewensi*	Winsor (1984)
buffered azure A	protein basiphilia	-	Lillie & Fullmer (1976)
biebrich scarlet	protein acidophilia	-	Lillie & Fullmer (1976)
alkaline Congo red	glycoprotein	human tissue containing amyloid	Puchtler *et al.* (1962)

3.2.1.3 Histology

The paragnaths, membranous lobe and labrum were removed from cooled specimens, that had been placed on ice for up to 20 min, and fixed in marine Bouin's fluid (3.7% formaldehyde; 5% acetic acid; 1.6% picric acid) (Winsor, 1984) for at least 48 h. They were then washed in several changes of 70% ethanol to remove excess picric acid. This fixative proved the best of those tested: formal calcium acetate (4% formaldehyde, 2% calcium acetate) (FCA), formal acetic acid calcium chloride (4% formalin, 1.3% calcium chloride, 5% acetic acid) (FAACC), 10% seawater formalin and Heidenhain Susa (Winsor, 1984). Marine Bouin's fluid contains a decalcifying agent, picric acid, which is essential when sectioning calcified material, whereas other fixatives require an additional decalcification step. Lipid specific histochemical tests such as Bromine Sudan Black (Winsor, 1984) can also be applied as marine Bouin's fluid is lipid soluble whereas most others are lipid insoluble (aqueous).

Specimens were processed automatically overnight (see Appendix 1) and embedded in paraffin wax in the correct orientation for sectioning. Sections (6 μm) were cut from wax blocks, mounted on slides and transferred to an oven at 60°C, overnight. They were then dewaxed and stained with haematoxylin-eosin and Mallory-Heidenhain (see Appendix 1). Specimens with a hard cuticle were chilled with ice for approximately 30 min before sectioning to minimise section tearing.

3.2.1.4 Histochemistry

The presence of carbohydrate, protein and glycoprotein in tissues was determined using the histochemical tests outlined in Table 3.1. All specimens were fixed in marine Bouin's fluid, except those tested for glycogen which were fixed in Gendre's fluid (Cook, 1974).

3.2.2 Correlation of tegumental gland mucus production to feeding

To determine whether tegumental gland mucus is produced continuously or only during ingestion, the paragnaths were dissected from specimens at specific times after feeding: 1 h, 6 h, 12 h and 24 h. They were fixed and processed as outlined in Ch 3.2.1.3 and stained with periodic acid Schiff (PAS)-alcian blue (Cook, 1974) to test for mucin in the secretory cells.

3.2.3 Transmission Electron Microscopy

For cytological examination of spherical cells and tegumental glands, 1 mm pieces of the membranous lobe and paragnaths were fixed for 2 h at 20°C in 4% glutaraldehyde in millipore filtered seawater (MFSW) pH 7.1. Following fixation, they were washed in 0.1 M cacodylate buffer in MFSW pH 7.1 and post-fixed in 1% osmium tetroxide in 0.1 M cacodylate buffer in MFSW pH 7.1 for 1 h at 20°C. These fixation periods were necessary as the cuticle impeded infiltration. Following a wash in cacodylate buffer they were dehydrated in graded ethanols and embedded in resin (Spurr, 1969). Optical sections (1.5 μm) were cut on an LKB Nova Ultramicrotome and stained with filtered 1% toluidine blue in 2% borax. Sections (60 nm - silver) were mounted on hexagonal 200 copper grids and stained with acidified, saturated uranyl acetate in 50% ethanol for 7 min followed by 1 min in lead citrate (Reynold, 1963). Grids were washed in distilled water and dried prior to examination on a JEOL 2000 fx transmission electron microscope at 80 kV.

3.2.4 Ingestion Mechanisms

Mouthpart movements of 15 individuals were observed and recorded using a Zeiss Tessovar microscope fitted with a JVC TK-870E colour video camera and a National 6010 time lapse recorder. The microscope was positioned above live specimens which were restrained ventral side up against a metal plate and immersed at an angle of approximately 30° from vertical in a small sea water tank (Fig. 3.1). Pereiopods were tied to prevent them obscuring the mouthparts. Ingestion sequences were initiated by stimulating either the antennules, antennae or pereiopod dactyls with scallop extract and then placing a piece of scallop on the dactylus and propus of the third maxillipeds. Mouthpart movements were analysed using slow speed playback of the video recordings. Illustrations of the relative positions of mouthparts during these sequences were prepared from high speed photography. To ensure that restriction of the specimen did not affect mouthpart movements, observations of unrestrained animals were made. This involved placing the specimen in a small glass tank and filming ingestion from beneath. No obvious differences in mouthpart movements from those of restrained animals were observed.

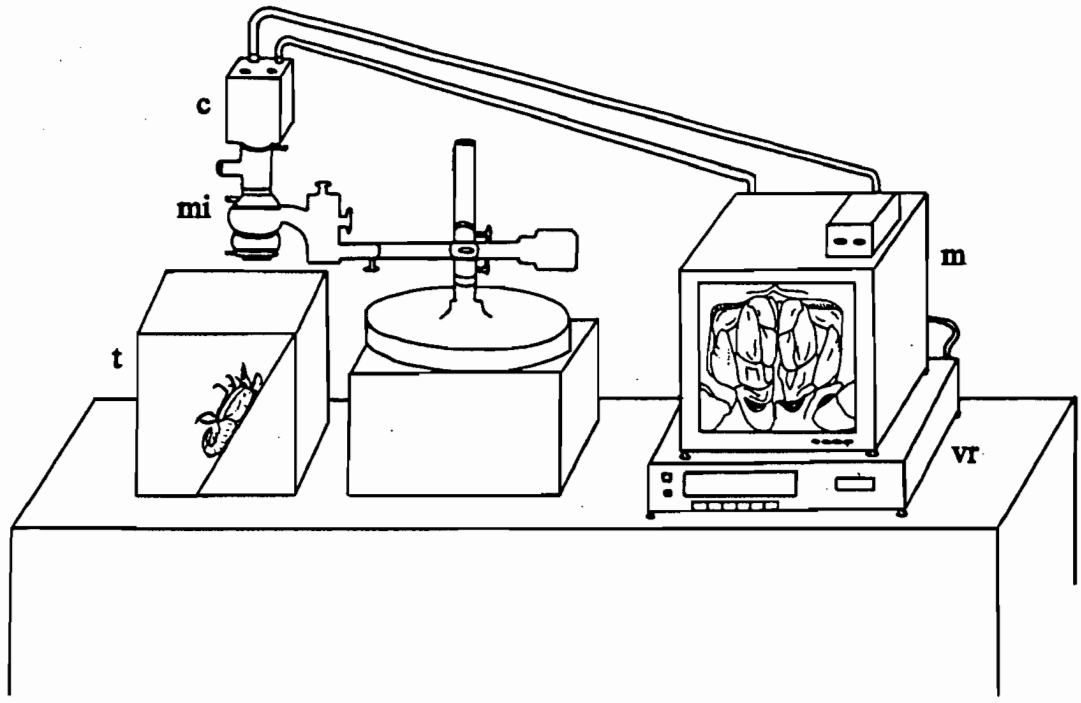

Figure 3.1. Apparatus used to examine the movements of mouthparts *in situ*. The Volpi 6000 fibre optics unit used to illuminate the mouthparts is not illustrated. For endoscopic filming of mouthparts, the microscope was replaced with the Volpi endoscope.
c, video camera; m, television monitor; mi, microscope; t, seawater tank; vr, video recorder

A range of foods commonly consumed by scyllarids (Suthers and Anderson, 1981; Lau, 1988; Jones, 1988) were offered at various sizes (2 mm^3 - 30 mm^3) to determine whether different sequences of mouthpart movements were adopted.

The opening and closing times of each mouthpart, the number of beats (one opening and closing event) performed and the rate of ingestion for a given food size were determined during 27 ingestion sequences by single frame advancement of the video recording. Results were analysed using Spearman rank correlations, to identify the correlations between mouthpart movements. Partial correlations were also made to determine whether the significant Spearman rank correlations evident were influenced by movements of other mouthparts. Correlation of mouthparts with the paragnaths and labrum could not be determined as they are frequently obscured during ingestion. Likewise, ingestion correlations could not be determined for large hard food items as the third maxillipeds obscured the other mouthparts. The number of beats of the third maxillipeds with ingestion of small soft and large hard items was analysed using a Mann-Whitney U test to verify functional differentiation and hence, the existence of two

ingestion modes. The relationship between mouthpart movements and their opening and closing times was graphically represented for each ingestion mode.

An endoscope was used to observe the actions of the membranous lobe, paragnaths and labrum, as these were often obscured during ingestion. Specimens were restained as described and positioned in the tank at an angle of approximately 45° from vertical. A Volpi 2,5/190 endoscope (external diameter 2 mm), attached to a JVC TK-870E colour video camera was inserted between the third and second maxillipeds allowing a clear view of the paragnaths, membranous lobe and labrum.

3.3 RESULTS

3.3.1 Mouthpart Structure

Position in Situ

At rest, the third maxilliped endopods are completely opposed, flexed at the merus-carpus articulation, with the dactylus resting on the inner edge of the ischium and the exopod lying flat against the carapace (Fig. 3.2A; see also 3.21A). The inner margins of the second maxillipeds and first maxillae form the walls of the pre-oral cavity and the membranous lobe forms the dorsal roof (Fig. 3.2A,B). The first maxilliped is located to the side of the second with its epipod in the branchial chamber and its exopod distal tip extends behind the second maxilliped exopod. The scaphognathite of the second maxilla is located to the side of the first maxilliped in the branchial chamber (Fig. 3.2A,B).

The opening to the oesophagus is bounded by the mandibles ventrally, the membranous lobe posterially and the labrum anteriorly; the lower part of the labrum lying between the incisor processes (Fig. 3.2B). The first maxillae lie to the side of the membranous lobe anterior lip, with the endites lying across the proximal half of the paragnaths. The paragnaths extend outwards along the lower aboral margins of the mandibular gnathobase (Fig. 3.2B).

Description of Setal Types

Setal classification is based on that of Thomas (1970) and Factor (1978). Setae not included by these authors were classified according to their external morphology, particularly the nature and distribution of setules/denticules and shaft characteristics. The term "comb" seta was taken from Kunze and Anderson (1979). While noting the setal characteristics outlined by Jacques (1989), his analytical notation system was not used as descriptive terms are more useful when relating setal structure to function.

To minimise confusion created by the range of classification systems published (refer Ch. 3.1.2), it is necessary to define the setal terminology used in this study. This is based on Pohle and Telford (1981) and Watling (1989) who recognise three types of cuticular outgrowths (Fig. 3.3A). All articulated cuticular extensions varying in size from very small (10-20 μm) to very large (> 1 mm) are setae. Non-articulated cuticular extensions with a base generally not as wide as thestructure is long, regardless of its size and shape, are spines. All non-articulated cuticular extensions of which the base is

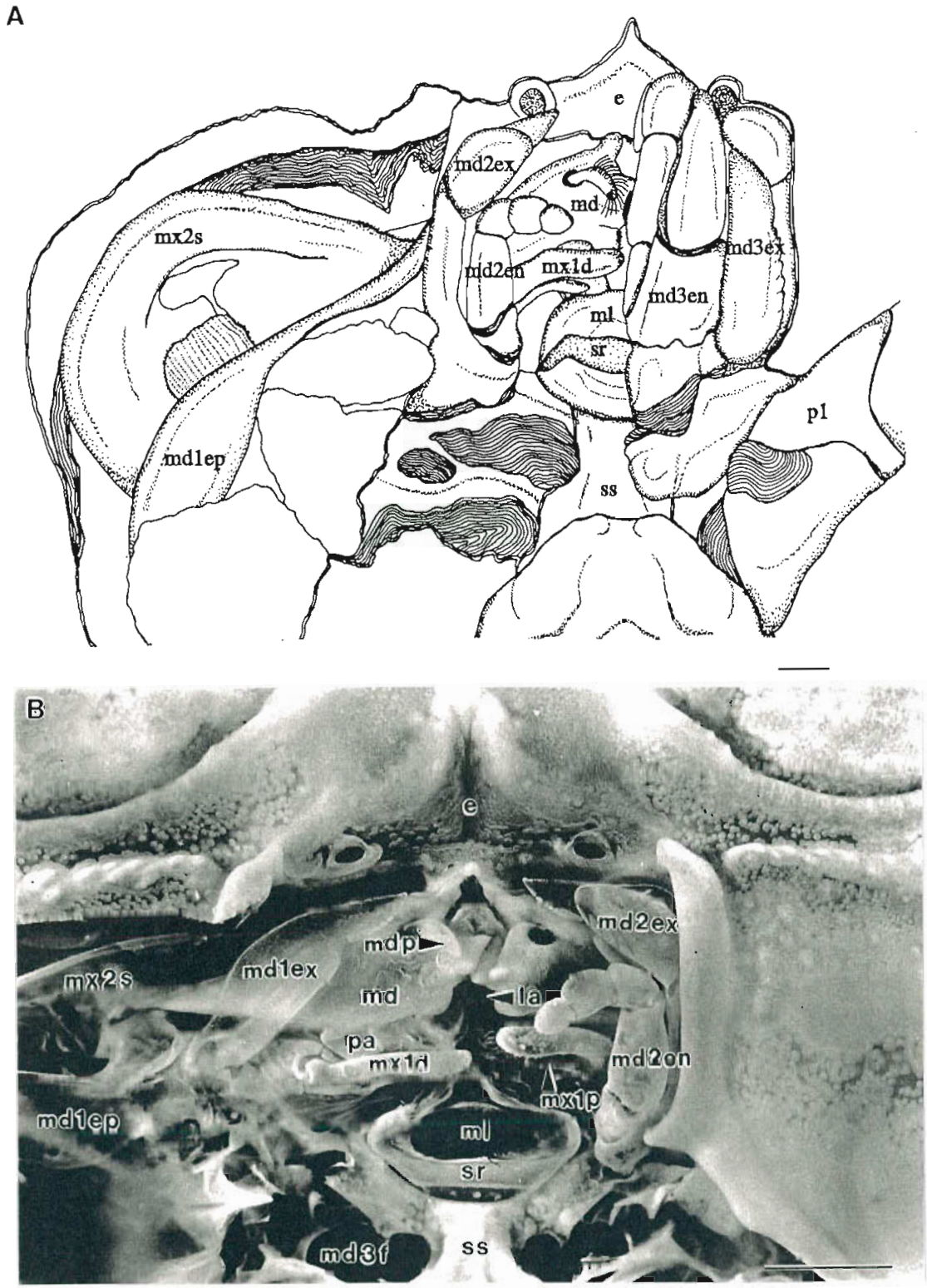

Figure 3.2. *In situ* positions of mouthparts in the oral cavity of *T. orientalis*, ventral view. **A.** The left third maxilliped and left side of the carapace have been removed to reveal the anterior mouthparts and those in the branchial chamber. Scale, 2 mm. **B.** Both the third maxillipeds and left second maxilliped have been removed to clearly reveal the position of the membranous lobe and its relation to the sternal skeleton. Scale, 4 mm. Note, the distal and proximal endite of the second maxilla are not visible.
e, epistome; la, labrum; md, mandible; mdp, mandibular palp; md1ep, first maxilliped epipod; md1ex; first maxilliped exopod; md2en, second maxilliped endopod, md2ex second maxilliped exopod; md3en, third maxilliped endopod; md3ex, third maxilliped exopod; md3f, foramen of third maxilliped; ml, membranous lobe; mx1d, first maxilla distal endite; mx2s, second maxilla scaphognathite; pa, paragnath; p1, first pereiopod; ss, sternal skeleton; sr, strengthening rod.

generally very wide relative to its length, are scales. The term sensilla, as defined by Derby (1982) to be setae with a known sensory function, will be avoided as physiological evidence for this role is not provided in this study.

Remaining terminology deals with the basic morphology of a seta and is illustrated in Fig. 3.3B. The shaft is the region of a seta between the base and tip. It may possess an annulus, a faint ring circumscribing the shaft which may be located near the base or along the shaft. Outgrowths are divided into two categories, setules and denticules. The former is an extension of the shaft, usually of uniform width from base to tip and forming an articulated or flexible junction with the shaft. In contrast, denticules are all non-atriculated extensions of the shaft.

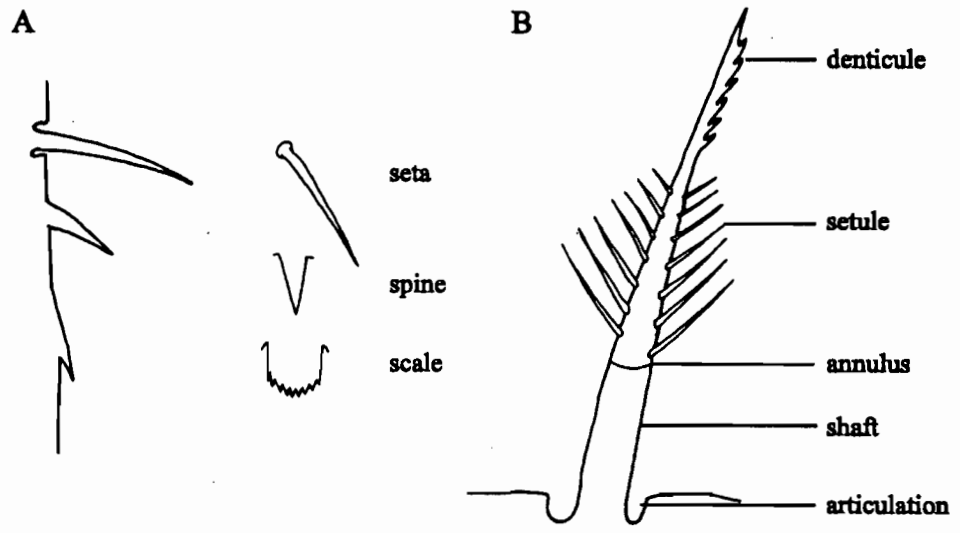

Figure 3.3. A. Diagrammatic representation of a seta, spine and scale, in side view on left and top view on right. **B.** Diagrammatic representation of a typical seta illustrating associated terminology. (Modified from Watling, 1989).

Setae are arranged into broad categories, most of which contain some variations. In many categories, the variation is sufficient to warrent subdivision into several types, each designated alphanumerically. Fig. 3.4 illustrates the types of setae identified on the mouthparts of *T. orientalis*.

Type A. SIMPLE. Setal shaft is smooth with setules/denticules absent.

A1. Stout - The shaft is broad with an obvious annulus and a rounded apex.

A2. Tapering (Acuminate after Thomas, 1979) - The shaft tapers markedly from a basal annulus to lie almost horizontal with the mouthpart surface. The apex is fine and pointed.

A3. Elongate - The setal shaft is thin and elongate, tapering distally to a fine pointed apex.

A4. Hamate (conate after Thomas, 1970) - These are small short setae with bulbous bases and pointed apices. They are often hook-shaped.

Type B. PLUMOSE. The elongate shaft arises from a supracuticular socket and bears two diametrically opposed rows of fine setules along its length. Adjacent plumose setae have overlapping setules which form a mesh between the shafts.

Type C. PAPPOSE. The shaft is elongate and tapered, bearing numerous radially arranged fine setules, most of which are directed distally. Setules are extemely long and densely arranged to obscure the shaft. They often intertwine giving a matted appearance.

Type D. MICROSCALES. Extremely small scales (approximately 5-8 μm in length) which arise directly from the appendage surface in varying densities and arrangements. The shaft is broad and tapered to a pointed apex. They may be clustered in groups of up to 12 scales.

Type E. MICROSPINES. Extremely small spines (approximately 8 μm) arising directly from the appendage surface in varying densities and arrangements. The shaft is narrow and tapered.

Type F. ANNULATE. Setal shaft has a number of closely arranged annulations along its length excluding the distal third which is smooth. The shaft tapers to a pointed apex and its length varies between 100-180 μm.

F1. Simple - Shaft is devoid of denticules.

F2. Cuspidate - A small number of randomly arranged cuneate denticules arise from one side of the proximal half of the shaft. They are directed distally and usually lie flat against the shaft surface, although they are often extended.

F3. Whorled - Elongate tapered denticules arise at an angle of 45° from the proximal

half of the shaft and are arranged in a whorl-like formation.

Type G. MULTIDENTICULATE. Setal shaft bears numerous denticules in various shapes and arrangements.

G1. Toothed - Elongate shaft bears radially arranged denticules along its distal half, increasing in density toward the apex. All denticules are distally directed at an angle of 20° to the shaft. They are narrow with their upper margin forming a number of serrations which taper to a pointed tooth-like apex.

G2. Cuneate - Elongate shaft bears cuneate denticules, with broad bases and tapered apices, in radially arranged longitudinal rows. Their angle to the shaft varies between 15° and 30°, lying flat against the shaft basally and distally.

G3. Digitate - (setobranchs after Thomas, 1979). Extremely elongate seta, up to 4 mm in length, with denticules on the distal third of its shaft. The shaft apex is curled; its underside devoid of denticules. Denticules have a narrow base which widens laterally; their upper margin rounded as a series of teeth. Their angle to the shaft varies between 30-45°.

G4. Spinose - The shaft is broad with rigid, radially arranged denticules arising from its middle third. Denticules have broad bases and pointed apices and are directed distally at approximately 45° to the shaft.

G5. Whorled - Setal shaft is short (150 μm long) and broad with denticules arranged in a whorl-like formation along its length; this formation being particularly obvious basally. Here the denticules are short and broad, directed at 90° to the shaft, whereas those in the distal two-thirds are more elongate and tapered, arising at an angle of 45° to the shaft.

G6. Pappose - Shaft is elongate and tapered with numerous radially arranged fine denticules along its length. Similar to C., except the denticules (instead of setules) are broader basally.

G7. Serrate - The setal shaft is broad with two rows of large cuneate denticules along its distal half, forming an angle of less than 180° with one another. Denticule size increases towards the apex; their tips becoming hook-like and directed distally. At the apex the two rows merge inwards on the upper shaft surface. Above each row of denticules is a row of smaller cuneate denticules which lie flat against the shaft and increase in number distally.

G8. Comb. The shaft is narrower than serrate with denticules in two rows along its distal half, separated from one another by a small ridge. Denticules arise from a narrow base

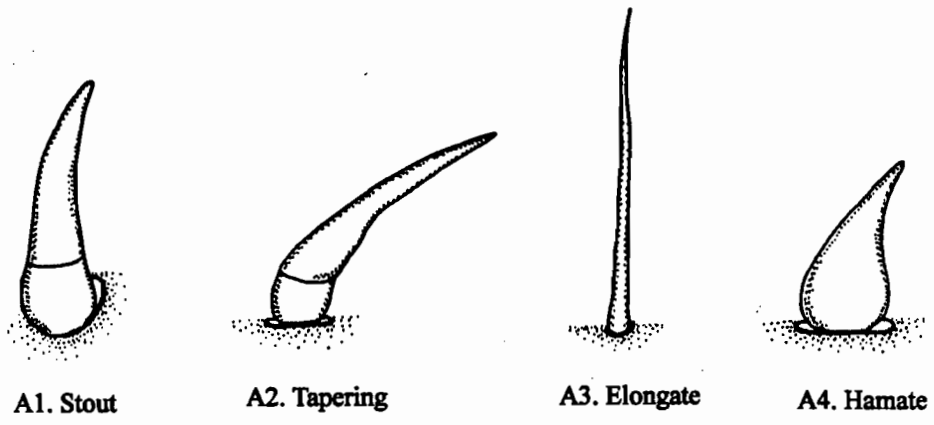

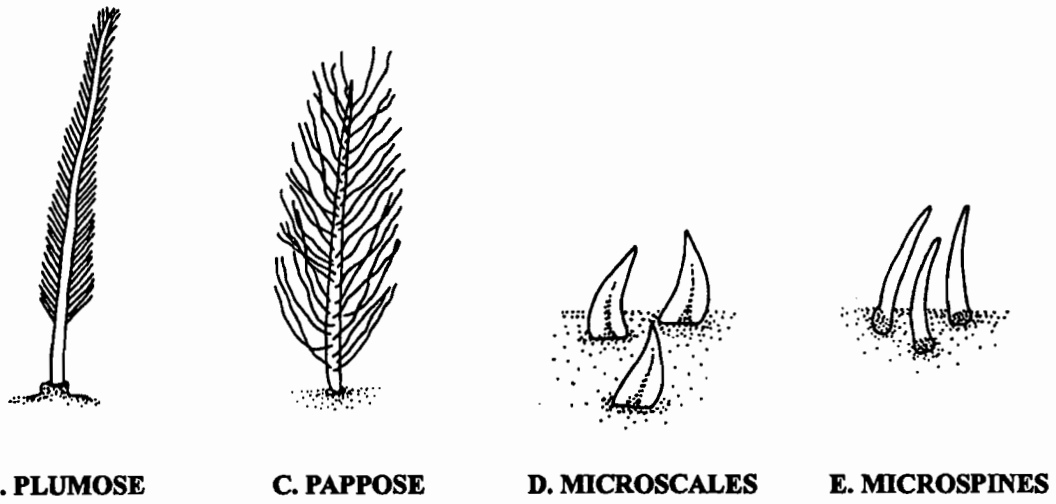

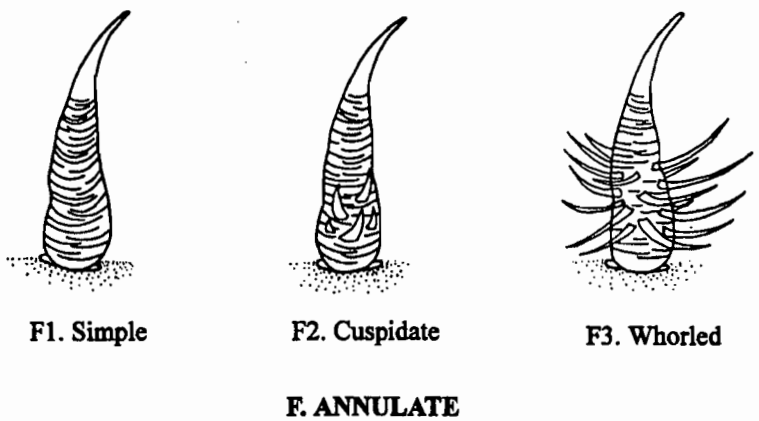

Figure 3.4. Diagrammatic representation of the types of setae, scales and spines on the mouthparts of *T. orientalis*. Illustrations are not to scale to allow visualisation of detail.

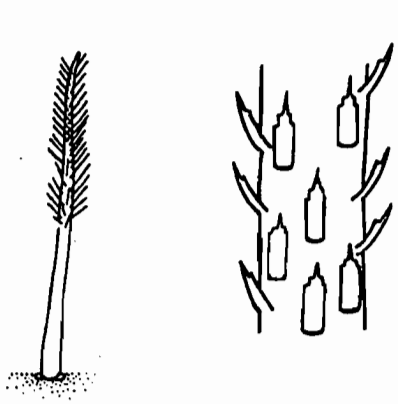

G1. Toothed

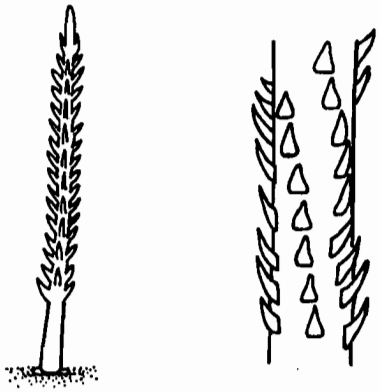

G2. Cuneate

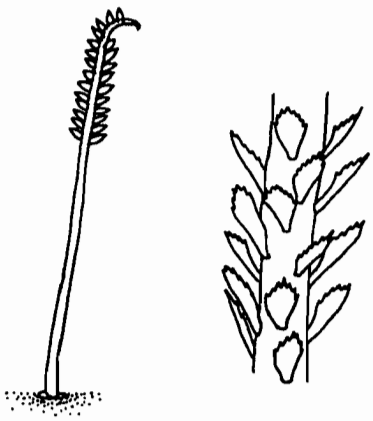

G3. Digitate

G4. Spinose

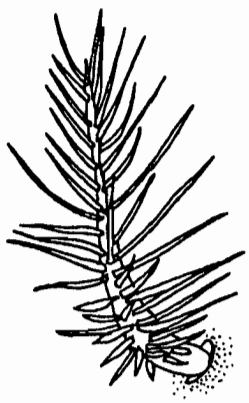

G5. Whorled

G6. Pappose

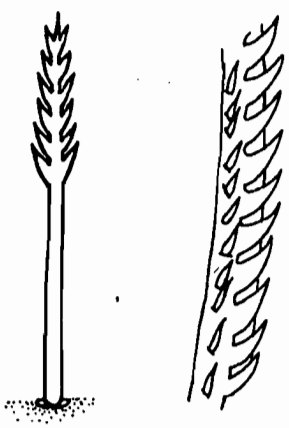

G7. Serrate

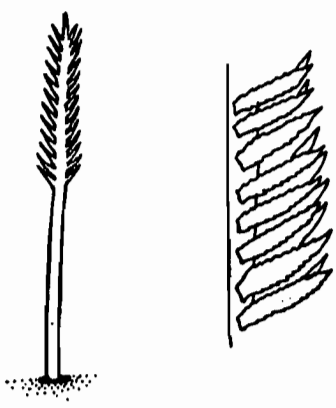

G8. Comb

G. MULTIDENTICULATE

Fig. 3.4. Continued.

and are tapered with serrated margins. They are densely arranged, each articulating at 90° to the shaft giving it a comb-like appearance.

Third Maxillipeds

The third maxillipeds are the largest and outermost pair of mouthparts; composed of a five-segmented endopod and a broad dorso-ventrally flattened exopod (Fig. 3.5A; 3.6A). The aboral surface of the broad coxa has a calcified protuberance (Fig. 3.5A) and pappose setae extend along its upper oral surface (Fig. 3.6B). The ischium has three lateral margins, the innermost with small blunt calcified teeth, otherwise known as crista dentata, which increase in size distally (Fig. 3.5A; 3.6A,C). A row of simple elongate setae, varying in length between 700 and 1200 μm extend along the inner margin of the merus (Fig. 3.5A,B) with multidenticulate spinose setae (300 μm long) interspersed between them on their aboral side (Fig. 3.5C,D).

Densely arranged multidenticulate comb setae cover the oral surface of the carpus (Fig. 3.6D,E) and projects distally over the carpus-propus articulation. Three types of similarly directed setae: simple stout, simple elongate and multidenticulate serrate line the upper, middle and lower oral surfaces, of the propus (Fig. 3.6F,G). Multidenticulate serrate setae are densely arranged and extend over the lower margin to intermesh with the simple elongate setae of the merus during ingestion. Simple stout setae also cover the distal margin of the aboral surface and the entire oral surface of the dactylus (Fig. 3.5A; 3.6H,I). These setae increase in size distally, and are particulary large at the apex. Here they appear hook-like and have an angle of articulation at more than 40°.

The aboral surface of the exopod is covered in a dense matt of multidenticulate whorled setae which decrease in density distally (Fig. 3.5E,F). The outer margin has a number of blunt protuberances, in between which are tufts of multidenticulate pappose setae (Fig. 3.5F). These protuberances become smaller and more pointed distally. Dense clusters of microscales and microspines cover the aboral surface as well as that of the basis, ischium and merus.

Second Maxillipeds

The second maxillipeds are less calcified than the third; the endopod smaller and the exopod more elongate and membranous (Fig. 3.7A,B). The coxa and basis are fused

Figure 3.5. A. Third maxilliped, right side, aboral view. Scale, 1.5 mm. Scanning electron micrographs (SEM): **B.** Simple elongate setae along the inner edge of the merus. Scale, 250 μm. **C.** Simple elongate setae interspersed with multidenticulate spinose setae along the inner aboral margin of the merus. Scale, 250 μm. **D.** Multidenticulate spinose setae. Scale, 50 μm. **E.** Multidenticulate whorled setae on the aboral surface of the exopod. Scale, 50 μm. **F.** Multidenticulate whorled and pappose setae on the outer aboral margin of the exopod. Note, the blunt protuberance. Scale, 200 μm.
b, basis; bp, blunt protuberance; c, carpus; cd, crista dentata; co, coxopodite; cp, calcified protuberance; d, dactylus; ex, exopod; i, ischium; m, merus; mps, multidenticulate pappose setae; msp; multidenticulate spinose setae; mws multidenticulate whorled setae; p, propus.

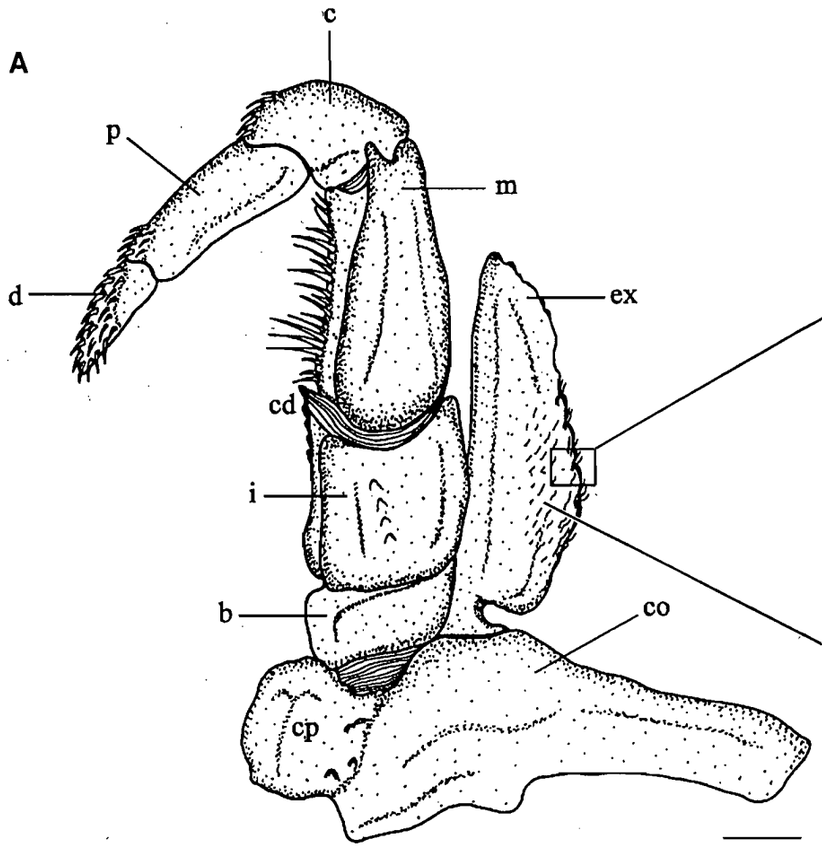
A
c
p
m
d
ex
cd
i
b
co
cp

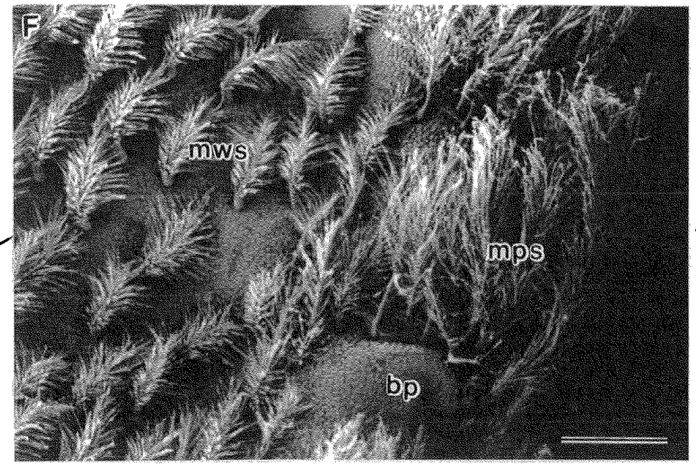
F
mws
mps
bp

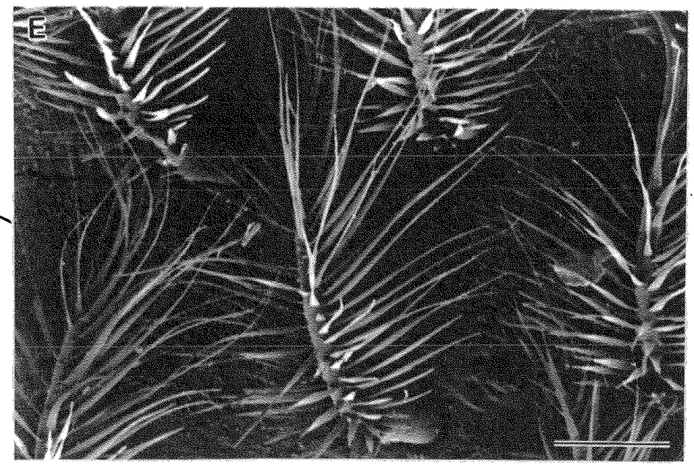
E

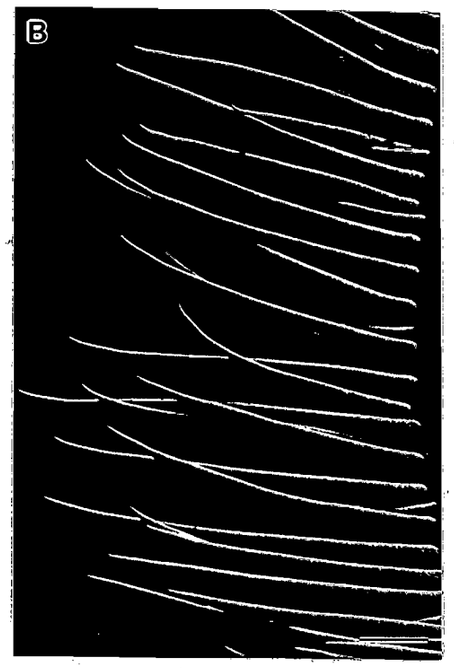
B

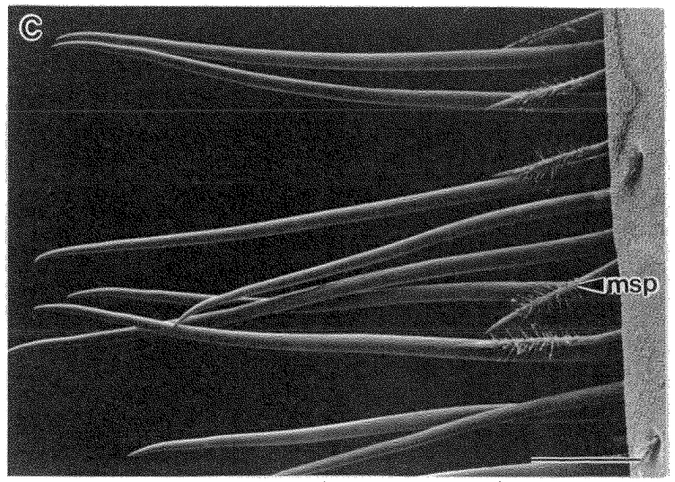
C
msp

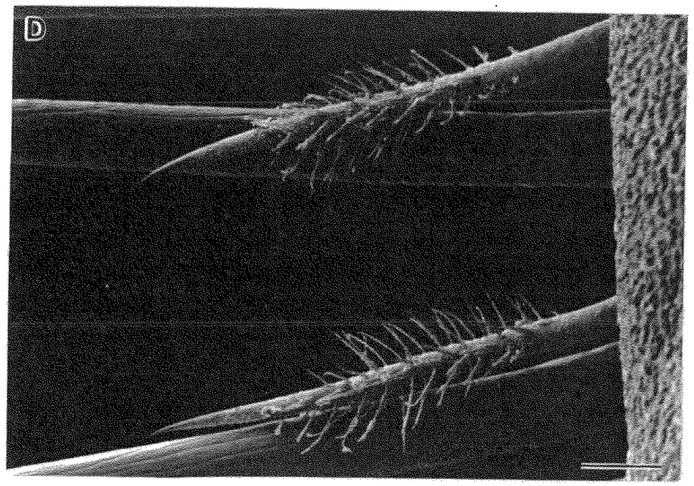
D

Figure 3.6. A. Third maxilliped, right side, oral view. Scale, 1.4 mm. SEM: **B.** Pappose setae. Scale, 100 μm. **C.** Small blunt crista dentata on the distal inner margin of the ischium. Scale, 500 μm. **D.** Multidenticulate comb setae on the carpus. Scale, 50 μm. **E.** Fine structure of multidenticulate comb setae. Scale, 20 μm. **F.** Arrangement of simple stout, simple elongate and multidenticulate serrate setae on the propus. Scale, 250 μm. **G.** Fine structure of multidenticulate serrate setae. Note, the small cuneate denticules along the setal ridge. Scale, 50 μm. **H.** Simple stout setae on the dactylus. Note, their hook-like appearance at the tip. Scale, 500 μm. **I.** Simple stout setae. Scale, 100 μm.
cd, crista dentata; ses, simple elongate setae, sss, simple stout setae; mse, multidenticulate serrate setae.

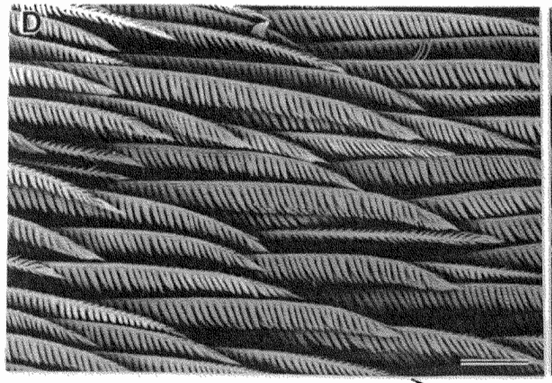
D

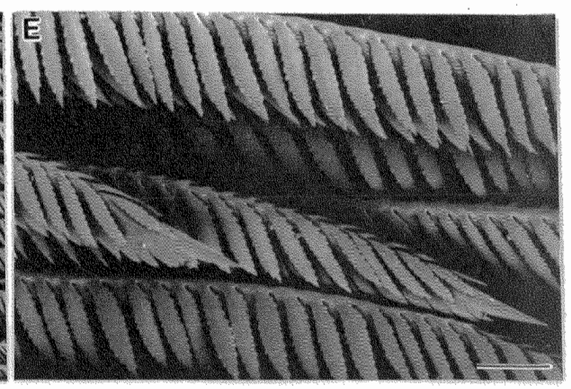
E

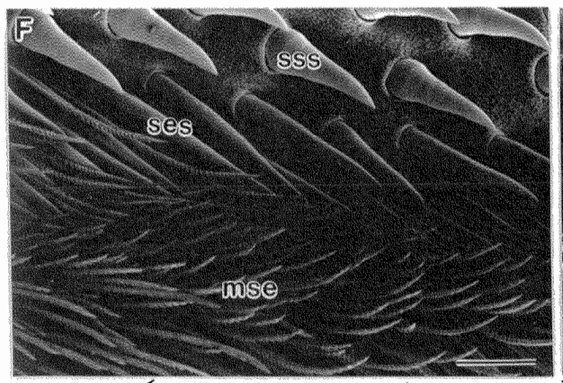
F
sss
ses
mse

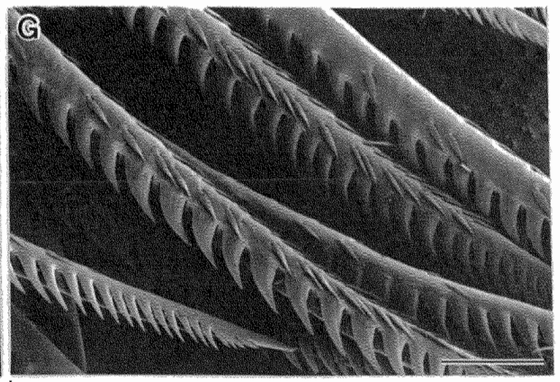
G

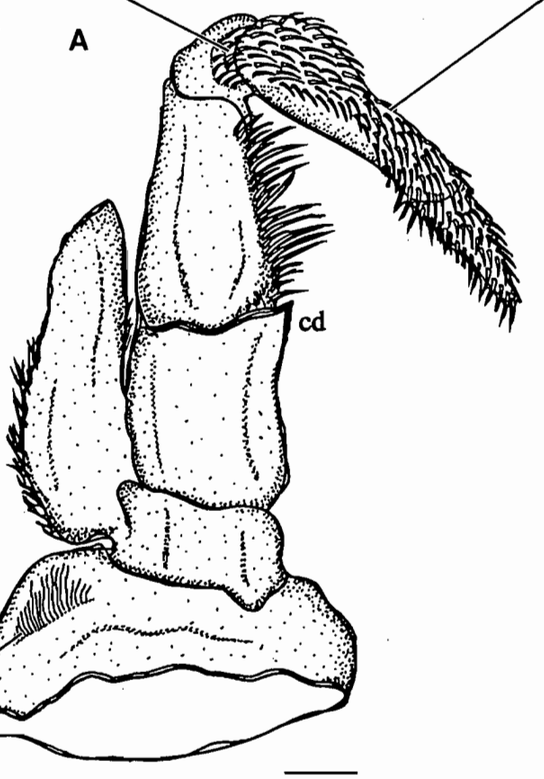
A
cd

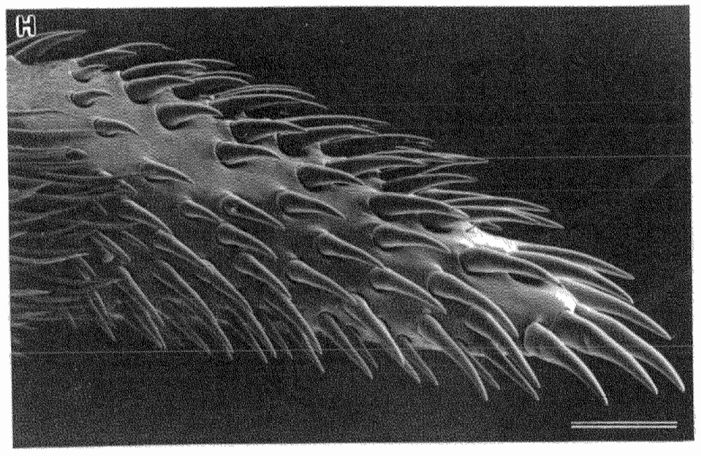
H

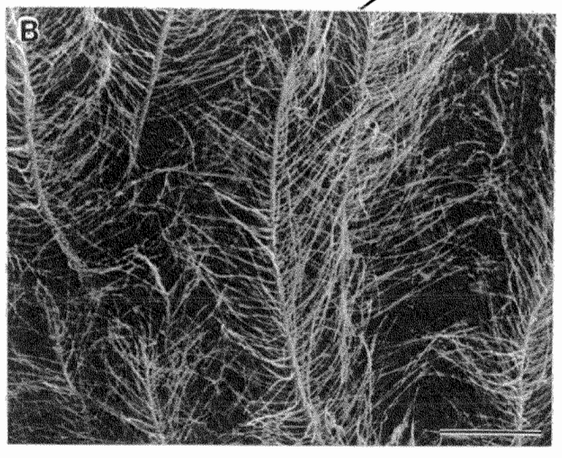
B

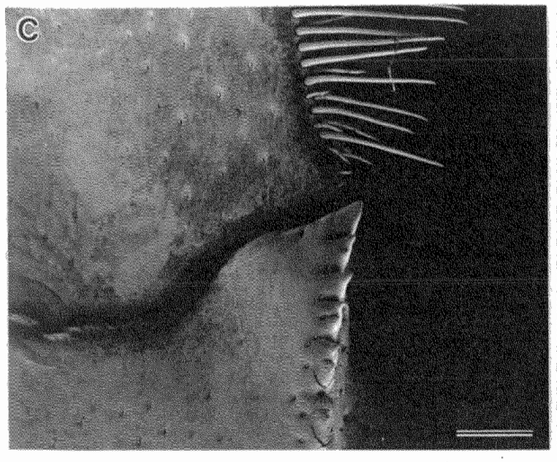
C

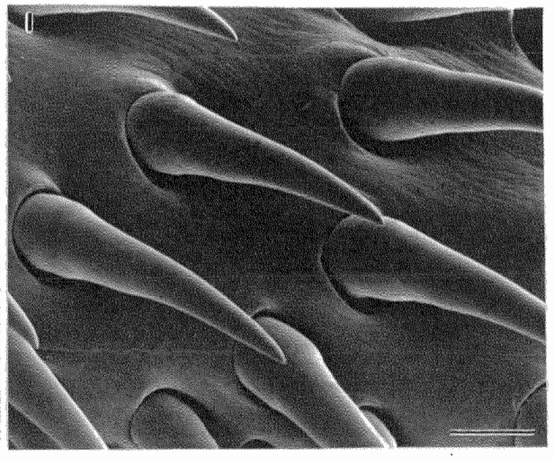
I

with a dense band of pappose setae extending along the outer oral and aboral surfaces. The ischium is reduced in size with a tuft of simple elongate setae on the distal medial margin which continues along the medial margin of the merus (Fig. 3.7A,B). Shorter more robust simple setae project medially from the distal upper margins of the propus and carpus (Fig. 3.7A,B,C). A number of small simple stout setae are distributed on the aboral surface of the carpus, propus and dactylus (Fig. 3.7D). The dactylus is dorso-ventrally flattened with well developed simple stout setae along its periphery which are larger and more hook-like distally (Fig. 3.7A,B,D,E).

The exopod is dorso-ventrally flattened and membranous distally, its outer proximal margin lined by densely arranged pappose setae (Fig. 3.7A,B). These merge distally into simple elongate setae which merge with plumose setae on the upper margin (Fig. 3.7F,G). Pappose setae also cover the proximal aboral surface of the exopod merging distally with multidenticulate whorled setae (Fig. 3.7A,H).

First Maxillipeds

The distal and proximal endites are very much reduced and the short endopod is fused with the elongate dorso-ventrally flattened membranous exopod (Fig. 3.8A,B). The endopod inner margin is lined by pappose setae which merge distally with serrate setae and hook-like simple stout setae at the apex. The exopod has densely arranged pappose setae lining its margins which merge with simple elongate setae and plumose setae at the apex (Fig. 3.8C). Simple hamate and tapering setae cover the exopod aboral surface, the former of which can be seen in Fig. 3.8C. A tuft of simple elongate and multidenticulate toothed setae arise medially from the oral surface of the protopod (Fig. 3.8D).

The epipod is large, flattened and membranous and is fused with the protopod to extend over gills within the branchial chamber. Sparsely arranged multidenticulate digitate setae cover the proximal aboral surface (Fig. 3.8E,F), whereas the oral surface is devoid of setae.

Second Maxillae

The scaphognathite (exopod) is fringed with plumose setae which increase in density along the lower margin (Fig. 3.9A,B). Simple stout and simple tapered setae cover the aboral and oral surfaces, respectively, and are directed towards the

Figure 3.7. Second maxilliped, right side. **A.** Aboral view. **B.** Oral view. Scale, 1.4 mm. SEM: **C.** Simple elongate setae on the distal upper margin of the propus. Scale, 250 μm. **D.** Simple stout setae on the dactylus. Note, their large and hook-like appearance at the tip and the smaller simple stout setae (arrows) on the aboral surface. Scale, 500 μm. **E.** Large and hook-like simple stout setae at the tip of the dactylus. Scale, 200 μm. **F.** Plumose setae on the distal margin of the exopod. Scale, 500 μm. **G.** Fine structure of plumose setae. Scale, 50 μm. **H.** Multidenticulate whorled setae on the aboral surface of the exopod. Scale, 50 μm. b/co, fused basis and coxopodite; c, carpus; d, dactylus; ex, exopod; i, ischium; m, merus; p, propus.

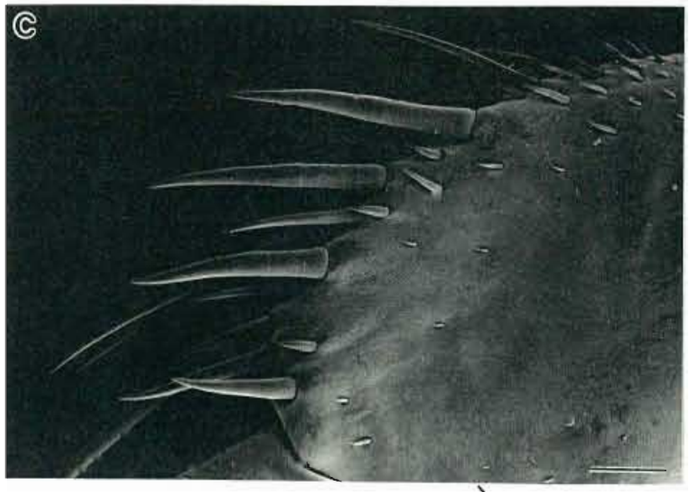
C


D

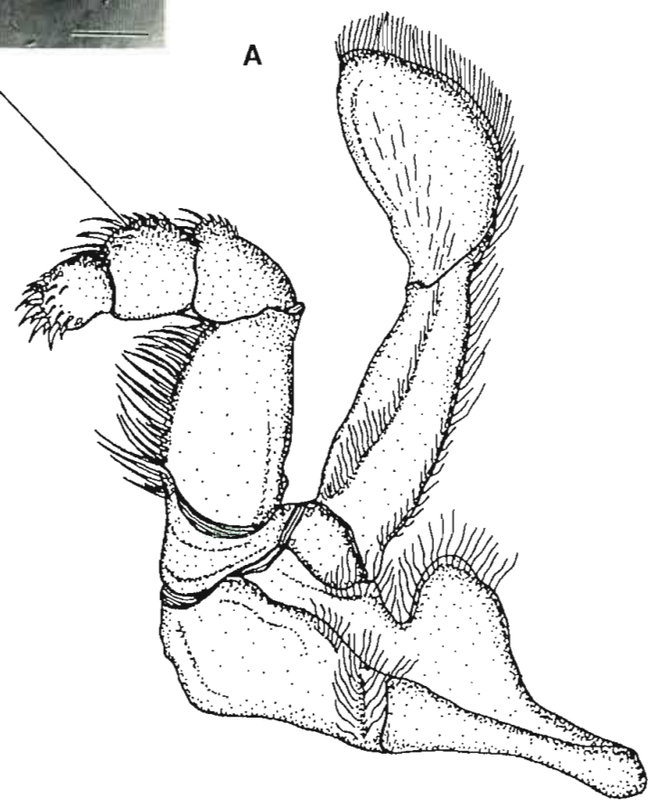
A

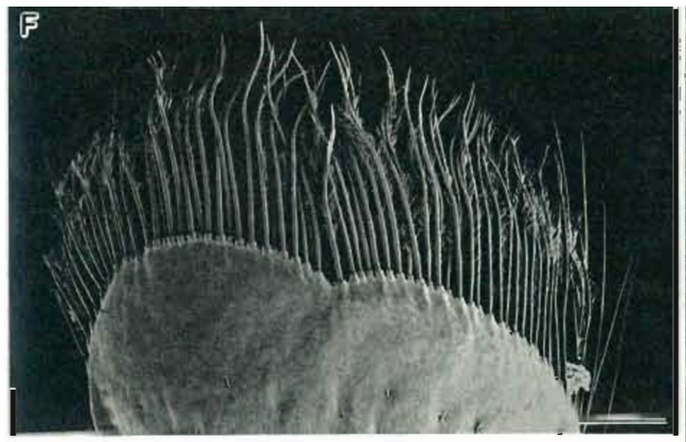
F


G

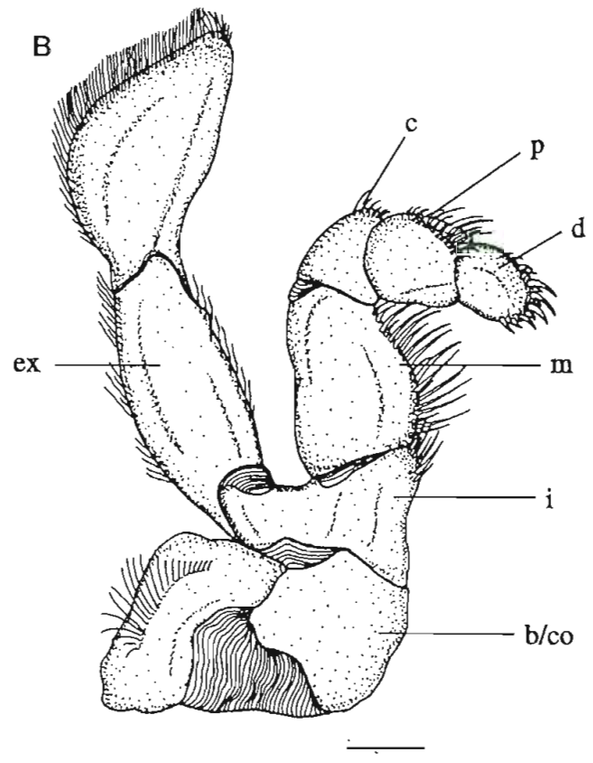
B
c
p
d
ex
m
i
b/co

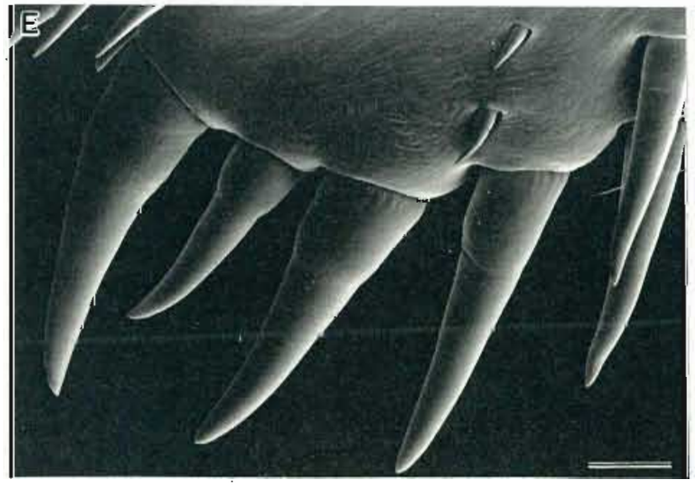
E

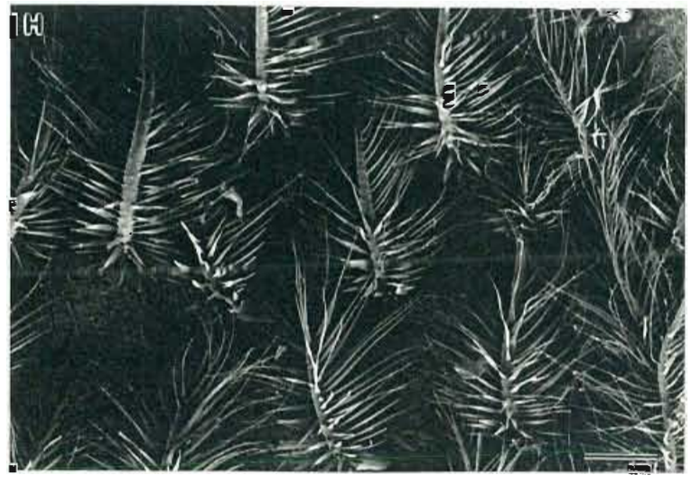
H

Figure 3.8. First maxilliped, right side. **A.** Oral view. **B.** Aboral view. Scale, 1.6 mm. SEM. **C.** Simple elongate and plumose setae along the distal margin of the exopod. Scale, 250 μm. **D.** Multidenticulate toothed setae and simple elongate setae on the oral surface of the protopod. Scale, 25 μm. **E.** Multidenticulate digitate setae dispersed on the aboral surface of the epipod. Scale, 250 μm. **F.** Fine structure of a multidenticulate digitate seta. Scale, 10 μm.
en, endopod; ep, epipod; ex, exopod; mts, multidenticulate toothed setae; pls, plumose setae; pr, protopod; shs, simple hamate setae; ses simple elongate setae.

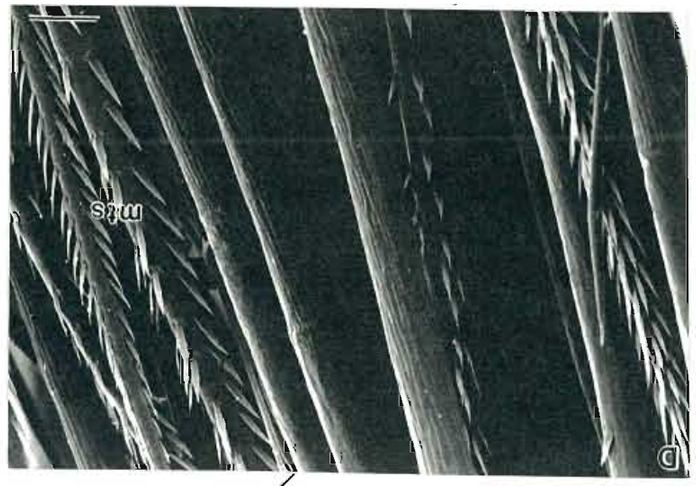
mts

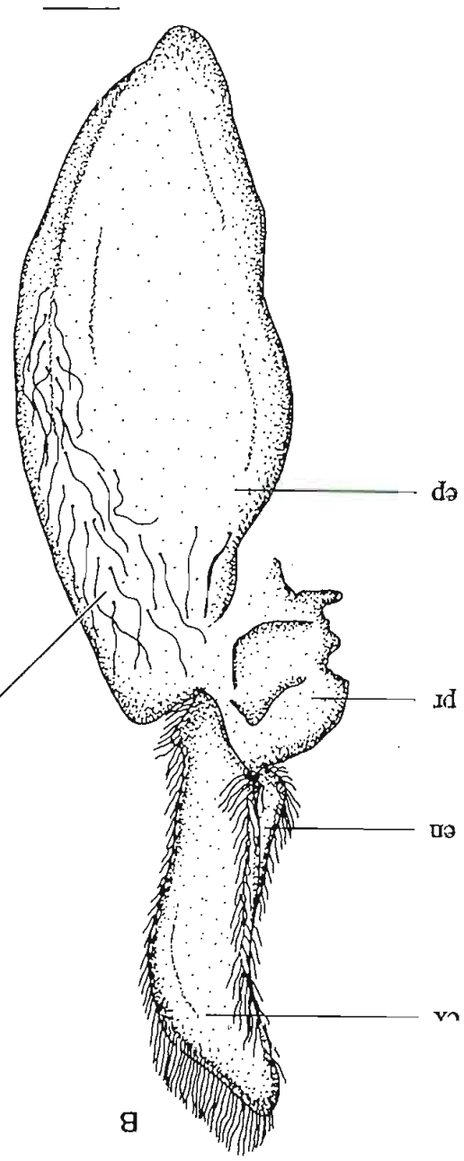
ep
pr
en
ca
B

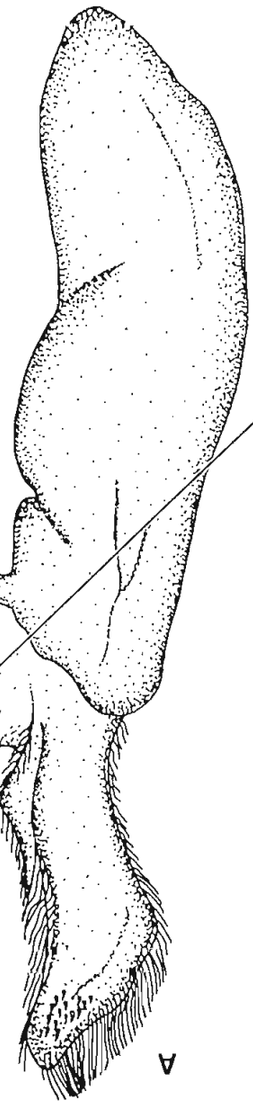
A

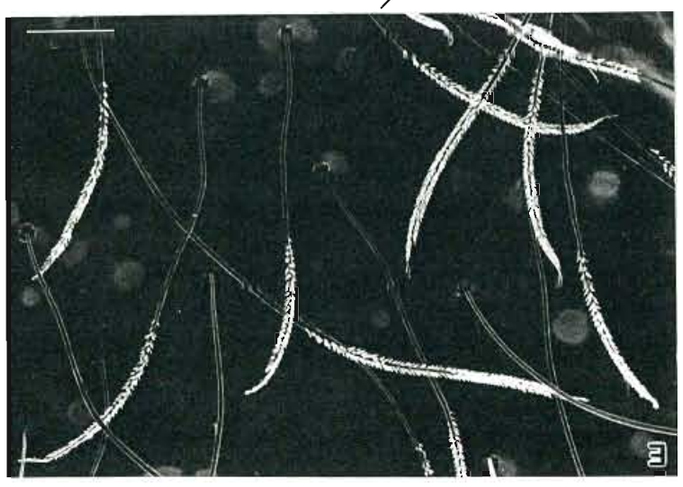

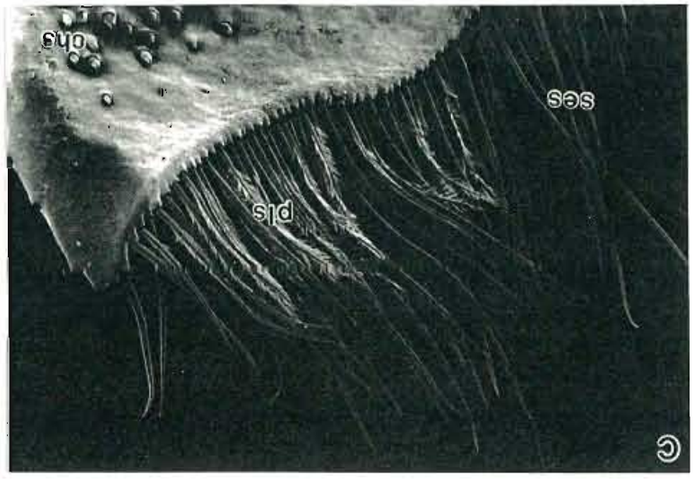
ons
ses
pls

scaphognathite margin (Fig. 3.9B,C). The distal and proximal endites are fused; the inner margin of the former lined with pappose setae and the aboral distal surface of the latter covered with numerous simple tapered setae.

First Maxillae

The first maxilla has a distal and proximal endite which articulate basally, the distal endite being considerably larger (Fig. 3.10A). Numerous simple stout setae cover the aboral surface and become extremely large and hook-like along the terminal margin of the distal endite (Fig. 3.10A,B). Two extremely elongate multidenticulate cuneate setae (700 μm and 1200 μm) project terminally from the proximal endite (Fig. 3.10A,C).

Mandibles

The mandibles are asymmetrical, the left having a well developed medially positioned molar process (Fig. 3.11). The medio-ventral incisor processes have small serrations, the most ventral enlarged to a sharp, upwardly directed hook. A row of simple hamate setae extend along the lower gnathobase margin. The mandibular palps are non-calcified but rigid and extend medially from the upper gnathobase. Densely arranged pappose setae along their upper margins decrease in number distally (not shown in Fig. 3.11).

Labrum

The labrum is a fleshy muscular structure, its lower part positioned between the incisor processes of the mandibles (Fig. 3.2B). It has numerous ventrally directed microspines, approximately 8 μm in length, arranged singley or in rows of 2 or 3. A cuticularised strengthening plate covers its proximal aboral surface.

Approximately 80% of labral tissue is muscle. Longitudinal muscle extends from the centre of the labrum into collagenic connective tissue at the periphery, between which are bundles of circular muscle. There is a well developed columnar epithelium beneath the thickened outer cuticle of the labrum. Tegumental rosette glands, similar in structure to those of the paragnath (refer Ch 3.3.2), are present beneath the epithelium. They are not, however, as abundant and form a narrow strip along the lower part of the labrum. They have been referred to as labral glands (Boxshall, 1982) and stain intensely blue with PAS-alcian blue and aldehyde fuchsin-alcian blue indicating that their secretions are carboxylated acidic mucopolysaccharides.

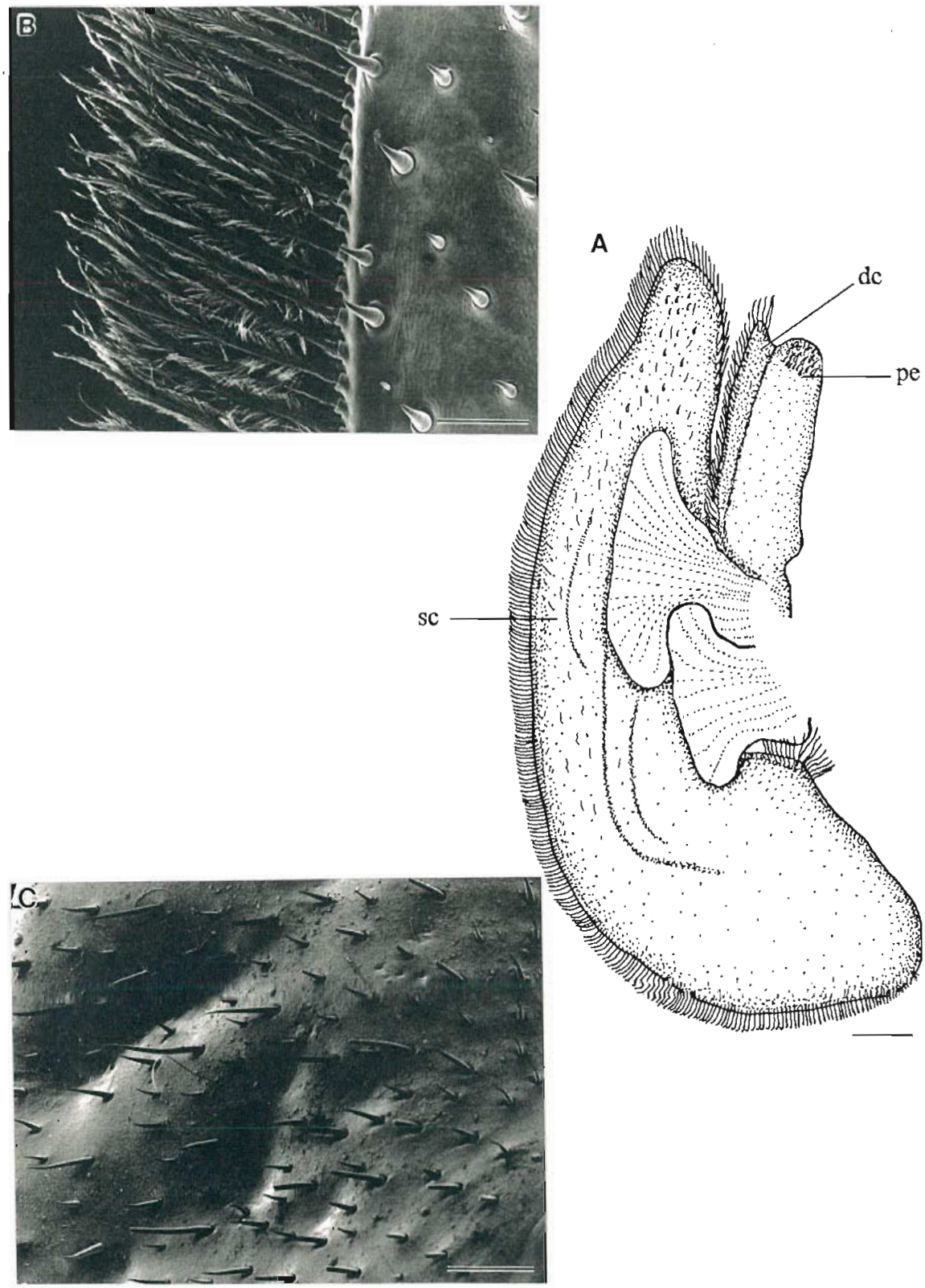

Figure 3.9. Second maxilla, right side. **A.** Aboral view. Scale, 1.2 mm. SEM: **B.** The fringe of plumose setae on the outer scaphognathite margin. Note, the simple stout setae on its aboral surface. Scale, 200 μm. **C.** Simple tapering setae on the oral scaphognathite surface. Scale 250 μm.
de, distal endite; pe, proximal endite; sc, scaphognathite.

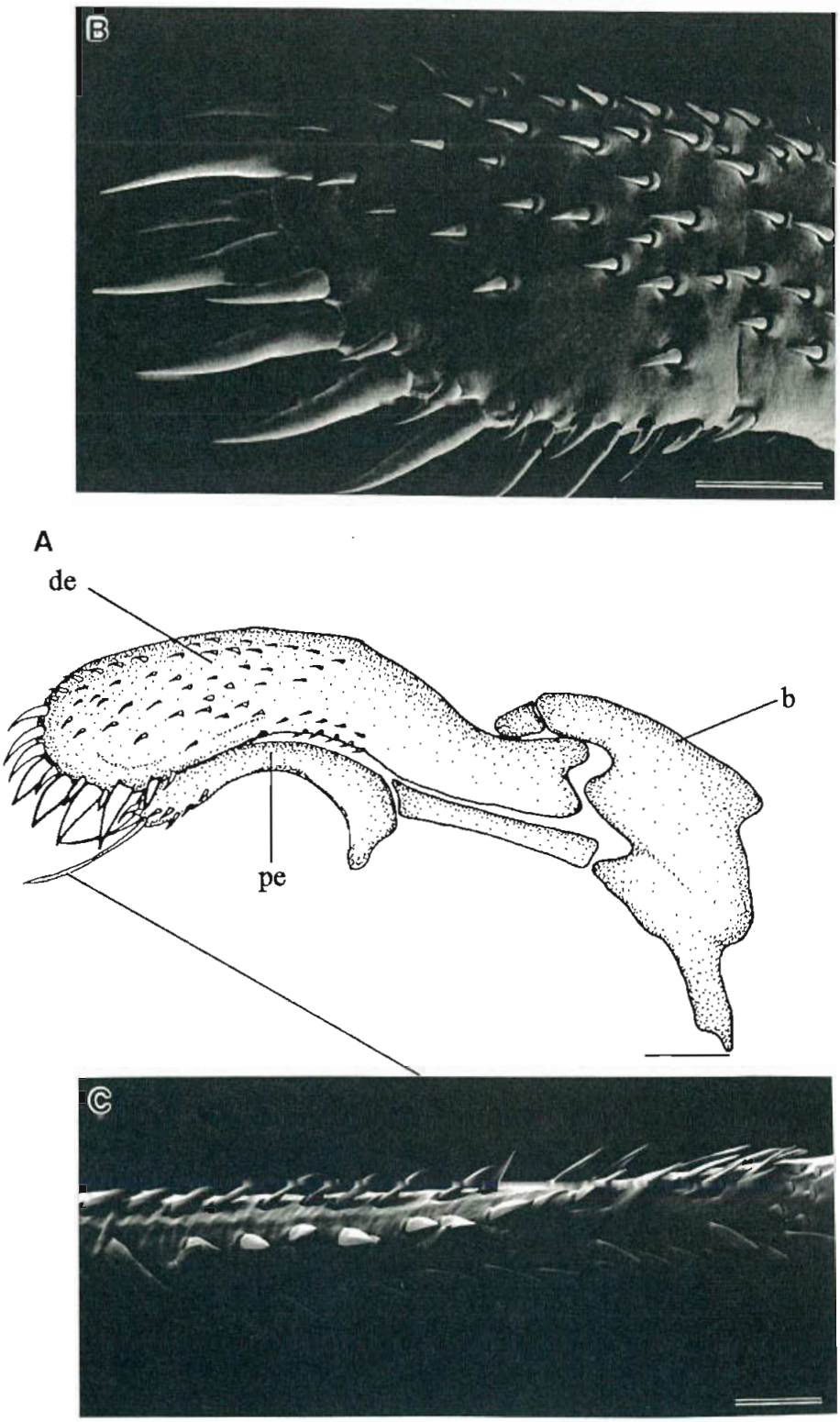

Figure 3.10. First maxilla, right side. **A.** Aboral view. Scale, 0.6 mm. SEM: **B.** Simple stout setae on the distal endite aboral surface and inner margin. Note, their size and hook-like appearance. Scale, 500 μm. **C.** Multidenticulate cuneate seta on the proximal endite. Scale, 25 μm.
b, basis; de, distal endite; pe, proximal endite.

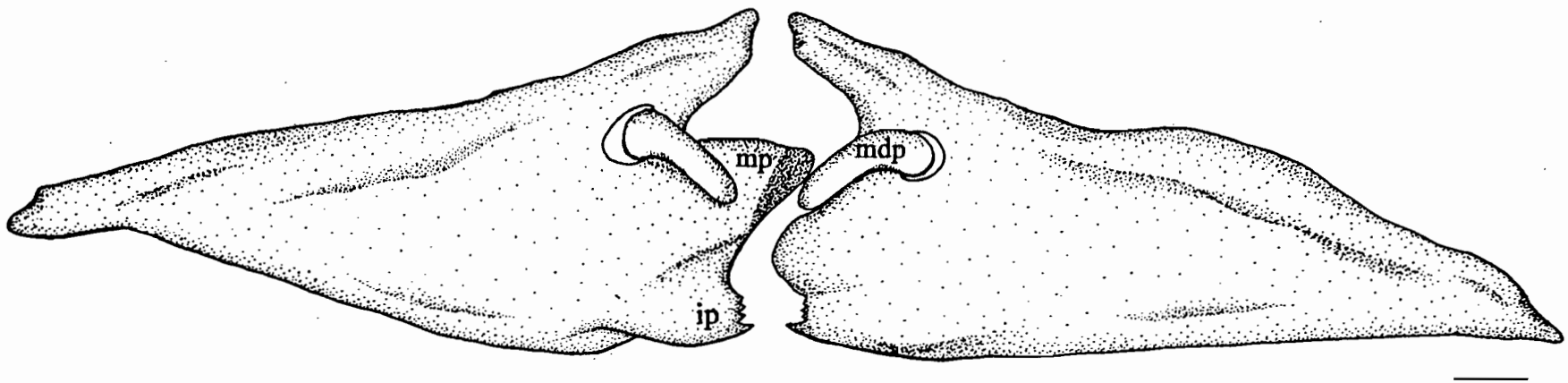

Figure 3.11. Mandibles, aboral view. Note, the well developed molar process on the left mandible and the teeth-like serrations of the incisor processes. Scale, 0.6 mm. mdp, mandibular palp; mp, molar process, ip, incisor process.

3.3.2 The Paragnaths

The paragnaths of *T. orientalis* are two fleshy outgrowths which are connected basally to the anterior lip of the membranous lobe and extend outwards along the lower aboral margin of the mandibular gnathobase (Fig. 3.2A,B). Their inner margins form the lateral boundaries of the mouth and an endophragmal skeletal extension extends a short distance along the proximal outer margin (Fig. 3.12).

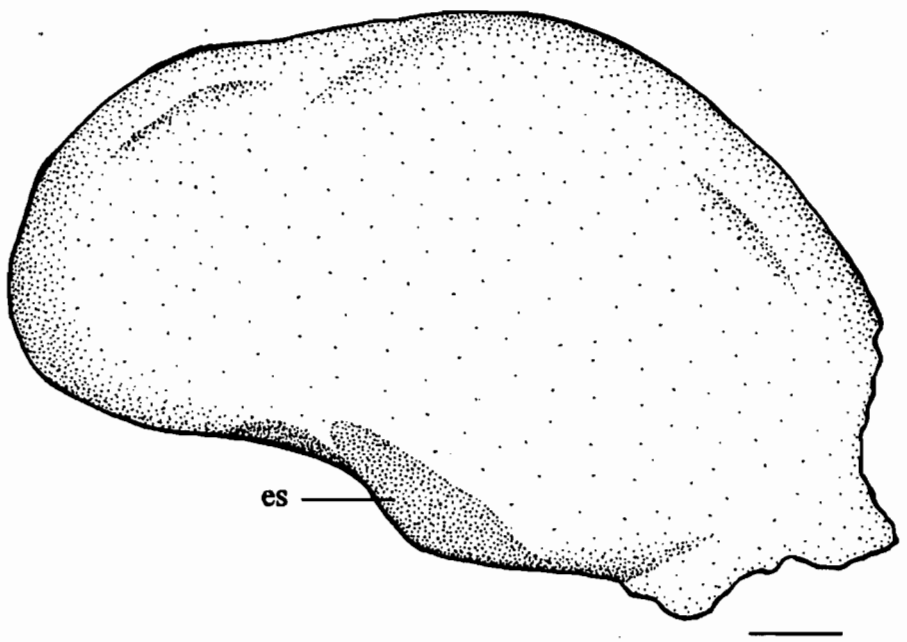

Figure 3.12. Aboral view of the left paragnath indicating the endophragmal skeletal extension. Scale, 0.3 mm.
es, endophragmal skeletal extension.

Pores are densely distributed over the oral and aboral surfaces, giving the paragnaths a pitted appearance (Fig. 3.13A). Each pore (1.5 μm in diameter) is surrounded by a raised area and is partially covered by a V-shaped lip (Fig. 3.13B). Scanning electron microscope examination of transverse sections through the paragnath revealed a multi-layered cuticle, traversed by ducts leading from pores to glands beneath. Each gland has a bulbous head and a narrow elongate duct. Their external appearance resembles that of rosette glands examined by Alexander (1989) in *Palaemon serratus* (Pennant).

The paragnaths have a thickened outer cuticle (28 μm), beneath which is a layer of columnar epithelial cells averaging 20 μm in length (Fig. 3.13C,D). Each cell has a prominent mid-basal nucleus and a granular cytoplasm (Fig. 3.13D), which stains positive for acidophil substances. Granules increase in density apically and often form a circular bolus directly beneath the cuticle. A central channel of connective tissue extends along the distal 2/3 of the paragnath which opens proximally into collagenic connective tissue (Fig. 3.13C).

Numerous tegumental rosette glands lie beneath the epithelium and are equally abundant on both sides of the central channel of connective tissue (Fig. 3.14A). They decrease in number distally. Between the glands are strands of connective tissue extending from the central channel toward the epithelium (Fig. 3.14A,B).

In section, each gland has 4-8 conical shaped secretory cells surrounding a central duct cell (Fig. 3.14C,D). From here, a single duct extends between two secretory cells to the gland periphery (Fig. 3.14C). Although pore channels were seen in the paragnath cuticle (see Fig. 3.14B), a direct link with the gland ducts was not obvious. However, it was noted that gland ducts often open alongside the strands of connective tissue which extend toward the epithelium in the vicinity of the pore channels (Fig. 3.14B,C).

Two forms of tegumental rosette gland can be identified: type 1 located in the distal half of the paragnath and type 2 in the proximal half. The secretory cells of type 1 are characterised by numerous vesicles which may contain one or more densely staining granules (Fig. 3.14C). Type 2 have a large metachromatic apical vacuole and small densely arranged vesicles proximally which are devoid of granules (Fig. 3.14D).

Ultrastructurally, secretory cells from both gland types contain smooth endoplasmic reticulum (SER) and numerous mitochondria in the basal cytoplasm, surrounding the nucleus and secretory vesicles (Fig. 3.15A). However, each gland type has distinct ultrastructural features.

Type One (Fig. 3.15B): Secretory vesicles vary between 1-3 μm and contain sparsely granular material and an obvious inner membrane. Electron dense granules are usually positioned around the outer periphery and vesicle fusion is common which suggests their

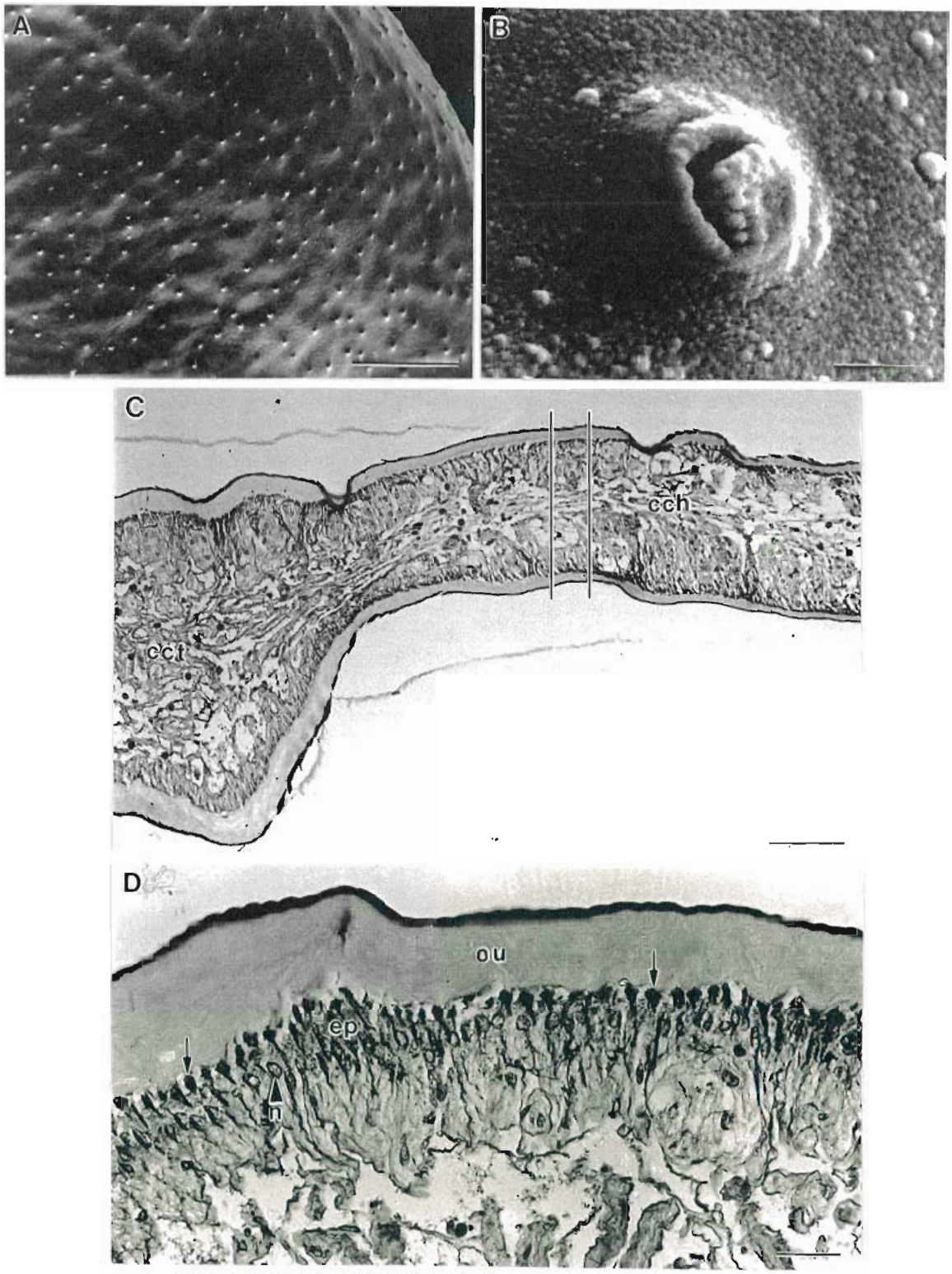

Figure 3.13 A. SEM of the aboral surface of the paragnaths, revealing its pitted appearance. Scale, 50 μm. **B.** SEM of a single pore. Scale, 1 μm. **C.** Longitudinal section (LS) (6 μm) of the paragnath showing the central channel of connective tissue opening proximally into collagenic connective tissue. Lines indicate the position in which the resin section (Fig. 3.14A) was taken. Scale, 100 μm. **D.** LS of paragnathal epithelial cells showing the apical bolus of acidophilic material directly beneath the cuticle (arrow). Scale, 25 μm. cch, central channel; cct, collagenic connective tissue; cu, cuticle; ep, epithelium; n, nucleus.

Figure 3.14. A. Transverse resin section (1.5 μm) of the paragnath in the position indicated in Fig. 3.13C, showing the tegumental rosette glands positioned on either side of the central channel of connective tissue. Scale, 50 μm. **B.** Tegumental rosette glands interspersed with strands of connective tissue leading toward the epithelium. Scale, 25 μm. **C.** Tegumental rosette gland, type 1. Note, the numerous vesicles and granules in each secretory cell cytoplasm and the central duct extending outwards between two secretory cells into the adjacent strands of connective tissue (arrow). Scale, 10 μm. **D.** Tegumental rosette gland, type 2. Note, the rosette of secretory cells surrounding a central duct cell, each secretory cell with a large apical vacuole, basal nucleus and proximal vesicles. Scale, 10 μm. Duct cell not indicated, refer to Fig. 3.15; 3.16.
cch, central channel; cts, connective tissue strands; cu, cuticle; du, duct; g, gland; n, nucleus; pc, pore channel; sc, secretory cell; v, vesicle; vac, vacuole.

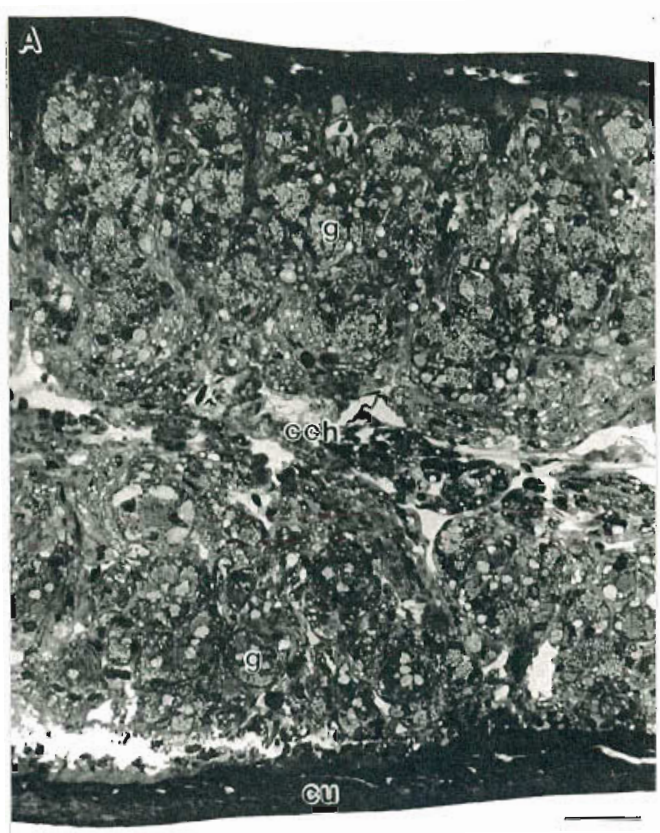
A
g
cch
g
cu


B
cu
pc
g
g
cts
cts


C
cu
v
n

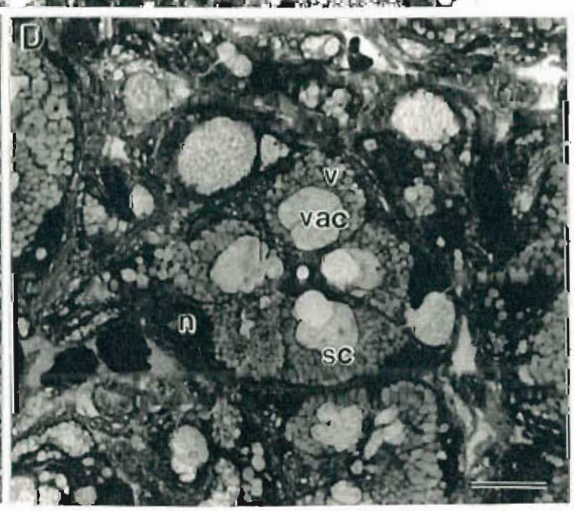
D
v
vac
n
sc

contents are sequestered prior to release via the central duct (Fig. 3.15C). There is an agranular central cell which interdigitates with a densely granular duct cell (Fig. 3.15B,D). The central cell cytoplasm extends into the secretory cell apex which is bordered on either side by two cytoplasmic extensions of the duct cell. Within the secretory cell apex is often a large vesicle bordering the central cell projection (Fig. 3.15D, labelled v). Smaller vesicles are apparent within the adjacent central cell cytoplasm (arrows). Extensions of the duct cell project into the secretory cells (dce), one of which forms the duct which extends outwards between two secretory cells toward the gland periphery (Fig. 3.15B,D).

Type Two (Fig. 3.16A): Densely arranged cytoplasmic vesicles contain fine granular material and fuse with one another and the large apical vacuole (Fig. 3.16B). Granulation is less marked in the large apical vacuole in which cytoplasmic extensions are prevalent. In contrast to type 1, the duct cell is spherical with a central agranular region surrounded by vesiclular tissue (Fig. 3.16A,C). A central cell is not present. Organelles were not observed within the duct cell cytoplasm of either gland type although mitochondria are present within the adjacent secretory cell cytoplasm (Fig. 3.16C).

Histochemical examination revealed the nature of glandular secretions and the results are summarised in Table 3.2. Gland cells stained intensely blue with PAS-alcian blue indicating their secretions are acidic mucopolysaccharides. Further identification using aldehyde fuchsin-alcian blue revealed that the mucopolysaccharides are carboxylated. Gland cells resisted diastase digestion indicating the absence of glycogen. Finally, glands reacted only marginally with mercuric bromophenol blue demonstrating that protein is present in small quantities.

Apical granules in the epithelial cells stained positive for alcian blue indicating they are acid mucopolysaccharides. The connective tissue strands also stained positive for acid mucins suggesting they may contain glandular secretions.

Acidic mucopolysaccharides were present in the secretory cells of tegumental glands regardless of the level of satiation.

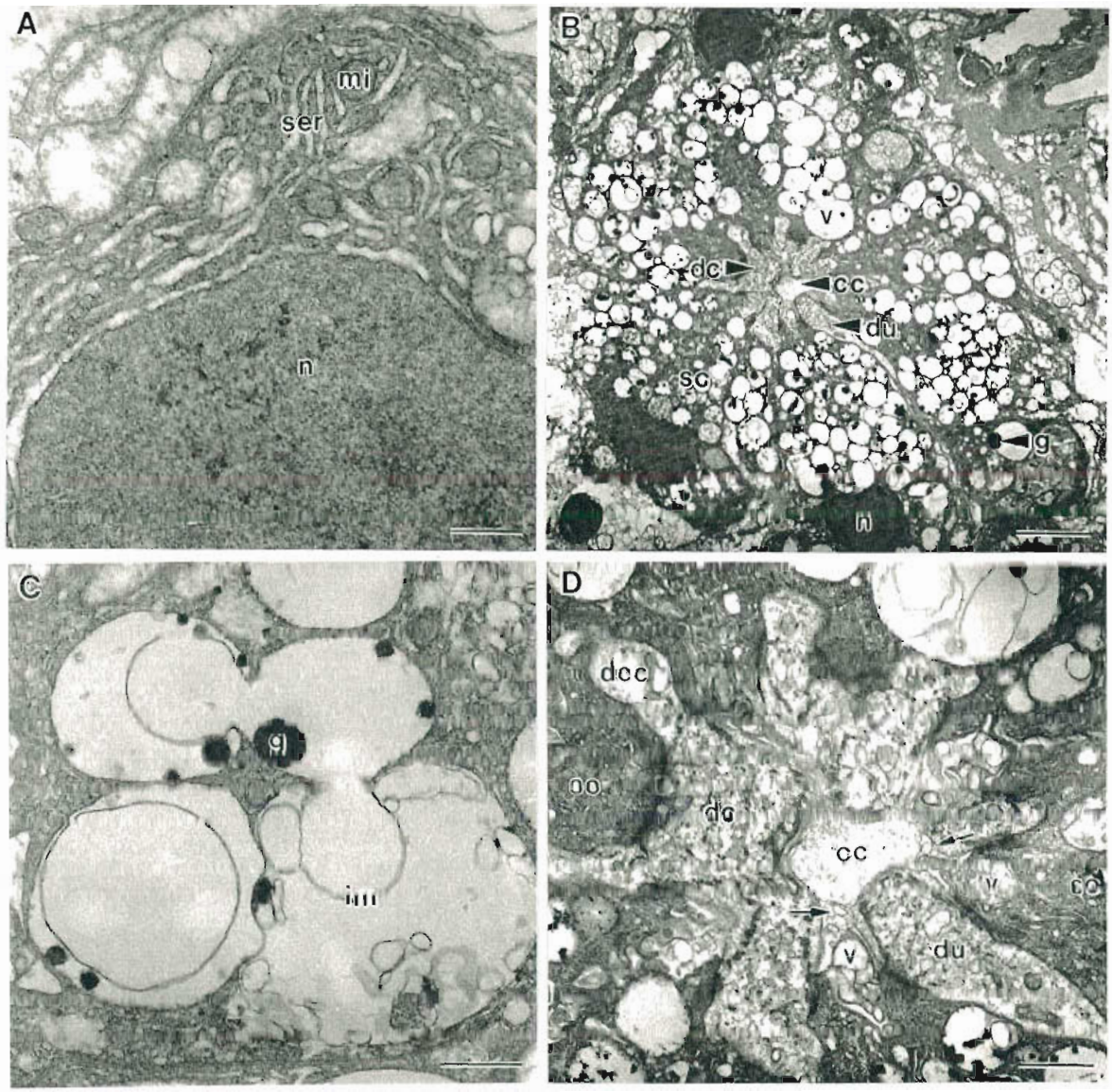

Figure 3.15. Transmission electron micrographs (TEM): **A.** Smooth endoplasmic reticulum and mitochondria surrounding a nucleus within the proximal cytoplasm of gland cells. Scale, 0.4 μm. **B.** Tegumental rosette gland, type 1, showing the characteristic secretory vesicles, granules, basal nucleus and central duct region. Scale, 6 μm. **C.** Fusion of secretory vesicles showing inner membranes and granules. Scale, 0.8 μm. **D.** Gland centre showing details of the central cell and duct cell. Note, the large vesicle in the secretory cell apex bordering the central cell projection (v). Arrows indicate small vesicles in the central cell cytoplasm. Scale, 0.4 μm.
cc, central cell; dc, duct cell; dce, duct cell extension; du, duct; g, granule; im, inner membrane; mi, mitochondria; n, nucleus; sc, secretory cell; ser, smooth endoplasmic reticulum; v, vesicle.

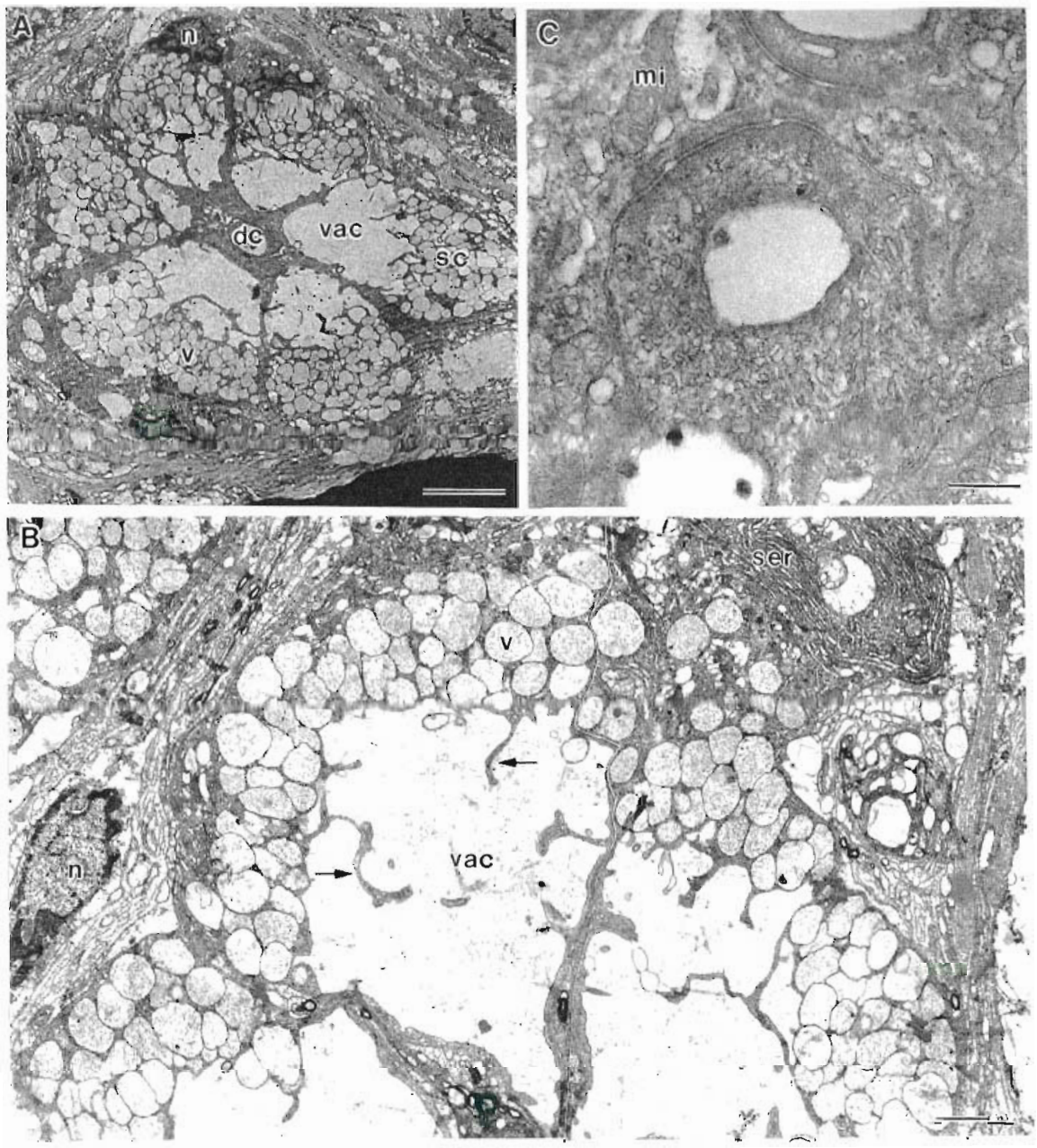

Figure 3.16. TEM: **A.** Tegumental rosette gland, type 2, showing the characteristic apical vacuole, proximal vesicles and duct cell. Scale, 6 μm. **B.** Secretory cells of gland type 2 showing the cytoplasmic extensions into the apical vacuole (arrows) and dense SER proximally. Scale, 0.8 μm. **C.** Duct cell. Note, its vesicular tissue and the mitochondria in the adjacent secretory cell cytoplasm. Scale, 0.5 μm.
dc, duct cell; mi, mitochondria; n, nucleus; sc, secretory cell; ser, smooth endoplasmic reticulum; v,vesicle; vac, vacuole.

Table 3.2. Results of the histochemical analysis on the paragnaths and membranous lobe of *Thenus orientalis*. +++, intensely stained; ++, moderately stained, +, weakly stained; -, negative (no reaction). Blank cells indicate the test was not applied. CT, connective tissue; glands, tegumental rosette glands; PAS, periodic acid Schiff.

Histochemical Test	PARAGNATHS			MEMBRANOUS LOBE		
	Glands	Epithelium	CT Strands	Glands	Spherical Cells	CT Granules
Carbohydrate						
PAS-alcian blue pH 2.5	blue +++	blue ++	blue ++	blue +++	dark pink +++ blue +	
alcian blue pH 0.2					purple +++	
aldehyde fuchsin-alcian blue pH 2.5	blue +++				-	
diastase-PAS	-	-	-	-		dark pink +++
Protein						
mercuric bromophenol blue	blue +	-	-	blue +	blue/red +++	-
Glycoprotein						
alkaline Congo red					-	

3.3.3 Membranous Lobe

The membranous lobe is a large fleshy protuberance arising midventrally from the sternal sclerite between the second maxillipeds (Fig. 3.2B). It extends towards the mandibles and forms the posterior boundary of the mouth. The anterior lip of the lobe is continuous with the oesophageal wall and paragnaths, which are in turn connected with the labrum (Fig. 3.2B).

A flattened strengthening rod extends across the aboral surface, which is densely covered with three types of ventro-anteriorly directed setae: annulate simple, cuspidate and whorled (Fig. 3.17A-D). The annulate simple setae are the most abundant and are also present posterior to the strengthening rod and in a row extending from the lower lobe margin, over the sternal skeleton (Fig. 3.17A,B). The anterior aboral surface largely lacks setae except for a few annulate simple setae along the lateral margins (Fig. 3.17A).

Three fields of microscales and microspines, anterior, middle and posterior, are also present on the strengthening rod. The anterior field is characterised by broad anteriorly-directed microscales, densely arranged (30 per 50 μm^2) in circular clusters of between 6 and 14 scales (Fig. 3.17E). The middle field has similar shaped microscales, but the clusters are less clearly defined and the numbers per cluster vary between 4 and 8 (Fig. 3.17F). The posterior field has narrow, tapered microspines (8 μm long) in groups of 4-5 spines, but most are quartets (Fig. 3.17G). Cluster density in the middle and posterior fields is approximately 20 per 50 μm^2.

The lobe has an outer cuticle of average width 50 μm, thickening to 100 μm along the aboral surface (Fig. 3.18A). Beneath the cuticle, epithelial cells have a densely granular, apical cytoplasm and a basal nucleus. Circular and longitudinal striated muscle bundles occupy a large amount of the lobe increasing towards the anterior lip. Strands of collagenic connective tissue are dispersed throughout the lobe, forming a band around the musculature. Tegumental rosette glands are located beneath the epithelium of the oral surface and contain sulphated acidic mucopolysaccharides, some protein but no glycogen (Fig. 3.18A; Table 3.2). They have 4-6 conical cells surrounding a central duct and are similar in structure to those of the paragnaths.

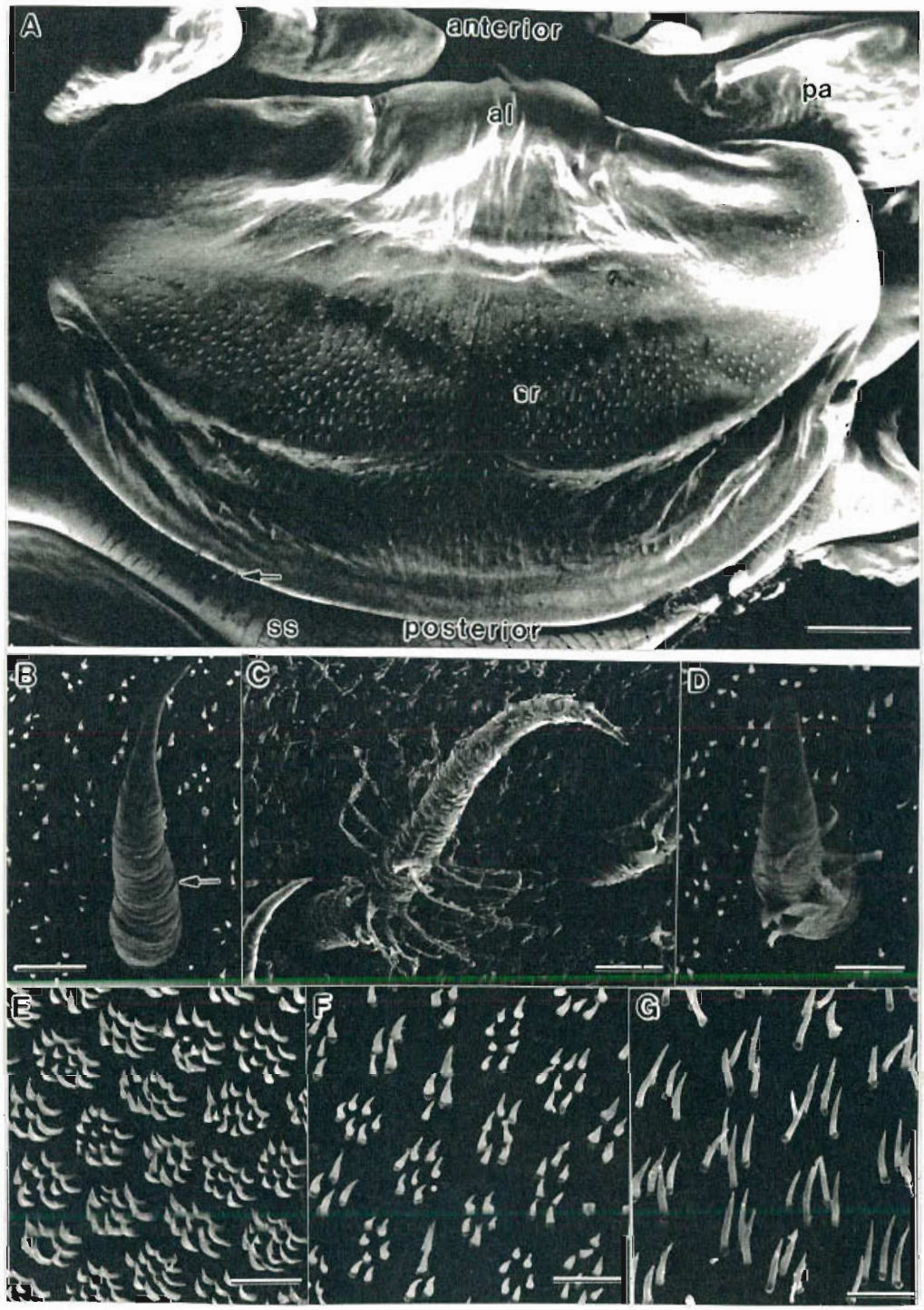

Figure 3.17. SEM of the membranous lobe of *T. orientalis*, aboral surface. **A.** Surface features and morphology of the membranous lobe. Note, setae on and posterior to the strengthening rod. Arrow indicates annulate simple setae on the posterior margin of the lobe. Scale, 1 mm. **B.** Annulate simple seta. Scale, 18 μm. Arrow indicates annulations on setal shaft. **C.** Annulate whorled seta. Scale, 20 μm. **D.** Annulate cuspidate seta. Scale, 15 μm. **E.** Circular clusters of anterior field microscales. Scale, 10 μm. **F.** Clusters of middle field microscales. Scale, 10 μm. **G.** Clusters of posterior field microspines. Scale, 10 μm.
al, anterior lip; pa, paragnath; sr, strengthening rod; ss, sternal skeleton.

Within the posterior region of the lobe there are numerous spherical cells embedded in the connective tissue beneath the aboral surface (Fig. 3.18B). They are distributed across its entire width, becoming confined to the outer aboral margins toward the middle of the lobe, and gradually decreasing anteriorly. The cells vary in size between 30 μm and 50 μm and contain numerous granules, the density of which varies considerably (Fig. 3.18B). In 1.5 μm resin sections their cytoplasm appears homogenous with much finer granularity (Fig. 3.18C). Many contain regions of dense granularity and intense staining which, ultrastructurally, are revealed as reticulum (Fig. 3.19A). The size and structure of these regions varies between cells (Fig. 3.18C). Nuclei are only visible ultrastructurally and are always located at the cell periphery (Fig. 3.19B,C). Vesicles of variable size commonly line the outer margin of the cell, many in close proximity to rough endoplasmic reticulum (Fig. 3.19B,D). Apart from these small quantities of rough endoplasmic reticulum, the cells are largely devoid of organelles.

Adjacent to the spherical cells are numerous glycogen granules (diastase-PAS positive) within the loose connective tissue (Fig. 3.18B) (Table 3.2).

Histochemically the cells stained moderately PAS positive (dark pink), revealing the presence of neutral mucopolysaccharides, but resisted diastase digestion, indicating the absence of glycogen (Table 3.2). Cells also stained intensely with mercuric bromophenol blue demonstrating that they contain large amounts of protein but the negative reaction to alkaline Congo red rules out glycoprotein.

There was no association between spherical cells and sex in the 30 adult male and females examined, nor was there a relationship with position in the moult cycle. Although cells were always present in both fed and starved individuals, cell granularity increased in starved individuals together with a reduction in amount of neutral mucin indicated by low staining intensity with PAS-alcian blue. An examination of another 18 individuals of various sizes revealed these cells were absent in juveniles less than 35 mm carapace width, whereas they were present in post-juveniles above this size and all adults.

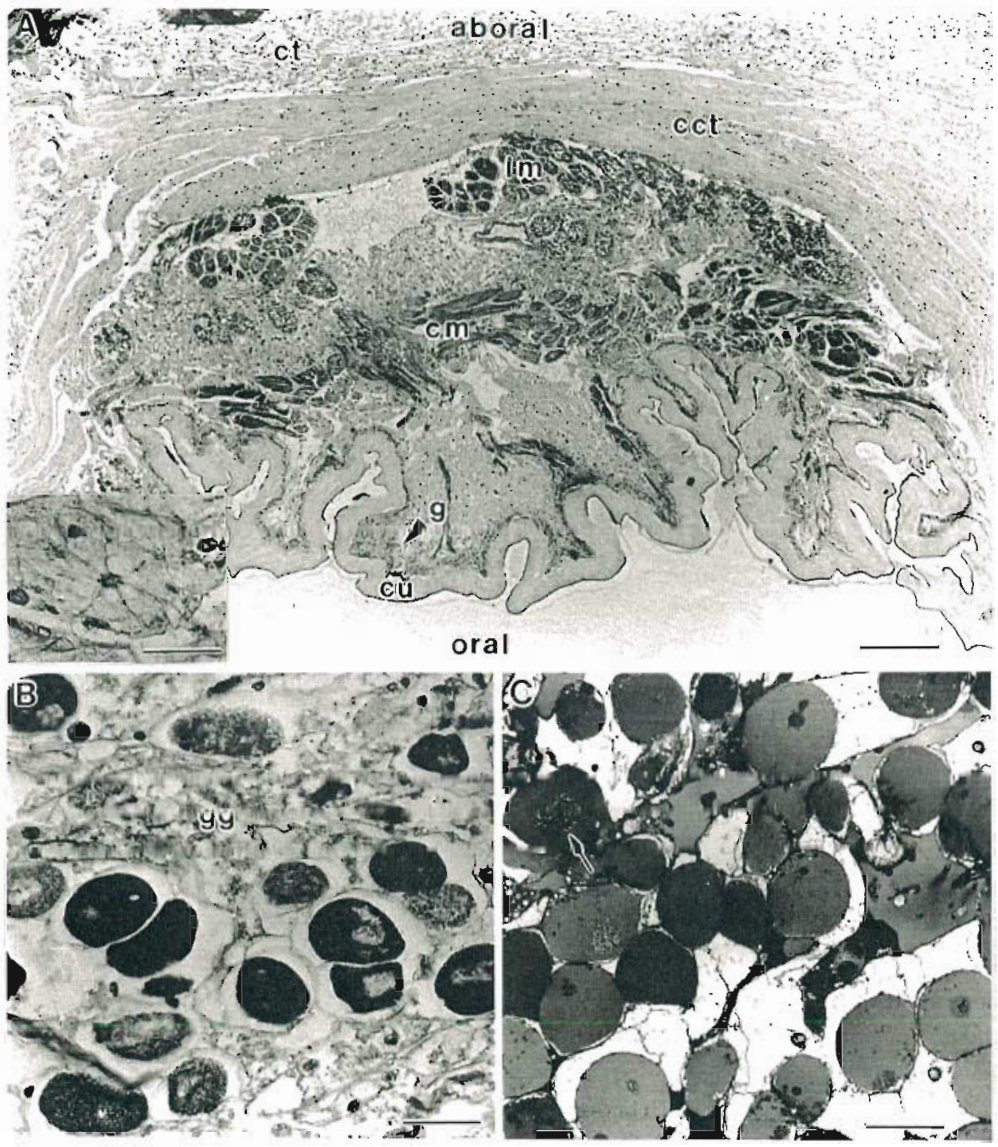

Figure 3.18. A. Transverse section (TS) (6 μm) through the central region of the membranous lobe illustrating the types and distribution of tissues. Scale, 400 μm. INSET, tegumental rosette gland. Scale, 25 μm. **B.** Spherical cells within the connective tissue. Note the adjacent glycogen granules and differences in granularity between cells. Scale, 40 μm. **C.** Resin section (1.5 μm) of spherical cells. Arrow indicates regions of increased granularity and staining within the cell cytoplasm. Scale, 30 μm.
cct, collagenic connective tissue; cm, circular muscle; ct, connective tissue; cu, cuticle; gg, glycogen granules; g, tegumental rosette glands; lm, longitudinal muscle.

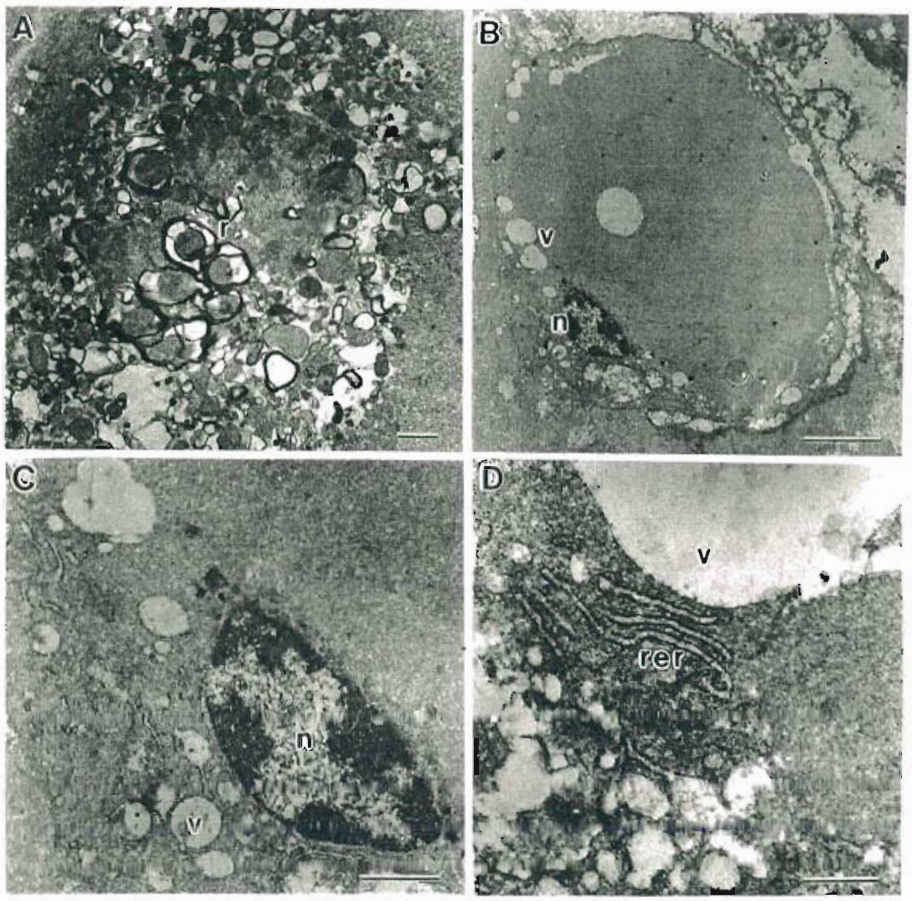

Figure 3.19. TEM of spherical cells within the membranous lobe. **A.** Reticulum within the cell cytoplasm. Scale, 1 μm. **B.** Whole spherical cell. Scale, 6 μm. **C.** Spherical cell nucleus. Scale, 2 μm. **D.** Spherical cell vesicle and adjacent rough endoplasmic reticulum. Scale, 1 μm.
n, nucleus; r, reticulum; rer, rough endoplasmic reticulum; v, vesicle.

3.3.4 Ingestion Mechanisms

Two ingestion modes are used according to the size and texture of food. To understand the process of ingestion the positions of mouthparts in the oral cavity are illustrated in Fig. 3.20 (also refer Fig. 3.2) and their sequential movements during ingestion are shown in Fig. 3.21 and 3.23. The first maxillipeds and second maxillae are not directly involved in ingestion and beating of the maxilliped exopods is minimal.

Mode 1: small soft food less than 10 mm^3

At the onset of ingestion, the third maxillipeds abduct and move ventro-laterally (Fig. 3.21B) as food is delivered to the mouth by the first and second pereiopods. The dactyli of the third maxillipeds alternate dorso-ventrally to insert food between the abducted second maxilliped endopods (Fig. 3.21C). The right second maxilliped endopod moves ventro-medially to receive the food while the left endopod remains stationary. With the aid of the dactyl simple stout setae, the right second maxilliped scrapes food dorsally over the membranous lobe and between the first maxillae (Fig. 3.21D). The left first maxilla moves ventro-medially and then dorsally to push food received from the right maxilliped endopod over the anterior lip of the membranous lobe and between the opened mandibles. This is followed by inward movement of the paragnaths across the lower mandibular gnathobase, but they are not involved in propulsion of food into the mouth. At this time, the lobe lip is retracted ventro-posteriorly and the labrum rotates antero-dorsally to enlarge the preoral cavity. The larger the food item, the greater the extent of retraction by the membranous lobe and labrum. At the most dorsal position of the right second maxilliped and left first maxilla, the left second maxilliped endopod moves ventro-medially inserting the dactyl setae into the food as it begins its dorsal propulsion (Fig. 3.21E). The first right maxilla then moves ventro-medially to receive food from the left second maxilliped and pushes it dorso-anteriorly over the anterior lobe lip and into the mouth (Fig. 3.21F). This occurs simultaneously with retraction of the left first maxilla and ventro-lateral movement of the right second maxilliped. Relative times of mouthpart movements during a representative ingestion sequence are shown in Fig 3.22.

Alternation of the first maxillae and second maxillipeds is repeated numerous times during ingestion with both second maxilliped endopods often moving dorsally together as food size decreases. After insertion between the mandibles the lobe lip

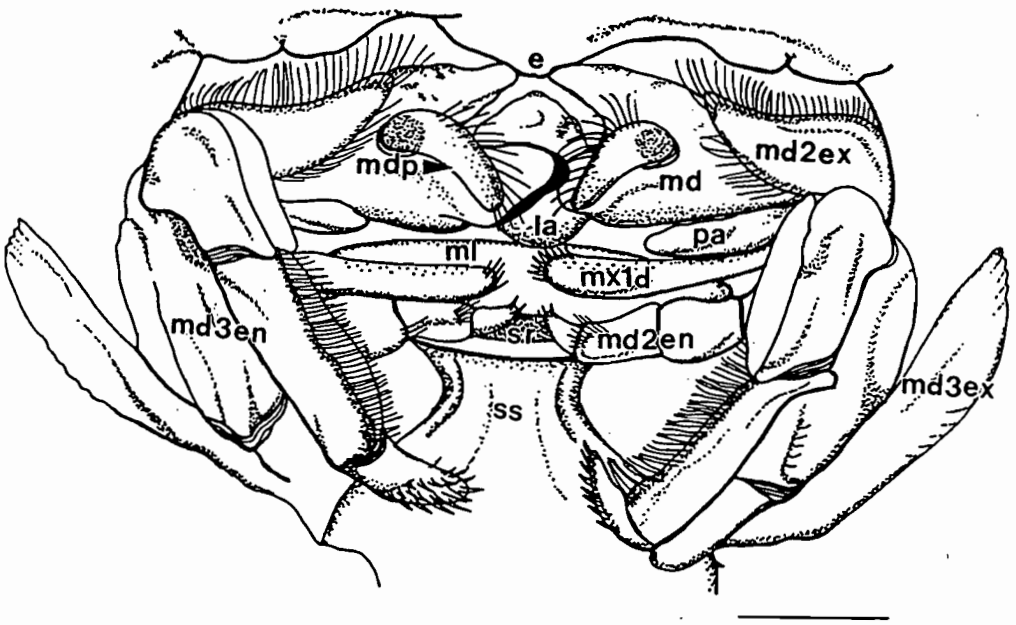

Figure 3.20. Ventral view of the mouthparts of *T. orientalis*, drawn open to show their relative positions within the preoral cavity. Note that the first maxillipeds and second maxillae are obscured under the carapace. Scale, 2.2 mm.
e, epistome; la, labrum; md, mandible; mdp, mandibular palp; md2en, second maxilliped endopod; md2ex; second maxilliped exopod; md3en, third maxilliped endopod; md3ex, third maxilliped exopod; ml, membranous lobe; mx1d; first maxilla distal endite; pa, paragnath; sr strengthening rod; ss, sternal skeleton.

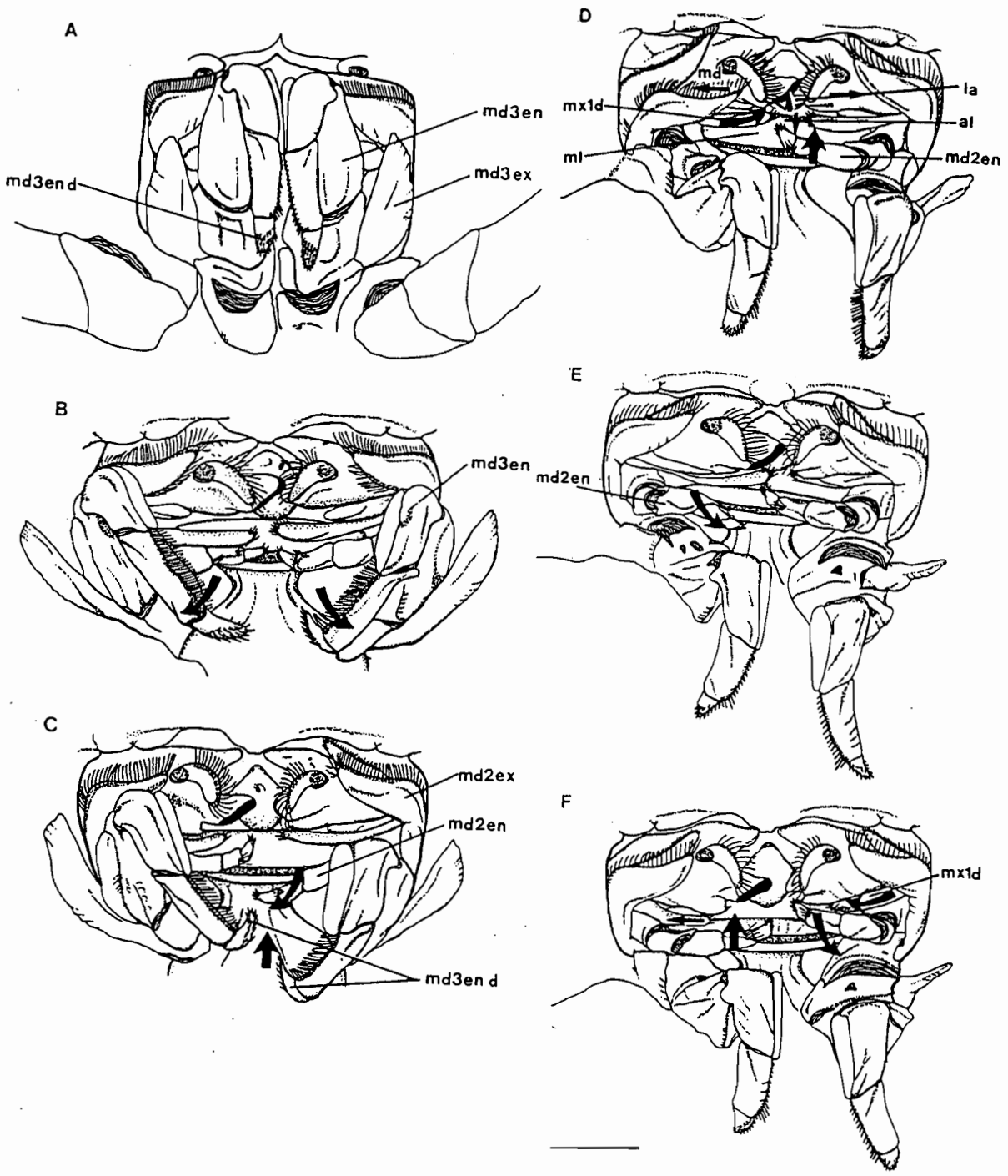

Figure 3.21. Sequential mouthpart movements of *T. orientalis* during small soft food ingestion. Refer to text for detailed explanation. Arrows indicate: **B.** outward ventral movement of the third maxillipeds; **C.** dorsal movement of the third maxilliped dactyli as the right second maxilliped moves ventro-medially; **D.** dorsal movement of the right second maxilliped and ventro-medial movement of the left first maxilla as the anterior lobe lip retracts ventro-posteriorly, the labral lip rotates antero-dorsally and the mandibles open laterally; **E.** ventro-medial movement of the left second maxilliped; **F.** dorsal movement of the left second maxilliped and ventro-medial movement of the right first maxilla as the left first maxilla retracts and the right second maxilliped moves ventro-laterally. Scale, 3 mm.
al, anterior lip of membranous lobe; md2en, second maxilliped endopod; md2ex, second maxilliped exopod; md3en, third maxilliped endopod; md3en d, third maxilliped endopod dactylus; md3ex, third maxilliped exopod; ml, membranous lobe; mx1d, first maxilla distal endite.

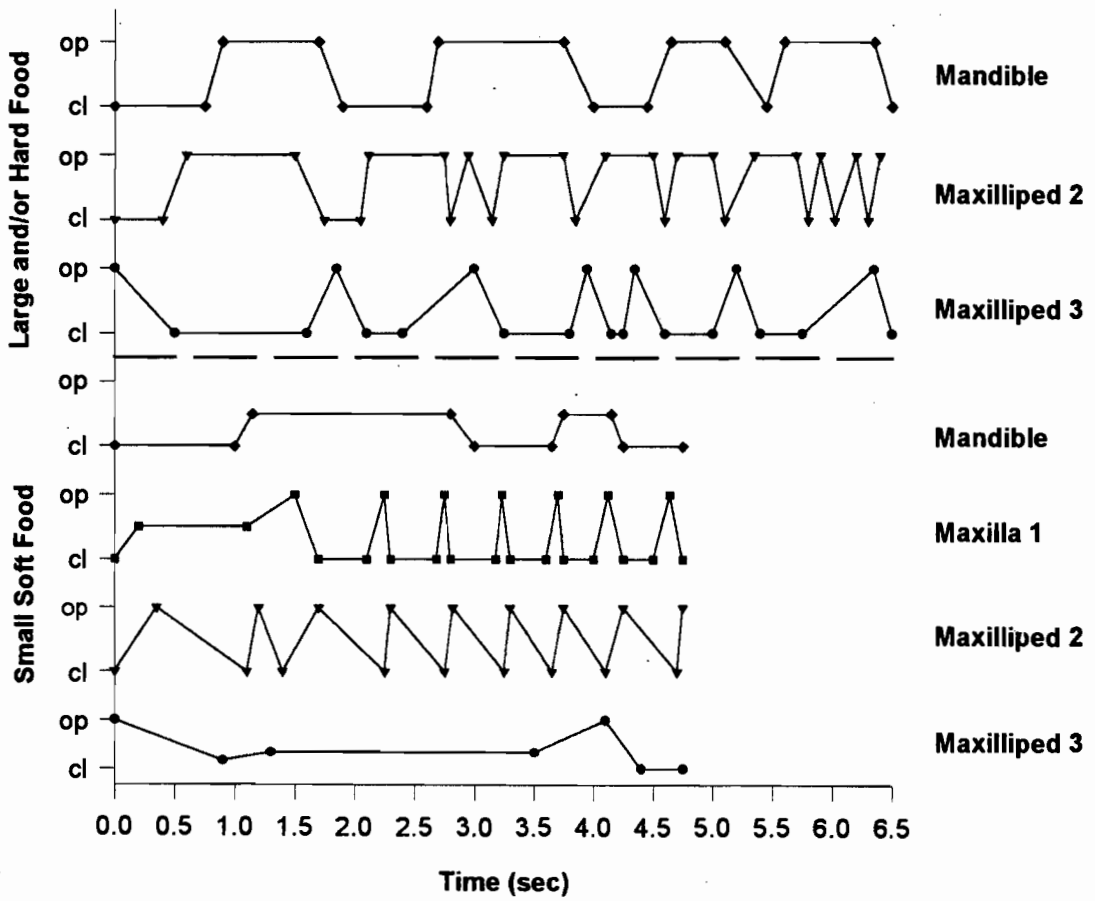

Figure 3.22. Timing of mouthpart movements during a representative small soft food and large and/or hard food ingestion sequence. Only movements of the left mouthparts are indicated. op, open and cl, close. Explanation: **Small soft food.** Third maxillipeds close passing food between the opened second maxillipeds. These alternate with the first maxilla to push food between the partially opened mandibles. The third maxillipeds remain partially open throughout ingestion. **Large and/or hard food.** The third maxillipeds close to grasp food, inserting it between the opened mandibles. During this time the second maxillipeds are held open. As the third maxillipeds open/pull ventrally the second maxillipeds close to insert the food between the mandibles which then close again. The first maxillae are obscured during this sequence and are not illustrated.

protracts ventro-anteriorly and the labrum ventro-posteriorly back to their original positions. Prior to dorsal propulsion of the next food item by the third maxilliped endopods, the second maxilliped endopods often move ventro-medially digging their dactyls into the membranous lobe around the strengthening rod and scraping their dactyl simple stout setae across its surface towards the mandibles. This action is also repeated after insertion. Endoscopic filming also revealed that, following ingestion, the membranous lobe and labral lip pulsate dorsally at regular intervals.

The average number of beats s^{-1} of the second maxillipeds and first maxillae is considerably higher than that of the third maxillipeds and mandibles, supporting their active role in small soft food ingestion (Fig. 3.22). These differences in beat number s^{-1} between the mouthparts are highly significant ($p<0.001$, $\alpha=0.05$) as determined by a One-Way Anova.

The highly significant correlation between the number of beats of the second maxillipeds and first maxillae (Spearman rank correlation $r_s = 0.632$, $p<0.001$, Table 3.3) verifies they have a highly co-ordinated role in inserting food into the mouth. Their alternating action is clearly demonstrated in Fig. 3.22 where the left second maxilliped is open when the left first maxilla is closed. This correlation is partially influenced by movements of the third maxillipeds (partial rank correlation $r_{pmxpdIII} = 0.327$, Table 3.3) and mandibles ($r_{pmand} = 0.270$, Table 3.3). This is expected as the second maxillipeds receive food from the third and opening of the mandibles is concurrent with insertion of food into the mouth by the first maxillae. Furthermore, the significant correlation between the mandibles and first maxillae ($r_s = 0.591$, $p<0.001$, Table 3.3) and the mandibles and second maxillipeds ($r_s = 0.457$, $p<0.02$, Table 3.3), indicates that movement of the mandibles is dependant on action of both the first maxillae and second maxillipeds, further verifying their importance in small soft food ingestion.

Movements of the mandibles, first maxillae and second maxillipeds are independant from those of the third maxillipeds ($r_s = 0.041$, $p>0.5$; -0.001, $p>0.5$; 0.246, $p>0.1$, respectively, Table 3.3) which highlights the reduced role of the third maxillipeds during small soft food ingestion. This is in contrast to large and/or hard food ingestion where the third maxillipeds play an active role in manipulating and passing food between the mandibles (see below and Fig 3.23A,B).

Table 3.3. Spearman rank (r_s) and partial rank correlations (r_p) between the number of beats of the mandibles, maxillae I, and maxillipeds II and III of *T. orientalis* during small soft food ingestion (27 sequences analysed). 1 beat = 1 opening and closing action of each mouthpart. Spearman rank statistical significance is shown (p) where α=0.05. Symbols: r_{pmand}, partial rank correlation between mouthparts irrespective of mandible movements; r_{pmaxI}, partial rank correlation between mouthparts irrespective of maxilla I movements; $r_{pmxpdII}$, partial rank correlation between mouthparts irrespective of maxilliped II movements, $r_{pmxpdIII}$, partial rank correlation between mouthparts irrespective of maxilliped III movements. Maxilla II and Maxilliped I were not included in the analysis as they do not participate in ingestion. Correlations with the paragnaths and labrum were not calculated as they were frequently obscured during ingestion.

Mouthparts	r_s	r_{pmand}	r_{pmaxI}	$r_{pmxpdII}$	$r_{pmxpdIII}$	p
Mandible Maxilla I	0.591	-	-	0.270	0.305	<0.001
Mandible Maxilliped II	0.457	-	0.360	-	0.172	<0.02
Mandible Maxilliped III	0.041	-	-0.199	0.172	-	>0.5
Maxilla I Maxilliped II	0.632	0.270	-	-	0.327	<0.001
Maxilla I Maxilliped III	-0.001	0.305	-	0.327	-	>0.5
Maxilliped II Maxilliped III	0.246	0.110	-0.193	-	-	>0.1

Following ingestion, the third maxillipeds close while debris lodged between setae of the second maxillipeds is removed by mutual rubbing of the endopods. The third maxillipeds then extend ventrally and rub the inner margins of the propus and carpus together allowing the multidenticulate comb and serrate setae to remove collected debris.

Rejection of Unpalatable Items

The rejection mechanism of unpalatable material is highly efficient in *T. orientalis*. A reversal in action by the first and second maxillipeds forcibly pushes it away from the mandibles, and simultaneously the anteriorly flowing feeding current is forced in the reverse direction, although the mechanism by which this is achieved is unclear. The third maxilliped dactyls then flick ventro-laterally to ensure the item is well clear of the oral region.

Mode 2: large and/or hard food greater than 10 mm^3

Food received from the first and second perieopods is grasped between the crista dentata of the third maxillipeds, with the simple stout and elongate setae on the dactylus and propus acting as accessory gripping structures (Fig. 3.23A). It is then presented to the mandibles which open to clamp the inner end of the food mass in a shearing action (Fig. 3.23B). However, compressional forces exerted are generally insufficient to cut through hard material. The third maxillipeds then pull ventrally on the food mass which is stretched between them and the mandibles in a tearing action (Fig. 3.23B). The stretched food is macerated by the second maxillipeds, which make alternating latero-medial strokes using primarily the dactyl simple stout setae as well as the simple elongate setae of the propus to fray the food. When food is cut, the inner end is pushed into the oesophagus by dorso-medial movement of the first maxillae (Fig. 3.23B). The third maxillipeds open and the dactyls re-position the remainder of the food between the crista dentata for another insertion between the mandibles (Fig. 3.23C). Movements of the membranous lobe, labrum and paragnaths are similar to that described in mode 1. The relative times of mouthpart movements during a representative ingestion sequence are shown in Fig. 3.22.

This sequence is repeated numerous times particularly with large hard items, where a resting period of up to 30 seconds is common between insertions. When a hard item (fish vertebra, prawn exoskeleton) is unable to be ingested, it is held between the third maxillipeds as the second maxillipeds pluck flesh from around the vertebrae/skin/scales using their dactyl setae. Flesh is then passed dorsally between the mandibles as the hard material is rejected by ventrally directed flicking of the third maxilliped dactyls.

The rate of ingestion is dependant on the size and texture of food, although in general, both ingestion modes enable *T. orientalis* to consume pieces of flesh very rapidly. This is particulary true of small soft flesh items (mode 1) where a regression analysis revealed a relationship between the rate of ingestion (seconds) and food size (mm^3) to be, Rate of Ingestion = 0.16 x (food size) + 3.18, where $r^2 = 0.55$. Hence a 10 mm^3 piece of flesh can be ingested in 4.8 s. Ingestion of hard items (mode 2) is considerably longer, up to several minutes, after which time they are generally rejected.

Figure 3.23. Sequential mouthpart movements of *T. orientalis* during large and/or hard food ingestion. Refer to text for detailed explanation. Arrows indicate: **A.** inward and dorsal movement of the third maxillipeds to grasp food and present it to the mandibles; **B.** the mandibles close and the third maxillipeds move ventrally as the second maxillipeds move latero-medially, followed by dorso-medial movement of the right first maxilla; **C.** after opening the third maxillipeds move inward and dorsally to insert another section of food between the mandibles. Scale, 3 mm.
cd, crista dentata; md, mandible; md2en; second maxilliped endopod; md3en, third maxilliped endopod; md3en i, third maxilliped endopod ischium; md3ex, third maxilliped exopod; ml, membranous lobe; mx1d, first maxilla distal endite.

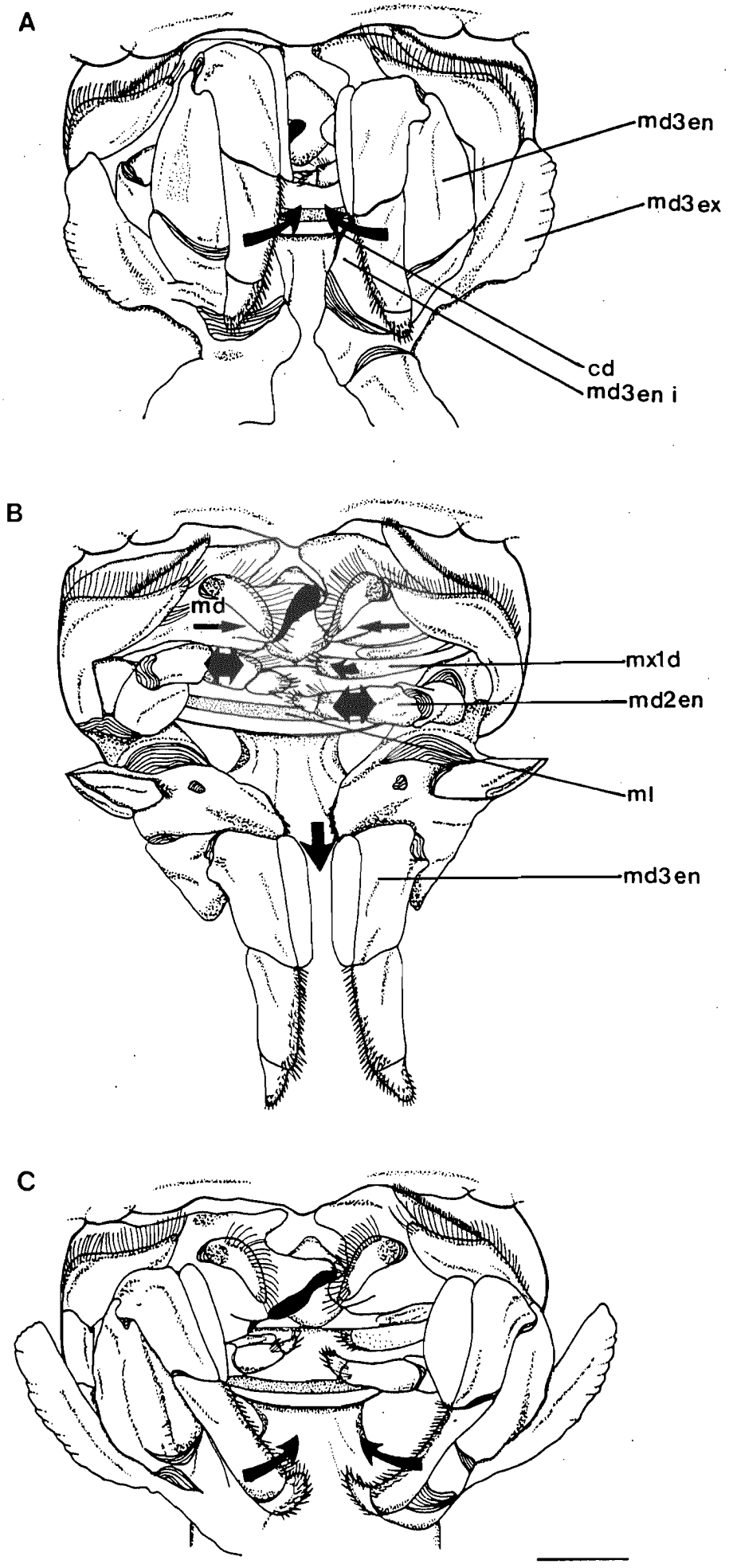
A
md3en
md3ex
cd
md3en i
B
md
mx1d
md2en
ml
md3en
C

There are also differences in both the relative times and number of mouthpart movements between the two modes of ingestion (refer Fig. 3.22), notably the increased mandibular chewing and third maxilliped movement with large hard items. This functional differentiation of the third maxillipeds during ingestion is supported by the highly significant difference in the number of beats between modes 1 and 2 (Mann Whitney statistic $U = 364.5$, $p<0.001$, Table 3.4).

Table 3.4. Mann Whitney U test on the number of third maxilliped beats between ingestion mode 1 and 2 where mode 1 is for small soft food items and mode 2 is for large and/or hard food items. Mann Whitney U statistical significance is shown (p) where $\alpha = 0.05$.

Ingestion Mode	Mean Rank	U	p
1	14.5	13.5	-
2	33.5	364.5	<0.001

3.4 DISCUSSION

Mouthpart Structure and Function

The application of video recording techniques together with SEM has provided detailed information on the process of ingestion and the functional morphology of the mouthparts of *T. orientalis*. Setae facilitate the specific roles of mouthparts in ingestion and perform accessory functions such as prevention of fouling and food loss. The feeding appendages are designed to handle soft flesh items which is consistent with the internal structure of the proventriculus (refer Ch 4).

In general, mouthpart structure is similar to that of the scyllarid *I. peronii* (Suthers and Anderson, 1981), reflecting a comparable body form, habitat and diet. The principal difference is the reduction of the distal and proximal endites of the first maxillipeds in *T. orientalis*. This is functionally significant as the first maxillipeds do not play an active role in ingestion, whereas the endites of this mouthpart aid in food transfer in *I. peronii* (Suthers and Anderson, 1981). Other relatively minor differences are that the third maxillipeds are less robust than in *I. peronii* and do not have its characteristic broad ridged merus. The maxilliped exopods are also broad and flattened in contrast to the tapered exopod flagellum on the maxillipeds of *I. peronii*, a feature consistent with other palinurans. Although SEM of mouthpart setation was not performed on *I. peronii* the distribution and density appears identical to that of *T. orientalis*.

Although both of these scyllarids share common structural characteristics and setation with the mouthparts of other macrophagous decapods, because of their dorso-ventrally flattened body form they differ fundamentally in dorso-ventral flattening of the maxillipeds and extensive fusion of anterior mouthpart segments. A reduction in development of the crista dentata and mandibles is also apparent. The crista dentata are blunt and few in number compared with the sharp massive teeth of many macrophagous groups such as hermit crabs (Kunze and Anderson, 1979) and predatory brachyurans (Skilleter and Anderson, 1986; Creswell and Marsden, 1990). The mandibles are also considerably less robust, lacking sharp incisor processes and a molar plate. Development of these macerating structures is positively correlated with macrophagy (Caine, 1975a; Kunze and Anderson, 1979) so differences may be attributable to the primarily soft flesh diets of *T. orientalis* and *I. peronii*. Strong gripping ability by the crista dentata and cutting and grinding by the mandibles is therefore unnecessary. Food is gripped by the

crista dentata as well as the simple stout setae on the dactylus and propus. The mandibles remain open during ingestion of small soft items (refer Fig. 3.22) and are capable of little compressional forces on large, hard items so that most are rejected. The primary role of the mandibles is to tear food during co-ordinated action with the third maxillipeds. Mastication is carried out primarily by the gastric mill (refer Ch 4). The food type ingested by macrophagous species is therefore an important factor in the development of macerating structures.

Two modes of ingestion allow *T. orientalis* to consume a range of food types and sizes that would otherwise be unavailable and by each mode specialising in a particular size range and type *T. orientalis* maximises ingestion efficiency. This increases survival advantage as scavengers such as *T. orientalis* must be capable of ingesting a variety of organisms, quickly and easily, if they are to exploit a habitat successfully. Mode 1 is used for small flesh items less than 10 mm^3 and is consistent with microphagous ingestion exhibited by many decapods (Caine, 1975b; Alexander and Hindley, 1985; Manjulatha and Babu, 1991). However, several differences in the role and participation of individual mouthparts exist, based primarily on the nature of food items being ingested as well as structural modifications of scyllarid mouthparts. Mode 2 is used for larger and harder items greater than 10 mm^3 and is consistent with macrophagous ingestion documented in other decapods (Kunze and Anderson, 1979; Alexander *et al.*, 1980; Suthers, 1984; Skilleter and Anderson, 1986). In contrast to mode 1 the role of the mouthparts is essentially the same as in macrophagous ingestion. Two ingestion modes were also confirmed by the functional differentiation of the third maxillipeds between modes (Mann Whitney U statistic, $p<0.001$, Table 3.4). In both modes the third maxillipeds receive food from the pereiopods. However they have a minor role in mode 1, simply passing food to the second maxillipeds, their movements independent of the second maxillipeds, first maxillae and mandibles (Spearman rank correlations, Table 3.3). In mode 2, they have an active role in manipulating food and passing it between the mandibles (Fig. 3.23A,B).

Mode 1 is characterised by the highly co-ordinated alternating action of the second maxillipeds and first maxillae which is responsible for the insertion of food between the mandibles (Spearman rank correlation, Table 3.3). The importance of the second maxillipeds and first maxillae is verified by their highly significant correlation with

the mandibles indicating that movement of the mandibles is entirely dependant on the action of these mouthparts. Their active role in mode 1 is shown by their greater number of beats compared with the other mouthparts (Fig. 3.22, One way Anova, $p<0.001$).

This functional integration between the second maxillipeds and first maxillae is not exhibited in microphagous ingestion by other decapods. The second maxillipeds are normally closed to prevent food loss and the simple elongate setae on the merus of the endopods roughly sorts particulate material. Furthermore it is the endites of the first maxillipeds and second and first maxillae which operate sequentially to pass food into the mouth (Caine, 1975b; Alexander and Hindley, 1985; Hunt *et al.*, 1992). Simple elongate setae are also present on the second maxillipeds of *T. orientalis* but their role in food loss prevention is reduced as particulate material and detritus is not a major component of the diet (Suthers and Anderson, 1981; Jones, 1988). They may, however, sort and prevent sand and silt from entering the preoral cavity. Simple stout setae on the dactylus and propus of the second maxillipeds and distal endites of the first maxillae of *T. orientalis* are particularly well adapted for gripping and digging into flesh to facilitate the transfer of food.

In contrast to microphagous ingestion, the first maxillipeds and second maxillae are not actively involved in the transfer of food in *T. orientalis*. The first maxillipeds have an accessory gripping and cleaning role using the hook-like simple stout setae on the apex of the endopod and multidenticulate toothed setae on the protopod. Multidenticulate digitate setae sparsely distributed on the aboral surface of the epipod are structurally similar to setobranchs reported on the epipodites of several other decapods. They prevent excessive deposition of mud and detritus in the branchial cavity and the fouling of gills (Thomas, 1979; Bauer, 1989). This is particularly important in *T. orientalis* which continually disturbs the substratum whilst foraging and feeding.

The scaphognathite of the second maxilla generates the respiratory current in the branchial chamber. This is enhanced by the peripheral plumose setae which enlarge the surface area of the appendage, as well as creating a seal between the edge of the scaphognathite and the branchial chamber (Factor, 1978; Lavalli and Factor, 1992). The interlocking arrangement of setules also form a palisade to filter particles, preventing their entry into the branchial chamber (Farmer, 1974; Pohle and Telford, 1981), as do

plumose setae on the distal margins of the second and first maxilliped exopods.

Pappose setae on the periphery of the third maxilliped exopods and endopod coxa and basis prevent sand and epizoic organisms from entering the preoral cavity during foraging and food transfer. Those on the outer margin of the first maxilliped exopods guard the branchial chamber and those lining the mandibular palps prevent the loss of food dorsally. Multidenticulate whorled setae on the aboral surface of the third and second maxilliped exopods also trap particulate matter and sand disturbed from the substratum during foraging.

Cleaning by reciprocal rubbing is a common post-ingestion behaviour in decapods to remove trapped particulate matter and food lodged between the mouthpart setae (Felgenhauer and Abele, 1983; Bauer, 1989). Serrate setae on the carpus and propus of the third maxillipeds are known to be involved in this process with the rigid sharp setules morphologically adapted to pick and scrape particles from other setae and appendages (Bauer, 1989). Additional denticules on the setal shaft increase the rasping surface of these setae in *T. orientalis* (Fig. 3.6G). Comb setae are similarly adapted where the serrated edge of each setule enhances scraping (Fig. 3.6E), as has been shown in other decapods (Caine, 1975a; Coombs and Allen, 1978). Sockets allowing some movement reduce setal damage and allows them to conform to the shape of the groomed surface. Multidenticulate spinose setae on the medial merus margin of the third maxillipeds are morphologically adapted for piercing tiny pieces of material trapped between opposing simple elongate and stout setae.

Serrate and comb setae on the third maxillipeds are also involved in antennular preening. The antennules are lowered between the distal segments of the third maxillipeds and pulled upwards to scrape the flagella and their aesthetascs clean (Felgenhauer and Abele, 1983; Bauer, 1989). This keeps sensory sites free of epizoic and sedimentary fouling which would impede distance chemoreception.

T. orientalis has an efficient rejection mechanism for unwanted material, similar to that exhibited by *P. merguiensis* (Alexander and Hindley, 1985). Reversal of the feeding current aids removal, although the mouthpart movements responsible remain unclear. Vigorous beating of the third and second maxilliped exopod flagella are

responsible for creating this current in most reptant decapods (Kunze and Anderson, 1979), but this action would cause contamination in scyllarids as they feed close to a sand or mud substratum. Minimal beating by the exopods and the absence of exopod flagella in *T. orientalis* suggest an alternative mechanism is likely.

Like macrophagous ingestion, mode 2 is characterised by the co-ordinated tearing action of the third maxillipeds and mandibles. It is similar to that exhibited by *I. peronii*, although items handled are larger in *T. orientalis* (>10 mm^3 compared with 5-10 mm^3) (Suthers and Anderson, 1981). Action by the robust simple stout setae on the dactylus and propus of the second maxillipeds of both scyllarids weakens the tissue which is important as the mandibles have little crushing and cutting ability. Manipulation of large items by the third maxillipeds is particularly efficient and is facilitated by simple stout setae on the dactylus and propus which pierce and grip flesh.

T. orientalis can ingest large pieces of flesh very rapidly, an advantage in scavengers. Regression analysis of mode 1 sequences revealed a rate of ingestion of 4.8 s for a 10 mm^3 piece of flesh. This rate of ingestion is attributable to the minimal amount of chewing by the mandibles as well as the co-ordinated action of the second maxillipeds and first maxillae. The longer ingestion rate of *I. peronii* (1-2 min) corresponds to macrophagous (mode 2) ingestion which requires greater manipulation (Suthers and Anderson, 1981). Nevertheless, the rate of ingestion in *T. orientalis* is generally faster as the grinding and rolling of the mandibles of *I. peronii* is not exhibited.

Ingestion mechanisms and mouthpart structure of *T. orientalis* are specialised for the consumption of fleshy items, of which a large size range can be quickly and efficiently ingested. Feeding efficiency is facilitated by the co-ordinated action of mouthparts and the ability to discriminate between different food sizes and textures and adopt the appropriate sequence. The use of two ingestion modes is instrumental in the survival of a slow moving, benthic, armoured scavenger.

Functional Morphology of the Paragnaths

The paragnaths of *T. orientalis*, like those of other decapods, are predominantly glandular. Cuticular pores are dispersed over the oral and aboral surface, beneath which are tegumental glands of the rosette type. Their singular distribution (Fig. 3.13A,B)

differs from *P. merguiensis* which has clusters of 3-5 pores (McKenzie and Alexander, 1989), although Alexander (1988) demonstrated that pore arrangement may differ significantly between groups of crustaceans. Setae were not present on the paragnaths of *T. orientalis*. Alexander (1988) believed that setae on the inner paragnath margins of microphagous feeders assist in the retention and transference of food from the food canal to the mouth. However, as *T. orientalis* is macrophagous this role is performed by the larger setose and more flexible second maxillipeds and first maxillae (refer Ch 3.3.4).

Each tegumental gland is composed of 4-8 secretory cells surrounding a central duct cell, from where a duct extends to the gland periphery (Fig. 3.14C,D). This structure resembles tegumental glands described by others (Gorvett, 1946; Aiken and Waddy, 1982; Alexander, 1989). Ultrastructural examination revealed two gland types in *T. orientalis*, whereas Alexander (1989) reported only one in *P. serratus*, but noted cytoplasmic differences between cells of the same gland and attributed their metachromasia to different physical and chemical properties of their mucosubstances. Based on cytological differences, two types were reported in the gills of *P. pugio* (Doughtie and Rao, 1982). Gland type 1 superficially resembles type A of *P. pugio* as both have similar secretory vesicles and central cell extensions into the secretory cell apices. However, the central cell of *P. pugio* forms part of the peripheral rosette, positioned adjacent to the duct, whereas that of *T. orientalis* does not. *P. pugio* also has a canal cell ensheathing the duct, whereas the duct of *T. orientalis* is simply an outward extension of the interdigitate duct cell. The large apical metachromatic vacuole in gland type 2 of *T. orientalis* has not been reported in any crustacean.

Cytological characteristics of both gland types, including numerous mitochondria, Golgi apparatus, endoplasmic reticulum and granular vesicles, confirm they are secretory (Arsenault *et al.*, 1979; Johnson and Talbot, 1987). Histochemical analysis revealed they both contain acid mucopolysaccharides (Table 3.2), indicating they are involved in the secretion of mucosubstances (Brimacombe and Webber, 1964). Although a single continuous duct between the gland and paragnath surface could not be identified, the opening of gland ducts into connective tissue strands (Fig. 3.14C), their acidophilic nature (Table 3.2) and proximity to pore channels in the cuticle (Fig. 3.14B) suggests the strands contain a common duct leading away from glands to the surface.

Many roles have been ascribed to the tegumental glands, the majority reflecting their position in the body (see review by Alexander, 1989). Of the 7 publications which histochemically detail the secretions of tegumental glands, all reported the presence of acid mucins (see Stevenson and Murphy, 1967; Shyamasundari and Hanumantha Rao, 1977, 1978; Shyamasundari, 1979; Erri Babu *et al.* 1979; Kumari *et al.* 1983; McKenzie and Alexander, 1989). In the paragnath glands of *T. orientalis* these were further identified as carboxylated, whereas Shyamasundari and Hanumantha Rao (1978) reported sulphated acid mucins in oesophageal glands of the same species. This difference is due to the presence of either active sulphate or carboxyl groups on the acid radicals of the mucin (Kiernan, 1990). Shyamasundari and Hanumantha Rao (1978) also detected neutral mucins and to some extent glycoproteins in the oesophageal glands of *T. orientalis*, both of which were absent in the paragnathal glands examined in this study.

It is well established that acid mucins contain hyaluronic and sialic acids (Cook, 1972). The presence of these compounds in the oesophageal glands of *T. orientalis* (Shyamasundari and Hanumantha Rao, 1978) and the isopod *Ligia exotica* Roux (Kumari *et al.*, 1983) led these authors to believe their secretions are used to lubricate the oesophageal lumen for easy passage of food. McKenzie and Alexander (1989) concluded glandular products of the paragnaths and second maxillipeds of *P. merguiensis* have a role in feeding by lubricating large particles and entangling particulate matter in mucus. A similar function was proposed by Shyamasundari and Hanumantha Rao (1977) for the oesophageal, maxillae and maxilliped glands of the amphipods *Talochestia martensii* Weber and *Orchestia platensis* Kröyer. These conclusions are verified by the physical properties of hyaluronic and sialic acids as both form highly viscous solutions, the former imparting to joint fluids their lubricating and shock absorption properties (Brimacombe and Webber, 1964) and the latter being commonly found in salivary and branchial glands (Cook, 1972).

Based on the histochemistry of paragnath tegumental glands of *T. orientalis* and their proximity to the oral cavity, it is likely their secretions are also lubricatory. This is important as *T. orientalis* ingests large items of flesh which require much lubrication for efficient passage into the mouth and oesophagus (refer Ch 3.3.4). The presence of acid mucopolysaccharide regardless of satiation level suggests secretory products are produced continuously and stored in the secretory cells. Thus a supply of mucus is

readily available whenever the need for ingestion arises. This is beneficial as *T. orientalis* is a scavenger (Jones, 1988) which must ingest food quickly as soon as it is located.

Based on the abundance of tegumental glands in the mouthparts and oesophagus of crustaceans many early workers such as Huet (1893 in Yonge, 1924) and Ide (1892 in Kumari *et al.*, 1983) believed they have a digestive function. The only biochemical evidence for this was detection of the carbohydrases: maltase, salicinase, lactase, amylase, invertase and glycogenase in the mandibular glands of *P. martensi* by Tyagi and Kaushik (1970). However, no methodology or quantitative data were provided. Histochemical analyses by a number of workers have cast doubt on the role of tegumental glands in digestion. Results demonstrated only marginal staining for glandular protein in all species tested (Stevenson and Murphy, 1967; Shymasundari and Hanumantha Rao, 1977, 1978; Erri Babu *et al.*, 1979; Kumari *et al.*, 1983). Likewise, tegumental glands in the paragnaths of *T. orientalis* stained only moderately positive for protein. This is most likely attributed to polypeptide chains covalently bound to the hexosamine sugars of the glycoprotein matrix of the mucin (Cook, 1972), rather than the presence of digestive enzymes. This is supported by the inability to detect the protease trypsin in the closely associated membranous lobe using immunohistochemical techniques (refer Ch 5).

In contrast to the majority of crustaceans, the paragnaths of *T. orientalis* are connected to the membranous lobe rather than the metastomal sclerite, and are supported only by an endophragmal rod along the proximal side (Fig. 3.2B; 3.12). Therefore they do not have the structural basis needed for extensive movement along the mandibular gnathobase, simply sliding inwards after food insertion between the mandibles. Consequently, the paragnaths of *T. orientalis* are incapable of total closure. In contrast, Alexander and Hindley (1985) and Hunt *et al.* (1992) reported that the paragnaths of *P. merguiensis* open laterally during feeding to allow food to enter the mouth and then close forming a tight seal to prevent food loss. Food loss in the scyllarid is prevented by a reduction in size of the oral cavity by coordinated protraction of the labrum and membranous lobe (see below). Therefore the paragnaths of *T. orientalis* do not participate actively in the ingestion mechanism; their primary role being the secretion of mucus for lubrication of large food items to aid in their swallowing.

Functional Morphology of the Membranous Lobe

Position of the Membranous Lobe

The membranous lobe of *T. orientalis* is similar to the metastome illustrated by Snodgrass (1951) in *Scyllarus americanus* Smith. He defined the metastome as a pair of anterior lobes, the paragnaths, and/or a single posterior lobe arising from the metastomal plate at the end of the maxillary sternum between the first maxillae. The membranous lobe of *T. orientalis,* however, arises from the sternal sclerite between the second maxillipeds (Fig. 3.2B). Suthers and Anderson (1981) illustrated the muscular protuberance (metastome) of *I. peronii* in a similar position to the lobe of *T. orientalis.* This position was also found in other scyllarid genera examined including: *Scyllarides, Scyllarus, Parribicus, Evibacus* and *Ibacus.* Consequently, the difference in lobe position in *S. americanus*, illustrated by Snodgrass (1951), is incorrect. The membranous lobe arises midventrally from the sternal sclerite between the second maxillipeds, as in all other scyllarids and not between the first maxillae as depicted by Snodgrass (1951). It is probable that the membranous lobe of scyllarids is a modified metastome arising posteriorly between the second maxillipeds.

Although Snodgrass' definition of the metastome includes a posterior lobe, no other decapod has a membranous lobe comparable with that of scyllarids. The scyllarid lobe does, however, superficially resemble the lingua of Isopoda, which is homologous to the posterior lobe of the metastome and is supported on the metastomal sclerite between the first maxillae (Snodgrass, 1951). Its morphology and role within the preoral cavity have not been documented so comparisons with the scyllarid lobe are difficult. Nevertheless, it would be interesting to ascertain whether possession of the posterior lobe is related to the dorsoventrally flattened body form characteristic of scyllarids and isopods.

The membranous lobe also superficially resembles the labium of insects which forms the posterior boundary of the mouth and is derived from fusion of a pair of appendages serially homologous with the second maxillae (Richards & Davies, 1977). Unlike the lingua their role is well established; the distal segment, or prementum, closes the preoral cavity and the palpi are mainly sensory (Chapman, 1982). Based on structural and feeding differences it is unlikely these functions are similar to those of the scyllarid lobe.

Role of the Membranous Lobe in Ingestion

The membranous lobe has a number of functions associated with ingestion. Numerous anteriorly directed annulate setae, microscales and microspines on the strengthening rod create a roughened surface to help grip food as it is passed by the second maxillipeds and first maxillae over the lobe surface, preventing it slipping away during ingestion. Setules on the whorled and cuspidate annulate setae are particularly suited for this.

Tegumental rosette glands beneath the oral surface contain acidic sulphated mucopolysaccharides and are comparable with those in the metastome of *P. merguiensis* (McKenzie & Alexander, 1989). Acidic mucopolysaccharides form the basis of muco-compounds which are primarily lubricatory in function (Brimacombe & Webber, 1964) and aid in the passage of food along the oesophagus. Mucus secreted onto the lobe surface coats food as it is passed over the aboral lobe surface by the second maxillipeds and first maxillae. Whorled and cuspidate annulate setae may also increase the surface area to facilitate mucus attachment. This lubricates the food prior to its insertion into the mouth for ease of swallowing, which is important for *T. orientalis* as it feeds on large pieces of bivalve mollusc and other items. Scraping of the second maxilliped dactyl tips over the lobe surface before and after insertion ensures mucus also coats the walls of the mouth and oesophagus. Much of this mucus may also be derived from the glandular paragnaths. Hence the lobe acts in concert with the paragnaths to lubricate large items to facilitate ingestion.

Retraction and protraction of the anterior lip is facilitated by the longitudinal and circular muscles within the lobe. Retraction is brought about by simultaneous contraction of the circular muscle which folds the lip ventrally and longitudinal muscle contraction which pulls the lip posteriorly. This dilates the preoral cavity and oesophagus, enabling large items to be swallowed quickly. This action is similar to that of the muscular protuberance of *I. peronii* which is drawn back during ingestion (Suthers & Anderson, 1981). Relaxation of these muscles allows the lobe to protract to its original position and prevent food loss after insertion. These movements and musculature are similar to those of the labrum of *Homarus gammarus* Linnaeus described by Robertson and Laverack (1979). During ingestion, the labrum moves simultaneously with the lobe lip so that both

act in concert to regulate the size of the preoral cavity and control the rate of food ingestion.

During retraction and protraction of the anterior lip structural support is provided by the median strengthening rod which prevents lateral compression of the lobe. Additional support is provided by the abundant collagenic connective tissue as the triple helix formation of polypeptide strands within the collagen fibrils provide strength and structural rigidity (Kiernan, 1990).

Small rhythmical pulsations of the lobe and labrum in *T. orientalis* followed ingestion. Robertson and Laverack (1979) noted small rhythmical swallowing movements in the labrum of *H. gammarus* following ingestion and found that it was related to the amount of food already consumed, with starved animals having short and fed animals much longer sequences. They concluded it was related to oesophageal peristalsis as is probably the case in *T. orientalis*.

It is unclear whether annulate setae serve a chemosensory or mechanosensory role during ingestion. Absence of an obvious apical pore suggests chemoreception is unlikely, as this pore enables the necessary diffusion of chemicals (Altner and Prillinger, 1980). However, an apical pore is not necessarily indicative of chemoreception as thin walled aesthetascs have been reported in which diffusion of chemicals occurs through the cuticle (Ghiradella *et al.*, 1968). Despite the absence of nervous tissue in the lobe electrophysiological examination of the setae is required before their chemoreceptive role is discounted. It may be inferred from their very abundance that microscales and microspines are not sensory as known sensilla tend to be restricted in their distribution and few in number (Ache, 1982).

It is possible that annulate setae are mechanosensors which, upon displacement by either the first maxillae or food itself, signal initiation of retraction of the anterior lip in preparation for ingestion. The general morphology of annulate setae conform to that of other cuticular mechanosensors; they are devoid of pores and bear a sharp tip, cuticular denticules and an articulating socket membrane (McIver, 1975).

Spherical Cells

Histochemical tests showed spherical cells contain protein and neutral mucopolysaccharide but no glycoprotein (Table 3.2). They have few cytoplasmic organelles and the peripheral nucleus indicates they are probably involved in the storage of these compounds.

The location of spherical cells in the lobe as well as the connective tissue of the paragnaths indicates a link with digestive processes. They stain intensely for protein but it is unlikely that they store digestive enzymes based on the inability to detect trypsin in membranous lobe tissue using immunohistochemical techniques (refer Ch 5). Furthermore, stored enzymes have only been reported in the form of inactive zymogen granules which are usually discrete structures in the cell cytoplasm (Al-Mohanna *et al.*, 1985b).

The cells may have an endocrine function as endocrine glands are not necessarily multicellular, but in invertebrates, they may be in groups of individual cells in the connective tissue (Welsch & Storch, 1975). Peptide hormones are associated with the alimentary tract and Kiernan (1990) states that endocrine cells often contain large quantities of secretory granules in which the biogenic amines are bound to a carbohydrate or protein matrix. The histological and histochemical features of these cells comply with these descriptions. However, they lack the obvious features of endocrine secretory cells which contain large quantities of endoplasmic reticulum, Golgi apparatus and mitochondria. They also show no obvious cytological changes with sex, time of moult and nutritional status, all of which influence the activity of endocrine glands.

Spherical cells increase in size and abundance as the animal matures and may be the result of accumulation of digestive products with age. Whether this is a reflection of different dietary preferences of juveniles and adults is not known. The increase in granulation and decrease in mucin concentration in starved individuals indicates their contents are either chemically modified or mobilised in response to nutritional requirements. In addition to a storage function of the spherical cells, the prevalence of glycogen granules in the lobe tissue demonstrates that it also stores metabolic products. These too would be mobilised during periods of nutritional stress.

As suggested by its size and conspicuous position within the preoral cavity the membranous lobe has several roles related to ingestion. Firstly, microscales, microspines and annulate setae grip food preventing its loss and provide a large surface area for mucus coverage. Secondly, it secretes acidic mucopolysaccharides which lubricate food during ingestion. Lastly, retraction and protraction of the anterior lip regulates the size of the preoral cavity and thereby controls (with the labrum) the passage of food during ingestion. Hence the unique possession of this specialised mouthpart in *T. orientalis* and other scyllarids is directly related to the ability to ingest particularly large items extremely quickly and efficiently, as demonstrated in Ch 3.3.4.

Chapter 4. Structure and Function of the Alimentary Tract

4.1 INTRODUCTION

The decapod alimentary tract performs a number of important roles including extra- and intracellular digestive processes, absorption and storage of nutrients and excretion and defecation of waste products. In all groups the tract is divided into an ectodermally derived, cuticle-lined foregut and hindgut and an endodermally derived uncuticularised midgut (Icely and Nott, 1992). The foregut occupies the anterior cephalothorax and is divided into an oesophagus and proventriculus, the latter being separated into a cardiac and pyloric stomach, containing the gastric mill and filter press, respectively. The midgut extends from the posterior of the pyloric stomach to the hindgut and varies in length from very short in the freshwater crayfishes (Astacidea:Astacidae) to very long in the lobsters (Astacidea:Nephropidae) (Icely and Nott, 1992). The paired digestive glands extend from the midgut. There may also be a pair of anterior midgut caeca adjacent to the sides of the foregut (Brachyura, Anomura) or a single caecum dorsal to the foregut (Penaeidae, Astacidae, Thalassinidea), as well as a posterior midgut caecum (Smith, 1978). The hindgut is essentially a simple tube leading from the midgut to the anus.

Foregut

Evolution

The proventriculus of all decapods has a similar structural plan (Mocquard, 1883; Yonge, 1924; Patwardhan, 1935a-d; Reddy, 1935; Schaefer, 1970; Powell, 1974). Based on numerous comparative studies it has been found that proventricular complexity and robustness, in particular that of the gastric mill, varies and tends to increase in parallel with decapod evolution (Caine, 1975a,b; Kunze and Anderson, 1979; Ngoc-Ho, 1984; Skilleter and Anderson, 1986; Growns and Richardson, 1990). This occurs through the infraorders Caridea, Astacidea, Thalassinidea, Palinura and Anomura and culminates in the Brachyura.

Although the form of the decapod proventriculus depends primarily on phylogenetic history of a species, it can also be modified by diet and feeding habit (Dall and Moriarty, 1983; Felgenhauer and Abele, 1989). In particular, gastric mill structure is

positively correlated with macrophagy, with increasing robustness and complexity through filtering, detrital, omnivore and carnivore feeders (Caine, 1975a,b; 1976). For example, detritivores have a finely toothed or setose gastric mill with blunt masticating ossicles, whereas in macrophagous carnivores it is strongly toothed and sparsely setose with the masticating portions sharp and cutting (Schaefer, 1970; Caine, 1975a; Kunze and Anderson, 1979). A similar trend is also shown by the cardio-pyloric valve which is setose in detritivores, but is spinose and has additional large teeth in carnivorous species. It is unclear whether variation in mesh sizes and spacing between longitudinal channels in the pyloric stomach filter press is similarly attributable to diet or is simply a function of an individual's size as suggested by Powell (1974). Schaefer (1970) and Caine (1976) believe increasing width between channels is indicative of macrophagy, whereas Kunze and Anderson (1979) found this relationship did not exist in anomurans.

Functional Morphology

Despite the diversity of internal foregut morphology in the decapods, its major features are remarkably uniform and are based on the close association between the stomach and the digestive gland to carry out the early phases of extracellular digestion (Icely and Nott, 1992). A number of structures are specialised to perform processes involved in the overall reduction of ingested food to a liquid state (Schaefer, 1970). These include i) physical degradation by gastric mill mastication; ii) chemical hydrolysis by digestive enzymes secreted from the digestive glands; iii) separation of particles and fluid from coarse material by setal filters; and iv) transport of particles and fluid into the digestive gland and transport of coarse indigestible material via the midgut for defecation from the hindgut (Icely and Nott, 1992).

The oesophagus is a highly muscular tube often possessing a series of longitudinal folds which expand to allow large food items to enter the cardiac stomach (Barker and Gibson, 1977). This passage is aided by peristaltic contractions of its walls and lubrication by mucus (acid mucoploysaccharides) secreted via ducts from abundant tegumental rosette glands, particularly beneath the anterior epithelium (Barker and Gibson, 1978; Erri Babu *et al.*, 1982). In many groups there is an oesophageal valve and/or sphincter at the junction with the cardiac stomach which prevents the regurgitation of food (Powell, 1974; Kunze and Anderson, 1979).

The cardiac stomach is a large distensible sac which acts as a crop in macrophagous species, allowing them to ingest large quantities of food at a time. Solids are passed posteriorly into the gastric mill by peristalsis of the cardiac wall together with ventral setal brushes and supralateral teeth, which form a line along the lateral walls (Powell, 1974; Kunze and Anderson, 1979). The cardio-pyloric valve lies at the back of the gastric mill and together with the setose lateral walls can completely close the aperture to the pyloric stomach (Coombs and Allen, 1978). This prevents large items leaving the cardiac stomach prior to trituration by the gastric mill.

Skeletal Structure

The chitinised walls of the proventriculus are variably thickened to produce an articulated network of up to 33 ossicles (Maynard and Dando, 1974). Although a basic arrangement of proventricular ossicles and musculature is shared by all decapods, distinctive modifications in the number, size, shape and degree of calcification exist between taxonomic groups (Meiss and Norman, 1977; Kunze and Anderson, 1979). Variations are usually more marked in the cardiac than pyloric stomach ossicles (Meiss and Norman, 1977). They serve as attachment sites for the proventricular muscles which are in turn controlled by a discrete extension of the central nervous system, the stomatogastric, that operates the proventriculus (Maynard and Dando, 1974).

The gastric mill comprises a median tooth mounted dorsally on the propyloric ossicle and a pair of lateral teeth mounted on the paired zygocardiac ossicles (Powell, 1974). The teeth move in rhythmic co-ordinated sequences brought about by contraction of musculature attached to supporting ossicles (Maynard and Dando, 1974). Essentially food is cut by the dorso-medial movement of lateral teeth and then ground on the ridged surface of the lateral teeth by the antero-ventral movement of the median tooth. Although this robust grinding action is characteristic of many higher Decapoda (Schaefer, 1970; Kunze and Anderson, 1981; Ngoc-Ho, 1984), several modifications exist which reflect tooth form and diet (Suthers and Anderson, 1984; Suthers, 1984). More than one type of action is also possible such as the "squeeze" and "cut and grind" modes documented by Heinzel (1988) and the "chewing" and "compression" modes reported by King and Alexander (1994). In higher decapods the cardio-pyloric valve may contribute to the gastric mill action by forcing material to accumulate between the teeth of the mill and by providing a surface on which material can be abraded (Icely and Nott, 1992).

During trituration, the fluids squeezed from food percolate ventrally through a primary setal filter overlying a pair of ventro-lateral channels on the cardiac floor (Powell, 1974). This filter allows only fine particles and fluid to enter the ventral fluid passageway which moves the fluid posteriorly around the cardio-pyloric valve and into the filter press located in the ventral pyloric chamber (Powell, 1974). Indigestible material passes directly into the dorsal chamber of the pyloric stomach which is separated from the filter press by a setose ventro-lateral partition.

The pyloric stomach is responsible for the final filtration of particles prior to their entry into the digestive gland, as well as regulating the movement of solids into the midgut. The filter press (or secondary filter) is morphologically consistent throughout the decapods and is separated into two halves by intrusion of the interampullary ridge from the stomach floor (Icely and Nott, 1992). The outer surface (valve) of each half is covered in a dense matt of dorsally directed filtration setae, whereas the inner surface (valve) has numerous longitudinal rows of filter setae that form a series of filtration channels. Each row of setae extends dorsally to overlie the setae of the upper row. The widths of the filtration channels range between 10 and 46 μm while the widths between the filter setae range from 0.5-4 μm (Schaefer, 1970; Powell, 1974; Kunze and Anderson, 1979). These channels merge at the ventro-posterior of the filter press and open into the primary ducts of the digestive gland (Lovett and Felder, 1989).

Fluid entering the filter press is squeezed against the inner valve filtration setae by compression of the outer valve. Fine particles (less than 1 μm) and fluids which pass between the setae move along the channels and are collected into the primary ducts of the digestive gland where the final stages of digestion (intracellular) and absorption take place. The filter press ensures only particles in the colloidal size range are able to enter the delicate digestive gland tubules (King and Alexander, 1994). Any material retained on the setae is deflected dorsally into the dorsal chamber for removal. Posteriorly the dorsal chamber is referred to as the faecal compaction zone where indigestible material is squeezed to extract any remaining juices before it enters the midgut (Powell, 1974). The efficiency of this process is enhanced in particulate feeders by pyloric fingerletts. Once fluids are removed, the solids pass out of the proventriculus and eventually leave the animal as faeces.

At the junction of the foregut and midgut is a pyloro-intestinal valve, descriptions of which remain incomplete (Lovett and Felder, 1989). It comprises cuticular protrusions

(sheaths) of the dorsal and lateral walls of the posterior pyloric stomach which terminate within the midgut lumen, and presumably control the final extrusion of faecal material without contaminating the filtrate entering the digestive gland (Icely and Nott, 1992).

Circulation of Fluids

There are three theories of fluid circulation within the proventriculus (see Icely and Nott, 1992), but that proposed by Powell (1974) is considered to be most accurate and applicable to the majority of decapods which possess similar internal structures (Dall and Moriarty, 1983). Based on the movement of injected dyes in a living thallasinid, Powell (1974) proposed that a pyloric pump drove fluid sequentially into the filter press and digestive gland. A dorsal passage booster pump moves digestive gland secretions dorsally, via a pair of ventrodorsal channels into the dorsolateral channels above the dorsal pyloric chamber. These secretions containing digestive enzymes move anteriorly along the channels into the cardiac stomach to complete the circulation of fluids and begin initial extracellular digestion.

Powell (1974) was unable to demonstrate the existence of the booster pump so that the problem of how fluid exited the digestive gland remained. This has been recently clarified by King and Alexander (1994) in the banana prawn *P. merguiensis*. They used similar techniques to demonstrate that fluids are removed from the digestive gland by suction created behind the median tooth as it swings anteriorly during normal gastric mill activity. This fluid then moves dorsally and anteriorly through the dorsoventral and dorsolateral channels, respectively, into the cardiac stomach thus verifying Powell's model of circulation.

Some confusion concerning the passage of fluid into and out of the digestive gland still remains. Other hypotheses proposed for the entry of fluids are: internal pressure of the proventriculus and action of the filter press (Dall, 1967) and antiperistaltic waves of the midgut (Lovett and Felder, 1990a). Further examination of this mechanism needs to be made in a number of groups before they can be applied to the majority of decapods.

Midgut

The midgut is responsible for the final stages of digestion including i) intracellular digestion of products received from the foregut; ii) production and supply of digestive enzymes for the foregut; iii) absorption and processing of digestive products either by

transport to the haemolymph or storage as lipid and glycogen; iv) detoxification of metals and foreign organic substances; and v) elimination of wastes (Icely and Nott, 1992). These functions are primarily attributable to the digestive gland which dominates the midgut in both volume and complexity and hence plays a central role in the digestive processes of decapod crustaceans (Brunet *et al.*, 1994). Consequently, its structure and function form an important part of this thesis and are considered separately in Ch 5.

Although digestive glands have been well studied, relatively little attention has focused on other regions of the midgut. The midgut trunk is a straight tube of varying length. The general size and shape of the caeca vary markedly between major subgroups of the Decapoda, but are conserved in form within given infraorders (Smith, 1978). These regions are lined with a simple columnar epithelium supported by a thick basal lamina. Epithelial cell cytology is characteristic of physiologically active tissue, exhibiting extensive mitochondria, Golgi apparatus and smooth and rough endoplasmic reticulum (Mykles, 1977; Lovett and Felder, 1990a; Felder and Felgenhauer, 1993).

Based on these structural characteristics, various roles have been attributed to the midgut trunk including i) absorption of nutrients from digested food (Yonge, 1924; Ahearn, 1974; Barker and Gibson, 1977; 1978); ii) absorption of ions and control of net water flux between the midgut lumen and the haemolymph (Yonge, 1924; Mykles and Ahearn, 1978; Mykles, 1980); iii) secretion of the peritrophic membrane (Dall and Moriarty, 1983); and iv) transport of fluids to the foregut and digestive gland by antiperistalsis (Yonge, 1924; Lovett and Felder, 1990a). Some of these functions, in particular the absorption of nutrients, have been assigned on the basis of assumed analogy with the vertebrate intestine. Ahearn and Clay (1988) found rates of solute transport across the midgut epithelium was considerably slower than in the digestive gland and concluded that the midgut trunk does not function significantly in absorptive processes. This was supported by Lovett and Felder (1990b) who found no evidence of alkaline phosphatase activity and hence absorptive ability in the midgut of an adult penaeid.

Functions of the anterior and posterior midgut caeca are equally obscure with the following proposals made: i) they may increase surface area for water absorption at ecdysis (Holliday *et al.*, 1980), or nutrients during digestion (Yonge, 1924); ii) secrete digestive enzymes (Holliday *et al.*, 1980); iii) function in water and ion balance (Mykles, 1977); iv) secrete the peritrophic membrane (Pugh, 1962; Dall, 1967); v) the anterior

caecum may accommodate volume changes during foregut contraction (Powell, 1974); and vi) the anterior caecum may contribute components of digestive fluid which activate enzymes or pH change (Dall and Moriarty, 1983). Lovett and Felder (1990b) could find no evidence of digestive enzyme production (proteases) in the anterior caecum of adult *Penaeus setiferus* Linnaeus. Secretion of the peritrophic membrane and its osmoregulatory role has also been refuted by Holliday *et al.* (1980). Whatever the varied roles of the midgut trunk and caeca may be, Icely and Nott (1992) concluded that their epithelial contributions to the processes of digestion and absorption are probably minor compared with those of the digestive glands.

Hindgut

The hindgut is involved in the expulsion of faeces, as well as anal drinking and antiperistaltic hydraulic functions (Lovett and Felder, 1990a). A peritrophic membrane generally surrounds the faeces containing it as a long pellet. The membrane probably protects the epithelium from abrasive material and may aid efficient defecation (Dall and Moriarty, 1983). Lovett and Felder (1990a) believe it separates chyme and faecal material from extraperitrophic water taken up during anal drinking.

The hindgut is a relatively simple cuticular tube extending from the midgut to the anus, which opens onto the ventral surface of the telson. Longitudinal foldings of the anterior hindgut are common in a number of groups (Dall, 1967; Barker and Gibson, 1977; 1978; Smith, 1978) and may expand to form a valve or sphincter at the midgut-hindgut junction. This was shown in the ghost shrimp *Lepidophthalmus louisianensis* Schmitt to have a dorso-lateral valve and a large mass of acinar glandular tissue (Felder and Felgenhauer, 1993). A range of functions were proposed for the acinar glands including mucus production, contribution to the peritrophic membrane or binding agents to faecal material. Antifouling, antibiotic or surfactant effects were also hypothesised based on knowledge of anal drinking in decapods which potentially introduces a host of microbes into the alimentary tract.

Tegumental glands are embedded in the connective tissue beneath the epithelium along the entire hindgut. Like those of the oesophagus, they secrete mucus which lubricates the passage of the faecal pellet (Barker and Gibson, 1977; 1978). Defecation is facilitated by peristaltic contractions of the muscular hindgut wall. During this process the wall grasps the peritrophic membrane via stout cuticular denticules on its surface, so a section of the faecal pellet is extruded during each contraction (Dall, 1967).

Status of Knowledge on Scyllarids and Objectives

Examination of the alimentary tract structure in a wide range of decapod groups has revealed the nature of, and region in which digestive processes take place. Despite such comprehensive knowledge of the decapod digestive system, the Scyllaridae have been relatively ignored with only two studies published on the proventriculus of *Ibacus*. Suthers and Anderson (1981) documented its external morphology and gastric mill structure and action in *I. peronii*. Internal proventricular structure has only been examined in the larval stages (phyllosoma to nisto) of *Ibacus ciliatus* (von Siebold) (Mikami and Takashima, 1993). Although functional inferences on proventricular digestive processes were made for the larval stages, differences in structure and diet with the adult form make direct comparison difficult.

The purpose of the present study was to provide a structural basis on which to understand the process of food digestion in the scyllarid *T. orientalis*. This was achieved by examination of alimentary tract structure, particularly the proventriculus and digestive gland (refer Ch 5) as they play an important role in the digestive processes of crustaceans (Icely and Nott, 1992; Brunet *et al.*, 1994). Complementary information gained from a wide range of techniques (histology, histochemistry and scanning electron microscopy) was collated to provide a detailed description of each region. By examining the entire tract an overall picture of scyllarid digestion, from initial chemical and physical degradation of food in the cardiac stomach to excretion of wastes in the hindgut, was realised. This approach is rare with most studies on decapods concentrating upon the structure and function of only one section of the digestive system (see Powell, 1974, Kunze and Anderson, 1979; Felder and Felgenhauer, 1993; King and Alexander, 1994).

4.2 MATERIALS AND METHODS

4.2.1 Dissection

General morphology of the alimentary tract was revealed by dissection. The proventriculus was sectioned in various orientations to determine the layout of its internal structures. Accurate illustration of all preparations were made with the aid of a camera lucida.

4.2.2 Histology

The alimentary tract was removed from the body (oesophagus to anus) and fixed in marine Bouin's fluid (Winsor, 1984) for at least 48 h. The proventriculus was cut to allow rapid infiltration of the fixative as well as paraffin wax during processing. The picric acid component of the fixative decalcified the ossicles and gastric mill teeth of the proventriculus minimising tearing during sectioning. Specimens were processed according to the method outlined in Ch 3.2.1.3; Appendix 1. Transverse serial sections (6 μm) were taken of the proventriculus to determine the consecutive positions of internal structures, whereas longitudinal and transverse sections (6 μm) were taken of the hindgut. Sections were stained with haematoxylin-eosin and Mallory-Heidenhain (see Appendix 1).

4.2.3 Histochemistry

Sections were stained with periodic acid Schiff (PAS)-alcian blue and mercuric bromophenol blue to determine the presence of mucopolysaccharides and proteins in the alimentary tract, respectively (refer Ch 3.2.1.4; Table 3.1).

4.2.4 Scanning Electron Microscopy of the Proventriculus

Internal morphology of the proventriculus was examined using scanning electron microscopy. Specimens were fixed in formal acetic acid calcium chloride (FAAC) for 24 h and then sectioned in a number of orientations to ensure all aspects of the proventriculus were viewed. In particular, the walls of the proventriculus were sectioned longitudinally and transversely at intervals to determine the precise layout of the gastric mill teeth and ventral floor channels. After sectioning, specimens were ultrasonicated for three x 30 s bursts to remove particulate matter. They were then routinely dehydrated to 100% ethanol, critical point dried, mounted on stubs and gold coated in a Hummer V sputter coater prior to examination on a Philips XL 20 scanning electron microscope at 15 kV.

4.3 RESULTS

The alimentary tract of *T. orientalis* is divided into three regions, the foregut, midgut and hindgut, each representing approximately 25%, 5% and 70%, respectively, of the total tract length. The foregut occupies the anterior cephalothorax and includes the oesophagus and proventriculus, the latter being divided into a cardiac and pyloric stomach (Fig. 4.1A). The midgut is reduced to a small dorsal caecum and a pair of large digestive glands which lie on either side of the proventriculus. Between the midgut and hindgut is the posterior pyloric sector, a region of the tract unique to *T. orientalis*. From here the hindgut extends through the abdomen to the ventrally positioned anus at the telson.

4.3.1 Foregut

4.3.1.1 Oesophagus

The oesophagus is a short tube leading from the mouth into the anterior floor of the cardiac stomach (Fig. 4.1A). Anteriorly, its walls form four longitudinal folds, the dorsal and ventral of which are continuous with the labrum and membranous lobe, respectively (Fig. 4.1B). A thick cuticle lines the columnar epithelium and tegumental rosette glands are densely arranged beneath the basal lamina (Fig. 4.1C). These glands are structurally similar to those of the paragnaths (refer Ch 3) and their contents stained positively with PAS-alcian blue indicating they secrete acid mucopolysaccharide. Longitudinal, circular and radial muscles are present throughout the connective tissue with radial muscles terminating at the epithelium-cuticle border (Fig. 4.1B,C).

4.3.1.2 Proventriculus

The cardiac stomach of *T. orientalis* is a voluminous membranous sac, which when full, occupies the entire anterior cephalothorax (Fig. 4.1A). Posteriorly, its chitinous lining is thickened at definite regions to form the teeth of the gastric mill. The smaller pyloric stomach extends ventro-posteriorly from the cardiac stomach and joins the posterior pyloric sector beneath the dorsal caecum (Fig. 4.1A; see also Fig. 4.13). It is divided into a dorsal and ventral chamber or filter press.

The arrangement of proventriculus ossicles in *T. orientalis* is similar to that of other decapods, although in general they are less calcified and many are much reduced. This is particularly so in the cardiac stomach and consequently a great proportion of its

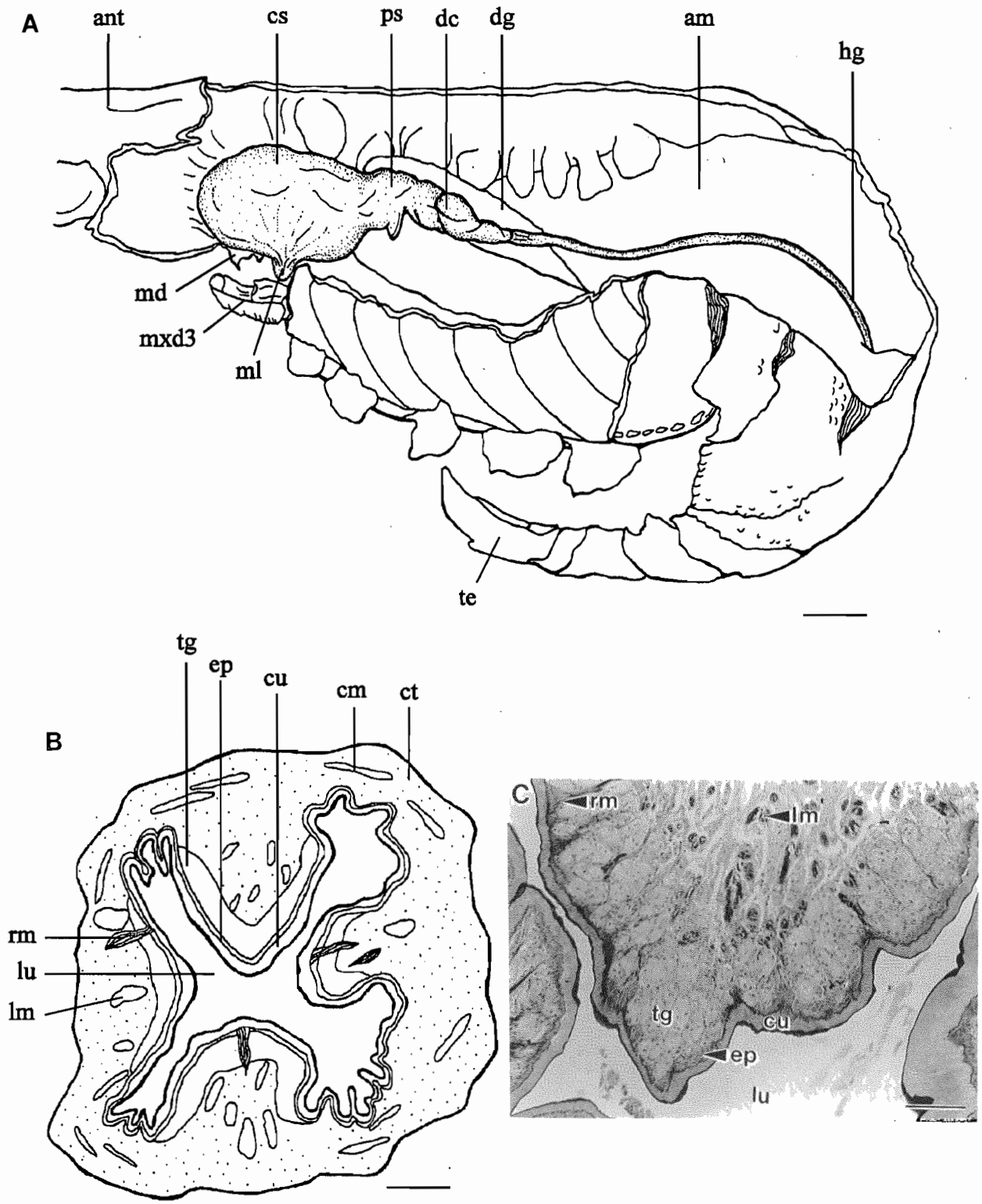

Figure 4.1. A. Sagittal section through *T. orientalis* showing the location of the alimentary tract and its components. Scale, 3 mm. **B.** Diagrammatic transverse section (TS) through the anterior oesophagus illustrating the distribution of tissues. Scale, 0.8 mm. **C.** TS (6 μm) through a lateral fold of the anterior oesophagus. Scale, 0.3 mm.
am, abdominal muscle; ant, antenna; cs, cardiac stomach; ct, connective tissue; cu, cuticle; dc, dorsal caecum; dg, digestive gland; ep, epithelium; hg, hindgut; lm, longitudinal muscle; lu, lumen; md, mandible; ml, membranous lobe; mxd3, third maxilliped; rm, radial muscle; te, telson; tg, tegumental glands.

posterior wall is soft membrane. The mesocardiac ossicle is a thin calcified plate the posterior margin of which hinges with the pterocardiac ossicles (Fig. 4.2; 4.3). The urocardiac ossicle is very much reduced and supports the median tooth of the gastric mill posterio-ventrally. Lateral teeth are supported by the zygocardiac ossicles, the inner margins of which hinge with the propyloric ossicles. The prepectineal ossicles supporting the anterior ends of the zygocardiac are rudimentary. The subdentary ossicle is well developed and extends the length of the gastric mill. Beneath it, the fused posterior lateral cardiac plates and the pectineal ossicles are reduced and pectineal teeth are absent (Fig. 4.2). Supporting the posterior wall of the cardiac stomach are the vertically directed postpectineal and inferior lateral cardiac ossicles.

Ossicles of the pyloric stomach are also less calcified than other decapods. The pyloric ossicle and anterior and middle supra-ampullary ossicles are absent. Nevertheless, the middle pleuropyloric and posterior mesopyloric are well developed, as are the upper ampullary roof ossicle and posterior supra-ampullary ossicle that support the pyloric filter press (Fig. 4.2; 4.3).

Cardiac Stomach

Anteriorly, the cardiac stomach wall is highly convoluted and lacks the complex arrangement of ventral filtration channels seen in other decapods such as prawns and crabs. The stomach surface is studded with minute dorsally directed rigid setae arranged in rows of 4 to 6 individual microspines. Within the posterior third of the stomach, a dorsal infolding of the floor forms two simple ventral channels that extend posteriorly into the gastric mill (Fig. 4.4A,B). Here they diverge to either side of the cardio-pyloric valve and enter the ventral pyloric chamber.

Above the ventral channels is a pair of ventro-lateral channels, which are supported on the postpectineal ossicles (Fig. 4.4A,B). These extend dorso-posteriorly to the cardio-pyloric valve where they merge with the ventral channels leading into the ventral pyloric chamber. Above each ventro-lateral channel is a densely setose outfolding of the cardiac stomach wall (Fig. 4.4A,B). A pair of lateral channels extend posteriorly between the setose outfolding and the lateral teeth of the gastric mill (Fig. 4.4A,B). These broad channels are not highly setose and transfer large indigestible material from the gastric mill into the dorsal pyloric chamber. These merge into two

Figure 4.2. Lateral external view of the proventriculus showing the location of ossicles. The musculature, dorsal caecum and digestive glands have been removed. The cardiac stomach is anterior. Scale: illustration, 3 mm; photograph, 1 mm.
cs, cardiac stomach; mt, median tooth. OSSICLES: aip, anterior inferior pyloric; amp, anterior mesopyloric; aplp, anterior pleuropyloric; exp, exopyloric; ilc, inferior lateral cardiac; lampr, lower ampullary roof; mc, mesocardiac; mplp, middle pleuropyloric; pe/plcp, pectineal/posterior lateral cardiac plate; pmp, posterior mesopyloric; pope, postpectineal; pplp, posterior pleuropyloric; prp, propyloric; psa, posterior supra-ampullary; pt, pterocardiac; sd, subdentary; uampr, upper ampullary roof; up, uropyloric; zc, zygocardiac.

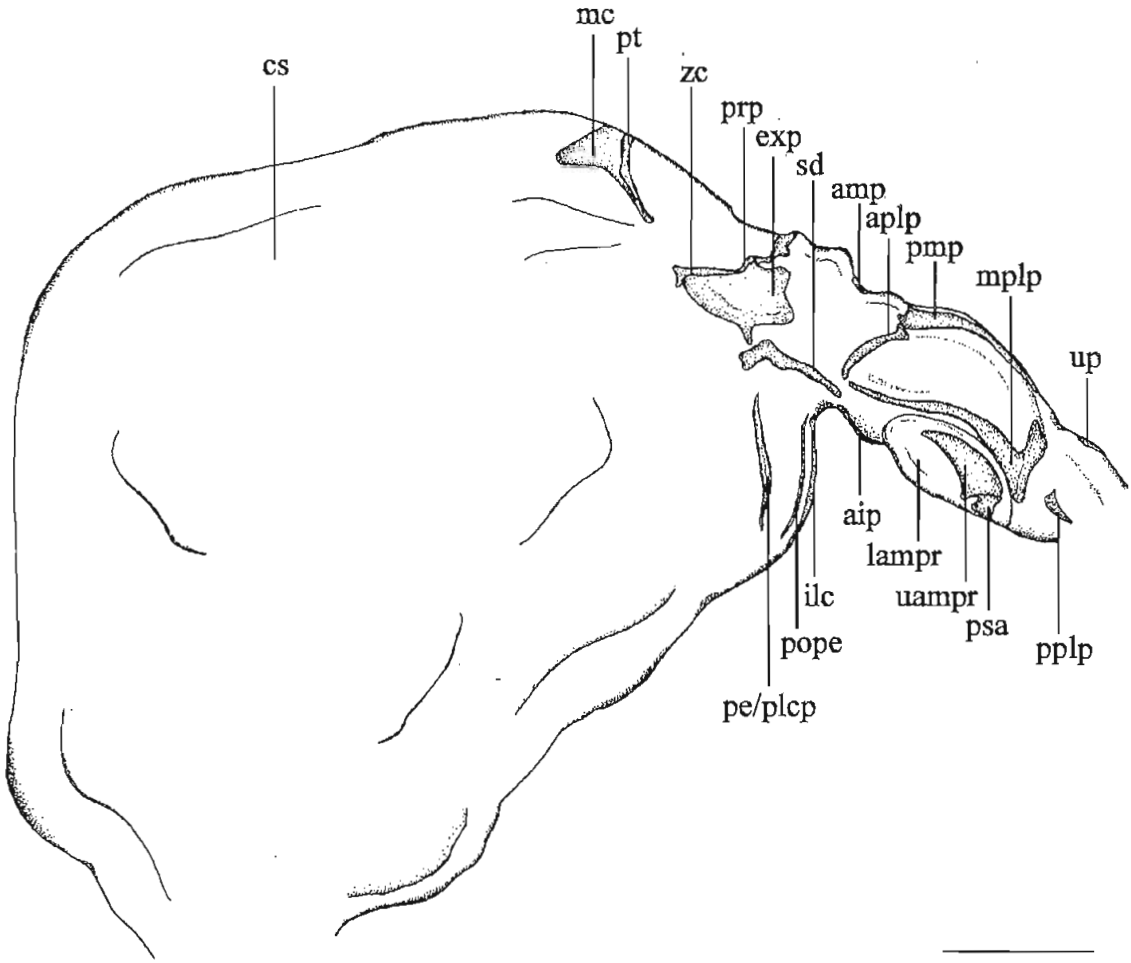
mc
pt
cs
zc
prp
exp
sd
amp
aplp
pmp
mplp
up
aip
lampr
uampr
psa
pplp
ilc
pope
pe/plcp

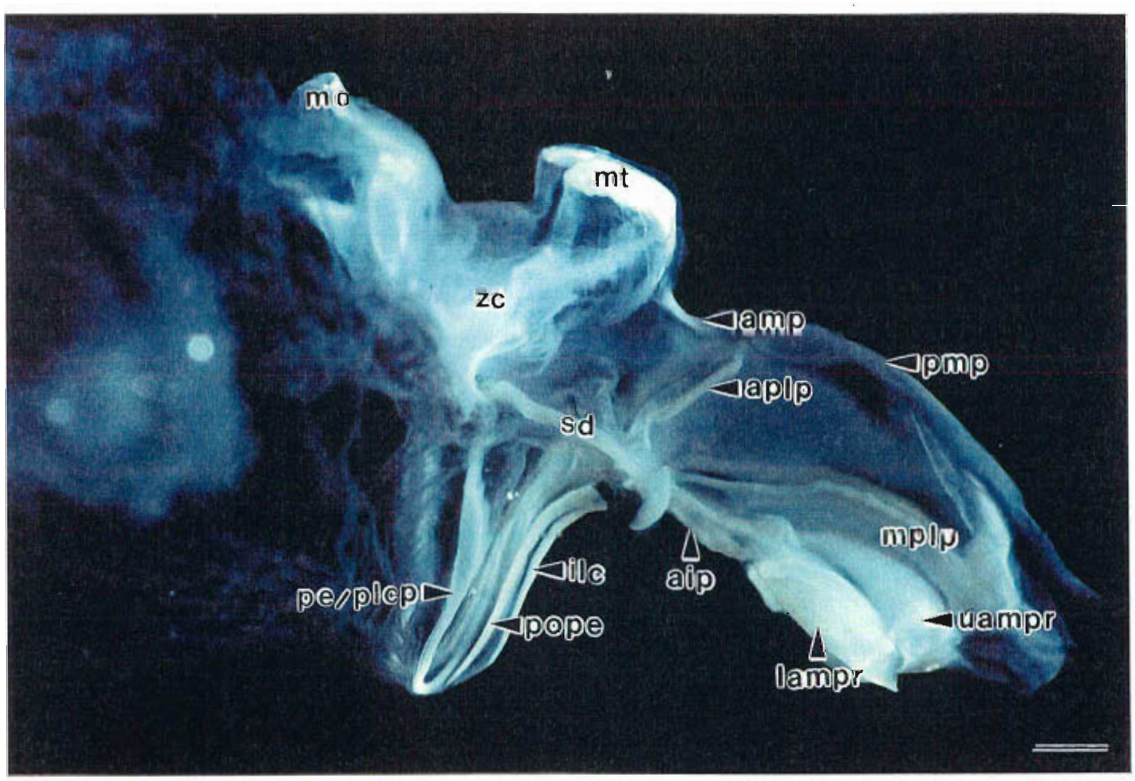
mc
mt
zc
amp
pmp
aplp
sd
mplp
ilc
aip
pe/plcp
pope
uampr
lampr

Figure 4.3. Dorsal external view of the proventriculus showing the location of ossicles. The musculature, dorsal caecum and digestive glands have been removed. The cardiac stomach is anterior. Scale: illustration, 2 mm; photograph, 1 mm.
cs, cardiac stomach; mt, median tooth. OSSICLES: amp, anterior mesopyloric; exp, exopyloric; mc, mesocardiac; mplp, middle pleuropyloric; pmp, posterior mesopyloric; pplp, posterior pleuropyloric; prp, propyloric; pt, pterocardiac; sd, subdentary; zc, zygocardiac.

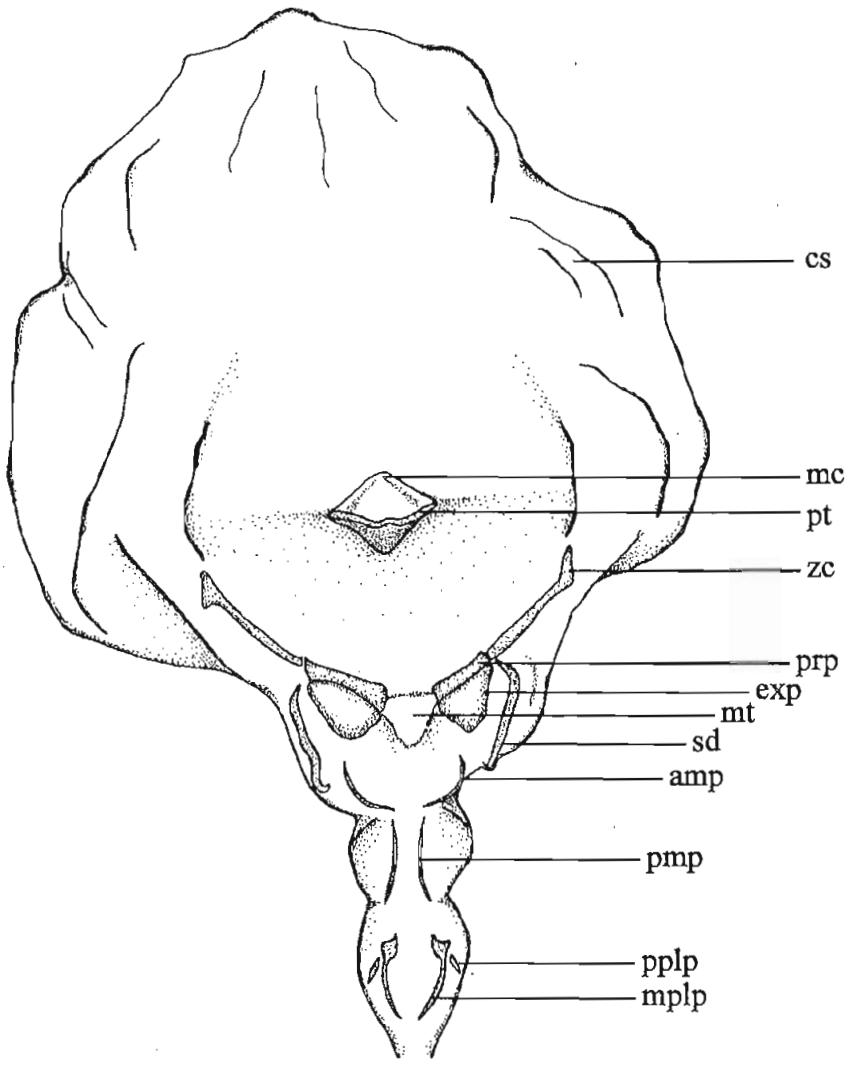
cs
mc
pt
zc
prp
exp
mt
sd
amp
pmp
pplp
mplp

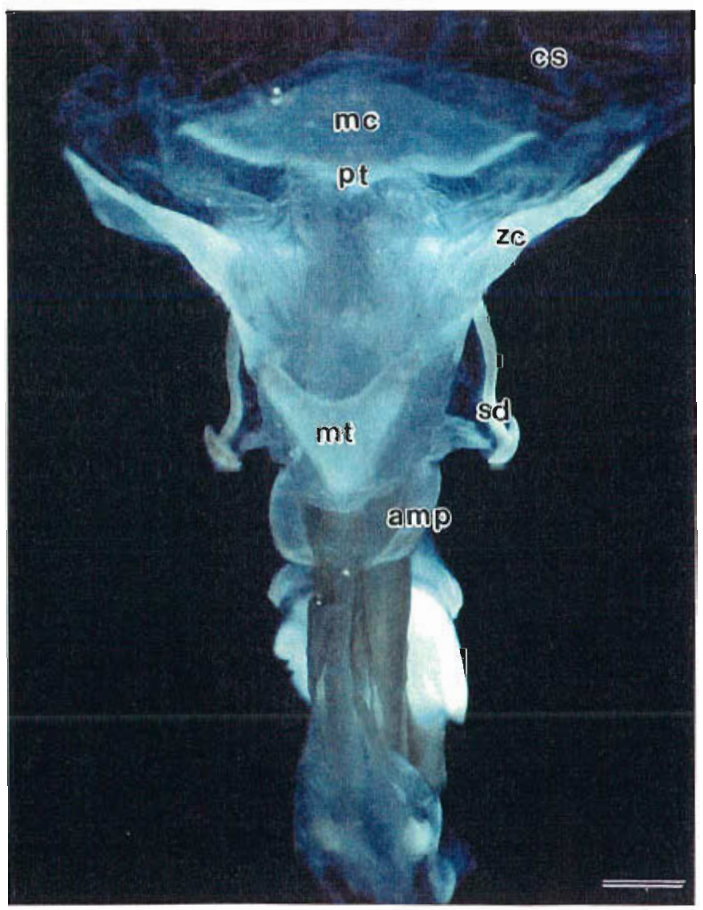
cs
mc
pt
zc
sd
mt
amp

Figure 4.4. A. Dorsal internal view of the proventriculus, the walls of which are folded out flat. Top is posterior. Scale, 2 mm. **B.** Diagrammatic TS through the cardiac stomach at position 1 indicated on A. Scale, 0.5 mm. **C.** Diagrammatic TS through the pyloric stomach at position 2 indicated on A. Scale, 0.5 mm. cb, central bulb; cpv, cardio-pyloric valve; dch, dorsal chamber; dfc, dorsal fluid channel; di, dorsal infolding; fc, filter crest; fp, filter press; iv, inner valve; lc, lateral channel; ls, lateral sheath; lt, lateral tooth; mplp, middle pleuropyloric; mt, median tooth; ov, outer valve; pope, postpectineal ossicle; post, posterior; so, setose outfolding; vc, ventral channel; vlc, ventro-lateral channel; vlp, ventro-lateral partition; vs, ventral sheath; zc, zygocardiac ossicle.

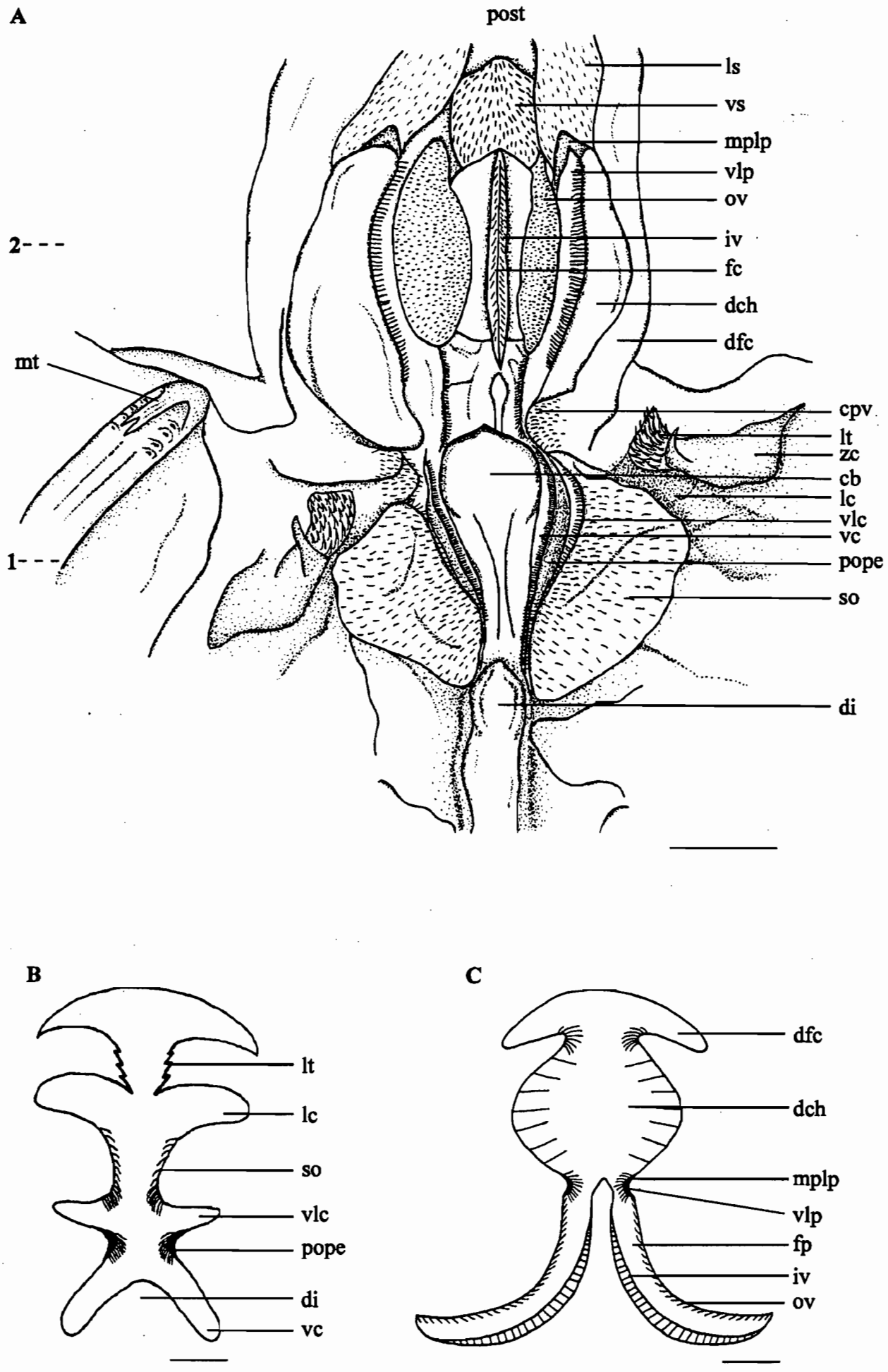
A
post
ls
vs
mplp
vlp
ov
iv
fc
dch
dfc
2
mt
cpv
lt
zc
cb
lc
vlc
vc
pope
so
1
di
B
lt
lc
so
vlc
pope
di
vc
C
dfc
dch
mplp
vlp
fp
iv
ov

dorsal fluid channels which run posteriorly along the length of the upper dorsal pyloric chamber (Fig. 4.4A, see also 4.7).

Elongate setae along the ventral edge of the setose outfolding overhang the ventro-lateral channel along its entire length and act as the first level of the primary filter (Fig. 4.4A,B). Beneath this, the dorsal margin of each ventral channel has a row of densely arranged rigid setae that form the second level of the primary filter (Fig. 4.4A,B). Both levels of the filter prevent large indigestible particles from entering the ventral channels. Small particles and fluid in the ventral channels pass through a posterior setal screen at its posterior margin prior to entry into the ventral pyloric chamber. Excluded particles pass directly into the dorsal pyloric chamber.

The gastric mill consists of a large forked median tooth and a pair of lateral teeth, both less calcified than those of other carnivorous decapods. The median tooth is a ventral extension of the propyloric ossicle and articulates anteriorly with the urocardiac ossicle (reduced) and posteriorly with the exopyloric ossicle. It has a slender molar process and a well developed bifurcate incisor process that projects ventro-posteriorly (Fig. 4.5A,B). The molar process usually has four raised molar cusps on its lateral margins and a set of raised chitinised ridges. The lateral teeth are mounted on the paired zygocardiac ossicles that are linked with the urocardiac anteriorly and propyloric ossicles medially and a pair of exopyloric ossicles posteriorly. Each has a medially directed incisor process at the anterior end with three smaller subsidiary teeth directed medially from its outer surface (Fig. 4.6A). Behind the incisor process are rows of vertical chitinous plates which are large and hook-like anteriorly and decrease in size posteriorly. The masticating surfaces of these plates are sharp and serrated and when the teeth are opposed they serve to macerate and tear food (Fig. 4.6B).

Separating the cardiac and pyloric stomachs is the cardio-pyloric valve. This comprises a central bulb-like structure and setose outfoldings of the posterior gastric mill wall (Fig. 4.4A; 4.6A). The outer margins of the bulb are supported by the inferior lateral cardiac ossicles and together with setose outfoldings can almost completely close the aperture to the pyloric stomach. The posterior surface of the bulb is densely covered in elongate ventrally directed setae (Fig. 4.6C).

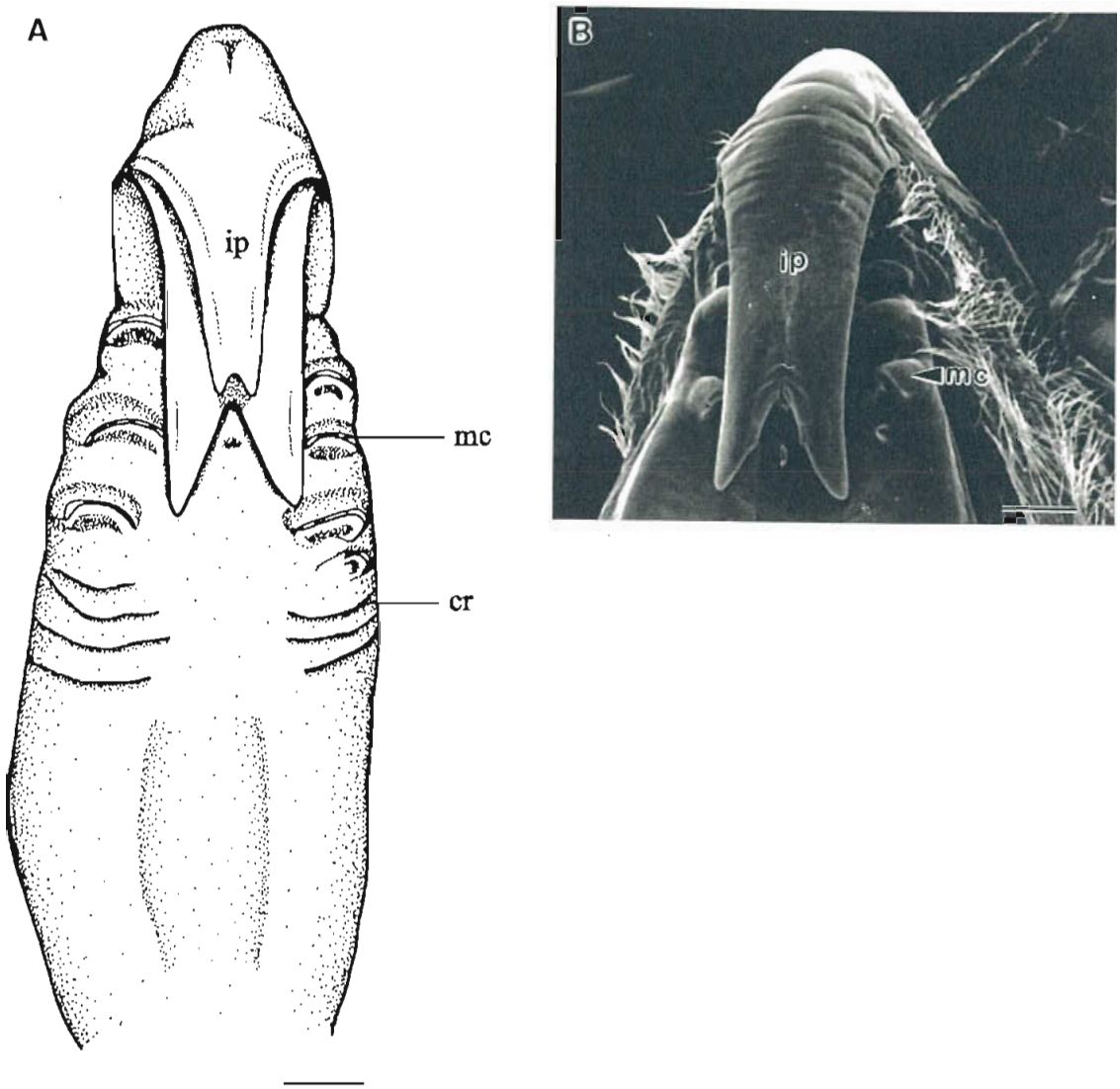

Figure 4.5. A. Median tooth of the gastric mill. Scale, 300 μm. **B.** Scanning electron micrograph (SEM) of the median tooth. Scale, 300 μm.
cr, chitinised ridge; ip, incisor process; mc, molar cusp.

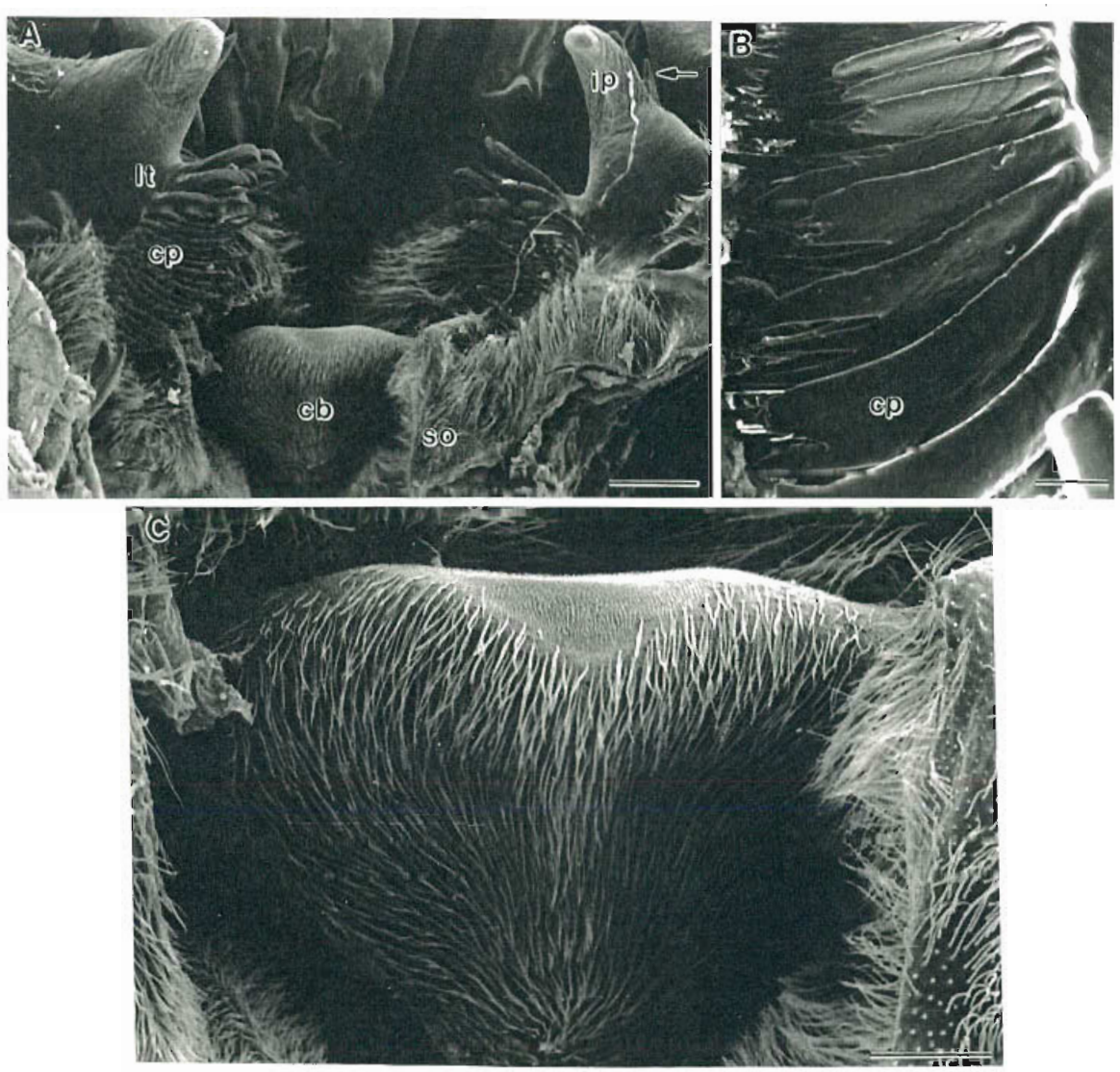

Figure 4.6. SEM of: **A.** Dorsal view of the lateral teeth of the gastric mill and cardio-pyloric valve, *in situ*. Top is anterior. Note the arrangement of chitinous plates and subsidiary teeth on the incisor process of the lateral teeth (arrow). Scale, 500 μm. **B.** Masticating edges of the chitinous plates. Scale, 150 μm. **C.** Central bulb of the cardio-pyloric valve. Note the ventrally directed setae on the posterior surface. Scale, 200 μm. cb, central bulb; cp, chitinous plates; ip, incisor process; lt, lateral tooth; so, setose outfolding.

Histologically, the cardiac stomach wall has a thick cuticle beneath which is a layer of cuboidal epithelium. Bundles of circular muscle are dispersed throughout its outer connective tissue.

Pyloric Stomach

The dorsal and ventral chambers of the pyloric stomach are separated by the ventro-lateral partition, a highly setose medially directed outfolding of the pyloric stomach wall (Fig. 4.4A,C; 4.7; 4.8A,B). This partition is supported along its length by the anterior extension of the middle pleuropyloric ossicle. Extensive musculature surrounds the dorsal and ventral chambers and the floor of the filter press (Fig. 4.8A). The dorsal chamber wall has numerous medially directed rigid setae, approximately 200 μm long and 20μm apart (Fig. 4.9A). These setae become thicker ventrally at the floor of the chamber, merging with the setose upper margin of the ventro-lateral partition. Above the dorsal chamber are 2 dorsal fluid channels (Fig. 4.4C; 4.7; 4.8A; 4.9B). They are devoid of setae except for the small ventral outfolding separating them from the dorsal chamber (Fig. 4.9B).

The pyloric filter press is a W-shaped chamber in cross section, formed from a dorsally directed medial infolding of the floor of the pyloric stomach (interampullary ridge) (Fig. 4.4C; 4.8A). Each side has an inner and outer valve; the two inner valves positioned on either side of the medial infolding. The inner valves are joined dorsally to form the filter crest, either side of which has a dense array of elongate dorsally directed setae along its length (Fig. 4.8A,B; 4.9C).

Fluid from the ventral and ventro-lateral channels flows between the inner and outer valves on either side of the filter crest. The outer valve is covered in a dense array of elongate simple setae up to 200 μm in length. These are directed dorsally and overlap one another to create a dense filtration matt (Fig. 4.10A,B). The inner valve has interlocking V-shaped longitudinal rows of filtration setae that project outwards from the valve at 90° and then terminate 90° dorsally so that the setae are parallel to the valve surface (Fig. 4.10A,C,D). Filtration setae are approximately 50 μm in length and each row is 25-30 μm apart creating a series of longitudinal channels (25-30 μm in width) along the length of the valve. The setae of each longitudinal row overlap those of the row above by more than half (30 μm) its length so that the setal filter is two layers thick

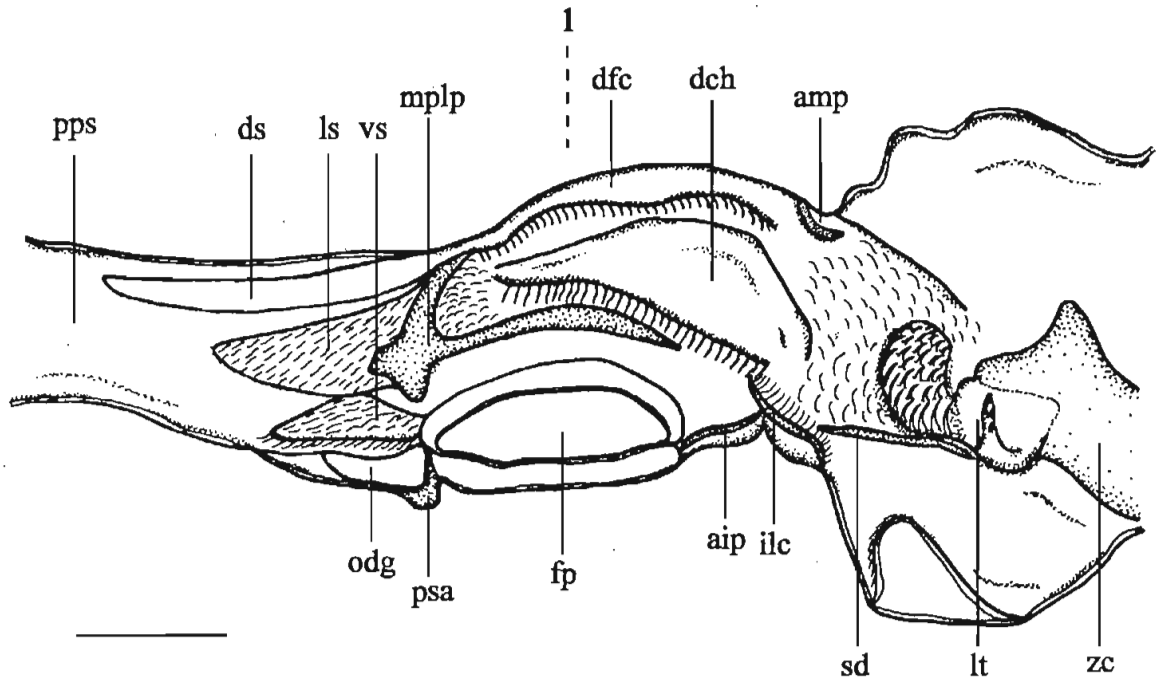

Figure 4.7. Lateral internal view of the pyloric stomach illustrating the external ossicles upon which the internal structures are supported. Left is posterior. Scale, 1.8 mm.
aip; anterior inferior pyloric ossicle; amp, anterior mesopyloric ossicle; dch, dorsal chamber; dfc, dorsal fluid channel; ds, dorsal sheath; fp, filter press; ilc, inferior lateral cardiac; ls, lateral sheath; lt, lateral tooth; mplp, middle pleuropyloric ossicle; odg, opening to digestive gland; pps, posterior pyloric sector; psa, posterior supra-ampullary ossicle; sd, subdentary ossicle; vs, ventral sheath; zc, zygocardiac ossicle.

Figure 4.8. (Opposite) **A.** TS (6 μm) through the pyloric stomach at position 1 indicated on Fig. 4.7. Scale, 500 μm. **B.** TS (6 μm) through the ventro-lateral partition and filter crest of the filter press. Note, the setae on the ventro-lateral partition (arrow). Scale, 100 μm.
dch, dorsal chamber; dfc, dorsal fluid channel; dg, digestive gland; fc, filter crest; iv, inner valve; m, musculature; mif, medial infolding; ov, outer valve; vlp, ventro-lateral partition.

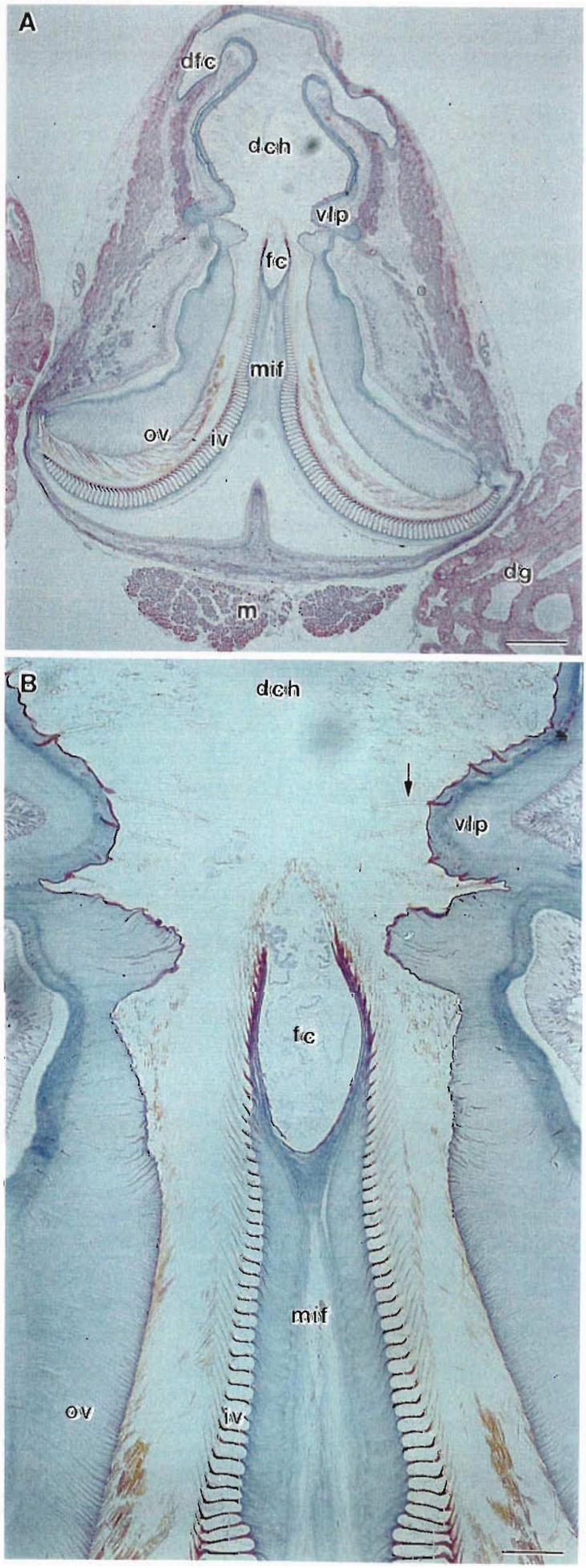
A
dfc
dch
vlp
fc
mif
ov
iv
dg
m
B
dch
vlp
fc
mif
ov
iv

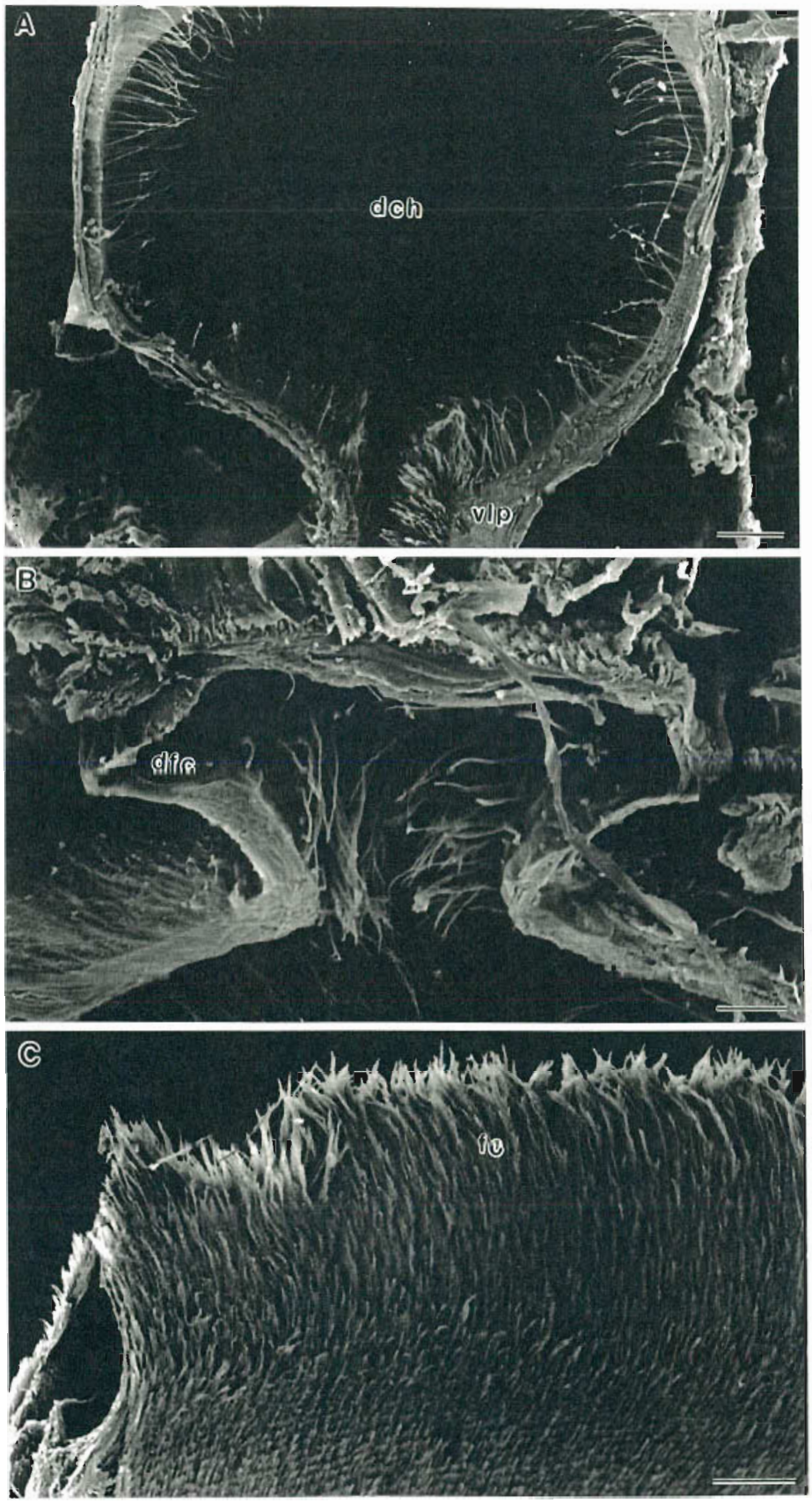

Figure 4.9. SEM: **A.** TS through the dorsal chamber. Scale, 160 μm. **B.** TS through the dorsal fluid channels. Scale, 80 μm. **C.** Filter crest setae. Scale, 100 μm.
dch, dorsal chamber; dfc, dorsal fluid channel; fc, filter crest; vlp, ventro-lateral partition.

Figure 4.10. A. TS (6 μm) of the filter press showing the arrangement of setae on the inner and outer valves. Scale, 50 μm. SEM: **B.** Outer valve setae. Scale, 50 μm. **C.** TS through the inner valve showing the arrangement of setae and longitudinal channels. Scale, 40 μm. **D.** Inner valve setae showing the extent of overlap and longitudinal channels. Scale, 20 μm. **E.** Compression of outer valve setae against the inner valve setae. Scale, 40 μm.
iv, inner valve; lc, longitudinal channel; ov, outer valve; s, setae.

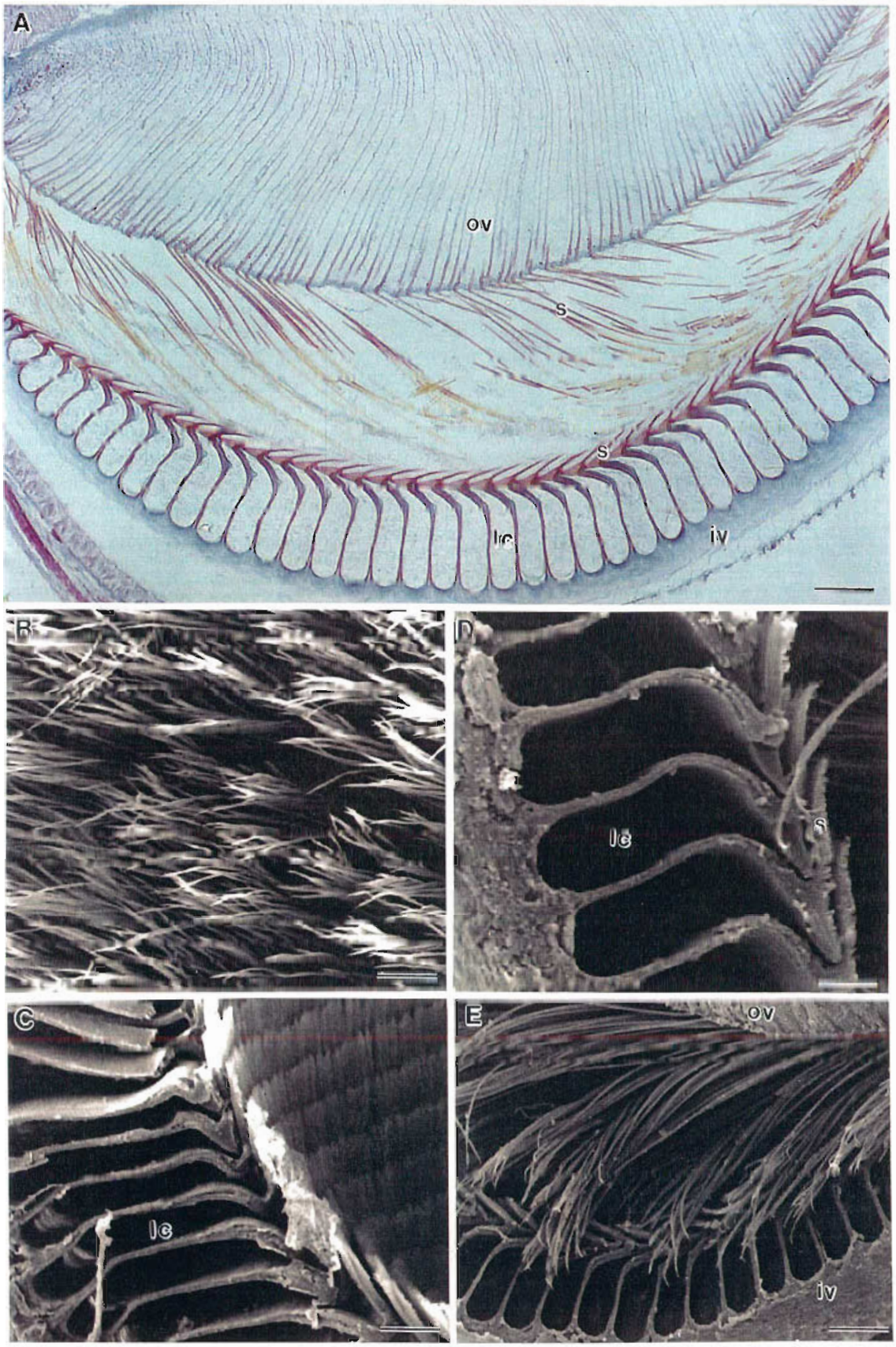
A
ov
s
s
ic
iv
B
D
ic
s
C
ic
E
ov
iv

(Fig. 4.10D). Compression of the outer valve setae against those of the inner valve forces fluid through this filtration screen into the longitudinal channels and prevents particulate material from entering the longitudinal channels (Fig. 4.10E).

Fluid that has passed through the filter screen moves posteriorly along the longitudinal channels. These eventually drain postero-ventrally into the openings of the digestive glands at the postero-ventral margin of the pyloric stomach (Fig. 4.7). Particles too large to pass through the filter setae move posteriorly between the valves. They are then deflected dorso-posteriorly by the posterior supra-ampullary ossicle over the ventral setose sheath, which protects the entrance to the digestive gland, and into the posterior pyloric sector to join indigestible material moving from the dorsal chamber (Fig. 4.7).

Three types of sheaths extend from the pyloric stomach into the posterior pyloric sector. Along the roof of the sector extend a pair of rigid dorsal sheaths originating from the dorsal filtration channels (Fig. 4.7). These are not highly setose but act as structural supports for the sector. Two highly setose lateral sheaths extend posteriorly from the dorsal chamber of the pyloric stomach and outer valves of the filter press to form the outer dorsal anterior margins of the sector (Fig. 4.4A; 4.7; 4.11). Lastly, a rounded flattened ventral sheath extends from the posterior margin of the inner valves of the filter press and overlies the entrance to the digestive gland primary ducts (Fig. 4.4A; 4.7). Both its upper and lower surfaces are covered in fine setae.

4.3.2 Posterior Pyloric Sector

An unusual feature of the alimentary tract of *T. orientalis* is the posterior pyloric sector which extends from the openings of the digestive gland at the posterior end of the pyloric stomach to the hindgut (see Fig. 4.13A). It is ensheathed by the dorsal caecum and has 2 chambers, separated by a narrow aperture created by the infolding of its walls (Fig. 4.11). The larger anterior chamber contains the sheaths extending from the pyloric stomach, whereas the posterior chamber is relatively simple and merges with the highly convoluted walls of the anterior hindgut. A bolus of indigestible material is often present which later forms a faecal pellet within the hindgut (Fig. 4.11).

In contrast to the foregut and hindgut, the posterior pyloric sector is characterised by a very thin layer of cuticle and a poorly developed epithelium and basal

lamina (Fig. 4.12A,B). Acidophilic secretory cells containing numerous acidophilic granules are densely distributed throughout the tissue (Fig. 4.11; 4.12A,B). Granules are also dispersed throughout the connective tissue adjacent to the cells. Duct-like structures leading to the lumenal border are present in the tissue with acidophilic material common on the cuticle surface and in the lumen (Fig. 4.12A,B). Similar secretory cells have been found beneath the basal lamina of the dorsal caecum and the primary duct of the digestive gland (see Ch 4.3.3.1 and Ch 5.3.1). These react positively with mercuric bromophenol blue indicating the secretory granules also contain protein (see Fig. 4.14B).

4.3.3 Midgut

4.3.3.1 Dorsal Caecum

The dorsal caecum arises immediately posterior to the pyloric stomach in line with the digestive gland primary ducts, and rests anteriorly on the roof of the pyloric stomach (Fig. 4.13A). At this point the caecum is a small semicircular chamber in cross section (Fig. 4.13B). Posteriorly its lateral walls extend ventrally to encircle the posterior pyloric sector completely at the region behind the digestive gland ducts (Fig. 4.13C,D). From here it continues to ensheath the sector up until the hindgut juncture.

The dorsal caecum lumen is lined by densely packed elongate columnar epithelial cells (100-150 μm in length) resting on a thick basal lamina (Fig. 4.14A). These cells have an apical brush border of microvilli and mid-basal nuclei and become more elongated posteriorly, once the caecum has completely encircled the posterior pyloric sector (Fig. 4.14B). Densely packed granules of acid mucin (blue with PAS-alcian blue) are present in the apical cytoplasm (Fig. 4.14A). Their cytoplasm stains differentially with mercuric bromophenol blue, the proximal third staining intensely blue indicating much protein is present, but the apical two-thirds remain unstained (Fig. 4.14B). Beneath the basal lamina are bands of circular muscle (Fig. 4.14B). Located close to these muscles are granular secretory cells similar to those in the connective tissue surrounding the posterior pyloric sector. These cells stain positive with mercuric bromophenol blue indicating they contain protein.

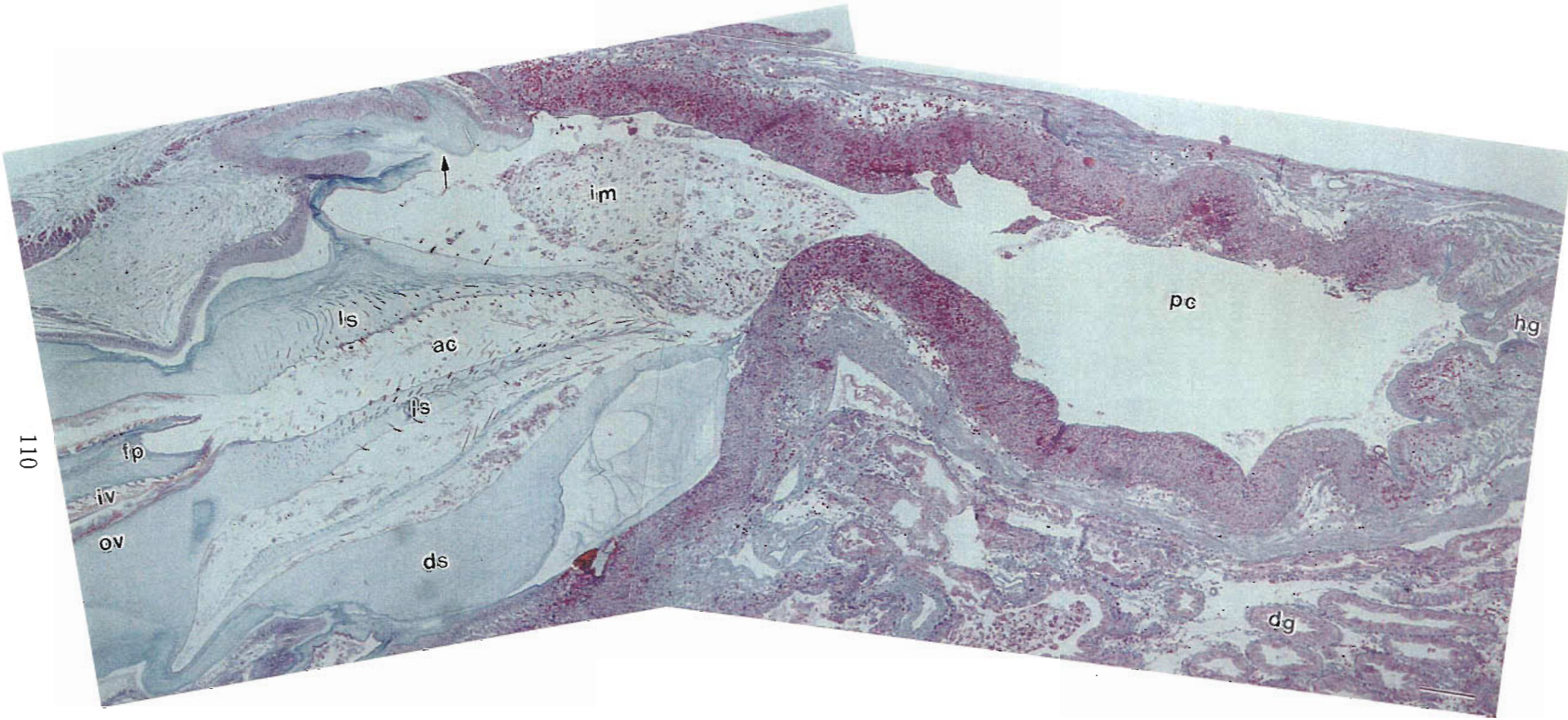

Figure 4.11. Longitudinal section (LS) (6 μm) through the posterior pyloric sector. Note, the setae on the lateral sheaths and entrance to the dorsal caecum (arrow). Scale, 300 μm.
ac, anterior chamber; dg; digestive gland; ds, dorsal sheath; fp, filter press; hg, hindgut; ls, lateral sheath; im, indigestible material; iv, inner valve; ov, outer valve; pc, posterior chamber.

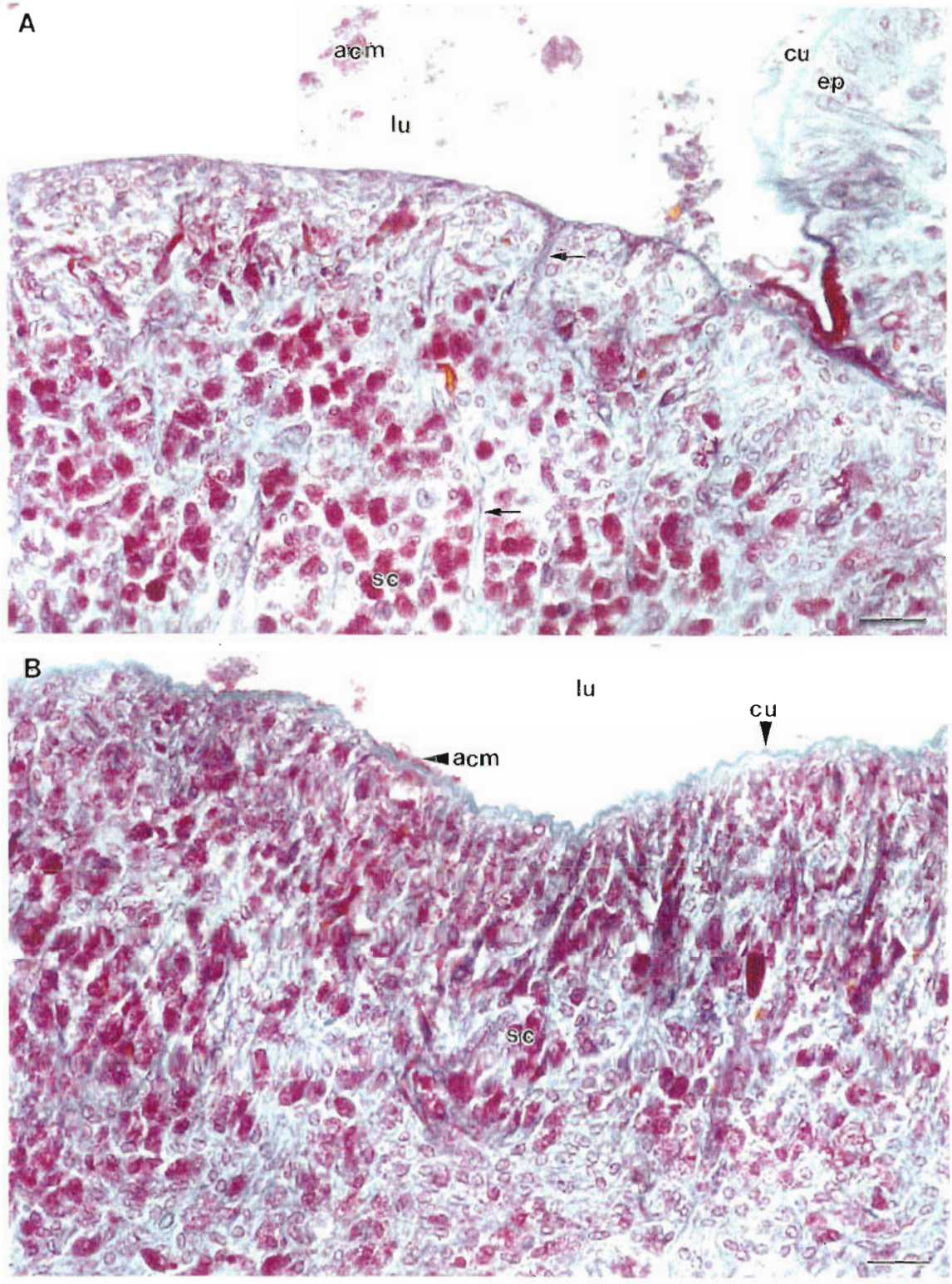

Figure 4.12. A. B. Walls of the posterior pyloric sector showing the absence of a well developed epithelium, a thin layer of cuticle, densely arranged acidophilic secretory cells and duct-like structures (arrows) leading toward the lumen. Note, the well developed epithelium and cuticle of the adjacent pyloric stomach (right) (A) and acidophilic material on the surface of the cuticle and in the lumen (A,B). Scale, 50 μm.
acm, acidophilic material; cu, cuticle; ep, epithelium; lu, lumen; sc, secretory cells.

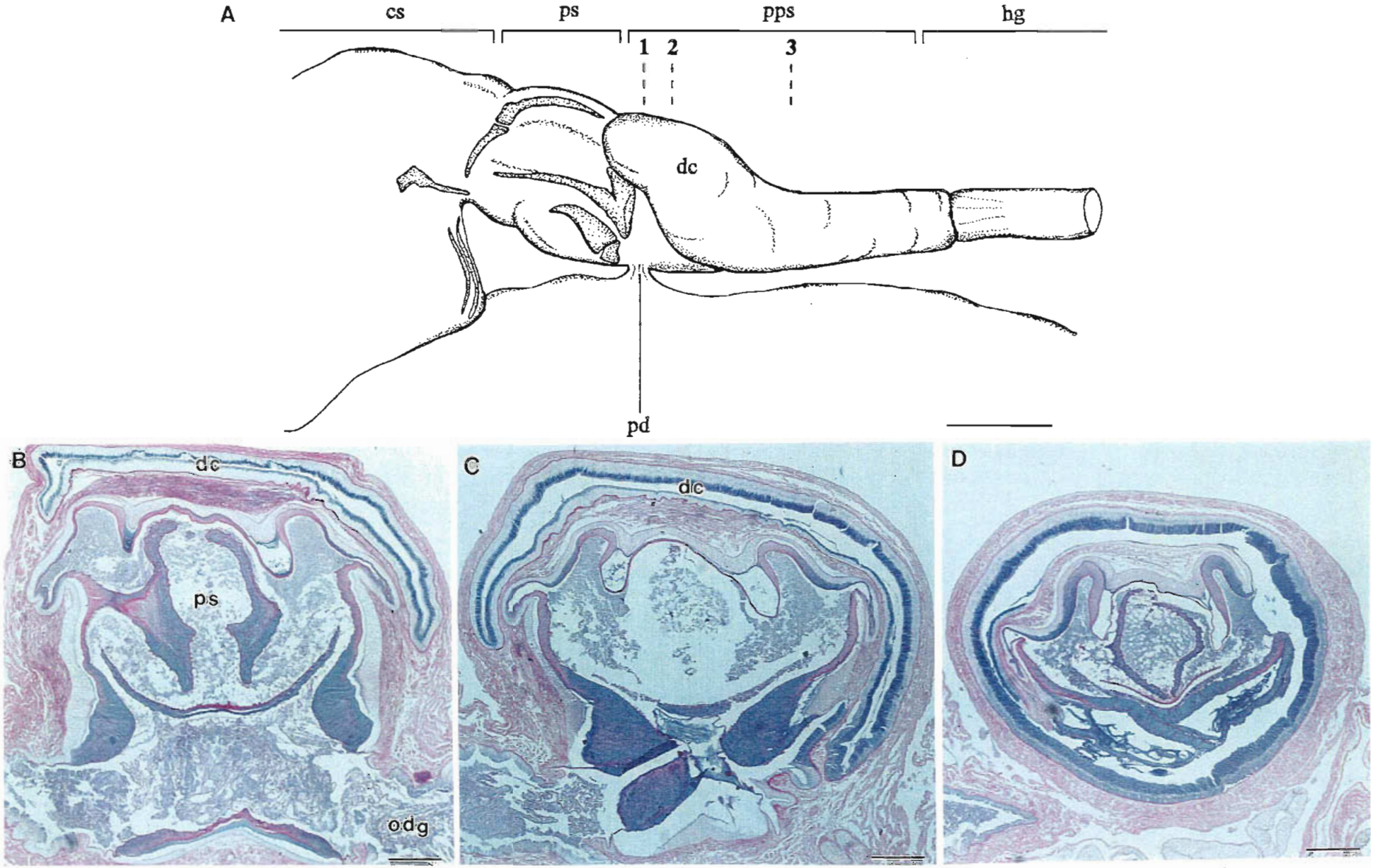
A
cs
ps
pps
hg
1
2
3
dc
pd
B
dc
ps
odg
C
dc
D

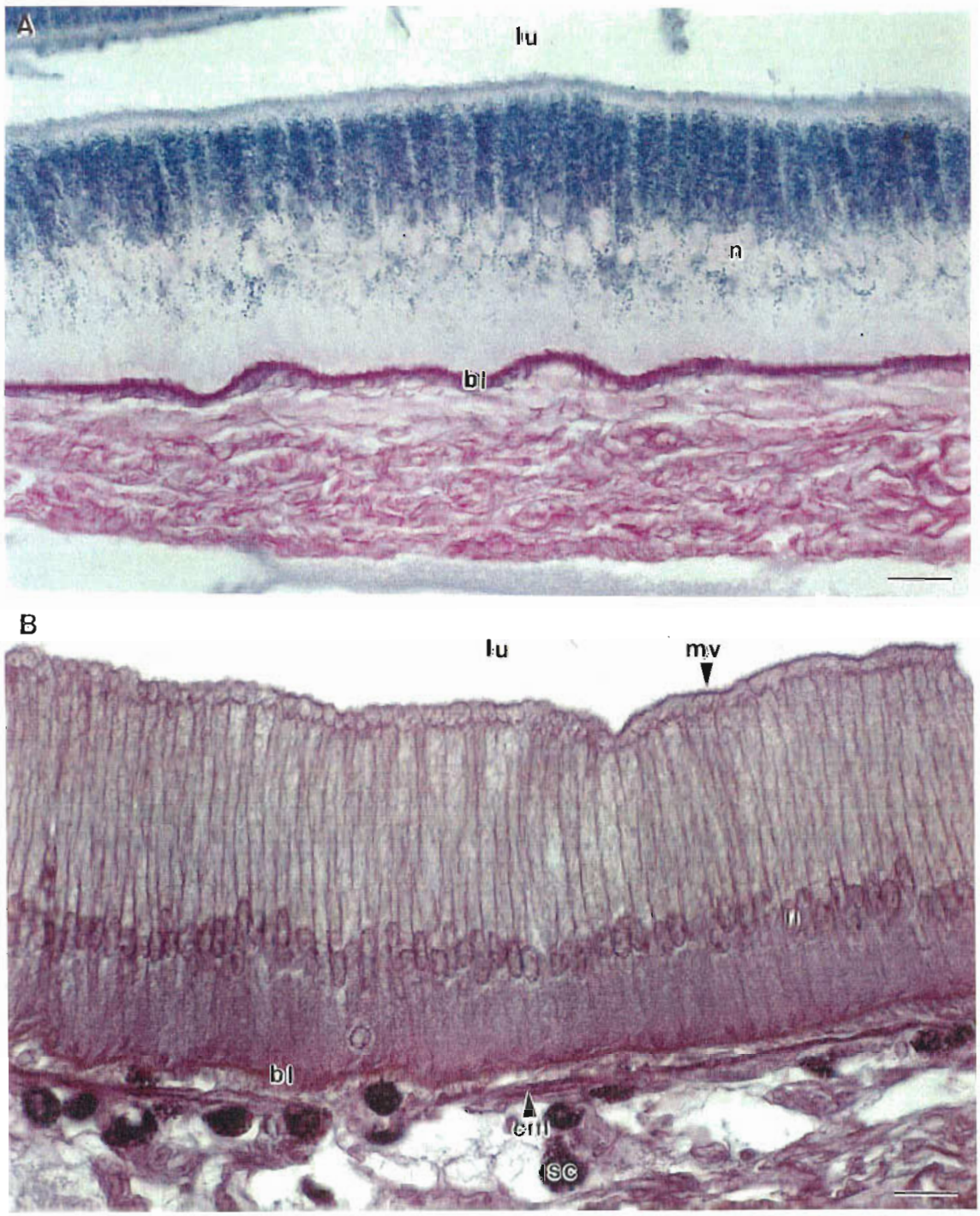

Figure 4.14. Epithelium of the dorsal caecum at position 1 and 3 in Fig. 4.13A. **A.** PAS-alcian blue stain showing acid mucin granules in the cytoplasm. Scale, 25 μm. **B.** Mercuric bromophenol blue stain showing the protein positive basal cytoplasm. Note, the micovillous brush border and secretory cells beneath the basal lamina. Scale, 25 μm.
bl, basal lamina; cm, circular muscle; lu, lumen; mv, microvilli, n, nuclei; sc, secretory cells.

Figure 4.13. (Previous Page) **A.** Lateral external view of the alimentary tract showing the position of the dorsal caecum. Left is anterior. Scale, 2.5 mm. **B.C.D.** TS (6 μm) through the alimentary tract at positions 1(B), 2(C), 3(D) indicated on A, to show ensheathing by the dorsal caecum. Scale, A,B, 200 μm; C, 150 μm.
cs, cardiac stomach; dc, dorsal caecum; hg, hindgut; odg; opening to digestive gland; pd, primary duct of digestive gland; pps posterior pyloric sector; ps pyloric stomach.

4.3.4 Hindgut

The hindgut is an elongated tube that extends posteriorly from the posterior pyloric sector through the abdominal muscles to the anus; a longitudinal slit bordered on either side by 2 hardened cuticularised lips. Anteriorly its walls are highly convoluted into numerous longitudinal folds as seen in Fig. 4.15A, and its surface is covered in fine setae arranged singly or in rows of 2 to 3 individual seta (Fig. 4.15B). A faecal pellet surrounded by a peritrophic membrane is usually present in the lumen of animals that have fed recently (Fig. 4.15C).

Like the foregut, columnar epithelial cells (30 μm in length) have basal nuclei, a granular cytoplasm and are lined by a thick layer of cuticle (Fig. 4.15D). Directly beneath the epithelium are bands of striated longitudinal muscles with bundles of circular muscle at their outer periphery. This musculature extends the length of the hindgut, with circular muscles, in particular, becoming larger towards the anus. Strands of convoluted collagen and smooth muscle fibres are located within the outer connective tissue.

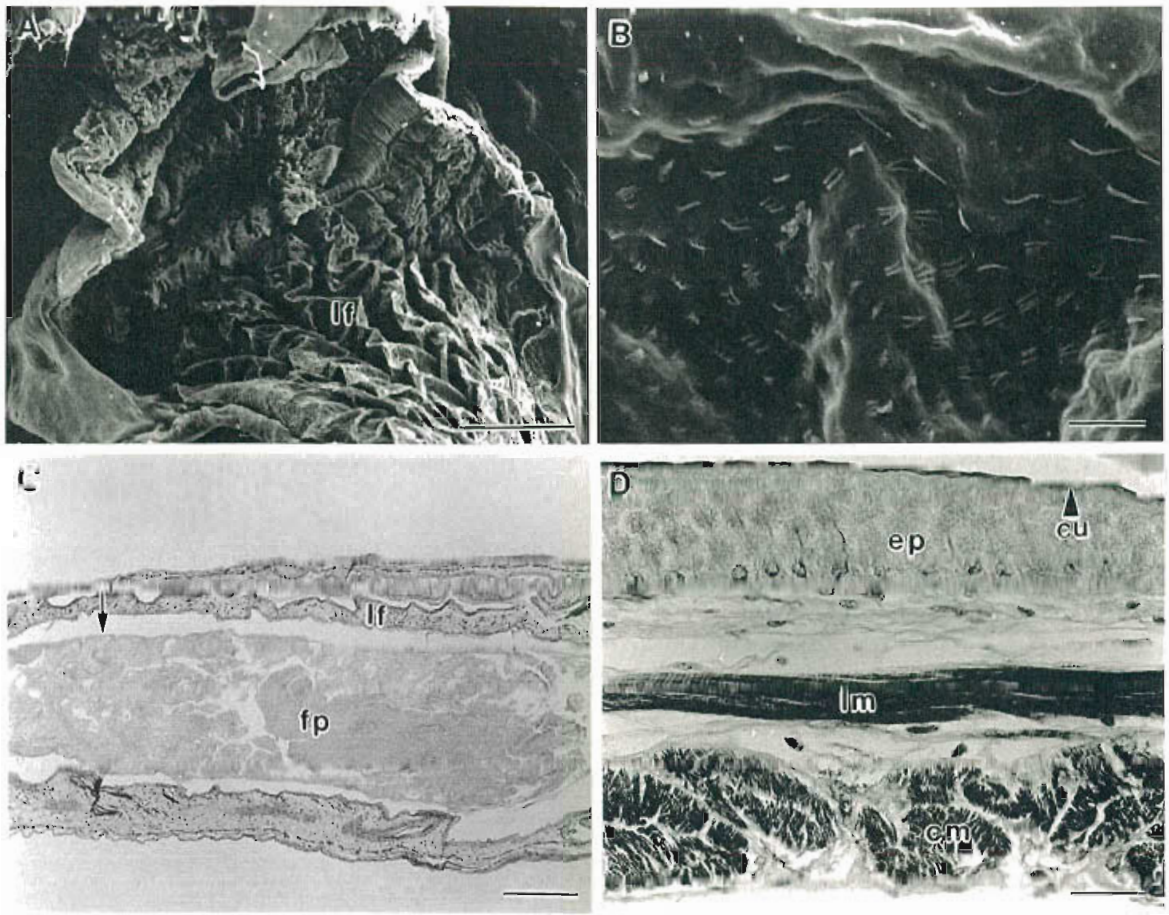

Figure 4.15. A. SEM of the anterior hindgut wall. Note, the longitudinal folds. Scale, 500 μm. **B.** SEM of setae on the wall of the hindgut. Scale, 20 μm. **C.** LS (6 μm) through the hindgut showing a large faecal pellet in the lumen. Arrow indicates the peritrophic membrane. Scale, 600 μm. **D.** TS of the hindgut wall. Note, the well developed musculature beneath the epithelium. Scale, 20 μm.
cu, cuticle cm, circular muscle; ep, epithelium; fp, faecal pellet; lf, longitudinal fold; lm, longitudinal muscle.

4.4 DISCUSSION

This study is the first to detail the structure of the entire alimentary tract of a scyllarid, *T. orientalis*. The alimentary tract conforms to the general plan exhibited by all decapods, although its proventriculus is simplified and the posterior pyloric sector appears to be unique to this scyllarid. Various structural specialisations are also evident and the functional implications of these will be discussed.

Longitudinal folds of the oesophageal walls enable considerable expansion of its lumen for the quick and efficient ingestion of large food items. This is particularly important as food entering the oesophagus of *T. orientalis* is often large because of the poor cutting ability of the mandibles (refer Ch 3). Peristaltic contractions of the oesophageal wall, often seen after food insertion (refer Ch 3), are likely to be facilitated by the longitudinal, circular and radial muscles along its length. This action together with mucus (acid mucin) secretions from tegumental glands beneath the epithelium facilitate the movement of food into the cardiac stomach (Barker and Gibson, 1977, 1978; Erri Babu *et al.*, 1982). Similar secretions by tegumental glands of the membranous lobe and paragnaths also aid this process (refer Ch 3). Thickened cuticle in the oesophagus protects the epithelium from large abrasive items ingested. Hence, structural features of the oesophagus of *T. orientalis* collectively promote a fast efficient passage of large food items into the cardiac stomach.

Proventricular morphology of *T. orientalis* is comparable with that of *I. peronii* (Suthers and Anderson, 1981). In particular, the arrangement of proventricular ossicles is similar and conforms, in general, to the proventricular ossicle anatomy common to the Decapoda (Maynard and Dando, 1974; Meiss and Norman, 1977; Kunze and Anderson, 1979). Both species of scyllarids are characterised by a reduction in ossicle framework and calcification, compared with that of other decapods. This reflects the relatively simple internal structure of the cardiac stomach of *T. orientalis*, as the absence of a complex ventral filtration system, except in the gastric mill region and the reduction in calcification of gastric mill teeth do not require the well developed structural supports of other decapods. Furthermore, the absence of accessory supralateral teeth and complex filtration channels common to many particulate feeders (Suthers, 1984; King and Alexander, 1994) is probably attributable to the small proportion of particulate material ingested by scyllarids (Suthers and Anderson, 1981; Jones, 1988; Lau, 1988). Hence, the

need for extensive filtration of indigestible particles in the cardiac stomach of this macrophage is reduced, as the majority of food items are large, and once triturated, are primarily digestible.

This reduced ossicle framework and calcification of the cardiac stomach together with extensive folding of its walls enable considerable expansion for accommodating large food items. This suggests the anterior cardiac stomach acts primarily as a crop, a beneficial adaptation for a scavenger like *T. orientalis* that relies on consuming as much as possible when food is located. This was verified by Suthers and Anderson (1981) who observed that food was kept in the cardiac stomach for 3-6 hours before being moved posteriorly by peristaltic action of the cardiac wall musculature to the gastric mill. Rigid microspines on the walls of the cardiac stomach of *T. orientalis* grip the food to aid this posterior movement. During food storage, chemical degradation by digestive enzymes weakens the tissue prior to trituration. During this process, the thickened cuticle of the foregut protects its epithelium from digestive hydrolysis.

The gastric mill teeth of *T. orientalis* are similar in structure to those of *I. peronii* (Suthers and Anderson, 1981). They are considerably less calcified than those of other macrophagous carnivores and lack a well developed molar process (Schaefer, 1970; Kunze and Anderson, 1979; Skilleter and Anderson, 1986). Their masticatory edges are sharp and serrated, particularly the chitinised plates of the lateral teeth which are well adapted to macerate and tear food when the teeth are opposed (Fig. 4.6B). Consequently, the teeth are extremely well adapted to cutting and macerating soft flesh from crustaceans, gastropods, bivalves and polychaetes, which are commonly ingested by *T. orientalis* and other scyllarids (Jones, 1988; Lau, 1988; Spanier *et al.*, 1988). This was verified by Suthers and Anderson (1981) who found the gastric mill of *I. peronii* to be a simplified cutting apparatus in which the major masticatory action is a cutting action of the lateral teeth, with only a minor role for the median tooth. The incisor process is pushed between the molar plates of the lateral teeth causing maceration. Reduced calcification and poorly developed molar processes reflect the few hard items ingested by scyllarids and they therefore lack the well developed grinding/crushing action common in other macrophagous decapods (Caine, 1975a,b; Suthers and Anderson, 1981, Heinzel, 1988). Hence, although *T. orientalis* generally conforms to the trend of increasing robustness and complexity of the gastric mill with macrophagy, food type is also

important in modifying tooth structure as was found with development of the crista dentata and mandibles (refer Ch 3).

To understand the nature of fluid flow in the proventriculus of *T. orientalis*, observations of injected dyes within a functioning individual are required. Nevertheless, based on a number of common structural features with *T. orientalis* it is assumed that the basics of fluid flow in this scyllarid is generally similar to that proposed by Powell (1974), Lovett and Felder (1990a) and King and Alexander (1994).

During trituration, fluids and small particles squeezed from the food percolate ventrally through the primary filter which comprises the two rows of setae overlying the ventro-lateral and ventral channels (Fig. 4.4A,B). Particles small enough to pass between the setae enter the ventro-lateral and ventral channels, sequentially, and flow posteriorly around the cardio-pyloric valve. Here they encounter the posterior setal screen overlying the ventral channel which further prevents large particles from entering the delicate pyloric filter press. A pyloric pump reportedly drives this movement of particles into the filter press (Powell, 1974). Excluded particles and indigestible material pass directly into the dorsal chamber of the pyloric stomach via the lateral channels directly beneath the lateral teeth (Fig. 4.4A,B).

The primary role of the cardio-pyloric valve is to prevent food from moving posteriorly into the dorsal chamber before completion of trituration (Coombs and Allen, 1978; Icely and Nott, 1992). In addition, the fine ventrally directed setae on the posterior surface of the central bulb of *T. orientalis* probably aid the ventral movement of fluid into the filter press. The absence of spines and accessory teeth common on the valve of other carnivorous decapods (Caine, 1975a,b) again reflects the soft flesh diet of this scyllarid, as additional mastication by the valve is not needed to reduce its food to a digestible size.

The pyloric filter press (secondary filter) of *T. orientalis* is responsible for the final filtration of particles prior to their entry into the digestive gland. Contraction of extensive musculature surrounding the pyloric stomach (Fig. 4.8A) compresses the outer against the inner valve setae to facilitate the removal of particles. Lovett and Felder (1990a) believe this process also promotes the final trituration and mixing of particles

with digestive enzymes prior to entry into the digestive gland. Fluid as well as particles fine enough to pass through the setal screen enter the longitudinal channels and move posterio-ventrally toward the primary ducts.

Setal overlap of one longitudinal channel on the inner valve of *T. orientalis* as opposed to two longitudinal channels is believed to be a macrophagous attribute (King, 1991) (Fig. 4.10D). The width of longitudinal channels in *T. orientalis* is also within the range of other macrophagous decapods such as the blue swimmer crab *Portunus pelagicus* Linnaeus (30 μm) (King, 1991) and the brachyuran *Cyclograpsus punctatus* Milne-Edwards (Schaefer, 1970). This supports the hypothesis of Caine (1976) and Schaefer (1970) that increasing channel width reflects macrophagy, which was also recently verified by King (1991) in his comparative study of *P. merguiensis* and *P. pelagicus*. Kunze and Anderson (1979) believed that no such relationship exists, with filter feeding species having a channel width (20 μm) not too dissimilar from carnivorous decapods like *T. orientalis* (30 μm). Hence, it is possible that the useable part of food is reduced to a similar consistency in all decapods, including *T. orientalis*, irrespective of diet, rendering their filtratory ability essentially similar. If so, accessory structures such as pyloric fingerletts would aid the efficiency of filtration in particulate feeders which have a greater need for efficient filtration than macrophages.

Intersetule distance of the inner valve of *T. orientalis* (100-200 nm) is within the same range as other decapods documented (Ngoc-Ho, 1984; King and Alexander, 1994). Thus only particles in the colloidal size range enter the longitudinal channels for passage into the digestive gland ducts of *T. orientalis*. This ensures that blockage or damage of delicate ducts and tubule epithelia by large particles does not occur.

Excluded particles outside this size range pass posteriorly between the valves and are deflected dorso-posteriorly to join indigestible material moving from the dorsal pyloric chamber. The elongate setae in this chamber protect the walls from abrasion whilst guiding the exit of material (Fig. 4.9A). Together with the filter crest, the densely setose ventro-lateral partition prevents this material from contaminating fluids entering the filter press (Fig. 4.8B; 4.9A,C). Similarly, setae between the dorsal chamber and dorsal fluid channels prevent contamination of fluid flowing anteriorly along these channels into the cardiac stomach (Powell, 1974; King and Alexander, 1994) (Fig. 4.9B).

The columnar epithelium of the dorsal caecum is lined by apical microvilli which indicates these cells are capable of absorption. Some workers believe that midgut caeca increase the surface area for water absorption at ecdysis (Holliday *et al.*, 1980), or nutrient absorption during digestion (Yonge, 1924). However, as nutrients are primarily absorbed by the B- and R-cells of the digestive glands (refer Ch 5), it is unlikely that they are absorbed by the dorsal caecum. It is possible, however, that water and ions may be absorbed for controlling water flux between the midgut lumen and the haemolymph. Failure to detect alkaline phosphatase in the anterior and posterior caeca of *P. setiferus* led Lovett and Felder (1990b) to conclude that this structure is incapable of absorption. Examination of epithelial transport, similar to the studies of Mykles and Ahearn (1978) and Mykles (1980), is necessary to verify whether absorption is indeed possible within the dorsal caecum of this scyllarid.

Granules of acid mucin are densely packed in the apical cytoplasm of the cells indicating they are actively involved in mucus production. Mucus secreted into the lumen would flow into the posterior pyloric sector for lubrication of the indigestible food bolus and possibly aid in binding this material prior to its enclosure within the peritrophic membrane. The role of protein present in the proximal cytoplasm of cells is unclear although it is unlikely to be digestive enzyme because Lovett and Felder (1990b) found no evidence of protease production in the anterior caecum of adult *P. setiferus*. Whether both secretions from the epithelium contribute toward production of the peritrophic membrane, as proposed by Pugh (1962) and Dall (1967), is unclear as Holliday *et al.* (1980) found that removal of the anterior caecum did not impair formation of the membrane in the crab *Cancer magister* Dana.

It is believed that the anterior caecum can accommodate volume changes during foregut contraction (Powell, 1974), as well as accepting digestive fluid and water flowing anteriorly from the midgut and hindgut during anal drinking and antiperistalsis (Lovett and Felder, 1990a). If this occurs in *T. orientalis*, the circular muscle bands beneath the basal lamina of the dorsal caecum may serve to control this fluid movement into and out of the lumen. In addition, muscular contractions may also transport epithelial secretions out of the caecum and into the posterior pyloric sector. Whatever the various roles of the dorsal caecum may be, their epithelial contributions to the

processes of digestion and absorption are probably minor compared with those of the digestive glands.

An unusual feature of the alimentary tract of *T. orientalis* is the posterior pyloric sector extending from the pyloric stomach to the hindgut (Fig. 4.11; 4.13A). The thin layer of cuticle indicates this region is not part of the midgut trunk, which is uncuticularised in all crustaceans (Dall and Moriarty, 1983). Structural characteristics of the midgut trunk of decapods, including columnar epithelial cells with an apical brush border and circular and longitudinal musculature beneath the basal lamina (Barker and Gibson, 1977; 1978; Coombs and Allen, 1978), are not present. The greater thickness of cuticle and well developed columnar epithelium of the foregut and hindgut, compared with that of the sector, indicate it is also distinct from these regions. Based on its position posterior to the midgut and its cuticle, it is more likely to be affiliated with the hindgut than the midgut.

The posterior pyloric sector is involved in processing indigestible material into a faecal pellet. At this stage the pellet lacks a peritrophic membrane, but it was present in the hindgut. This indicates the membrane is derived from a region anterior to the hindgut, and is probably formed from secretions produced in the sector. Acidophilic and proteinaceous material produced in the granular secretory cells dispersed throughout the tissue, are most likely secreted from these cells via the duct-like structures into the lumen. The peritrophic membrane is made up of a microfibrillar network rich in chitin, included in a protein and mucopolysaccharide matrix (Brunet *et al.*, 1994). Hence, one or both these secretions probably contribute to the peritrophic membrane. Alternatively, acid mucopolysaccharide released from the dorsal caecum may bind with the secreted protein to form the protein and mucopolysaccharide matrix. To verify these hypotheses the nature of the acidophilic material produced by cells in the posterior pyloric sector and the mechanism by which the membrane matrix is formed needs to be examined further before the origin of the peritrophic membrane is elucidated.

Cuticular dorsal and lateral sheaths in the anterior chamber passively guide indigestible material leaving the dorsal chamber of the pyloric stomach into and through the posterior pyloric sector. This is primarily accomplished by the setose lateral sheaths, with the rigidity of the dorsal sheaths providing additional support to the roof of the

chamber. Powell (1974) also believed the sheaths provided a durable lining against abrasive material and allowed fluids to flow around the faecal column without disrupting the compacted material.

Powell (1974) termed the region immediately behind the pyloric stomach, the faecal compaction zone. Although the anterior chamber of the sector superficially resembles this zone in that both contain cuticular sheaths protruding from the pyloric stomach, the absence of well developed musculature in the sector suggests it is not involved in faecal compaction. The final process of squeezing the remaining fluids from indigestible material probably occurs in the dorsal chamber of the pyloric stomach in *T. orientalis*, as the walls of the stomach are highly muscular and capable of much compression (Fig. 4.8A). The absence of musculature also indicates the sector is incapable of extensive peristaltic and antiperistaltic contractions exhibited by the midgut trunk and hindgut of decapods (Lovett and Felder, 1990a). Hence an active role in the regurgitation of incompletely digested material and/or faecal movement is unlikely.

Like all other decapods, the hindgut of *T. orientalis* is primarily involved in defecation, facilitated by peristaltic contractions of the muscular hindgut wall (Coombs and Allen, 1978; Icely and Nott, 1992). These peristaltic contractions grasp the faecal pellet via fine setae on the hindgut surface to maintain traction on the peritrophic membrane as it moves posteriorly toward the anus (Fig. 4.15B). The majority of setae are directed posteriorly to prevent back-flow of material. Circular muscle is extremely well developed around the anus and is probably involved in constricting the hindgut lumen to force the faecal pellet through the anus to the exterior. This process is aided by smooth muscles located in the outer connective tissue.

Tegumental glands, common in the majority of decapod hindguts, are not present beneath the epithelium in *T. orientalis*. They have been reported to secrete mucus and binding agents to lubricate the faecal pellet during egestion (Barker and Gibson, 1977; 1978).

In addition to defecation, the hindgut of *T. orientalis* is probably involved in anal drinking. Antiperistaltic contractions of the hindgut wall, known for other decapods (Lovett and Felder, 1990a), could not be seen but the extensive musculature suggests it

occurs. The peritrophic membrane, in addition to protecting the epithelium from abrasive solids within the faecal pellet, may also separate chyme and faecal material from extraperitrophic water taken up during this process (Lovett and Felder, 1990a).

Information on the structure and function of the entire alimentary tract of *T. orientalis* forms the basis upon which comparisons with other scyllarids can be made. It conforms to the general plan of all decapods although its structural characteristics, in particular those of the proventriculus, reflect its primarily soft flesh diet, for example, the simplification of the ventral filtration system of the cardiac stomach and sharp cutting and macerating edges of the gastric mill teeth. An unusual region of the tract, the posterior pyloric sector appears to be unique to scyllarids.

Chapter 5. Structure and Function of the Digestive Gland

5.1 INTRODUCTION

The digestive gland plays a central role in the digestive processes of decapod crustaceans (refer Ch 4.1). It is morphologically similar in most decapods, although the number of lobes may vary between species (see reviews by Gibson and Barker, 1979; Icely and Nott, 1992; Brunet *et al.*, 1994). The digestive gland is a large organ which occupies much of the cephalothoracic cavity and is connected to the ventro-posterior of the pyloric stomach by two primary ducts. Each duct branches extensively into numerous blind-ending tubules which comprise the digestive gland. The tubules are supported by a continuous network of connective tissue rich in blood sinuses and vessels (Factor and Naar, 1985), and have circular and longitudinal muscles beneath their basal lamina (Al-Mohanna and Nott, 1989).

The epithelial cells of the tubules are differentiated into 4 cell types, conventionally classified as E-(embryonic/embryonalenzellen), R-(resorptive/resorptionzellen), F-(fibrillar/fibrillenzellen) and B-(blisterlike/blasenzellen), according to the scheme of Jacobs (1928) and Hirsch and Jacobs (1928). In some decapods a fifth cell type is present, which Al-Mohanna *et al.* (1985a) termed the M-(midget) cell. As they are not universal to all decapods these cells will not be discussed further.

Despite extensive research over the past 30 years, controversy still exists over the functions of the various cell types. The digestive gland is very fragile and death or trauma is rapidly followed by proteolytic autolysis within the cells. Consequently, workers have relied on histological and cytological techniques which, because of the inherent limitations of cell fixation, are often difficult to interpret. Rapid autolysis may also significantly change intracellular proteins so that mis-identification during histochemical examination is possible. Different stages of the feeding and moult cycles, both of which affect cell cytology, have often been ignored. Recent application of advanced techniques such as X-ray microanalysis, immunohistochemistry and Percoll density-gradient centrifugation (Al-Mohanna and Nott, 1987; Vogt *et al.*, 1989; Toullec *et al.*, 1992) have clarified some cell functions.

Based on unambiguous ultrastructural evidence, the role of E-cells in mitotic differentiation (Al-Mohanna *et al.*, 1985b; Vogt, 1993) and R-cells in absorption of diffusible metabolites and storage of lipid and glycogen (Al-Mohanna and Nott, 1987) is widely accepted. Furthermore, X-ray microanalysis of R-cells has revealed a role in the detoxification of heavy metals by storing them in an insoluble form within the cytoplasm for subsequent elimination and excretion from the body (Hopkin and Nott, 1979; Lyon and Simkiss, 1984). Accumulation and mobilisation of lipid and glycogen, as well as calcium, magnesium and copper, within the R-cells has also been found to be closely linked with the moult cycle (Al-Mohanna and Nott, 1989).

In contrast, F- and B-cell function has been variously explained, largely because of inadequate techniques of enzyme identification and localisation. For example, the site of enzyme biosynthesis has often been deduced from activity within tissue homogenates, which is incapable of determining the particular cell type involved (Gibson and Barker, 1979). In addition, evaluation by histochemical techniques was often inaccurate because of the unsatisfactory specificity of chromogenic and fluorogenic substrates used, as well as the inactivation of enzymes during fixation. Consequently, the histochemical identification of enzymes within the central vacuole of B-cells and their subsequent extrusion into the lumen, led workers to conclude incorrectly that the B-cells were involved in enzyme synthesis and secretion (Loizzi and Peterson, 1971; Gibson and Barker, 1979; Caceci *et al.*, 1988).

This has been refuted by Al-Mohanna and Nott (1986) who provided evidence for their role in absorption and intracellular digestion of nutrients, a role which has been widely accepted over the past few years. Evidence included the active uptake of thorium dioxide and colloidal gold via pinocytosis and the presence of numerous digestive bodies in the cytoplasm. Al-Mohanna and Nott (1986) were able to identify various cytological features consistent with pinocytosis and the digestion of absorbed nutrients such as the sequential formation of subapical vacuoles, digestive bodies and the large central vacuole. In addition, the presence of intact B-cells and their central vacuoles in the faeces provided evidence of an excretory function for waste products from intracellular digestion (Hopkin and Nott, 1980).

In contrast, Vogt (1993) proposed that B-cells are involved in the absorption of

remnants of digestion from the tubule lumen for degradation and eventual excretion. He concluded that the sub-apical vacuoles and central vacuole identified by Al-Mohanna and Nott (1986) are in fact lysosomes which facilitate the breakdown process. He considered that a nutrient absorbing function is unlikely as they were unable to discriminate selectively against the biologically inert materials, colloidal gold and thorium dioxide. Vogt (1993) concluded that the majority of digestion occurs extracellularly in the tubule lumen, with nutrients being absorbed only by R-cells for either storage or mobilisation. Before acceptance, these hypotheses require verification by other workers, particularly in the identification of lysosomes and their degrading enzymes.

The cytological features of F-cells, including extensive rough endoplasmic reticulum, mitochondria, Golgi apparatus and Golgi vesicles migrating to the apical brush border, led workers to conclude that F-cells were involved in the synthesis and secretion of protein (Dall and Moriarty, 1983; Al-Mohanna *et al.*, 1985b; Vogt, 1985). The application of immunohistochemical techniques by Vogt *et al.* (1989) showed conclusively that the protein was digestive enzyme. Immunohistochemistry uses antibodies specific for a purified digestive enzyme to localise it within a tissue and therefore identify the intracellular site of biosynthesis directly and unambiguously. The considerable specificity and sensitivity of immunolocalisation techniques is due to the high binding affinities of antibodies for their respective epitopes (Stryer, 1988). Thus immunolocalisation of *Astacus* protease in dictyosomes and vesicles of the F-cells of *A. astacus* by Vogt *et al.* (1989) clearly identified these cells as the site of enzyme synthesis. This has since been verified by detection of α-amylase activity in F-cell homogenates separated by Percoll density-gradient centrifugation (Toullec *et al.*, 1992).

A number of interpretations of cell genealogy exist, although most workers advocate the two-cell lineage proposed by Hirsch and Jacobs (1928; 1930). This was based upon distribution of the four cell types along each tubule as follows. E-cells are located only at the distal zone. The following zone of cell differentiation comprises young R- and F-cells, the mid-region mature R-, F- and B-cells and the proximal region only R- and F-cells (Gibson and Barker, 1979; Dall and Moriarty, 1983). Based on the lack of B-cells in the differentiation zone, B-cells were thought to have originated from F-cells with R- and F-cells originating from mitotic differentiation of E-cells.

Using an ultrastructural distinguishing mark, the apical complex, Vogt (1993) identified B-cells within the differentiation zone. He concluded that B-cells originate directly from E-cells, and therefore advocated a three-cell-lineage. The fact that a transition of F- to B-cells has never been convincingly demonstrated further supports his hypothesis.

The primary focus of this study was to examine the structure and function of the digestive glands of *T. orientalis*. Identification of tubule epithelial cells (R-, F-, B-) was based on their structural and cytological characteristics, which were investigated using histology and transmission electron microscopy, respectively. Specialised procedures were also applied to determine the role of each recognised cell type and help resolve some of the controversy surrounding cell function.

The role of R-cells in metal accumulation and excretion was by X-ray microanalysis to identify the cytoplasmic structures responsible and the types and relative concentrations of metals stored. The role of F-cells in enzyme synthesis and secretion was verified using immunohistochemistry against purified *T. orientalis* trypsin (refer Ch 7). Other possible sites of trypsin production in the alimentary tract was also investigated by immunolocalisation of representative areas: the oral region (membranous lobe), proventriculus and hindgut. Cytological evidence was used to verify active absorption by B-cells as well as excretion of cell contents.

Structural characteristics of the primary duct were used to identify any possible contribution to the mechanism by which fluid enters and exits the digestive gland, an area of much contention in decapods (see Ch 4.1).

5.2 MATERIALS AND METHODS

5.2.1 Histology and Histochemistry

Owing to the highly fragile nature of digestive gland tissue, care was needed during examination. Rapid proteolytic autolysis after death or trauma was minimised by rapid dissection and placement in fixative. The fixative used was marine Bouin's fluid (Winsor, 1984), selected after extensive trials (see Ch 3.2.1.3).

Animals were placed on ice for up to 20 min, depending on their size, prior to gland removal. Glands were cut into 5 mm x 5 mm blocks to promote rapid infiltration of the fixative over 24 h and processed and sectioned routinely as described in Ch 3.2.1.3. Sections (6 μm) were stained with haematoxylin-eosin and Mallory-Heidenhain (see Appendix 1).

The location of protein in the digestive gland and associated tissues was investigated using mercuric bromophenol blue as described in Ch 3.2.1.4; Table 3.1.

5.2.2 Cytology

Cell cytology was examined using transmission electron microscopy (TEM) according to the method outlined in Ch 3.2.3 with the following amendments concerning the length of fixation. Fresh tissue was cut into small pieces (1 mm x 1 mm) and fixed in 4% glutaraldehyde in Millipore filtered seawater (MFSW) pH 7.1 for 1 h at 20°C. Tissue was washed in 0.1 M cacodylate buffer in MFSW pH 7.1 to remove the fixative and then post-fixed in 1% osmium tetroxide in 0.1 M cacodylate buffer in MFSW pH 7.1 for 30 min at 20°C.

5.2.3 Immunohistochemistry

Enzyme localisation was undertaken using a modified version of the immunohistochemical technique outlined by Foster (1988). This initially required purification of an enzyme known to be produced by the digestive gland in high concentrations. For this reason the protease trypsin was chosen (see Ch 6) and its purification by ion exchange chromatography and gel filtration are described in Ch 7. *T. orientalis* trypsin antisera (1° antibody) was raised in mice as outlined in Ch 7.

The digestive glands of recently fed individuals were cut into small pieces

approximately 2 mm thin and fixed for 24 h in marine Bouin's fluid (Winsor, 1984). This fixative was selected from a range tested, including "Histochoice™", 4% formaldehyde, 15% picric acid in 0.1% phosphate buffer pH 7.1 and 4% formaldehyde, 0.1% glutaraldehyde, 15% picric acid in 0.1% phosphate buffer pH 7.1, as it maintained greatest tissue integrity without affecting protein antigenicity. After fixation, the glands were washed numerous times over 12 h in 70% ethanol, to remove the picric acid, and then processed routinely for paraffin wax infiltration (see Ch 3.2.1.3; Appendix 1).

Sections (6 μm) were dewaxed (see Appendix 1) and incubated at room temperature for 1 h in *T. orientalis* trypsin antiserum diluted 1:200 with 10% sheep sera in 0.1 M phosphate buffered saline (PBS), pH 7.0. After three 5 min washes in PBS, the sections were incubated for 1 h in rabbit anti-mouse antibodies conjugated to horseradish peroxidase (HRP) (2° antibody) (Dakopatts, Denmark) diluted 1:200 in 10% sheep sera in PBS. The sections were then washed again in PBS (3 x 5 min) and developed in 0.05% 3,3'-diaminobenzidine (DAB) in 50 mM Tris-HCl pH 7.5 in the presence of 1 μl H_2O_2 ml^{-1} for approximately 10 min (Harlow and Lane, 1988). The location of immunoreactive trypsin was visualised by a golden brown / dark brown colouration attributable to the precipitate formed upon reaction of DAB with HRP. Sections were counterstained in haematoxylin-eosin (5 min) and blued using Scotts tapwater substitute (2 min). They were then routinely dehydrated, cleared and mounted in DePeX (BDH Chemicals) (see Appendix 1).

Nickel ammonium sulphate enhancement was also used in concert with DAB for greater development sensitivity. Sections were incubated in reaction mixture, 1% nickel ammonium sulphate, 0.05% DAB, 0.4% NH_4Cl, 20% D-glucose in 0.2 M sodium phosphate pH 7.4, for 3 min and developed by addition of 1 μl of glucose oxidase ml^{-1} reaction mixture for 20 min. Location of trypsin was visualised by a blue/black chromogenic colouration. Sections were counter stained in Light Green for 1-2 min, dehydrated, cleared and mounted.

A number of control screenings were performed to test the specificity of the 1° antibody (*T. orientalis* trypsin antiserum) and to ensure that staining was not attributable to nonspecific reactions (false positives). These were as follows:

i) 2° antibody + DAB only, to detect any nonspecific binding of rabbit anti-mouse

antibodies to the section. This is generally prevented by blocking any nonspecific binding sites which may react with the 2° antibody using either sheep or rabbit sera.
ii) DAB only, to detect any endogenous HRP activity within the section.
iii) Negative control tissue, using *T. orientalis* adductor muscle, which does not contain digestive enzymes such as trypsin to ensure staining of normal tissue does not occur.
iv) Antigen/antibody control which verifies that no nonspecific binding of *T. orientalis* trypsin antiserum occurs to regions of the section, that is, the *T. orientalis* trypsin antisera is only specific for the antigen trypsin and no other protein.

The technique was also applied to 6 μm sections of other regions of the alimentary tract including the oral region (membranous lobe), the proventriculus and the hindgut. Tissues were treated identically to the digestive gland following the protocol outlined above.

5.2.4 X-Ray Microanalysis

X-ray microanalysis was used to determine whether unusual osmiophilic structures (residual bodies) within the R-cells were metal deposits and if so, which types were present and in what relative concentrations. Thick resin sections (1 μm) were cut on an LKB Nova Ultratome, mounted on hexagonal 200 copper grids and carbon coated for conductivity. Grids were stuck onto stubs using carbon tape and examined with a JEOL JX-840A Electron Probe Microanalyser, at 25 kV. Metal deposits located within residual bodies were identified by back-scatter analysis. X-ray microanalysis was carried out by focussing the electron probe on each deposit for 400 s. This ensured that sufficient X-ray counts diffracting off the metals were accumulated. At least three replicate analyses per residual body were carried out. X-ray microanalysis was also performed on organelles as well as areas of pure resin as a control to establish background levels of metals.

5.3 RESULTS

5.3.1 Digestive Gland Morphology, Histology And Cytology

The digestive gland of *T. orientalis* is a large organ which occupies most of the cephalothoracic cavity, extending antero-posteriorly on either side of the proventriculus (see Ch 4; Fig. 4.1). It has two lobes, each connected to the ventro-posterior of the pyloric stomach by a primary duct (Fig. 5.1A). Each duct ramifies into ductules which open into hundreds of blind-ending tubules.

Primary Duct

A flattened setose ventral sheath extending from the posterior margin of the inner valves of the filter press overlies the openings to the primary ducts (see Ch 4.3.1.2). Each duct is composed of a single type of epithelial cell which is more elongated and densely arranged than those of the pyloric stomach and digestive gland tubules (Fig. 5.1B). Epithelial cells have an apical brush border, mid-basal nuclei and a highly granular cytoplasm (Fig. 5.1C). Beneath the basal lamina are bands of longitudinal striated muscle and bundles of circular muscle which extend the length of the primary duct. Located close to these muscles are granular secretory cells similar to those of the posterior pyloric sector (refer Ch 4.3.2) (Fig. 5.1C). Both the epithelial and secretory cells stain intensely positive with mercuric bromophenol blue which indicates they contain considerable amounts of protein (Fig. 5.1B,C).

Digestive Gland Tubules

The tubules are densely arranged, separated by loose connective tissue which contains blood sinuses and vessels (Fig. 5.2A). Each tubule has a central lumen surrounded by columnar epithelial cells which rest on a thin basal lamina (Fig. 5.2B). There are four cell types: E- (embryonic/embryonalenzellen), R-(resorptive/resorptionzellen), F-(fibrillar/fibrillenzellen) and B-(blisterlike/blasenzellen), according to the original scheme of Jacobs (1928). E-cells were not positively identified in specimens of *T. orientalis* but are presumably found at the distal tips of tubules and are of similar structure and function to those documented for other decapods (Al-Mohanna *et al.*, 1985b; Vogt, 1993). The remainder of each tubule consists of R-, F- and B-cells with R-cells and F-cells the most and least abundant, respectively (Fig. 5.2B; 5.3). Small bundles of circular muscle are located in isolated pockets beneath the basal lamina (Fig. 5.3).

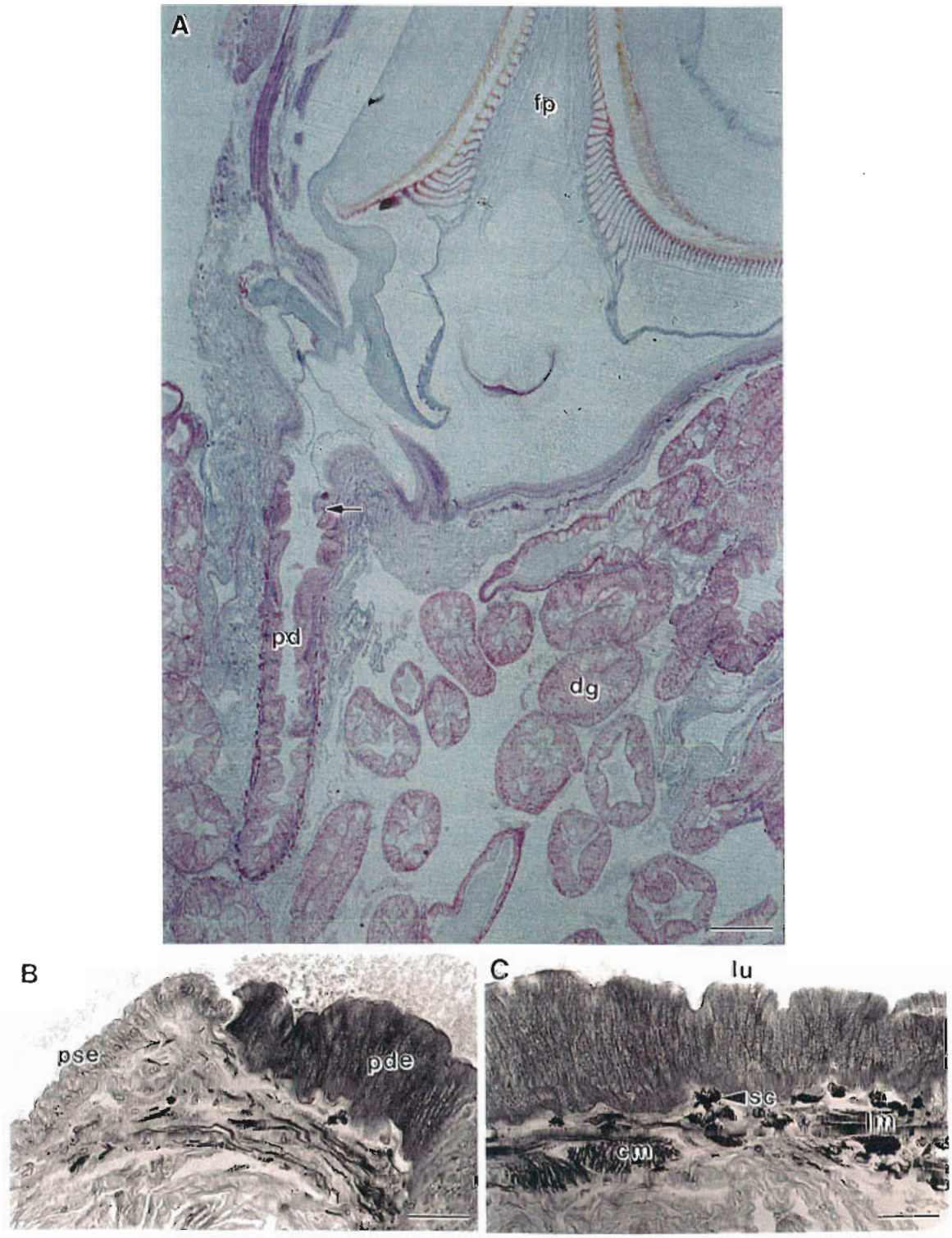

Figure 5.1. A. Transverse section (TS) (6 μm) through the ventro-posterior of the pyloric stomach showing the location of the digestive gland primary duct (left side). Scale, 1 mm. **B.** Junction of the pyloric stomach and primary duct at the position indicated in A (arrow), showing the difference in epithelial cell structure. Mercuric bromophenol blue stained. Scale, 50 μm. **C.** Epithelial cells of the primary duct, stained with mercuric bromophenol blue. Scale, 50 μm.
cm, circular muscle; dg, digestive gland; fp, filter press; lm, longitudinal muscle; lu, lumen; pd, primary duct; pde, primary duct epithelium; pse, pyloric stomach epithelium; sc, secretory cell.

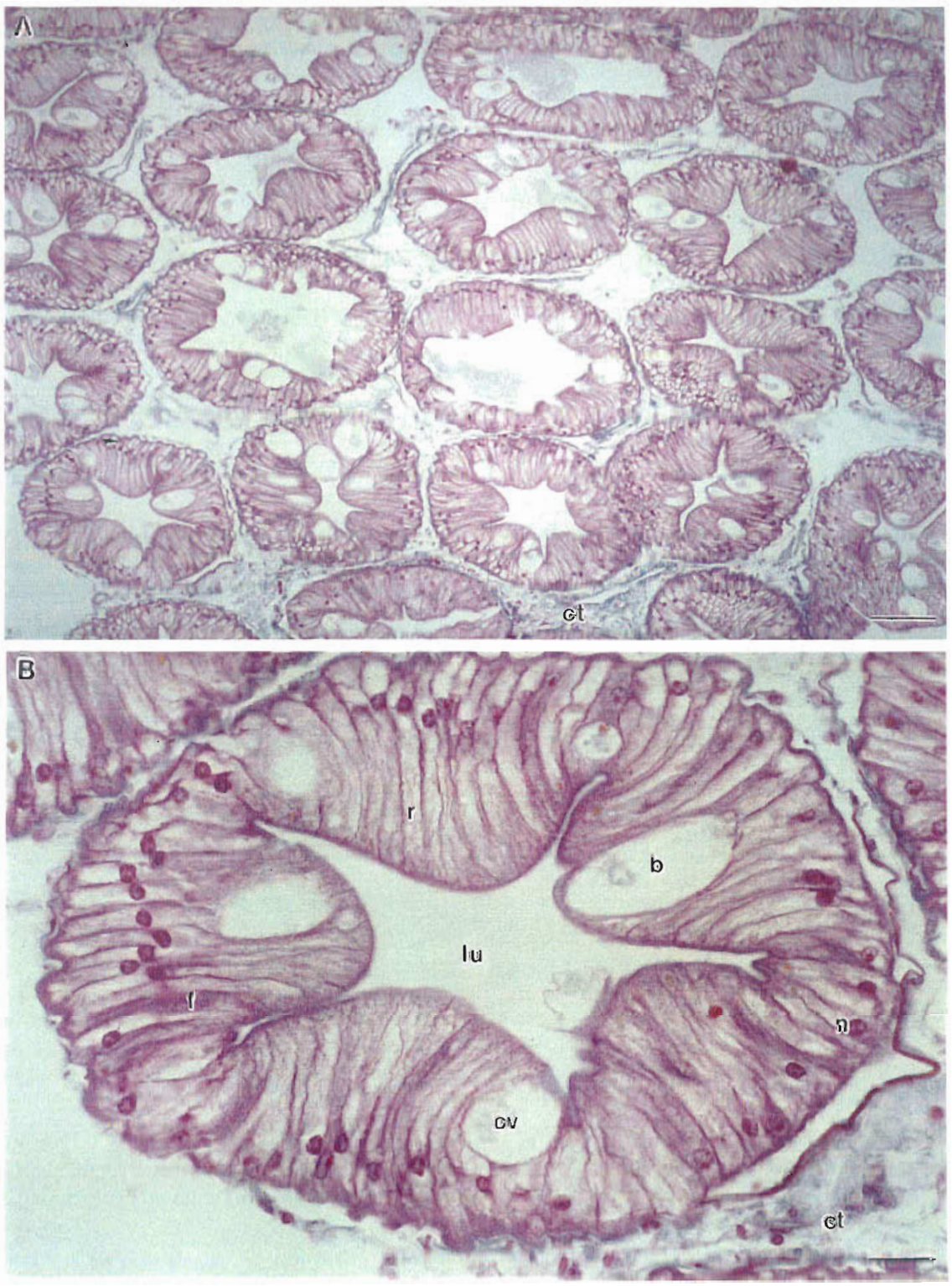

Figure 5.2. A. TS (6 μm) through the digestive gland tubules showing their dense arrangement and supporting connective tissue. Scale, 200 μm. **B.** TS through a single digestive gland tubule showing the types of epithelial cells (R-,F-,B-). Note the obvious central vacuole in the B-cells. Scale, 60 μm.
b, B-cell; ct, connective tissue; cv, central vacuole; f, F-cell; lu, lumen; n, nucleus; r, R-cell.

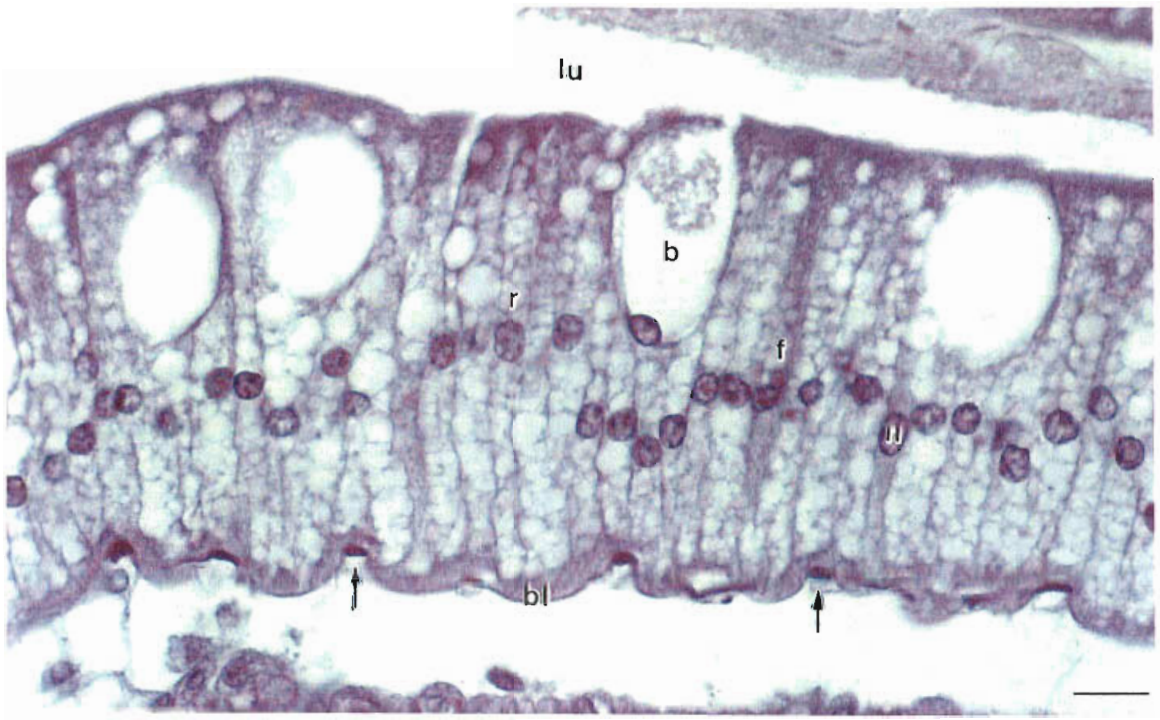

Figure 5.3. Longitudinal section (LS) through a digestive gland tubule showing cell types and small bundles of circular muscle beneath the basal lamina (arrows). Mercuric bromophenol blue stained. Scale, 25 μm. b, B-cell; bl, basal lamina; f, F-cell; lu, lumen; n, nucleus; r, R-cell.

Degradation of the apical membranes of R- and B-cells was often observed, providing evidence for the release of cell contents into the tubule lumen by entire cell decomposition (Fig. 5.4A). Consequently, remnants of B-cell vacuoles were often seen in the tubule lumen.

All cells have a brush border of dense microvilli, approximately 1.2 μm in length (Fig. 5.4B). The lumenal periphery of microvilli is often lined with one or more layers of amorphous material, termed the surface enteric coat (Loizzi, 1971; Lyon and Simkiss, 1984) or "fuzz layer" (Loizzi and Peterson, 1971) (Fig. 5.4B,C). These strands are thickened in common regions and form a continuous sheath over the cell surfaces (Fig. 5.4C).

R-(Resorptive/Resorptionzellen) Cells

Mature R-cells are characterised by lipid deposits (1-10 μm) throughout their cytoplasm (Fig. 5.5A). They are intensely osmiophilic and increase in size apically being either absent or very small basally. Closely associated with lipid deposits are empty vacuoles varying in size between 0.5-8 μm (Fig. 5.5B). They have a well defined outer membrane, which when bordering a lipid deposit, have darkly staining granules along the common membrane (arrow).

There are numerous irregular-shaped mitochondria dispersed throughout the cytoplasm, often located near the lipid droplets (Fig. 5.5A). Dense rough endoplasmic reticulum (RER) is concentrated in the mid to proximal cytoplasm with many vesicles budding from the cisterna (Fig. 5.5C, inset). A basal system of smooth endoplasmic reticulum (SER) is present in the proximal cytoplasm, together with numerous pinocytotic vesicles above the basal lamina. Large numbers of active Golgi apparatus are dispersed throughout the cell, with vesicles budding from the distal margins of cisterna fusing with one another to form large vacuoles (Fig. 5.5D).

Many R-cells have an intensely osmiophilic residual body within the apical cytoplasm which often contains electron dense granular inclusions (Fig. 5.5A, also see Fig. 5.12A). These range in size from 0.8-6 μm and appear to be correlated with the yellow staining granules commonly found in their apical cytoplasm in optical sections stained with Mallory-Heidenhain (Fig. 5.6).

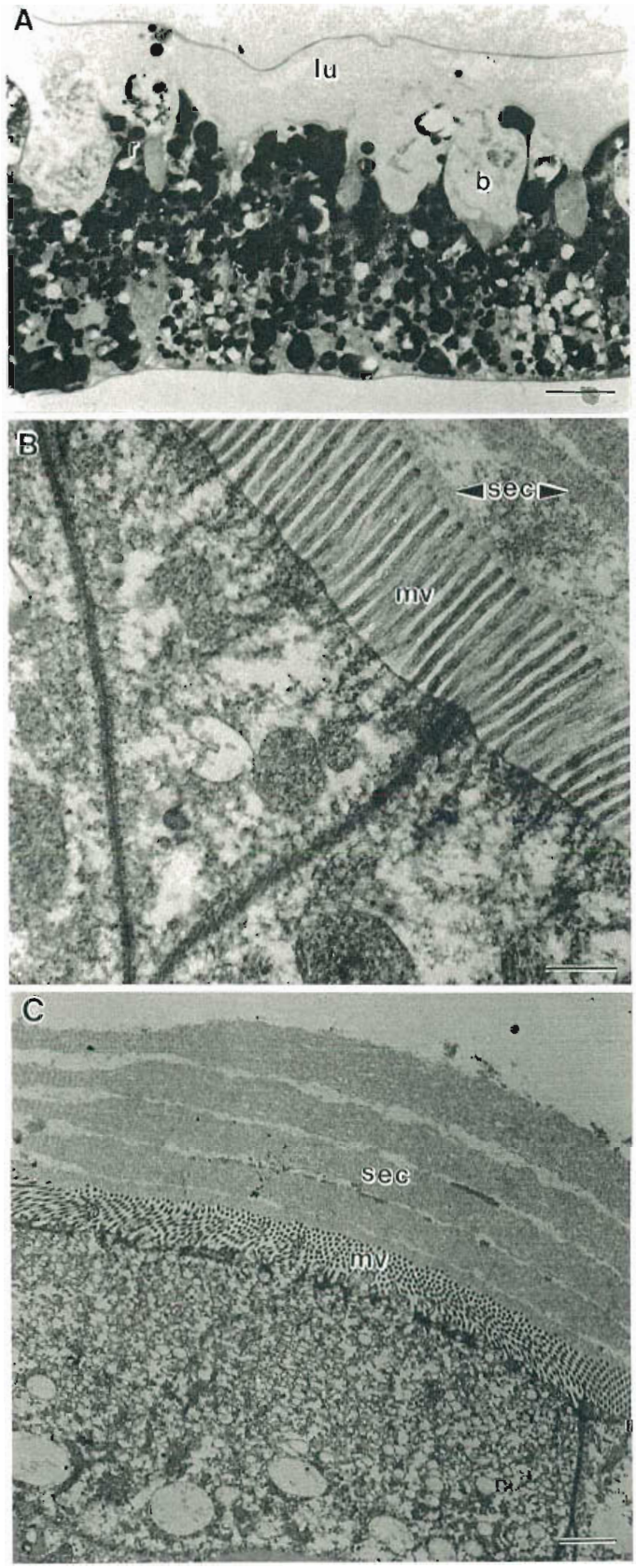

Figure 5.4. A. Longitudinal resin section (1 μm) through a digestive gland tubule demonstrating degradation of the apical membrane of R- and B-cells. Note, the release of contents of the central vacuole of the B-cells and contents of the R-cells into the lumen. Scale, 40 μm. **B.** Transmission electron micrograph (TEM) of the microvillous brush border and its surface enteric coat. Scale, 0.6 μm. **C.** TEM of the multiple layers of the surface enteric coat. Note, the common thickening of layers. Scale, 1 μm.
b, B-cell; lu, lumen; mv, microvilli; r, R-cell; sec, surface enteric coat.

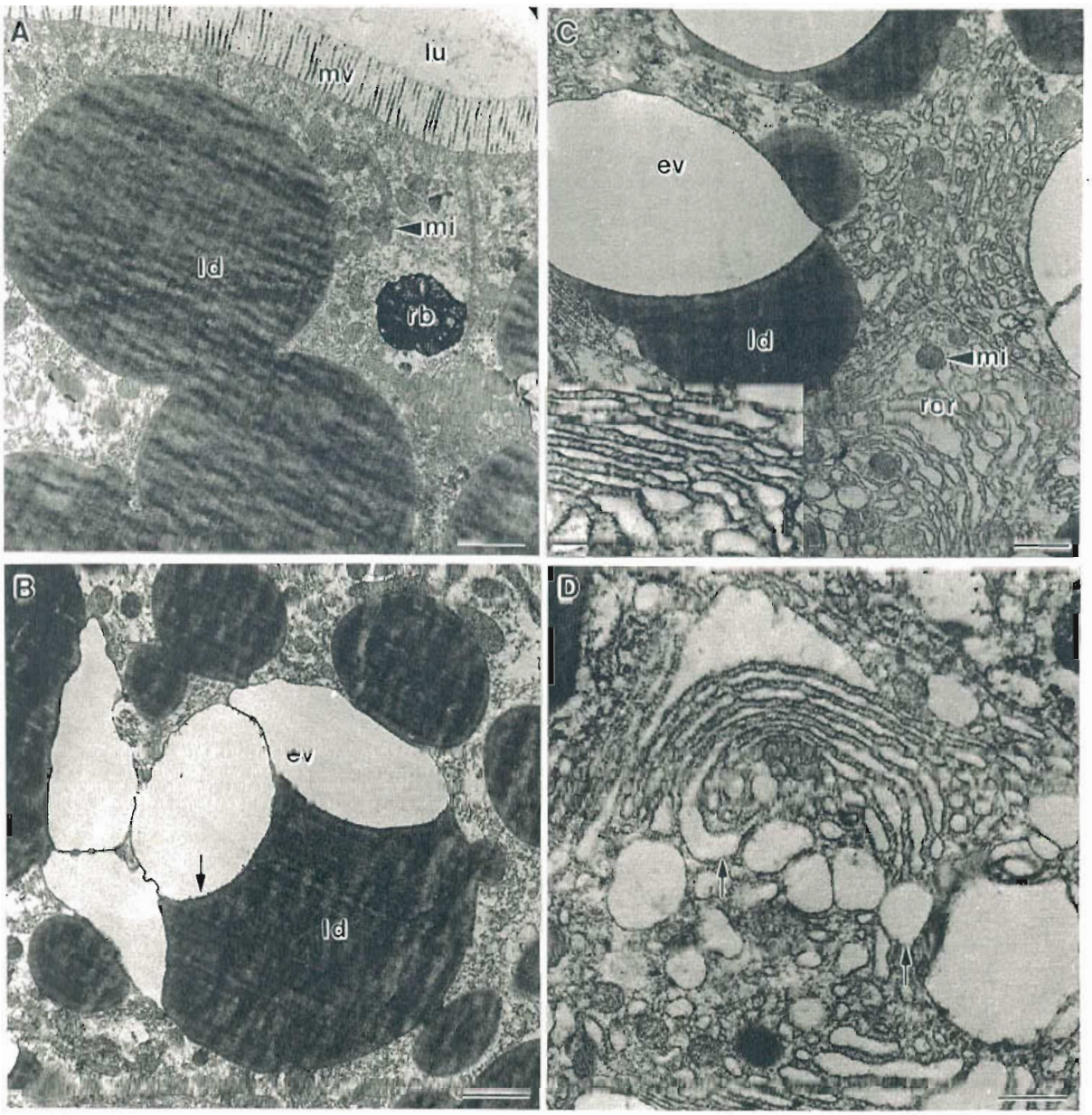

Figure 5.5. TEM of R-cells. **A.** Lipid deposits and residual body in the apical cytoplasm. Scale, 2 μm. **B.** Lipid deposits and adjacent empty vacuoles. Arrow indicates darkly staining granules. Scale, 2 μm. **C.** Rough endoplasmic reticulum (RER) and mitochondria within the mid to proximal cytoplasm. Scale, 1 μm. INSET, budding vesicles at the distal tips of the RER cisterna. Scale, 0.3 μm **D.** Golgi apparatus and budding vesicles (arrows). Scale, 0.8 μm.
ev, empty vacuole; ld, lipid deposit, lu, lumen; mi, mitochondria; mv, microvilli; rb, residual body; rer, rough endoplasmic reticulum.

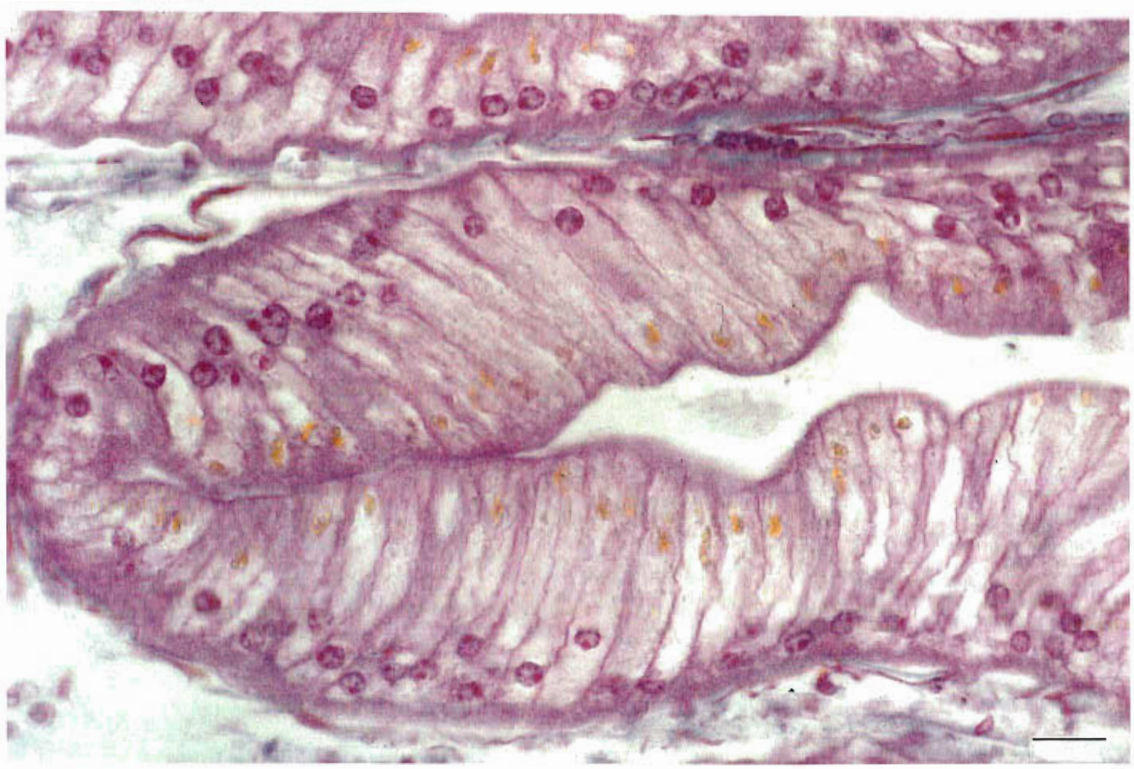

Figure 5.6. LS (6 μm) through a digestive gland tubule showing the yellow staining granules within the apical cytoplasm of R-cells. Mallory-Heidenhain stained. Scale, 60 μm.

B-(Blister-like/Blasenzellen) Cells

B-cells are generally larger than R- and F-cells and are characterised by a single swollen central vacuole which occupies up to 80% of the cell volume (Fig. 5.2B; 5.3). The vacuole contains electron-lucent and flocculent material and the cytoplasm is confined to a thin layer around the cell periphery, often with a compressed basal nucleus. Invagination of the apical membrane forms large numbers of pinocytotic vesicles in the apical cytoplasm directly beneath the microvilli (Fig. 5.7A). These coalesce to form larger sub-apical vacuoles that fuse with the single swollen central vacuole (Fig. 5.7B). These features has been referred to as the apical complex in a number of other decapods (Lyon and Simkiss, 1984; Al-Mohanna and Nott, 1986; Vogt, 1993). Mitochondria are always associated with the apical complex (Fig. 5.7B). Extensive RER and numerous Golgi apparatus occupy the proximal cytoplasm.

F-(Fibrillar/Fibrillenzellen) Cells

F-cells are the least abundant cell type, occurring approximately one in every 15 cells (Fig. 5.2B; 5.3). They are characterised by a densely granular cytoplasm which stains purple with haematoxylin-eosin (Fig. 5.2B). Cytoplasmic granularity in light micrographs is partly attributable to extensive RER, which is closely associated with numerous mitochondria (Fig. 5.7C). Golgi apparatus are abundant and the nucleus, with a prominent nucleolus, is slightly larger than those of R- and B-cells. F-cells give a strongly positive response with mercuric bromophenol blue indicating large quantities of protein (Fig. 5.7D).

5.3.2 Immunohistochemistry

The immunohistochemical procedure produced no ambiguities or false positives, since all immunohistochemical controls for nonspecific reactions were negative.

F-cells in sections developed with DAB stained golden brown indicating the presence of trypsin in the cytoplasm and microvilli (Fig 5.8B; 5.9A,B). This was supported by DAB/nickel-ammonium sulphate enhancement which stained the F-cells blue/black, positive for trypsin. Comparison with almost identical digestive gland sections stained with haematoxylin-eosin confirmed the identification of F-cells as they characteristically stain purple with this oversight stain (Fig. 5.8A,B). Trypsin is usually concentrated toward the apical membrane (Fig. 5.9B; 5.10). It is secreted into the lumen

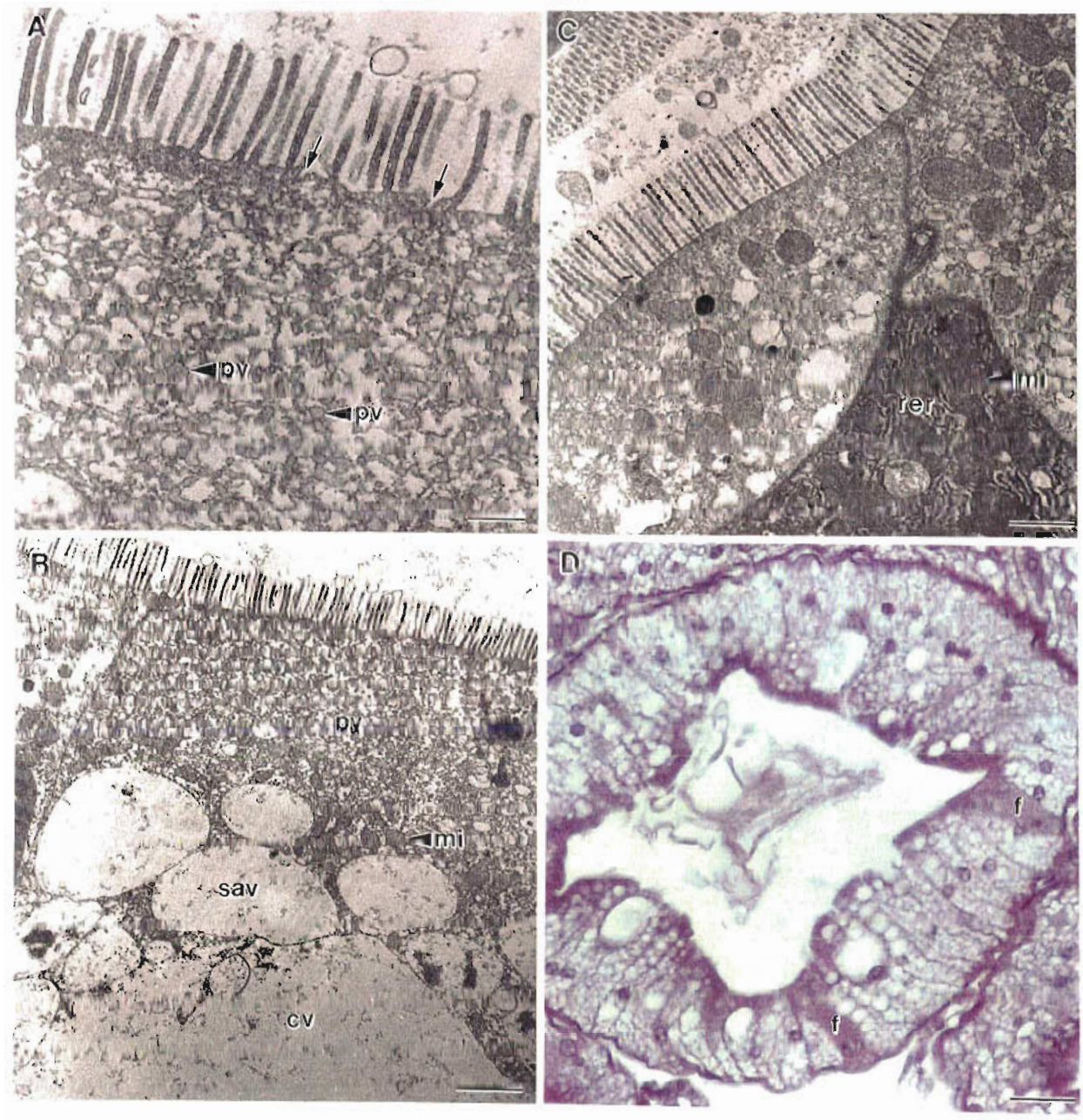

Figure 5.7. TEM. **A.** Invagination of the apical membrane (arrows) and numerous pinocytotic vesicles within the apical cytoplasm of a B-cell. Scale, 0.4 μm. **B.** The characteristic apical complex of a B-cell comprising pinocytotic vesicles, sub-apical vacuoles and the large central vacuole. Note, fusion of the subapical vacuoles with the central vacuole. Scale, 2 μm. **C.** Section of an F-cell indicating the extensive RER and numerous mitochondria. Scale, 1 μm. **D.** Mercuric bromophenol blue stain of a TS (6 μm) through a digestive gland tubule showing the positively stained F-cells. Scale, 80 μm.
cv, central vacuole; f, F-cell; mi, mitochondria; pv, pinocytotic vesicle; rer, rough endoplasmic reticulum; sav, subapical vacuole.

as verified by the absence of trypsin basally within the F-cell indicated in Fig. 5.9A and the intense staining of digestive fluid in the lumen.

The contents of the B-cell central vacuole rarely contained trypsin, but occasionally, faint staining of the entire vacuole contents or concentrations around the periphery and apical membrane, indicated minimal amounts were present (Fig. 5.9B; 5.10).

Digestive enzyme production in other regions of the alimentary tract

Trypsin was not present in the membranous lobe. The slight brown colouration of tissue adjacent to the area without cuticle at the anterior lip (Fig. 5.11A) is attributable to exposure to digestive fluid containing trypsin.

Epithelial cells in the cardiac and pyloric stomachs contained no trypsin, although digestive fluid in these regions did. Similarly, epithelial cells of the hindgut did not contain trypsin, whereas digestive fluid surrounding the indigestible food bolus did (Fig. 5.11B).

5.3.3 X-Ray Microanalysis

X-ray microanalysis was applied to R-cell residual bodies to determine their role in metal accumulation (Fig. 5.12A). Areas of pure resin and typical cell organelles were analysed to determine the background levels of metals inherent in either the resin or the cell itself. Major peaks for copper and silicon were found in all organelles tested as well as pure resin. Zinc was present in smaller amounts and only in pure resin (Fig. 5.12B).

Metal deposits in the R-cells were localised in residual bodies. A total of 10 residual bodies were analysed and representative traces from two are shown in Fig. 5.12C,D and their cytological appearance in Fig. 5.12A. Major peaks for copper and osmium were universal to all residual bodies but are contaminants derived from the grid and fixative, respectively (refer discussion). Aluminium and potassium were also present, often in large concentrations, as indicated by the major peaks in Fig. 5.12C,D. Chromium was only present in one of the residual bodies tested, although its peak was extremely high suggesting a large concentration of this metal (Fig. 5.12C). Iron, manganese,

calcium and magnesium were detected in a number of residual bodies but only in small concentrations as indicated by the minor peaks in Fig. 5.12C,D.

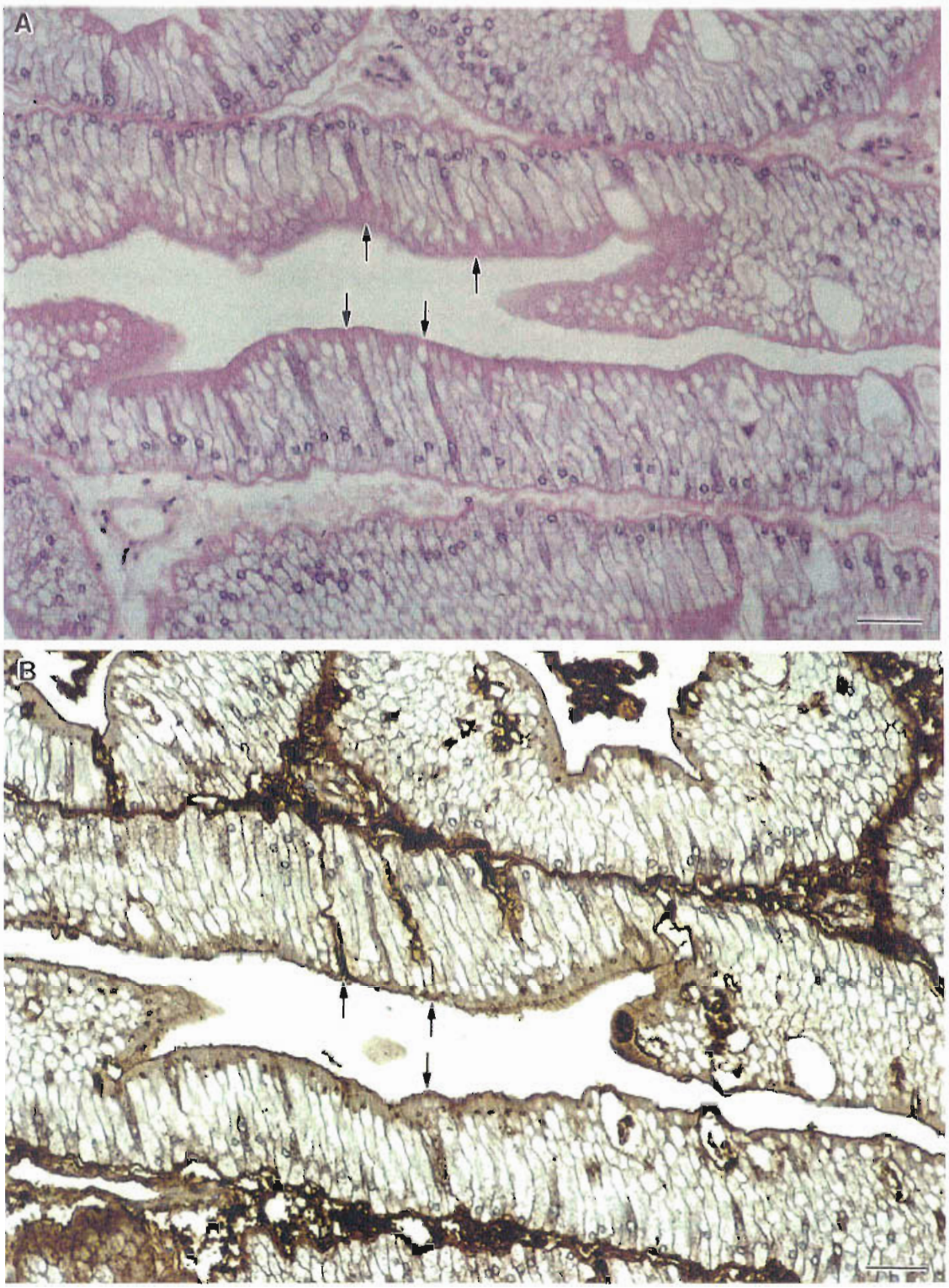

Figure 5.8. Longitudinal serial sections (6 μm) of a digestive gland tubule confirming *T. orientalis* trypsin is localised only in F-cells (arrows). **A.** The characteristic densely staining F-cells with haematoxylin-eosin. Scale, 70 μm. **B.** Immunohistochemistry: the positive reaction of F-cells to trypsin with DAB. Scale, 70 μm.

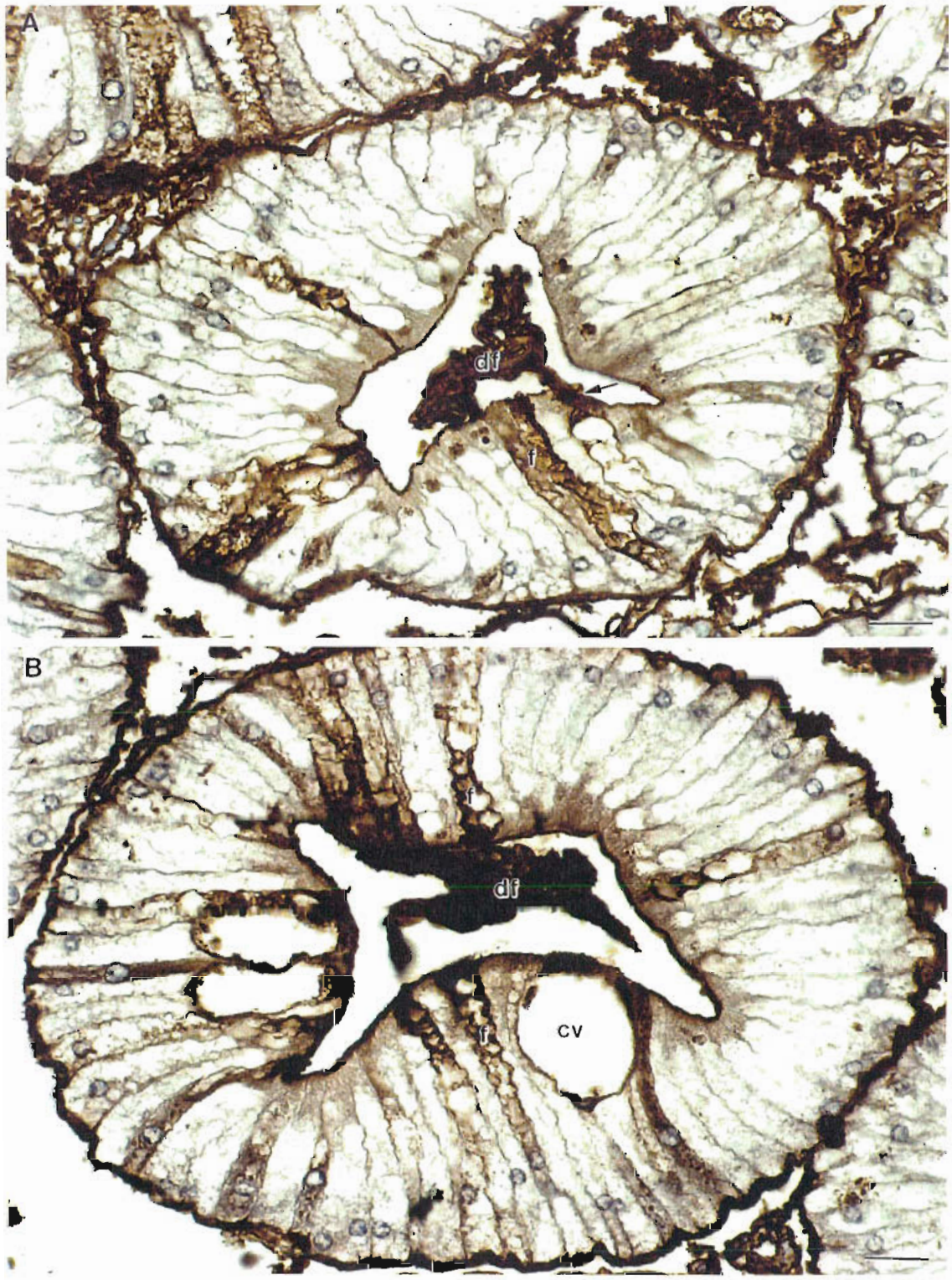

Figure 5.9. TS of a digestive gland tubule illustrating the positively reacting F-cell cytoplasm, microvillous brush border and digestive fluid with DAB. **A.** Note, the secretion of trypsin into the lumen from the F-cell in which trypsin is absent from its basal cytoplasm (arrow). Scale, 40 μm. **B.** Note, the apical accumulation of trypsin and its location around the B-cell central vacuole periphery and apex. Scale, 30 μm.
cv, central vacuole; df, digestive fluid; f, F-cell.

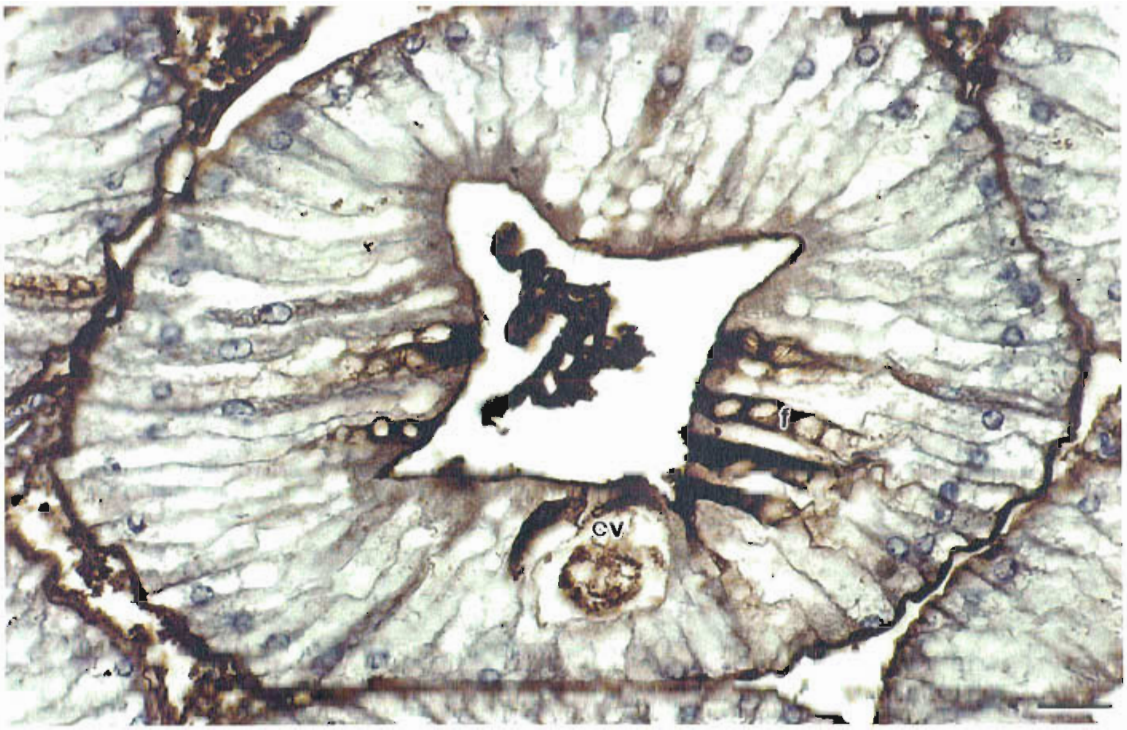

Figure 5.10. TS of a digestive gland tubule illustrating the apical accumulation of trypsin in the F-cells and the positively staining contents of the B-cell central vacuole. Scale, 40 μm.
cv, central vacuole; f, F-cell.

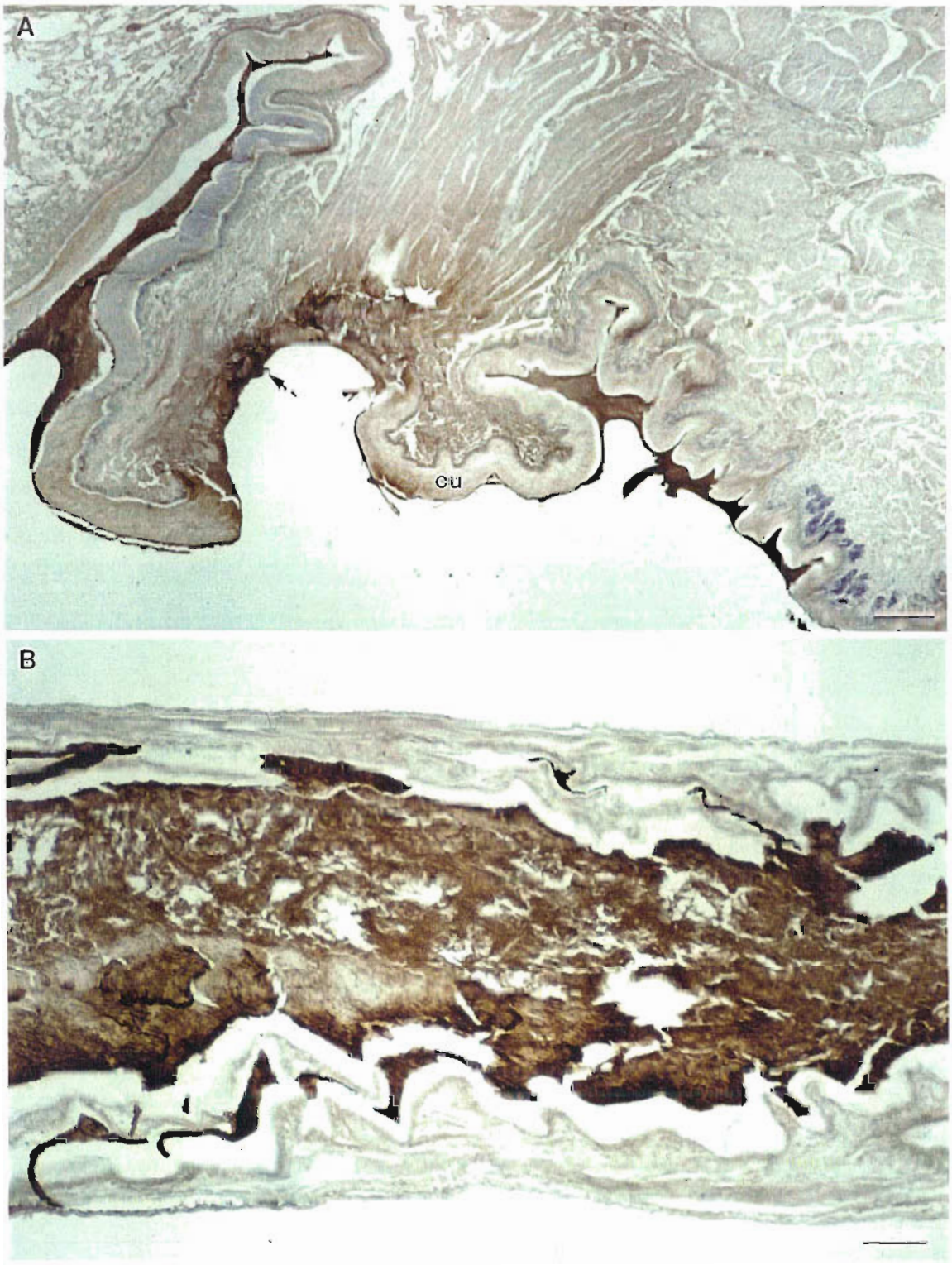

Figure 5.11. A. TS of the membranous lobe anterior lip indicating the absence of trypsin within its tissues, but its presence in the digestive fluid and tissue adjacent to the area without cuticle (arrow). Scale, 200 μm. **B.** LS of the anterior hindgut indicating the absence of trypsin within its tissues, but its presence in the digestive fluid surrounding the indigestible food bolus. Scale, 250 μm.
cu, cuticle.

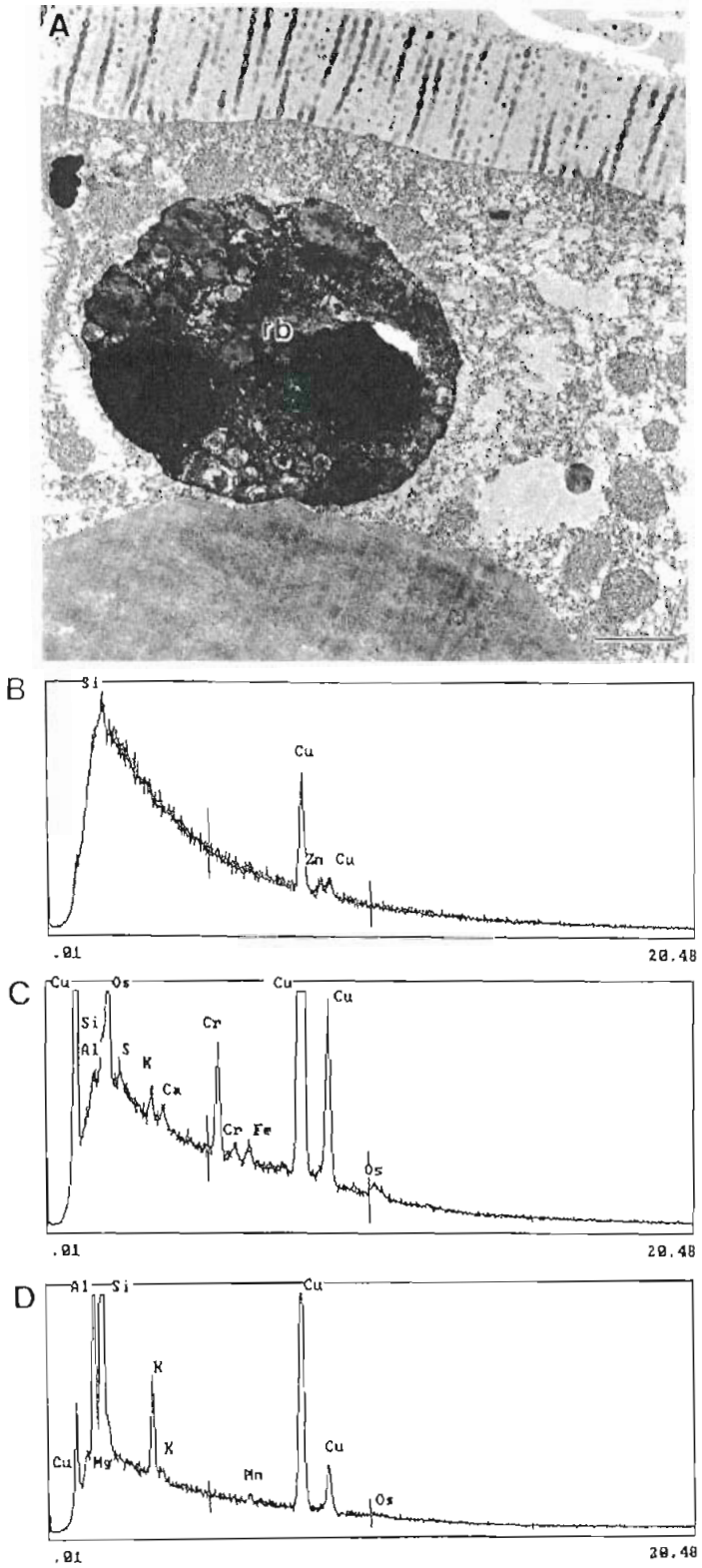

Figure 5.12. A. TEM of an R-cell residual body. Scale, 1 μm. X-ray microanalysis spectra of: **B.** pure resin, to detect background levels of metals inherent in the processing of digestive gland tissue, with major peaks for silica and copper and a minor peak for zinc. Full vertical scale = 1160 x-ray counts; horizontal scale = x-ray energy in KeV. **C,D.** two representative residual bodies, with major peaks for copper, silicon, aluminium, potassium and chromium and minor peaks for calcium, iron, osmium, magnesium and manganese. Full vertical scale = 2050 x-ray counts; horizontal scale = x-ray energy in KeV.
Al, aluminium; Ca, calcium; Cr, chromium; Cu, copper; Fe, iron; K, potassium; Mg, magnesium; Mn, manganese; Os, osmium; rb, residual body; S, sulphur; Si, silicon; Zn, zinc.

5.4 DISCUSSION

The general morphology of the digestive gland of *T. orientalis* is similar to that of all other decapods documented. Likewise the types and structural characteristics of the tubule epithelia (R-, B-, F-) are comparable. However, in contrast to the majority of studies which only applied cytology to elucidate cell function, this study combines a suite of techniques including histology, histochemistry, electron microscopy, x-ray microanalysis and immunohistochemistry to investigate the various roles of each cell type more thoroughly. A number of studies have accomplished this for a single cell type only, for example F-cells - Vogt *et al.* (1989); R-cells - Loret and Devos (1992); B-cells - Hopkin and Nott (1980) and Vogt (1993).

Primary duct

Each lobe of the digestive gland of *T. orientalis* is connected to the ventro-posterior of the pyloric stomach by a single primary duct (Fig. 5.1A). Although the digestive gland has been extensively researched, this is the first study to detail the structure and possible function of the primary duct. Lack of prior information probably arises from difficulties resulting from its small size and orientation so that it cannot easily be identified and traced in histological sections.

The flattened setose ventral sheath which overlies the entrance to each duct (see Ch 4, Fig. 4.7) ensures that only fluid and small particles enter the digestive gland tubules. Large particles rejected from the filter press are channelled into the dorsal pyloric chamber to join indigestible material passing into the posterior pyloric sector (refer Ch 4). This protects the delicate duct and tubule tissues from mechanical damage. A similar role was attributed to the ventral sheath in the thallasinid, *Callianassa californiensis* Dana by Powell (1974).

The mechanism by which fluids enter and exit the digestive glands remains highly controversial. Several theories have been proposed although only those by Powell (1974) and King and Alexander (1994) have supporting evidence based on observations of live specimens. Powell (1974) proposed that fluid enters the digestive gland via a pyloric pump and exits via a booster pump, although he could not verify this second mechanism. Recently, King and Alexander (1994) found that suction created behind the median tooth during gastric mill action was responsible for the exit of fluid from the glands. The

extensive system of circular and longitudinal musculature beneath the basal lamina of the primary duct has not been previously reported and indicates an active role in the movement of fluids into and out of the digestive gland of *T. orientalis*. Although the aforementioned mechanisms possibly operate in this scyllarid, peristaltic contraction and relaxation of duct musculature may also facilitate the entry and exit of fluid from the digestive gland. This may clarify the confusion about the dual passage of fluid along the duct as a reversal in peristalsis by duct musculature would allow the opposite flow of fluid to occur simultaneously. King and Alexander (1994) believe that the suction mechanism created during gastric mill action was also important in this process. Internal observations of peristalsis are now necessary to verify this hypothesis. Based on the extensive development of this musculature it would be possible to observe peristaltic contractions by inserting an endoscope through the carapace of a live animal.

Small bundles of circular muscle found in isolated pockets beneath the basal lamina of digestive gland tubules (Fig. 5.3) appear consistent with the arrangement of circular muscles in *Penaeus semisulcatus* de Haan (Al-Mohanna and Nott, 1989). It is possible their contraction aids the movement of fluid within the tubule lumen. Extensive arrangements of circular and longitudinal muscle have also been found in the digestive gland tubules of *Orconectes virilis* (Hagen), *Procambarus clarkii* (Girard) (Loizzi, 1971) and *A. pallipes* (Lyon and Simkiss, 1984), with Loizzi (1971) stating that these muscles force fluid out of the tubules and into the stomach. However, the apparent lack of longitudinal muscle and the small size of circular muscles in *T. orientalis* suggest it is more likely that the combined action of tubule and primary duct musculature facilitates the passage of fluid into and out of the digestive gland of this scyllarid. Although hypothesised, peristaltic contractions have never been observed in the digestive tubules of decapods but they have been observed in the paired digestive diverticula of amphipods (Kanneworff and Nicolaisen, 1969).

It is likely that the primary duct of *T. orientalis* has functions other than the facilitation of fluid movement. For example, epithelial cells are involved in the production of protein, as determined from mercuric bromophenol blue. However, further examination is needed before the significance of this and other possible roles are elucidated.

Tubules

All tubule epithelial cells are bordered apically by dense microvilli, the lumenal periphery of which is lined with one or more layers of amorphous material (Fig. 5.4B,C), referred to as the surface enteric coat or "fuzz layer" (Loizzi, 1971; Loizzi and Peterson, 1971: Lyon and Simkiss, 1984; Al-Mohanna and Nott, 1987). This is hypothesised to be involved in contact digestion, that is, the hydrolysis of nutritive substrates and subsequent absorption, based on the findings of lipolytic activity in the coat (Loizzi and Peterson, 1971; Momin and Rangneker, 1975). Trypsin located at the microvillous border of cells by immunohistochemistry, may also be present in the surface enteric coat, given their close proximity, suggesting it too could be involved in contact digestion in *T. orientalis*.

Alternatively, Hopkin and Nott (1980) believed similar strands of amorphous tissue at the microvillous border in the crab *Carcinus maenas* Linnaeus were peritrophic membrane. However, this is unlikely to be the case in *T. orientalis* as indigestible material in the posterior pyloric sector of the tract lacked this membrane, which did not appear until the hindgut, indicating a more posterior origin than the digestive glands (refer Ch 4). Furthermore, digestive proteases (trypsin) secreted into the digestive gland lumen from the F-cells would probably hydrolyse the protein matrix, a known component of the membrane (Brunet *et al.*, 1994), prior to its release into the tract.

Although cell genealogy is an important aspect of digestive gland studies, it was not the purpose of this study and will not be discussed in this chapter. The recent findings of Vogt (1993) in support of a three-cell lineage have re-ignited the existing debate and future work on the digestive gland of scyllarids should encompass this issue.

B-Cells

Presence of numerous pinocytotic vesicles formed by invagination of the apical membrane (Fig. 5.7A,B) provides evidence for absorption, by pinocytosis, of fluid and small particles from the digestive gland lumen. Pinocytotic vesicles fuse with one another to form larger sub-apical vacuoles which coalesce and fuse with the large central vacuole. These structural features are collectively termed the apical complex, and are characteristic of all decapod B-cells (Vogt, 1993). Consequently, an absorptive role has

been postulated by all workers (Brunet *et al.*, 1994). However, the nature of the material absorbed and accumulated in the subapical vacuoles and central vacuole is difficult to determine using histological and cytological techniques so that various interpretations of B-cell function have been hypothesised.

Based on tracer experiments and cytological features during a feeding cycle, Al-Mohanna and Nott (1986; 1989) believed the B-cells of *P. semisulcatus* were nutrient absorbing cells involved in intracellular digestion. Several other studies reported enzyme activity in B-cells including proteases in the amphipod *Corophium volutator* (Pallas) (Icely and Nott, 1985), acid phosphatase and aryl sulphatase in the calanoid copepod *Centropages typicus* Kröyer (Arnaud *et al.*, 1984) and α-amylase and trypsin activities in the lobster *Orconectes rusticus* (Girard) (DeVillez and Fyler, 1986) and crab *C. maenas* (Loret and Devos, 1992). This active enzyme activity, particularly the digestive enzymes α-amylase, trypsin and proteases is consistent with a digestive role. Similarly, detection of *T. orientalis* trypsin within the central vacuole suggests that B-cells of this scyllarid may also be involved in intracellular digestion. However, it is not known whether *T. orientalis* trypsin and the aforementioned enzymes are endogenous to the B-cell or have been absorbed from the tubule lumen for excretion (see below). It is also unusual to find α-amylase and trypsin, which hydrolyse large carbohydrates and proteins, in B-cells that are presumably absorbing partially digested nutrients for the final stages of digestion. If this is so, one would expect glycosidases and peptidases to be present as they are involved in the final hydrolysis of glycosides and peptides into their component sugars and amino acids (refer Ch 6). In addition, immunohistochemical identification of trypsin gives no indication of whether this protease is active or inactive. Hence further investigation on the origin and activity of trypsin and the presence of active glucosidases and peptidases in the B-cell is required to verify their digestive role in *T. orientalis*.

In contrast to previous workers, Vogt (1993) has hypothesised that B-cells have an excretory role based on their cytological features, holocrine secretion and presence of entire B-cells in the faeces (Hopkin and Nott, 1980). Holocrine secretion of B-cells and the presence of central vacuoles in the tubule lumen of *T. orientalis* are consistent with an excretory function. Vogt (1993) believes excretion involves absorption of waste products of digestion and degradation of the pinocytosed material via the following process. Pinocytotic vesicles fuse with Golgi vesicles to form subapical vacuoles which

he considers are secondary lysosomes. These coalesce to form the central vacuole which he regards as a "huge" lysosome.

Although a similar progression is evident in *T. orientalis*, the size, density and structure of the subapical vacuoles and central vacuole are not consistent with conventional primary and secondary lysosomes. Lysosomes vary between 0.25-0.8 μm in diameter and are generally electron-dense structures often containing myelin bodies, pigments and crystals once fusion and digestion of pinosomes and phagosomes has occurred (Weiss, 1983; Fawcett, 1994). The size of subapical vacuoles and the central vacuole is considerably larger than typical lysosomes, with the latter often occupying up to 80% of the cell. Similarly, both are electron-lucent, containing flocculent material in contrast to the electron-dense lysosomes reported by others. Given that Vogt (1993) believes Golgi vesicles fuse with pinocytotic vesicles to form secondary lysosomes, one would anticipate a greater abundance of Golgi in the apical region, adjacent to the pinocytotic vesicles, of *T. orientalis* B-cells.

Application of conventional identification methods such as histochemical detection of acid phosphatase, a characteristic lysosomal enzyme (Weiss, 1983; Fawcett, 1994), in the subapical and central vacuoles of *T. orientalis* is required to verify whether these structures are lysosomes. Trypsin is not a known lysosomal enzyme and according to Vogt's (1993) theory may have been absorbed and accumulated in the central vacuole for degradation, as crustacean digestive enzymes are resistant to autolysis (Zwilling and Neurath, 1981).

In conclusion, although an absorptive role by *T. orientalis* B-cells is evident, the unknown nature of material absorbed and accumulated in the subapical and central vacuoles and the obscure origin and state of activity of trypsin prevents a role in either intracellular digestion or lysosomal degradation and excretion being conclusively determined. Nevertheless, absence of apical accumulation of trypsin in the B-cell and its confinement in the central vacuole contradicts proposals that B-cells are a source of enzymes for extracellular digestion (Loizzi, 1971; Gibson and Barker, 1979; Caceci *et al.*, 1988).

R-Cells

Substantial accumulations of lipid throughout the R-cell cytoplasm of *T. orientalis* (Fig. 5.5) suggests a role in the absorption and storage of digestion products; a role which is irrefutably assigned to the R-cells of all decapods examined (Brunet *et al.* 1994). Pinocytosis was not observed at the apical membrane so it is possible that soluble substances are taken up by diffusion or an active transport system, as reported in *P. semiculcatus* (Al-Mohanna and Nott, 1987). Components of the active transport system: SER, RER and Golgi apparatus are all abundant in the R-cells of *T. orientalis*.

Another prominent feature of R-cells is the large number of empty vacuoles in close association with lipid deposits. Their contents are water soluble, as they dissolve during processing and consequently their role is difficult to determine. Similar vacuoles have not been previously reported in the R-cells of other decapods.

Intensely osmiophilic residual bodies unique to R-cells may be the yellow staining granules observed in the apical cytoplasm in light micrographs stained with Mallory-Heidenhain (Fig. 5.5A; 5.6). Based on their electron dense granular inclusions and inhomogeneity of contents, the residual bodies appear to contain cellular debris (Fig. 5.5A; 5.12). Similar yellow-brown granules in the distal cytoplasm of R-cells in *P. clarkii* were also found to contain myelin figures and cellular debris by Bunt (1968), who concluded their contents represented undigested residues remaining after absorption. Barker and Gibson (1977) found similar granules in *Homarus gammarus* Linnaeus to be sites of ATPase, acid phosphatase and possibly lipase activity and suggested they were involved in preparing the debris for elimination. Examination of residual bodies (granules) in *T. orientalis* using X-ray microanalysis revealed they contain metal accumulations, substantiating the role of R-cells in the detoxification of metals by storing them in an insoluble form in this structure. This role in metal accumulation and elimination has also been attributed to the R-cells of several other decapods (Hopkin and Nott, 1979; Lyon and Simkiss, 1984; Al-Mohanna and Nott, 1987; Loret and Devos, 1992). As a result, the digestive gland has often been used as a monitoring organ for levels of pollution in the marine environment (Vogt, 1987).

X-ray microanalysis of pure resin sections revealed peaks of copper, silicon and zinc (Fig. 5.12B), suggesting the presence of these elements in residual bodies is derived

from processing. In particular, copper is attributable to the copper grids upon which sections were mounted (refer Ch 5.2.4). Likewise detection of osmium in residual bodies, but not in areas of pure resin, is credited to the absorption of osmium tetroxide fixative used during tissue processing, as indicated by the extremely osmiophilic nature of residual bodies (Fig. 5.12A,C). Nevertheless higher concentrations of copper in the residual bodies above that of pure resin (Fig. 5.12B,C,D), indicates a genuinely significant accumulation of this metal, as was found in R-cells of several other decapods (Ogura, 1959; Lyon and Simkiss, 1984; Loret and Devos, 1992). Accumulation of copper in dense granules in the caeca of amphipods was found to be directly related to levels in the environment with more mature cells accumulating highest concentrations (Icely and Nott, 1980). This accumulation in *T. orientalis* is beneficial as copper is primarily stored and subsequently transferred to the haemolymph of crustaceans for the production of haemocyanin (Al-Mohanna and Nott, 1989).

Aluminium, potassium and chromium are all metals detected in high concentrations in residual bodies (Fig. 5.12C,D). Potassium is likely to be accumulated for physiological and metabolic purposes and would therefore be mobilised to other cellular regions. In contrast, metals such as aluminium and chromium have no physiological purpose and are most likely stored for detoxification and waste removal. Calcium is often present within R-cells and its levels are synchronised with stages of the moult cycle, where it is accumulated during premoult in preparation for ecdysis and then mobilised during postmoult for calcification of the exoskeleton (Al-Mohanna and Nott, 1989). Similarly, magnesium has also been associated with the moult cycle with low levels indicating its mobilisation for hardening of the exoskeleton during post-moult (Al-Mohanna and Nott, 1989). Iron has not been found previously in R-cells, although it has been detected in the supranuclear vacuoles of F-cells in several decapods (Ogura, 1959; Loizzi, 1971; Lyon and Simkiss, 1984). Its presence is often associated with ferritin, derived either from ingested food or seawater (Lyon and Simkiss, 1984). Manganese has only been found in the R-cells of a crayfish after its injection into the haemocoel (Lyon and Simkiss, 1984).

Similar metal storing structures termed supranuclear vacuoles were reported in *P. semisulcatus* although they primarily contained phosphorus, sulphur, zinc and magnesium (Al-Mohanna and Nott, 1987; 1989). Granular inclusions in the amphipod

C. volutator are also very similar to *T. orientalis* residual bodies and contain copper, sulphur and calcium (Icely and Nott, 1980). Differences in the types and concentrations of metals accumulated may be attributed to variation in diet, environmental levels of metals and moult cycle stage.

R-cells eliminate lipid deposits, accumulated metals and residual material by degradation of the apical membrane resulting in deterioration of the entire cell (Fig. 5.4A). The apical accumulation of lipid deposits was probably in preparation for this process, during which lipids are mobilised for metabolic requirements and metals and residual material are excreted as waste. Mobilisation of lipid often occurs during nonfeeding post moult stages to sustain the enlargement of body tissue and muscle prior to calcification of the new exoskeleton (Al-Mohanna and Nott, 1989).

The R-cells of *T. orientalis* are involved in the absorption, storage and mobilisation of lipid for metabolic purposes and the detoxification of metals by their storage in an insoluble form in the residual body for subsequent mobilisation, or excretion from the body. The mobilisation of metals such as calcium, copper and magnesium is closely linked with the moult cycle.

F-Cells

F-cells are characterised by considerable RER, Golgi apparatus and mitochondria, contributing to their osmophilia and densely granular appearance in light micrographs. These features are common to all other decapods examined and suggest a role in protein synthesis. This is based upon the involvement of RER in protein translation (synthesis), and Golgi apparatus in post-translational modification of the newly synthesised amino acid chain and its subsequent packaging into secretory vesicles for cytoplasmic transport (Mathews and van Holde, 1990). Mitochondria are responsible for the production of adenosine triphosphate (ATP), a crucial energetic requirement of protein synthesis. This role was further verified by the positive reaction of these cells to mercuric bromophenol blue, a histochemical stain specific for protein (Fig. 5.7D). The nature of this protein, however, could not be ascertained using conventional histochemistry. It was not until the use of immunohistochemistry identified trypsin in the F-cells of *T. orientalis* that their role in digestive enzyme synthesis was verified.

Immunolocalisation clearly identified F-cells as the primary site of trypsin synthesis based upon their intense cytoplasmic staining compared with all other cell types in the digestive gland (Fig. 5.8; 5.9). Using similar techniques Vogt *et al.* (1989) found protease to be located in dictyosomes within the F-cell cytoplasm of *A. astacus*. *T. orientalis* trypsin is likely to be found in similar cytoplasmic structures or vesicles although further cytological examination of the entire cell cytoplasm is needed to verify this. Apical accumulation of trypsin, its release from the cell and presence in the digestive fluid indicate F-cells secrete this enzyme for extracellular digestion (see Fig 5.9; 5.10). Vogt *et al.* (1989) provided cytological evidence for the transport of *Astacus* protease vacuoles from the dictyosomes to the cell apex where they are discharged into the gland lumen by exocytosis. It is probable that a similar secretory mechanism occurs in *T. orientalis* although electron microscopy of the cell apex is needed to confirm this.

In the past there has been much confusion over the role of F-cells. This can be attributed to indirect cytological evidence and from the detection of enzyme activity in tissue homogenates or by histochemistry using synthetic substrates. Based only on cytological features, Al-Mohanna *et al.* (1985b) believed F-cells were the sites of enzyme synthesis and secretion. This role was supported by Toullec *et al.* (1992) who detected α-amylase in F-cell suspensions separated by Percoll density-gradient centrifugation. However, studies on whole cell homogenates only indirectly associate F-cells with enzyme production and therefore evidence remained relatively inconclusive. By using immunohistochemistry the present study has unambiguously and directly localised *T. orientalis* trypsin in the F-cells of *T. orientalis* providing conclusive evidence for their role in trypsin biosynthesis. Using similar immunohistochemical techniques to localise *Astacus* protease within the F-cells of *A. astacus*, only Vogt *et al.* (1989) has provided comparable evidence. Direct cellular localisation of a range of enzymes is needed in a number of groups before F-cell function in enzyme biosynthesis and secretion can be confirmed in the Decapoda.

The inability to detect trypsin in the membranous lobe, proventriculus and hindgut tissues suggest that they are not involved in trypsin biosynthesis. Nevertheless, extracellular digestion still occurs as revealed by the positive staining of their associated digestive fluid to trypsin (Fig. 5.11). Consequently, it appears that F-cells of the digestive gland are the primary site of trypsin biosynthesis and secretion in the alimentary tract of

T. orientalis and it contributes to extracellular digestion in the oral region (membranous lobe), proventriculus and anterior hindgut. This is verified by biochemical studies which identified the digestive glands as the site of greatest digestive enzyme activity compared with all other regions of the alimentary tract (Tsai *et al.*, 1986a; McClintock *et al.*, 1991).

In conclusion, the morphology and epithelial cell structure of the digestive gland of *T. orientalis* is consistent with that of all other decapods. It is central to all digestive processes in this scyllarid and the roles of the R-, B- and F-cells have been determined using a suite of specialised techniques including X-ray microanalysis and immunohistochemistry. Although resolution of some of the controversy surrounding cell function has been achieved, further examination of B-cells is necessary to verify their role in either intracellular digestion or degradation and excretion. It is evident their role will remain a contentious issue. Live observations of peristaltic movements are also required to justify the role of the primary ducts in facilitating fluid movement into the digestive glands.

Chapter 6. Types and Concentration of Digestive Enzymes Produced

6.1 INTRODUCTION

A knowledge of the types and concentration of digestive enzymes produced by the digestive gland of decapods is fundamental to our understanding of digestive processes, namely chemical degradation.

Relationship Between Diet and Digestive Enzymes

The close relationship between diet and the range of digestive enzymes produced has been well documented in crustaceans (Kristensen, 1972; Lee *et al.*, 1984; Bärlocher and Porter, 1986; McClintock *et al.*, 1991; Rodriguez *et al.*, 1994). It is known that the types and concentration of digestive enzymes reflect the predominant dietary components of a given animal. In general, carnivorous species that ingest large quantities of dietary protein exhibit a wide range and greater concentration of proteases, whereas those ingesting large amounts of carbohydrate in the form of algae or phytoplankton exhibit a greater range and higher activity of carbohydrases. Based on the range and concentration of digestive enzymes produced, this relationship enables the assessment of which dietary components a crustacean is able to hydrolyse and utilise for metabolic purposes. Consequently, the digestive capabilities of a particular species can be determined (Galgani *et al.*, 1984; Galgani and Nagayama, 1987). This has been utilised by aquaculturalists to formulate commercial feeds to maximise shrimp production and growth. For example, Lee *et al.* (1984) found that dietary protein levels affected protease activity in shrimp of all sizes and concluded that when formulating diets the source and level of protein must be carefully chosen.

A wide range of digestive enzymes has been reported in decapod crustaceans over the last 30 years. Early studies were essentially qualitative, listing an enzyme(s) produced either in a single species, for example, the American lobster *H. americanus* (Brockerhoff *et al.*, 1970; Wojtowicz and Brockerhoff, 1972), or a number of invertebrate groups or species (Sather, 1969; Telford, 1970). Only recently have advances in biochemical techniques enabled the purification and characterisation of enzymes for more accurate comparison between groups. These studies are, however, few in number, concentrating on well known proteases such as trypsin, and commercially

viable species such as penaeid prawns and crayfish (Dendinger and O'Connor, 1990; Honjo *et al.*, 1990; Guizani *et al.*, 1992). As a result, although understanding of the structure and function of these crustacean enzymes is increasing, knowledge of the majority of crustacean digestive enzymes remains limited.

Protein Digestion

Proteins are complex molecules that are initially hydrolysed into polypeptide fragments by endoproteases. These fragments are then further hydrolysed by exopeptidases, which cleave terminal peptide bonds, liberating simpler tri- and dipeptides and amino acids (Stryer, 1988). There are four major families of proteolytic enzymes: serine, zinc, thiol and carboxyl; characterised according to structure and catalytic mechanism (Stryer, 1988). Of these, serine proteases play a substantial role in the digestive process of crustaceans. They are characterised by a uniquely reactive serine residue at the active site which is crucial for catalysis. The two most extensively studied are the endoproteases, trypsin and chymotrypsin. The zinc proteases (exopeptidases), carboxypeptidases, and aminopeptidases are also represented in the Crustacea, although they have been studied to a lesser degree. In contrast to serine proteases, a zinc ion bound to the active site of these proteases is essential for catalysis.

In the many reports of proteases found in crustaceans, almost all have detected at least one trypsin-like enzyme, their classification based primarily on the ability to cleave substrates C-terminal to an arginine or lysine residue. This is considered to be one of the most important proteolytic enzymes in crustaceans with Galgani *et al.* (1984) reporting that 40-50% of total proteolysis was carried out by trypsin in the prawns *Penaeus japonicus* Bate and *Penaeus kerathurus* Forskal.

Some of the groups found to produce this enzyme are: crayfish (Zwilling and Neurath, 1981), lobster (Galgani and Nagayama, 1987), prawn (Lu *et al.*, 1990), krill (Osnes and Mohr, 1985) and crab (Dendinger, 1987). Recently, many of these trypsins have been purified and some of their characteristics determined (Dendinger and O'Connor, 1990; Honjo *et al.*, 1990; Guizani *et al.*, 1992). This has enabled comparisons to be made between the Decapoda and the comprehensively studied mammalian trypsins (refer Ch 7).

Chymotrypsin is an endoprotease which hydrolyses peptide bonds where the carboxyl group is donated by the aromatic amino acids phenylalanine, tyrosine or tryptophan (Stryer, 1988). In contrast to trypsin, detection of chymotrypsin is not universal, with negligible activity reported for many crustaceans including crayfish (Zwilling and Neurath, 1981), shrimp/prawns (Lee *et al.*, 1980; Galgani *et al.*, 1984) and crabs (Brun and Wojtowicz, 1976). However, Van Wormhoudt *et al.* (1992) and Tsai *et al.* (1986a) believe the use of substrates benzoyl-L-tyrosine ethyl ester (BTEE) and N-acetyl-L-tyrosine ethyl ester (ATEE) in these studies hampered the detection of chymotrypsin. Tsai *et al.* (1986a) believe the size of substrate is particularly important for chymotrypsin, with its specificity determined not only by primary aromatic sites but also secondary interactions. This was later verified by the stringent selectivity of shrimp chymotrypsin for substrates with extended polypeptide chains (Tsai *et al.*, 1991). Use of substrates such as Suc-L-$(Ala)_2$-Pro-Phe-ρ-nitrophenyl and radiolabelled peptides enabled them to detect substantial amounts of chymotrypsin in prawns such as *P. japonicus*, which was previously recorded with only traces of activity by Galgani *et al.* (1984), using BTEE. Nevertheless, chymotrypsin has been reported in the crab *Callinectes sapidus* Rathbun by Dendinger (1987) and *P. kerathurus* by Galgani *et al.* (1984) using BTEE as substrate. These discrepancies emphasise the need for caution when choosing substrates for examination of crustacean enzymes, particularly chymotrypsin.

Detailed characterisation of prawn (*Penaeus* spp.) chymotrypsins by Van Wormhoudt *et al.* (1992) and Tsai *et al.* (1986b, 1991) revealed that they are similar in N-terminal amino acid sequence, inhibition and stability to other crustacean serine proteases and have a molecular weight between 25-27 kDa. Interestingly, Van Wormhoudt *et al.* (1992) detected an additional collagenolytic activity in the two chymotrypsins he purified. Such activity was also exhibited by fiddler crab trypsin and chymotrypsin (Eisen *et al.*, 1973; Grant and Eisen, 1980) and shrimp trypsins (Lu *et al.*, 1990). Other studies indicate the existence of a discrete collagenase enzyme in penaeids (Galgani *et al.*, 1984) and the lobster *Panulirus japonicus* von Siebold (Galgani and Nagayama, 1987), many of which exhibit a trypsin-like specificity (Grant *et al.*, 1983). Production of these enzymes is necessary as they feed on animal tissues frequently containing collagen as a major constituent protein.

The exopeptidases, carboxypeptidases A and B, and leucine aminopeptidase are widely represented in decapod crustaceans being reported in prawns (Gates and Travis, 1973), lobsters (Galgani and Nagayama, 1987), crayfish (Zwilling *et al.*, 1979) and crabs (Dendinger, 1987). Carboxypeptidases are the most studied group with an amino acid composition similar to mammalian pancreatic carboxypeptidases, except that they have a higher number of acidic amino acid residues (Zwilling *et al.*, 1979). Carboxypeptidases A and B have been characterised chemically and enzymatically by Gates and Travis (1973) who reported them as separate molecular entities in the prawn *P. setiferus*. Their molecular weights are identical at 35 kDa in the prawns *P. kerathurus* and *P. japonicus* (Galgani *et al.*, 1984). Most studies have, however, simply documented their activity as part of a survey on digestive proteases (Dendinger, 1987). Unlike the carboxypeptidases, leucine aminopeptidases have not yet been characterised in decapods.

Reports of other proteases and peptidases in decapod crustaceans are few in number but it is likely that many, like the seven unidentified proteolytic enzymes found in *H. americanus* by Brockerhoff *et al.* (1970), contribute to protein digestion. No doubt many more will be discovered with increasing interest in biochemical studies attributable to the developing aquacultural potential of many crustacean species.

Carbohydrate Digestion

Digestion of carbohydrates is a complex process often involving at least two enzyme reactions. Structurally complex carbohydrates are initially hydrolysed into smaller oligosaccharides by glycanases (polysaccharases), which cleave internal glycosidic linkages. These in turn are hydrolysed into constituent monosaccharides by numerous glycosidases, specific for terminal glycosidic linkages. Enzyme specificity is determined mainly by the nature of the sugar contributing the reducing group and the type of linkage.

A considerable range of carbohydrases has been detected in decapod crustaceans. However, less emphasis has been placed on these enzymes compared with proteases and only in the last few years have selected carbohydrases been purified and characterised, namely: α- and β-glucosidase (Chuang *et al.*, 1992a,b) and chitinase/chitobiase (Kono *et al.*, 1990; Lynn, 1990; Essaiassen *et al.*, 1992).

α-Amylase (endo-α-1,4-glucanase) is responsible for hydrolysing starch and glycogen, the major storage polysaccharides in plant and animal tissues, respectively. Starch contains two types of glucose polymer, α-amylose and amylopectin. Both consist of long chains of glucose units connected by α-1,4 linkages, although amylopectin is highly branched with the branch points being α-1,6 linkages (Stryer, 1988). Glycogen is similar in structure to amylopectin except that it is more highly branched. α-Amylase activity has been demonstrated in all crustaceans investigated (Sather, 1969; Telford, 1970; Kristensen, 1972; Lee *et al.*, 1980; Glass and Stark, 1995). Early studies attempted to isolate and identify some of its basic features, such as molecular weight (41 kDa) and pH optima (Blandamer and Beechey, 1964; Wojtowicz and Brockerhoff, 1972). Only recently have its characteristics been comprehensively detailed for the brown shrimp *Penaeus californiensis* Holmes (Vega-Villasante *et al.* 1993). These workers found that amylase has a pH optimum of 7.5 and that its activity was enhanced by Mg^{2+} and Ca^{2+} ions. In contrast to the comprehensive characterisations of trypsin, these workers did not purify the enzyme but used crude extract in their studies.

After initial digestion of starch and glycogen by α-amylase, complete hydrolysis is achieved by α-1,4-glucosidase (maltase). This enzyme has been detected in a range of decapods including *H. americanus* (Brockerhoff *et al.*, 1970) and various crab species (Brun and Wojtowicz, 1976; McClintock *et al.*, 1991). Only recently has it been purified and characterised from the prawn *P. japonicus* by Chuang *et al.* (1992a) who determined some of its structural features as well as simple kinetics.

Other complex carbohydrates which are potential energy sources in the crustacean diet are chitin and cellulose. Chitin is a polymer of β-1,4 linked amino-sugars, predominantly N-acetyl glucosamine and to a lesser degree, glucosamine. It is found in a variety of animal phyla, but is best known as a major component of the exoskeleton, gut lining and peritrophic membrane of arthropods, in particular insects and crustaceans. The complete enzymatic hydrolysis of chitin to free N-acetyl glucosamine is performed by a chitinolytic system consisting of chitinase which splits chitin into dimers and trimers of N-acetyl glucosamine which are in turn hydrolysed by N-acetyl β-D glucosaminidase, also known as chitobiase or N-acetylhexosaminidase (Jeuniaux, 1966).

Chitin degrading enzymes have been studied extensively in fish (Danulet and

Kausch, 1984; Lindsay, 1987; Clark *et al.*, 1988) and insects (Koga *et al.*, 1986; Kramer and Aoki, 1987). Much less is known of these enzymes in crustaceans although it is well established that an epidermal chitinase is secreted for resorption of the old exoskeleton (Dall and Moriarty, 1983). Since their early detection in a range of crustaceans by Elyakova (1972) and Kristensen (1972) they have been studied in lobsters (Lynn, 1990), krill (Spindler and Buchholz, 1988) and shrimps (Spindler-Barth *et al.*, 1990; Clark *et al.*, 1993). Most of these studies are aquaculturally orientated; relating the ability of shrimp to utilise chitin in commercial diets for growth, production and survival. Purification and characterisation of chitinase on a range of decapods including the American lobster *H. americanus* (Lynn, 1990) and shrimps *Pandalus borealis* Kroyer (Essaiassen *et al.*, 1992) and *P. japonicus* (Koga *et al.*, 1990, Kono *et al.*, 1990), has only occurred in the last few years. This has provided detailed information on molecular weight, amino acid composition, inhibition and kinetic parameters. Their importance in crustacean digestion is only now being realised despite the predominance of chitobiase in *Cancer* spp., reported almost 20 years ago by Brun and Wojtowicz (1976).

Inability to detect chitinases in a number of crustaceans (Telford, 1970; Fox, 1993; Glass and Stark, 1995) has fuelled debate about whether they can digest and utilise chitin. These studies generally used powdered chitin substrates which are poor in comparison with chito-oligosaccharides or synthetic substrates such as ρ-nitrophenyl N-acetyl glucosamine that have been used in many recent studies.

Cellulose is hydrolysed by a mixture of enzymes loosely referred to as cellulase. The main components are endo-β-1,4-glucanase, exo-β-1,4-glucanase and β-1,4-glucosidase (cellobiase) (Dall and Moriarty, 1983). Cellulases have been poorly studied in crustaceans with considerable confusion about their origin, endogenous versus microbial, and functional significance. Only a few studies have identified cellulases in decapods (Yokoe and Yasumasu, 1964; Elyakova, 1972; Kristensen, 1972), with only minimal activity reported in penaeids (New, 1976). Substrate type is possibly responsible for the reported absence or negligible activity with many studies advocating the use of water soluble cellulose derivatives, namely carboxymethyl cellulose, for accurate determination. Activity detected in *Penaeus aztecus* Ives was found to be attributable to gut bacteria (Dempsey and Kitting, 1987), although the concentration of the enzymes was small and unlikely to play an appreciable role in cellulose digestion. It is believed

that cellulase would be absent from carnivorous crustaceans (Dall and Moriarty, 1983). Additional information such as that provided by the present study is needed for this to be verified.

β-1,3-Glucans are storage or structural polymers in many algae, fungi and protozoans and are therefore a potential source of energy for crustaceans that feed on algae or micro-organisms. β-1,3-Glucanases and glucosidases (laminarinases) hydrolyse laminarin, the major storage polysaccharide in brown algae (Division Phaeophyta) and diatoms (Division Crysophyta) (Percival, 1970). Considerably higher laminarinase activity has been found in Crustacea and Mollusca than any other marine invertebrate group (Sova *et al.*, 1970; Kristensen, 1972). There are, however, no detailed studies despite the fact that laminarinases would be expected to contribute greatly to digestion in herbivorous and detritivorous species.

In this study the types and concentration of proteases and carbohydrases produced by the digestive glands of *T. orientalis* were determined using a range of specific enzyme assays. By correlating these enzymes with dietary components known to be ingested by this and other scyllarids, the digestive capabilities of *T. orientalis* were assessed and compared with other decapods. pH profiles for each carbohydrase were determined and their pH of optimal activity was related to gut fluid pH to reveal whether *T. orientalis* enzymes were well adapted for extracellular digestion; a feature well documented for other crustacean enzymes (van Weel, 1970).

6.2 MATERIALS AND METHODS

6.2.1 Enzyme Extraction

Adult *T. orientalis* collected by otter trawling in Cleveland Bay (refer Ch 2.2.1) were immediately transferred to the laboratory and placed on ice for 20 min prior to digestive gland removal. The digestive glands were used in this study as greatest enzyme activity has been reported in this organ compared with other regions of the alimentary tract (Tsai, *et al.*, 1986a; McClintock *et al.*, 1991). Individual glands were homogenised for 5 min with an UltraTurrax homogeniser in 30 ml of chilled 200 mM Tris pH 7.5 containing 100 mM NaCl. The homogenate was centrifuged at 18000 g for 20 min at 4°C to pellet debris and remove the buoyant lipid fraction. The supernatant, or crude digestive gland extract, was then stored at -20°C.

6.2.2 Enzyme Activity Measurement

All enzyme assays were conducted in duplicate at 37°C in a Hewlett-Packard 8452A diode-array spectrophotometer using crude digestive gland extract. A linear rate of substrate hydrolysis through time was established for each assay to ensure substrate depletion did not affect the estimation of enzyme activity. The appropriate concentration of commercial enzymes were used as positive controls to ensure assay conditions were optimal for enzyme detection. Negative controls in which dH_2O was substituted for enzyme extract monitored possible residual substrate hydrolysis over long incubation periods. Any residual rates were subtracted from the initial rate of hydrolysis to calculate the net rate of hydrolysis. Enzyme activity was generally measured as specific activity in units mg^{-1} digestive gland protein where units are defined in each assay using the appropriate absorption coefficient, ϵ. Protein concentration was measured by the method of Bradford (1977) using reagents supplied by Bio-Rad Laboratories. Bovine serum albumin (BSA) was used as the protein standard.

6.2.2.1 Proteases

i) *Trypsin*

Trypsin (amidase) activity was determined using N-α-benzoylarginine-ρ-nitroanalide (BAPA) (Sigma B4875) as substrate. 50 μl from a stock solution of 20 mM BAPA dissolved in dimethylformamide (DMF) was used per assay. The assay mixture (1 ml) contained a final concentration of 1 mM BAPA, 5% DMF, 200 mM Tris, 200 mM NaCl, 10 mM $CaCl_2$ and 0.2% poly-ethylene glycol 6000 (PEG) pH 7.5. Assays were

conducted at 37°C and initiated by the addition of substrate. Release of ρ-nitroanalide was measured at $A_{400-410}$. One unit of BAPA activity was defined as the amount of trypsin that releases 1 nmole *ρ*-nitroanalide s^{-1} and specific activity as units mg^{-1} where ϵ is 9300 $M^{-1}cm^{-1}$ for *ρ*-nitroanaline (Stone *et al.*, 1991). A positive control of 3 mg ml^{-1} porcine pancreas trypsin (Sigma T7418) in 1 mM HCl was used.

ii) *Chymotrypsin*

Esterase activity was determined using benzoyl-L-tyrosine ethyl ester (BTEE) (Sigma B6125) as substrate. 50 *μ*l from a stock solution of 20 mM BTEE dissolved in DMF was used per assay. The assay mixture (1 ml) contained a final concentration of 1 mM BTEE, 5% DMF and 200 mM Tris, 200 mM NaCl, 10 mM $CaCl_2$, and 0.2% PEG pH 7.5. Release of benzoyl-tyrosine was measured at A_{256}. One unit of BTEE activity was defined as the amount of chymotrypsin that releases 1 nmol of benzoyl-tyrosine s^{-1} and specific activity as units mg^{-1} where ϵ is 964 $M^{-1}cm^{-1}$ for benzoyl-tyrosine (Walsh and Wilcox, 1970). A positive control of 3 mg ml^{-1} bovine pancreas chymotrypsin (Sigma C4129) in 1 mM HCl was used.

iii) *Carboxypeptidase A and B*

Carboxypeptidase A and B activities were determined using the substrates hippuryl-phenylalanine (Hipp-Phe) (Sigma H6875) and hippuryl-arginine (Hipp-Arg) (Sigma H2508), respectively. The assay mixture (1 ml) contained a final concentration of 1 mM substrate and 200 mM Tris, 200 mM NaCl, 10 mM $CaCl_2$ and 0.2% PEG pH 7.5. Activity was monitored as the increase in absorbance s^{-1} at A_{254} resulting from the liberation of hippuric acid. Positive controls were 0.4 mg ml^{-1} bovine pancreas carboxypeptidase A (Sigma C0386) and porcine pancreas carboxypeptidase B (Sigma C7261) in 5 mM $KHPO_4$ buffer containing 1 M NaCl.

6.2.2.2 Carbohydrases

Assays were conducted at a range of pH values to estimate the pH optima of each carbohydrase. The following buffers were used: 100 mM citrate-phosphate at pH 4.0, 5.0, 5.8, 6.5, 7.2 and 100 mM sodium phosphate at pH 5.8, 6.5, 7.2, 8.0. Considerable pH overlap between the buffers ensured any trends in enzyme activity were correctly identified.

i) *α-Glucosidase and β-Glucosidase*

α- and β-Glucosidase activities were determined using the substrates ρ-nitrophenyl α-D glucopyranoside (Sigma N1377) and ρ-nitrophenyl β-D glucopyranoside (Sigma N7006), respectively. Each assay mixture (1 ml) contained a final concentration of 4 mM substrate and 100 mM buffer. Aliquots (100 μl) of assay mixture were removed at time intervals and added to 900 μl of 1 M Na_2CO_3 pH 11 to terminate the reaction and liberation of ρ-nitrophenol measured at A_{400}. One unit of activity was defined as the amount of glucosidase that releases 1 nmol ρ-nitrophenol s^{-1} and specific activity as units mg^{-1} where ϵ is 18 300 $M^{-1}cm^{-1}$ for ρ-nitrophenol at pH>9 (Erlanger *et al.*, 1961).

ii) *N-Acetyl β-D glucosaminidase (chitobiase)*

Glucosaminidase activity was determined using ρ-nitrophenyl N-acetyl β-D glucosaminide (Sigma N9376) as substrate. Assay conditions and units were identical to 6.2.2.2 i).

iii) *β-Galactosidase*

β-Galactosidase activity was determined using o-nitrophenyl β-D galactopyranoside (Sigma N1127) as substrate. Assay conditions were identical to 6.2.2.2 i) with the liberation of o-nitrophenol monitored at A_{420}. One unit of enzyme activity was defined as the amount of β-galactosidase that releases 1 nmol o-nitrophenol s^{-1} and specific activity as units mg^{-1} where ϵ is 21 300 $M^{-1}cm^{-1}$ for o-nitrophenol at pH>9 (Hestrin *et al.*, 1957).

iv) *α-Amylase*

α-Amylase activity was determined using iodine staining. Aliquots (100 μl) were removed at time intervals from assays (1 ml) containing 1% soluble potato starch (Sigma S20004) (300 μl), 100 mM buffer (300 μl) and crude digestive gland extract (400 μl) and added to iodine reagent (5 ml) (0.2% iodine in 2% potassium iodide (50 ml) made up to 60 ml with 6 mM HCl, diluted to 500 ml). Iodine staining was measured at A_{600} to determine the pattern of starch hydrolysis. Activity was defined as change in absorbance min^{-1}. The shape of the curve for starch hydrolysis was used to verify that the enzyme was α-amylase.

v) *Enzyme linked glucose-6-phosphate dehydrogenase and hexokinase assays (G-6-PDH/HK)*

The hydrolysis of a number of carbohydrates: cellulose (Sigma C8758), cellobiose (Pfansteihl Laboratories Inc. 11281A), maltose (Sigma M2250) and laminarin (Koch-Light Laboratories Ltd. 3423h) was determined using the G-6-PDH/HK assay.

Each assay mixture (1 ml) contained 100 μl of crude enzyme extract and 10 mg of substrate in 100 mM buffer. Aliquots (150 μl) of assay mixture were removed and heated (100 °C) for 5 min to inactivate the enzyme. 100 μl was then added to the G-6-PDH/HK assay containing 150 mM adenosine triphosphate (ATP) (Sigma A3377) and 12 mM nicotinamide adenine dinucleotide phosphate (NADP) (Sigma N0505) in 300 mM triethanolamine, 3 mM $MgSO_4$ pH 7.5. The reaction was initiated with G-6-PDH/HK suspension (Boehringer 127825) and liberation of NADPH (reduced form) measured after approximately 15 min at A_{340}. Production of NADPH reflects the concentration of glucose released (Bergmeyer *et al.*, 1984). The amount of glucose (μg) released was then determined from a standard curve of glucose vs. A_{340} and converted into nmol glucose using its molecular weight, 180 g. One unit of activity was defined as the amount of enzyme to release 1 nmol glucose s^{-1} and specific activity as units mg^{-1} digestive gland protein.

6.2.3 pH of Digestive Fluid

Individuals were fed overnight with scallops and placed on ice for 20 min the following morning before dissection. This ensured ample digestive fluid was present for pH determination. The alimentary tract was removed and the digestive gland primary ducts cut from the pyloric stomach. Digestive fluid was then carefully drained from the primary ducts into microfuge tubes which were then centrifuged for 5 min to pellet debris and remove the lipid component. Sufficient fluid was collected from two individuals for pH measurement (approximately 200 μl). Fluid was then transferred to a clean microfuge tube and its pH measured using an Activon BJ331 microelectrode (5 mm x 180 mm). Readings were averaged for final pH determination. Negligible amounts of fluid from the cardiac stomach prevented its inclusion for pH determination.

6.3 RESULTS

6.3.1 Digestive Enzymes

The endoprotease trypsin exhibited high amidase activity against BAPA (Table 6.1). By comparing the specific activity of pure trypsin (0.375 μmol s^{-1} mg^{-1} - refer Ch 7.3) with the total activity of crude extract trypsin (1.52 μmol s^{-1}) it was calculated that trypsin was 4.1 mg of crude extract protein. As the total amount of protein in the crude extract was 183.1 mg, trypsin therefore represents approximately 2% of total protein in the crude extract. Similar calculations from the purification of other crude extracts reveal trypsin may be as high as 13% of total protein which reflects the varying concentrations of this enzyme between individuals of different feeding status. Hence *T. orientalis* trypsin is a large proportion of the total protein extracted from the digestive gland.

Purified trypsin (refer Ch 7) was tested against BTEE to determine whether possible activity from crude digestive gland extract was attributable to trypsin or a discrete chymotrypsin enzyme. Hydrolysis of BTEE by purified trypsin was negligible. Thus the considerable esterase activity exhibited against BTEE by crude digestive gland extract is a discrete chymotrypsin enzyme (Table 6.1).

Negligible hydrolysis of Hipp-Phe and Hipp-Arg suggests carboxypeptidase A and B are produced in undetectable concentrations by *T. orientalis* (Table 6.1).

Table 6.1. Specific activity of proteases from two crude digestive gland extracts of *T. orientalis*. Values are in units mg^{-1} ± standard errors of duplicate determinations, where units are nmol ρ-nitroanalide s^{-1} and nmol benzoyl tyrosine s^{-1} at pH 7.5 and 37 °C for trypsin and chymotrypsin, respectively. -, no activity detected.

Enzyme	Substrate	Extract A	Extract B
trypsin	BAPA	4.5 ± 0.02	3.2 ± 0.01
chymotrypsin	BTEE	22.4 ± 1.5	20.2 ± 1.2
carboxypeptidase A	Hipp-L-Phe	-	-
carboxypeptidase B	Hipp-L-Arg	-	-

A wide range of carbohydrases was detected including glycanases, glycosidases and galactosidases, although the majority of these are produced in relatively low concentrations. Their optimal specific activities and the respective pH values against synthetic and natural substrates are summarised in Table 6.2. Considerable activity was exhibited by N-acetyl β-D glucosaminidase (chitobiase) at 7.0 units mg^{-1}, which is nearly 20-fold greater than the next most active glycosidase, α-glucosidase. α-glucosidase activity was 5-fold higher than β-glucosidase but only 3-fold greater than β-galactosidase (Table 6.2). Cellulose hydrolysis to glucose could not be detected over a range of pH values and cellobiase and laminarinase were present in negligible concentrations.

6.3.2 pH Optima

The carbohydrases are active over a wide pH range (pH 4-8) with all enzymes exhibiting greatest activity at acid pH. Of these the majority are at pH 5.0 (Table 6.2, Fig. 6.1; 6.2). This trend is particularly clear for α-amylase, α-glucosidase, β-glucosidase, β-galactosidase and N-acetyl β-D glucosaminidase and is substantiated by the close overlap between buffer systems (Fig. 6.1; 6.2). All enzymes demonstrate negligible activity at pH 8.0 indicating that alkaline conditions are unsuitable for carbohydrate hydrolysis.

Although quantitative comparison of α-amylase with these carbohydrases cannot be made based on the technique used, the exponential decline in iodine staining of starch over a short time period indicates that a substantial amount of this enzyme is produced by *T. orientalis* (Fig. 6.2C). The concave pattern of starch iodine staining with time verifies that the enzyme is α-amylase and not an exo-hydrolytic enzyme such as α-glucosidase (Fig. 6.2C).

6.3.3 pH of Digestive Fluid

Digestive fluid produced by *T. orientalis*, post feeding, was acidic at pH 5.9.

Table 6.2. Optimal specific activity and pH values of carbohydrases from crude digestive gland extract of *T. orientalis*. Values are in units mg^{-1} ± standard errors of duplicate determinations where units are nmol ρ-nitrophenol s^{-1} at 37 °C for all enzymes with ρ-nitrophenyl substrates and nmol glucose s^{-1} at 37 °C for maltase, cellulase, cellobiase and laminarinase. Specific activity units were not calculated for α-amylase. The buffers used were 100 mM citrate-phosphate (pH 4.0-7.2) and 100 mM phosphate (pH 5.8-8.0). -, no activity detected; neg., negligible activity.

Enzyme	Substrate	pH Optima	Specific Activity
Polysaccharases			
α-amylase	starch	5.0-5.8	
cellulase	carboxy-methyl cellulose		-
laminarinase	laminarin		neg.
Glycosidases			
α-glucosidase	ρ-nitrophenyl α-D glucopyranoside	5.0	0.37 ± 0.004
β-glucosidase	ρ-nitrophenyl β-D glucopyranoside	4.0	0.072 ± 0.001
β-galactosidase	o-nitrophenyl β-D galactopyranoside	5.0	0.11 ± 0.005
N-acetyl β-D glucosaminidase	ρ-nitrophenyl N-acetyl β-D glucopyranoside	5.0	7.0 ± 0.3
maltase	maltose	5.0	0.22 ± 0.003
cellobiase	cellobiose		neg.

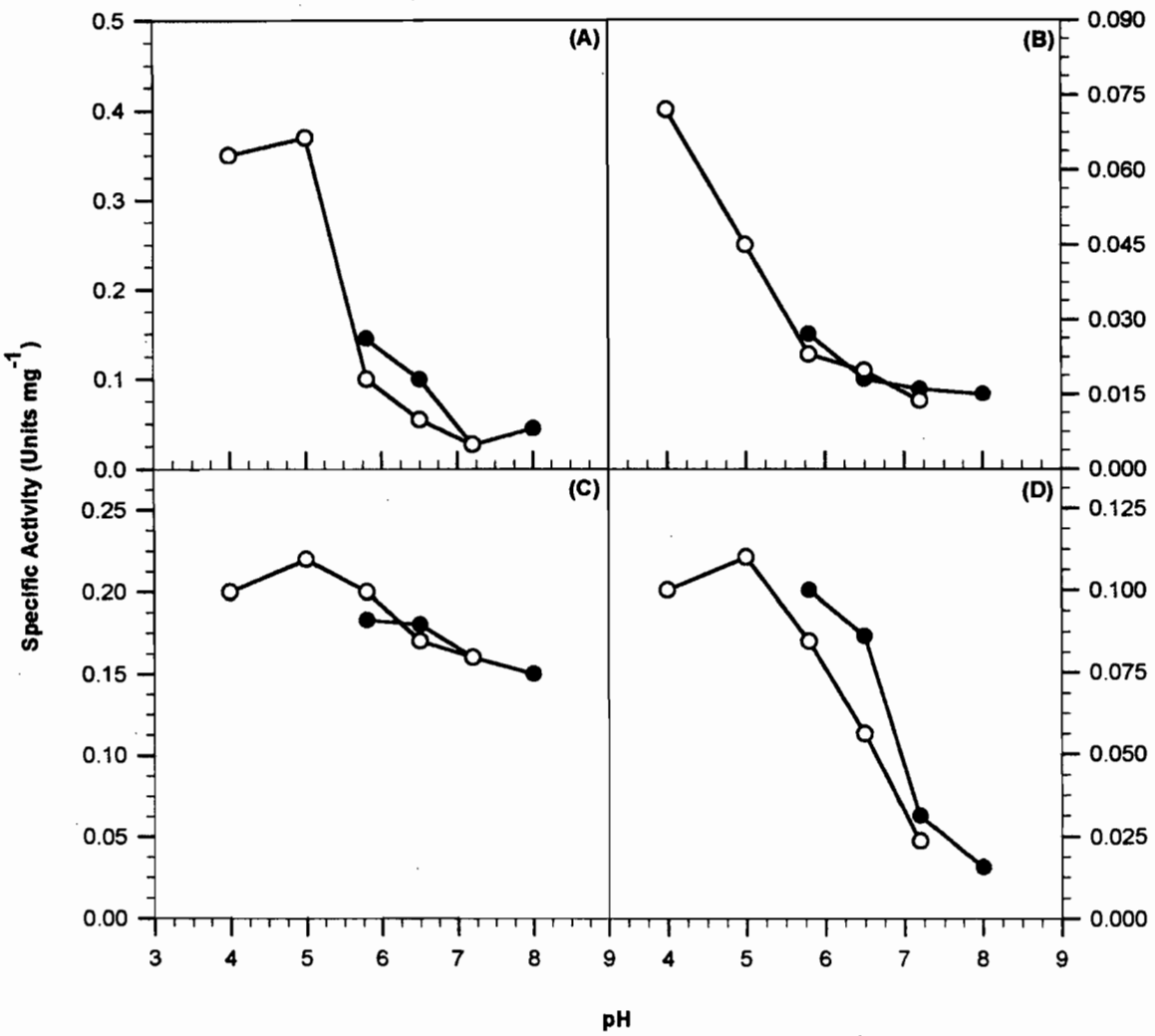

Figure 6.1. Effect of pH on the specific activity of carbohydrases from crude digestive gland extract of *T. orientalis*. **A.** α-glucosidase, **B.** β-glucosidase, **C.** maltase and **D.** β-galactosidase. The buffers used were 100 mM citrate-phosphate (○) and 100 mM phosphate (●). Values are in units mg^{-1} where units are in nmol ρ-nitrophenol s^{-1} for α-glucosidase, β-glucosidase and β-galactosidase and nmol glucose s^{-1} for maltase.

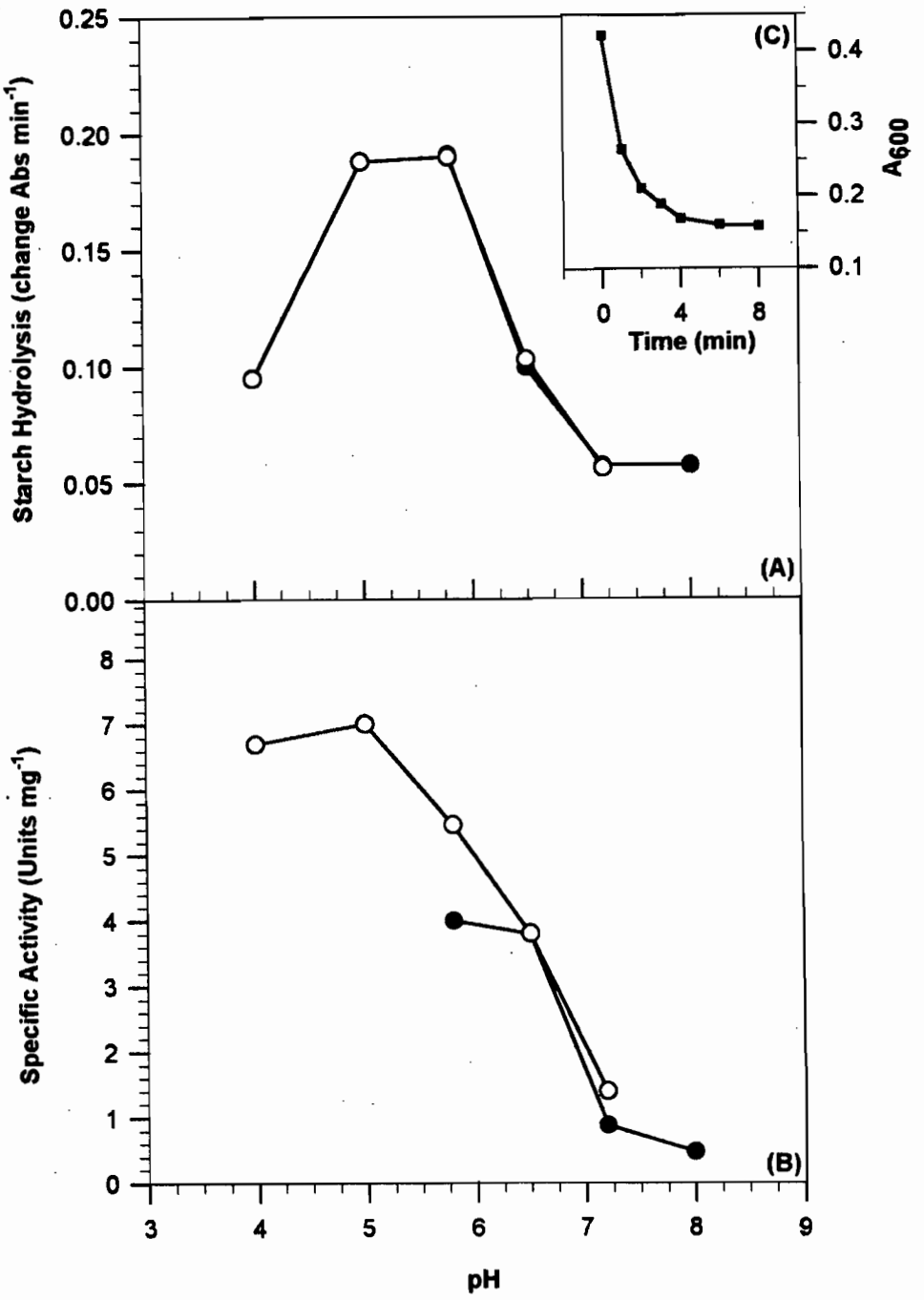

Figure 6.2. Effect of pH on the activity of carbohydrases from crude digestive gland extract of *T. orientalis*. **A.** α-amylase, **B.** N-acetyl β-D glucosaminidase. The buffers used were 100 mM citrate-phosphate (○) and 100 mM phosphate (●). Values are in change in absorbance min^{-1} for α-amylase and units mg^{-1} where units are in nmol ρ-nitrophenol s^{-1} for N-acetyl β-D glucosaminidase. **C.** Starch hydrolysis profile for α-amylase as determined by reduction in the iodine staining properties of solubilised starch.

6.4 DISCUSSION

Digestive Enzymes

Considerable trypsin and chymotrypsin activity indicates *T. orientalis* possesses the enzymes necessary for hydrolysing the large protein component of its carnivorous diet, which includes the adductor muscle of bivalves. It is also consistent with dietary components of other scyllarids including small benthic invertebrates such as crustaceans, polychaetes and gastropods (Ch 1,2; Suthers and Anderson, 1981; Lau, 1987; 1988; Spanier, 1987). Both proteases are important in extracellular digestion as they are endoproteases responsible for the initial hydrolysis of large structural proteins into smaller oligopeptides.

Trypsin has been found in all crustaceans studied and plays a major role in proteolysis. For example, 40-50% of total proteolysis is carried out by trypsin in the prawns *P. japonicus* and *P. kerathurus* (Galgani *et al.*, 1984). Based on the following evidence trypsin is of similar importance in *T. orientalis*.

Trypsin exhibited substantial amidase activity against BAPA (Table 6.1) indicating that it is produced in large concentrations by this scyllarid. It is also a significant proportion (up to 13%) of total protein extracted from the digestive gland. This is substantiated by the ability to visualise the trypsin band clearly when a crude extract is fractionated on SDS-PAGE (refer Ch 7; Fig. 7.6). Trypsin from *P. japonicus* represents a similar proportion of digestive gland protein (11%) (Honjo *et al*, 1990), further verifying the importance of this enzyme in decapod proteolysis.

Although there are several quantitative studies on decapod digestive enzymes, the use of different substrates and activity units makes comparison with data obtained for *T. orientalis* difficult. Nevertheless, comparable values were calculated for the majority of enzymes tested from studies where identical substrates and hence specific activity units were used. These values are presented in Table 6.3.

Table 6.3. Comparison of specific activities of crustacean proteases and carbohydrases from crude digestive gland extracts. Chymo, chymotrypsin; α-glu, α-glucosidase; β-glu, β-glucosidase; β-gal, β-galactosidase; N-AcG, N-acetyl β-D glucosaminidase; malt, maltase. Substrates and units are identical with those used in *T. orientalis* assays (refer Ch 6.2), with values in units mg^{-1} where units are $nmol\ s^{-1}$. Extract A and B values for *T. orientalis* trypsin and chymotrypsin are provided. Trypsin activity in parentheses are against the substrate TAME. *Euphausia superba* values are for three forms (I,II,III) of trypsin.

	Enzyme							
Species	**Trypsin**	**Chymo**	**α-Glu**	**β-Glu**	**β-Gal**	**N-AcG**	**Malt**	**Reference**
Thenus orientalis	4.5, 3.2	22.4, 20.2	0.37	0.072	0.11	7.0	0.22	
Homarus americanus		0	0.1	0.15	0.003	78		Brockerhoff *et al.* (1970)
Cancer borealis			0.016	0.13	0.1	1.5		Brun & Wojtowicz (1976)
Cancer irroratus			0.016	0.15	0.117	3.8		Brun & Wojtowicz (1976)
Callinectes sapidus			0.16	0.17	0.176		0.007	McClintock *et al.* (1991)
Procambarus clarkii		0						Guizani *et al.* (1992)
Callinectes sapidus		0.8						Dendinger (1987)
Penaeus kerathurus	1.0 (350)	3.4						Galgani *et al.* (1984)
Penaeus japonicus	1.0 (816)	0						Galgani *et al.* (1984)
Euphausia superba								Osnes & Mohr (1985)
Enzyme I	2.3 (383)							
Enzyme II	24 (1683)							
Enzyme III	14 (1766)							

The activity of *T. orientalis* trypsin against BAPA is generally similar to trypsins of other decapods which have a similarly high protein component in their diet (Table 6.3). The greater activity of *T. orientalis* trypsin than in the prawns *P. kerathurus* and *P. japonicus* (Galgani *et al.*, 1984) may be correlated with the larger quantity of protein ingested by the carnivorous scyllarid, compared with penaeids which are primarily detritivores scavenging on vegetation, organic detritus and microfauna and only small amounts of animal tissue when available (Chong and Seskumar, 1981; Alexander and Hindley, 1985). The three forms of trypsin in the Antarctic krill, *Euphausia superba* Dana (Osnes and Mohr, 1985), are particularly active with forms II and III being 6-fold and 3-fold greater than *T. orientalis* trypsin. This is unexpected as krill are filter feeders ingesting primarily phytoplankton (Hamner, 1988).

It must be noted that esterase activity against the substrate ρ-tosyl-L arginine methyl ester, TAME, is up to 800 times higher than amidase activity against BAPA for all decapods examined (Table 6.3). This is because trypsin (and most other enzymes) hydrolyse ester bonds more easily than amide bonds because of the weaker structural characteristics of ester bonds. For this reason comparison between the activity of chymotrypsin and trypsin cannot be made in the present study as BTEE is an ester compared with the amide BAPA.

The substantial activity exhibited against BTEE by crude extract is attributable to a discrete chymotrypsin enzyme, based on the negligible hydrolysis of this substrate by pure trypsin. Hence, chymotrypsin also plays an important role in proteolysis in *T. orientalis*. Chymotrypsin has been detected in a number of other decapods including a range of penaeid species (Tsai *et al.* 1986a,b; 1991; Van Wormhoudt *et al.*, 1992), krill (Kimoto *et al.*, 1985) and crabs (Dendinger, 1987). The substantially higher activity of chymotrypsin in *T. orientalis* than the prawn *P. kerathurus* (Table 6.3) is attributable to the greater amount of dietary protein ingested by *T. orientalis* in comparison with the detritivorous penaeid. However, it is difficult to explain why chymotrypsin activity is so low in the crab *C. sapidus* as it is known to ingest similar quantities of protein to scyllarids (Creswell and Marsden, 1990).

Negligible chymotrypsin activity reported for many crustaceans including *H. americanus* (Brockerhoff *et al.* 1970), *P. japonicus* (Galgani *et al.*, 1984) and *P. clarkii*

(Guizani *et al.*, 1992) (refer Table 6.3) has been attributed by Van Wormhoudt *et al.* (1992) and Tsai *et al.* (1986a) to the use of BTEE. Although it is possible that the use of this substrate contributed to poor activity in *C. sapidus*, considerable chymotrypsin activity against BTEE in the present study indicates that other factors may be involved. Either the absence or low activity of this enzyme in other decapods is genuine or factors such as unfavourable assay conditions have prevented workers from accurately demonstrating chymotrypsin activity.

Negligible carboxypeptidase A and B activity in *T. orientalis* is unusual as they are responsible for the final hydrolysis of oligopeptides and dipeptides into amino acids for subsequent absorption (Stryer, 1988). These exopeptidases have been detected in all crustaceans studied including prawns, (Galgani *et al.*, 1984), crabs (Dendinger, 1987) and lobsters (Galgani and Nagayama, 1987). It is unlikely that poor affinity of these enzymes for Hipp-Phe and Hipp-Arg prevented their detection in *T. orientalis* as both substrates have been successfully used for detecting these enzymes in other studies. It is therefore likely that other exopeptidases are produced by *T. orientalis* which facilitate this final hydrolytic step. For example, numerous low molecular weight exopeptidases such as leucine aminopeptidase have been documented in other crustaceans (Galgani *et al.*, 1984; Galgani and Nagayama, 1987).

The relatively low activity of most carbohydrases reflects the small proportion of carbohydrate, compared with protein, ingested by *T. orientalis* and other scyllarids (Suthers and Anderson, 1981; Lau, 1988). Nevertheless, the wide range of carbohydrases produced, including polysaccharases, glucosidases and galactosidases, indicates the majority of dietary carbohydrates can be hydrolysed into their component monosaccharides by this scyllarid.

Detection of N-acetyl glucosaminidase (chitobiase) indicates that *T. orientalis* is capable of hydrolysing chito-oligosaccharides for subsequent absorption and utilisation of glucosamine for metabolic purposes. Its substantial activity (7 units mg^{-1}) compared with other glycosidases (Table 6.2) strongly suggests that *T. orientalis* can digest large quantities of chitin from crustacean exoskeletons and polychaete acicula, which are common dietary components of other scyllarids (Suthers and Anderson, 1981; Lau, 1988). Hence it appears that although feeding behaviour and structural characteristics of

the mouthparts and proventriculus reflect a soft flesh diet, it is possible that chitin rich components are also ingested by *T. orientalis*. A comprehensive dietary analysis is needed to confirm this.

Such high activity with respect to other glycosidases was also documented by Brun and Wojtowicz (1976) in the crabs *C. borealis* and *C. irroratus* at 1.5 and 3.8 units mg^{-1}, respectively (Table 6.3). Hence the relative importance of this enzyme in *T. orientalis* is similar to other carnivorous decapods which have a significant proportion of chitinous material in their diets, further supporting the likelihood of a chitin component within the diet. The importance of this enzyme is exemplified in *H. americanus* where N-acetyl β-D glucosaminidase is over 500 times more active than all other glycosidases produced by this lobster (Table 6.3).

Several authors have postulated that gut bacteria are responsible for the production of chitin digesting enzymes. Chandramohan and Thomas (1984) found 67% of gut bacteria showed chitinolytic activity in the gut fluid of *Penaeus indicus* Milne-Edwards, whilst in *P. setiferus* 85% showed activity (Hood and Meyers, 1973). It is unlikely that N-acetyl β-D glucosaminidase activity in *T. orientalis* is attributable to gut bacteria as digestive gland extract used in the present study is largely devoid of these organisms as it is totally separate from gut fluid.

α-amylase is an endo-α-1,4 glycanase responsible for the hydrolysis of starch and glycogen, the major storage polysaccharides in plant and animal tissues, respectively. Detection of both the polysaccharase, α-amylase and the glycosidases, maltase and α-glucosidase suggests *T. orientalis* is capable of completely hydrolysing starch and glycogen to glucose. In particular, glycogen is an important dietary component of bivalve adductor muscle which is commonly ingested by *T. orientalis*. The ability to digest the components of glycogen is consistent with the general observation that many crustaceans utilise this compound for metabolic purposes (van Weel, 1970).

Although α-amylase has been found in a range of crustaceans, quantitative comparison is difficult because of the wide range of assay techniques used in experiments. Nevertheless, based on the marked hydrolysis of starch over a short time period, it is evident that a substantial amount of α-amylase is produced by *T. orientalis*

(Fig. 6.2C). The concave iodine staining profile verifies that *T. orientalis* α-amylase is an endo-hydrolase, causing the rapid reduction in molecular weight of the starch polymer. An exo-hydrolysis profile is convex, typical of the slower reduction in the iodine stain leaving the bulk of the molecule intact.

The greater α-glucosidase and maltase activity in *T. orientalis* compared with the lobster *H. americanus*, and crabs *C. borealis, C. irroratus* and *C. sapidus* (Table 6.3) reveals that this scyllarid hydrolyses the oligosaccharides of starch and glycogen more efficiently than these carnivorous decapods. Despite similar dietary preferences with lobsters and crabs, this is probably attributable to the greater amount of glycogen ingested by scyllarids based on its large concentration in adductor muscles of bivalves which are unique to the diet of scyllarids (Ch 2; Lau, 1987; Jones, 1988).

The considerable amount of α-amylase combined with the significantly greater α-glucosidase than β-glucosidase activity reflects the greater proportion of animal tissue ingested by *T. orientalis*, which contain polysaccharides such as glycogen, compared with plant and algal tissues rich in cellulose and laminarin (Suthers and Anderson, 1981; Jones, 1988). This is verified by the absence of cellulase and the negligible concentrations of cellobiase and laminarinase (Table 6.2). Consequently, *T. orientalis* is unable to digest cellulose and its β-1,4 oligosaccharides, the major constituents of plant cell walls, supporting the view of Dall and Moriarty (1983) that carnivorous crustaceans do not produce cellulase enzymes. Only minimal cellulose hydrolysis has been reported in penaeids with cellulase activity in *P. aztecus* attributable to gut bacteria (Dempsey and Kitting, 1987).

Negligible laminarinase activity reveals that *T. orientalis* is incapable of hydrolysing laminarin, a major storage polysaccharide of brown algae (Division Phaeophyta) and diatoms (Division Crysophyta) (Percival, 1970). This enzyme has been detected in large concentrations in a range of crustaceans including the crab *C. maenas*, the barnacles *Balanus crenatus* Bruguière (Kristensen, 1972) and *Tetraclita squamosa* Bruguière (Johnston *et al.*, 1993) and the amphipod *Gammarus tigrinus* Sexton (Bärlocher and Porter, 1986). The majority of these ingest large quantities of algae, particularly the planktivorous barnacles and detritivorous amphipod, reflecting the considerable activity of this enzyme in these species.

Furthermore small concentrations of β-galactosidase in *T. orientalis* reflect the rarity of carragheenan and agar, constituents of some marine algae that are rich in β-galactoside linkages (McClintock *et al.*, 1991), in the diet of *T. orientalis*. Low levels of activity have been similarly reported in the carnivorous lobster *H. americanus* and crabs *C. borealis*, *C. irroratus* and *C. sapidus* (Table 6.3).

pH of Digestive Fluid/pH Optima

The acidic digestive fluid of *T. orientalis* (pH 5.9) is consistent with that reported in other crustaceans (Table 6.4). This reflects the acid pH optima of all carbohydrases (Table 6.2) and verifies that digestive enzymes produced by the digestive gland of *T. orientalis* are well adapted for extracellular digestion as they are optimally active in an acidic environment. A similar correlation between acidic gut pH and the pH optima of carbohydrases is also evident for other decapods. For example, the gut pH of *H. americanus* (5.0) is almost identical with the pH optima of carbohydrases produced (Table 6.4; 6.5).

Optimal activity of carbohydrases at acid pH in *T. orientalis* is comparable with those found in other decapods (Table 6.5). In particular, the pH optima of N-acetyl β-D glucosaminidase is identical with that of *H. americanus* and *P. japonicus*, as is β-galactosidase with *H. gammarus*. This clearly demonstrates that decapod digestive enzymes operate under similar acidic conditions for optimal activity. However, although the acidic pH optima of *T. orientalis* α-amylase is consistent with that of the lobsters *H. americanus* and *H. gammarus* (Table 6.5), neutral pH optima reported for other decapods indicates that crustacean α-amylase is capable of catalysis over a wide range of pH conditions.

Table 6.4. Gut fluid pH of various crustaceans. For each species determinations were made after feeding. All references except for Brockerhoff *et al.* (1970) are cited in van Weel (1970).

Species	Gut Fluid pH	Reference
Thenus orientalis	5.9	
Astacus fluviatilis	5.8-6.0	Mansour-Bek (1954)
Astacus leptodactylus	5.0	Mansour-Bek (1954)
Procambarus clarkii	5.0-5.3	Fingerman *et al.* (1967)
Homarus americanus	5.0	Brockerhoff *et al.*(1970)
Cancer pagurus	5.8-6.0	Mansour-Bek (1954)
Carcinus maenas	6.42	Mansour-Bek (1954)

Table 6.5. pH optima of various crustacean carbohydrases. α-am, α-amylase; α-glu, α-glucosidase; β-glu, β-glucosidase; β-gal, β-galactosidase; N-AcG, N-acetyl β-D glucosaminidase.

	Enzyme					
Species	**α-am**	**α-glu**	**β-glu**	**β-gal**	**N-AcG**	**Reference**
Thenus orientalis	5.0-5.8	5.0	4.0	5.0	5.0	
Homarus americanus		5.5	5.0		5.0	Brockerhoff *et al.* (1970)
Homarus americanus	5.2					Wojtowicz & Brockerhoff (1972)
Homarus gammarus	4.8	5.5	5.0	5.0		Glass & Stark (1995)
Cancer irroratus	7.0	5.5	5.0	5.5	6.0	Brun & Wojtowicz (1976)
Carcinus maenas	7.0					Blandamer & Beechy (1964)
Pandalus borealis					4.0-6.0	Essaiassen *et al.* (1992)
Penaeus japonicus			4.5		5.0	Chuang *et al.* (1992a,b)
Penaeus californiensis	7.5					Vega-Villasante *et al.* (1993)

The range and concentration of proteases and carbohydrases produced reflects the carnivorous diet of *T. orientalis*. The considerable N-acetyl β-D glucosaminidase activity indicates that chitin may also be ingested in the form of crustacean exoskeletons

which is consistent with the dietary regime of other scyllarids. The correlation between acid gut pH and the pH optima of carbohydrases indicates that the scyllarids' enzymes are well adapted for extracellular digestion, a common feature of all crustacean enzymes. To understand fully the nature of digestive processes of *T. orientalis* future research should focus on the purification and characterisation of a number of these enzymes. For this reason, an extensive examination of trypsin was conducted (refer Ch 7) involving determination of its structure and catalytic mechanism to reveal the nature of proteolysis in this scyllarid. Lipases, another important group of digestive enzymes, should also be investigated before a comprehensive picture of scyllarid digestion can be achieved.

Chapter 7. Purification and Characterisation of the Serine Protease, Trypsin

7.1 INTRODUCTION

Serine proteases comprise one of the largest and best characterised protein families of the animal kingdom. They are of extremely widespread occurrence and include a whole range of enzymes of diverse function including trypsin, chymotrypsin, elastase (digestion), acrosin (ovulation), thrombin (blood coagulation) and plasmin (fibrinolysis) (Powers and Harper, 1986). Of these the trypsin-related enzymes have been especially well studied, and are present in a wide range of marine and terrestrial vertebrate and invertebrate phyla, as well as the prokaryotes (Kraut, 1977).

Serine proteases are characterised by a uniquely reactive serine residue (Ser195), and display a significant degree of similarity in primary structure and catalytic mechanism. In particular, their amino acid sequence is highly conserved and a universal numbering system, based on that of bovine chymotrypsinogen (Hartley and Shotton, 1971), has been adopted. Hence, identical residues are consistently numbered between different enzymes, regardless of any insertions or deletions, allowing comparisons in primary structure to be made between serine proteases.

All serine proteases possess a catalytic triad of three amino acid residues: histidine (His57), aspartate (Asp102) and Ser195, clustered about the active site depression (Fersht, 1985). These residues are actively involved in the catalytic mechanism, the details of which are presented in Fig. 7.1. In summary, this mechanism involves the acylation and protonation of Ser195 and His57, respectively, to form an acyl enzyme intermediate with the appropriate substrate (Fersht, 1985). Another feature of their active site is the "primary specificity pocket" (or substrate binding site) located close to Ser195. Small structural differences in this pocket give each serine protease its specificity. For example, the pocket is deep and narrow in trypsin, with a negatively charged carboxylate at its base to attract the long positively charged side chain of lysine and arginine (Mathews and van Holde, 1990).

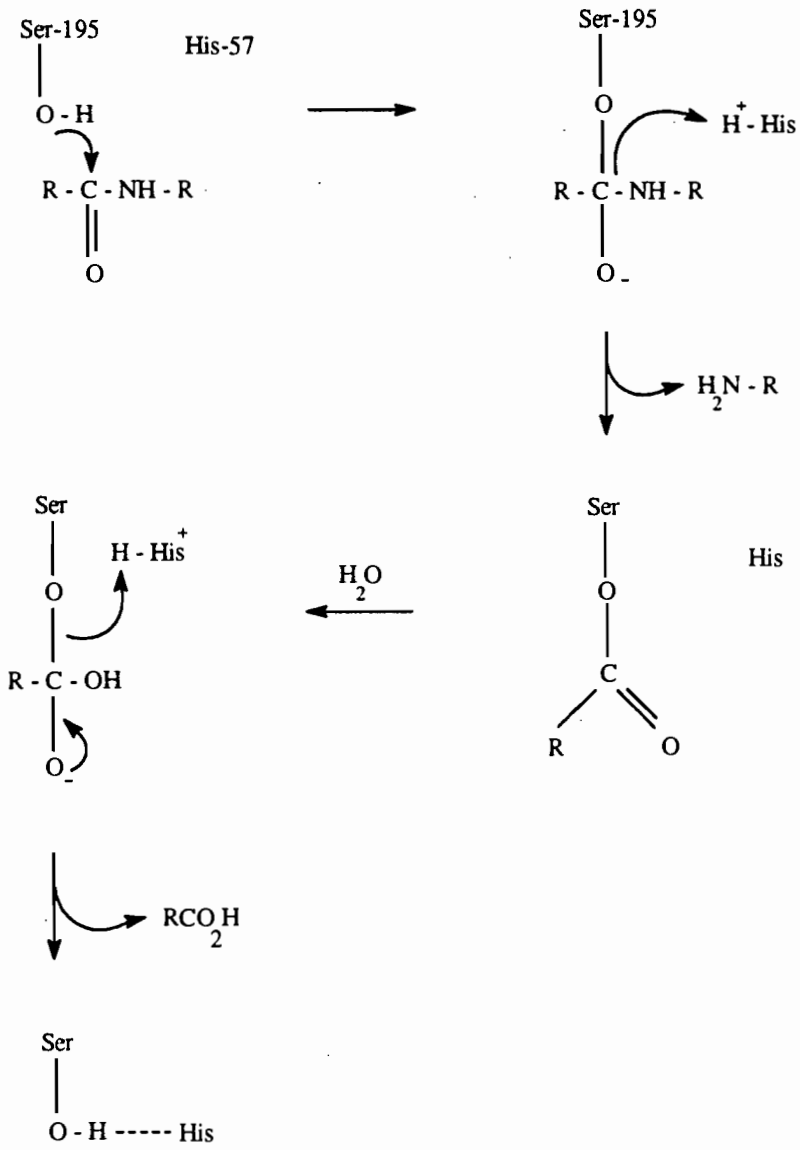

Figure 7.1. Catalytic mechanism of a serine protease (Powers and Harper, 1986). After substrate binding, the reactive hydroxyl group of Ser195 attacks the carbonyl group of the amide bond of the substrate forming a tetrahedral transition state (top right). This process is facilitated by protonation of the imidazole ring of His57. Asp102 (not shown) acts to stabilise the positively charged His57 as well as ensuring it is in the appropriate tautomeric form to accept the proton from Ser195 (Stryer, 1988). Decomposition of the tetrahedral state results in release of the amino portion of the substrate and formation of an acyl enzyme intermediate (middle right). The departing amino group receives a proton from the imidazole ring of His57. Subsequent hydrolysis of the acyl enzyme to active enzyme and the carboxylic acid product occurs through a reaction sequence analogous to that which formed the acyl enzyme.

Inhibitors play an important role in determining the catalytic mechanism of an enzyme as they interact with and therefore identify amino acid residues at the active site and/or substrate binding site. Hence an enzyme can be assigned to a particular family in which the amino acid residues involved in catalysis are known. Since Asp102 is buried deep in the structure of serine proteases, Ser195 and His57 are by far the most frequent targets for inhibitors. For example, sulphonyl fluorides such as phenylmethylsulphonyl fluoride (PMSF) are used to determine the presence of Ser195 within the catalytic triad of serine proteases such as trypsin. PMSF acts as a substrate analogue by deprotonating the hydroxyl group of Ser195 forming a covalent bond with oxygen (Fig. 7.2). This hydrogen ion is accepted by His57 and the fluoride ion is removed from PMSF. Consequently, the tetrahedral transition state is formed with the sulphonyl fluoride inhibitor, instead of the substrate, preventing formation of the acyl enzyme intermediate (Powers and Harper, 1986). This reaction with Ser195 by sulphonyl fluorides has resulted in their widespread use in general identification of serine proteases.

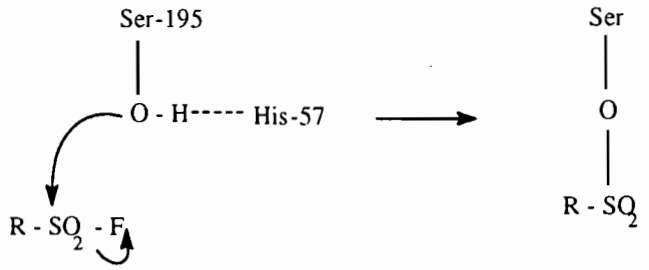

Figure 7.2. Inactivation of serine proteases by sulphonyl fluorides (Powers and Harper, 1986).

In contrast, chloromethyl ketone inhibitors determine the presence of His57 in the catalytic triad serine proteases. In particular, tosyl lysine chloromethyl ketone (TLCK) and tosyl-L-phenylalanine chloromethyl ketone (TPCK) have been developed specifically for trypsin and chymotrypsin, respectively. After recognition of the peptide moiety by the enzyme, Ser195 reacts with the carbonyl of the chloromethyl ketone to give a tetrahedral structure (Powers and Harper, 1986). Alkylation of the ϵ-nitrogen in the imidazole ring of His57 then occurs. Thus the structure of the inactivated enzyme at neutral pH contains 2 covalent bonds (Fig. 7.3). Formation of the covalent bond between the chloromethyl ketone and the ϵ-nitrogen of His57 has recently been verified by X-ray crystallography (Bode *et al.*, 1989).

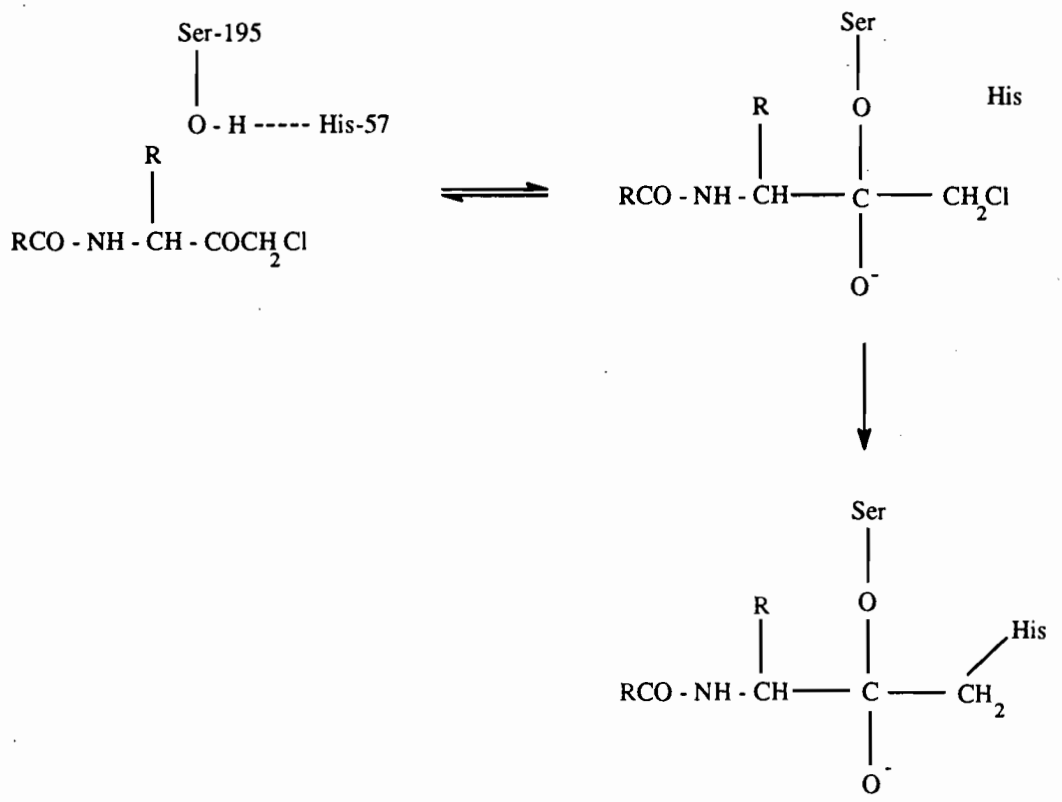

Figure 7.3. Mechanism of inactivation of serine proteases by peptide chloromethyl ketones (Powers and Harper, 1986).

Status of Knowledge on Crustacean Trypsins

Trypsin has been detected in all crustaceans examined and plays an important role in proteolysis in this phylum (Galgani *et al.*, 1984; Dendinger, 1987; Lu *et al.*, 1990). Furthermore, the detection of large concentrations of trypsin from the digestive gland extract of *T. orientalis*, together with its substantial proportion of dietary protein (see Ch 1,6), confirms its importance in scyllarid digestion. Recent data on the structure of this enzyme has enabled comparisons to be made with mammalian trypsins. In particular, decapod and mammalian trypsins share several common features including conservative regions of amino acid sequence, a similar molecular weight (approximately 25 kDa), substrate specificity and reaction with inhibitors (PMSF, TLCK and soybean trypsin inhibitor: SBTI) (Dendinger and O'Conner, 1990; Honjo *et al.*, 1990; Guizani *et al.*, 1992). Nevertheless, several differences do exist, for instance, the extreme stability of

decapod trypsins in the absence of calcium ions, their instability at acid pH, and low isoelectric point (Gates and Travis, 1969; Zwilling *et al.*, 1969; Dendinger and O'Connor, 1990).

It is known that mammalian trypsin and chymotrypsin evolved from a common ancestral enzyme and diverged in structure and function based on mutations in gene duplication (Stryer, 1988). Consequently, these differences between mammalian and decapod trypsins demonstrate the evolutionary divergence of this serine protease which may have been influenced by dietary and environmental (marine versus terrestrial) variation between these two groups.

Despite the increasing number of studies characterising crustacean trypsins (see Ch 6), a number of aspects have yet to be studied before their structure and function can be fully understood. One of the most important is that of kinetic characteristics, as they underly an understanding of catalytic mechanisms. Lack of knowledge in this area makes analysis of crustacean digestive function (proteolysis) difficult and comparison with catalytic mechanisms of vertebrate trypsins almost impossible. Some studies documented pH and temperature optima based on profiles of activity at one substrate concentration with no attempt at Michaelis-Menten kinetics (Galgani *et al.*, 1984; Dendinger and O'Connor, 1990; Honjo *et al.*, 1990). Guizani *et al.* (1992) recently documented the first pH profiles of the kinetic parameters K_m, V and V/K_m for crayfish trypsin and the substrate tosylarginine methyl ester (TAME). They did not, however, determine the amino acid groups involved in catalysis nor did they give estimates of these parameters for comparative purposes. In contrast, Grant *et al.* (1983) and Osnes and Mohr (1985) documented values of K_m, k_{cat} and k_{cat}/K_m in the fiddler crab and Antarctic krill, respectively, but did not describe their pH profiles. Such incomplete analysis of one species prevents a detailed picture of digestive mechanism, in this case proteolysis, being made in any decapod.

Are Zymogens Produced?

There has been considerable debate over the production of inactive enzyme precursors, or zymogens, by the crustacean digestive gland. Al-Mohanna *et al.* (1985b) have been the only workers to find zymogen granules in the F-cells of *P. semisulcatus*. Brunet *et al.* (1994) believe that the inability to detect zymogens cytologically by other

investigators may be due to their short cellular phase, going from production to secretion of most granules in *P. semisulcatus* in less than 90 minutes. In contrast, Vogt *et al.* (1989) found no evidence for the intracellular storage of enzymes as zymogen granules, or even cytological features supporting zymogen production during their extensive examination of the F-cells in the crayfish *A. astacus*. They believe enzymes are produced and released simultaneously from the digestive gland for extracellular storage within the cardiac stomach, in readiness for feeding. This was based on the automatic filling of the cardiac stomach of *A. astacus* within 4-6 hours of gut evacuation.

Very few biochemical studies on digestive enzymes have investigated the issue of zymogen production. There is, so far, no evidence for activation of precursors and it has been suggested that a zymogen form does not exist (Gates and Travis, 1969; Brockerhoff *et al.* 1970). If this is the case the greater stability of crustacean compared with mammalian trypsin is of definite adaptive value. Attributes including resistance of proteases to self digestion based on very few autolysis sites (Zwilling and Neurath, 1981) and stability at acid pH, found within the majority of crustacean guts (van Weel, 1970), verifies Vogt's (1989) belief that crustacean enzymes are well adapted for extracellular digestion. Nevertheless, Galgani and Nagayama (1987) believe further investigation of zymogens is needed after they found an increase in proteolytic activity after incubation of digestive gland extract at low temperature, indicating activation may have occurred. It is possible that zymogen activation differs from that in mammals so that different experimental conditions are needed to demonstrate their presence in crustaceans. Further studies are required to understand this important aspect of crustacean digestive processes. For example, the presence or absence of a trypsinogen zymogen would require the isolation and sequencing of the gene coding trypsin.

The major objectives of this study were to examine, in detail, the structure and catalytic mechanism of *T. orientalis* trypsin. This characterisation involved purification of the enzyme from crude digestive gland extract and examination of several structural features including its molecular weight, N-terminal amino acid sequence and antibody cross reaction against other crustacean and mammalian trypsin-like enzymes. Reaction with known serine protease and trypsin inhibitors (PMSF, TLCK, SBTI) was used to identify particular amino acid residues at the active site involved in catalysis.

The catalytic mechanism of *T. orientalis* trypsin was further detailed by a comprehensive kinetic analysis involving calculation of the kinetic parameters: V, K_m, V/K_m, k_{cat} and k_{cat}/K_m. pH profiles of V and V/K_m were used to verify the specific amino acid residues that play a role in catalysis. Comparison with other crustacean and mammalian serine proteases confirmed structural and catalytic features in common with this well characterised protein family.

7.2 MATERIALS AND METHODS

7.2.1 Protein Determination and Trypsin Activity Measurement

Protein concentration was measured by the method of Bradford (1977) using reagents supplied by Bio-Rad Laboratories. Bovine serum albumin (BSA) was used as the protein standard. Trypsin was assayed by its amidase activity using N-α-benzoylarginine-ρ-nitroanalide (BAPA) (Sigma B4875) as previously described (Ch 6.2.2.1).

7.2.2 Sodium Dodecyl Sulphate Polyacrylamide Gel Electrophoresis (SDS-PAGE)

Proteins were fractionated by SDS-PAGE according to the method of Laemmli (1970), to determine purity of the fractions eluted during the purification procedure (Ch 7.2.3). Protein bands were visualised using Coomassie brilliant blue. Phosphorylase b (94 kDa), BSA (67 kDa), ovalbumin (43 kDa), carbonic anhydrase (30 kDa), soybean trypsin inhibitor (SBTI) (20.1 kDa) and α-lactalbumin (14.4 kDa) were used as molecular weight standards (Pharmacia Biotech). SDS-PAGE was also used to determine the subunit molecular weight of trypsin by comparing its migration (R_f) with that of the standards. A plot of log molecular weight versus R_f of standards was used to estimate this value.

7.2.3 Purification of *T. orientalis* Trypsin

Trypsin was purified from crude digestive gland extract, prepared according to the method outlined in Ch 6.2.1. Digestive gland extracts of *Cherax quadricarinatus* (von Martens) (red claw crayfish), *Tetraclita squamosa* (barnacle) and *Penaeus merguiensis* (prawn) used in the antibody study (Ch 7.2.7) were also prepared according to this method. The purification procedure involved a combination of ion exchange chromotography and gel filtration and was conducted on a Pharmacia fast protein liquid chromatography system (FPLC) at 22°C.

i) Ion Exchange Chromatography: Thawed crude digestive gland extracts were pooled and centrifuged (18000 xg, 4°C, 20 min) and the supernatant applied at 4 ml min^{-1} to a DE-52 (Whatman) column (2 cm x 12 cm) pre-equilibrated with 20 mM Tris-HCl pH 7.3 containing 400 mM NaCl. A linear gradient of 0.4 to 2 M NaCl in 20 mM Tris-HCl pH 7.3 was applied to the column and 1 ml fractions collected. The eluate was monitored for protein concentration by absorbance at A_{280} using a datalogger connected to a single

path UV monitor (Pharmacia). Fractions absorbing at A_{280} were assayed for trypsin by the hydrolysis of BAPA using an ELISA plate reader. Active fractions were pooled, diluted 4-fold with chilled 20 mM Tris-HCl pH 7.3 to reduce the salt concentration and applied at 2 ml min^{-1} to a Bio-Rad Econo-Pac Q ion exchange column (0.5 cm x 5 cm) pre-equilibrated with 20 mM Tris-HCl pH 7.3 containing 400 mM NaCl. Protein was eluted using a 0.4 to 2 M NaCl linear gradient. Fractions (1 ml) were collected and monitored for protein (A_{280}) and trypsin. Active fractions were pooled, diluted 4-fold and re-applied to the Econo-Pac Q column. The sample was concentrated to minimal volume by direct elution with 2 M NaCl in buffer and fractions (0.5 ml) containing trypsin activity were pooled.

ii) Gel Filtration: The pooled sample (<800 μl) was applied at 0.5 ml min^{-1} to a Pharmacia Superose 12 column equilibrated with 20 mM Tris-HCl pH 7.3 containing 100 mM NaCl. Fractions (0.5 ml) were monitored for protein (A_{280}) and trypsin and active fractions were pooled and stored at -20°C.

7.2.4 Molecular Weight Determination

Native molecular weight of pure trypsin was estimated on the same Pharmacia Superose 12 gel filtration column using the molecular weight markers: ferritin (440 kDa), catalase (232 kDa), ovalbumin (45 kDa), carbonic anhydrase (30.5 kDa) and cytochrome C (12.5 kDa). Proteins were eluted at 0.5 ml min^{-1} with 20 mM Tris-HCl pH 7.3 containing 200 mM NaCl. A plot of log molecular weight versus the calculated partition coefficient (K_{av}) of each standard was used to determine the molecular weight of *T. orientalis* trypsin.

7.2.5 Glycosylation

The unusually large molecular weight of *T. orientalis* trypsin prompted an investigation into whether the enzyme was a glycoprotein. The presence of glycoproteins on SDS-PAGE was detected by the method of Dubray and Bezard (1982) using the periodic acid-Schiff reagent (PAS) which stains for 1,2-diol groups of glycoproteins in polyacrylamide gels. Tridacnin (7.5 μg), a C-type lectin from haemolymph of the giant clam *Hippopus hippopus* Linnaeus (Puanglarp *et al.*, 1995), and BSA (5 μg) were used as positive and negative controls, respectively. To determine whether the glycoprotein contained mannose residues, a Western blot of *T. orientalis* trypsin (5 μg) and tridacnin

lectin (2 μg) was probed with concanavalin A conjugated to horseradish peroxidase (HRP) (Sigma Chemical Co.) and developed with 4-chloro-1-naphthol according to the method of Kijimoto-Ochiai *et al.*, (1985).

The presence of N-glycosidic linkages was determined by digestion with N-glycanase (peptide-N^4-(N-acetyl-β-glucosaminyl) asparagine amidase F (EC 3.5.1.52)) (Oxley and Bacic, 1995) using tridacnin lectin as a positive control. Purified trypsin was first concentrated to approximately 1 mg ml^{-1} by ultrafiltration in a Centricon ultrafilter (10,000 kDa exclusion limit). An aliquot (45 μl) was boiled for 2 min with 5 μl of 10% sodium dodecyl sulphate (SDS). After cooling, 425 μl of buffer (100 mM sodium phosphate pH 7.2, 25 mM EDTA, 5 mM sodium azide) and 25 μl of 10% nonidet-P40 were added and boiled for a further 2 min. The mixture was cooled and then digested with 0.6 units (U) of N-glycanase (Boehringer) for 18 h at 37°C. Digested samples were then examined by SDS-PAGE.

7.2.6 N-Terminal Amino Acid Sequence

The N-terminal amino acid sequence of trypsin was determined following separation of the purified enzymes on SDS-PAGE and transfer onto polyvinylidene difluoride membrane (Problott membrane, Applied Biosystems). Sequencing was conducted by Dr Dennis Shaw (John Curtin School of Medical Research, Canberra) on an Applied Biosystems Model 477A Protein Sequencer using standard protocols for the instrument.

7.2.7 Antibody Preparation

Antiserum was prepared in male Quackenbush mice by subcutaneous injection of a solution of approximately 100 μg pure trypsin dissolved in 100 μl 0.1 M Tris-glycine buffer after emulsification with an equal volume of Freund's Complete Adjuvant (Gibco Laboratories 660-5721AD). Prior to the initial injection a prebleed was taken from the tail to obtain control serum to determine whether residual antibodies against trypsin were present. Two booster injections of the same amount of protein were emulsified with an equal volume of Freund's Incomplete Adjuvant (Gibco Laboratories 660-5720AD) and administered at two week intervals. The mouse was then bled through the tail 5 days after the last injection. The blood was allowed to clot overnight and the clot removed by centrifugation. Sera (700 μl) was stored at -20°C.

Antigenic similarity between *T. orientalis* trypsin and serine proteases from mammalian and different groups of crustaceans was determined by Western Blotting of SDS polyacrylamide gels. This was performed in a Bio-Rad mini transblot electrophoretic transfer cell. Digestive gland extracts of *T. orientalis* (20 μg), *C. quadricarinatus* (red claw crayfish) (28 μg), *T. squamosa* (barnacle) (25 μg) and *P. merguiensis* (prawn) (13 μg) and commercial porcine pancreas trypsin (Sigma T1418) (10 μg) and bovine pancreas chymotrypsin (Sigma C4129) (10 μg) were separated on SDS-PAGE. The gels were then equilibrated for 2 min in transfer buffer (25 mM Tris and 192 mM glycine, pH 8.3) and blotted at 25 V for 2 h at 4°C onto nitrocellulose. Membranes were probed with *T. orientalis* anti-trypsin primary antibodies (1:5000 dilution) for 1 h and then a 1:5000 dilution of rabbit anti-mouse antibodies conjugated to HRP (Dakopatts, Denmark) for 1 h. Immunoreactive polypeptides were visualised using 3 mM 3,3-diaminobenzidine (DAB) and H_2O_2 (Harlow and Lane, 1988).

Specificity and concentration of *T. orientalis* anti-trypsin antiserum was determined using a series antisera dilutions: 1:1000, 1:5000, 1:10000 against *T. orientalis* crude digestive gland extract. The blots were treated as above and then developed with 3 mM DAB and H_2O_2 (Harlow and Lane, 1988).

7.2.8 Inhibitor Studies

Inhibitors are often used in the characterisation of enzymes as they reveal chemical characteristics, such as active site amino acid residues, which are generally common to a type or family of enzyme. Prior to assay with BAPA, the enzyme was incubated for 30 min at 37°C with 1 mM of each of the following inhibitors: phenylmethylsulphonyl fluoride (PMSF) (Sigma P7625), tosyl lysine chloromethyl ketone (TLCK) (Sigma T7254) and soya bean trypsin inhibitor (SBTI) (Calbiochem 65035). PMSF and TLCK are specific inhibitors of serine proteases, whereas SBTI is a specific inhibitor of trypsin. The effect of each inhibitor on enzyme turnover of BAPA indicated whether inhibition has occurred.

7.2.9 Kinetics

All enzyme assays were conducted at 37°C using a Hewlett-Packard 8452A diode-array spectrophotometer and multiple cell changer. Michaelis-Menten kinetics were performed using a three component buffer system containing 50 mM acetic acid,

50 mM 4-Morpholinethane sulphonic acid (MES), 100 mM Tris, 200 mM NaCl, 0.2% (w/v) poly(ethylene glycol) 6000 and 10 mM $CaCl_2$. The pH of the assay buffer was adjusted to the desired pH at 37°C. The three component buffer system was chosen because it maintained constant ionic strength at 0.3 M, achieved by the wide spread of pK_a values (> 2) between each component (Ellis and Morrison, 1982). Kinetic constants were determined between pH 3.7-8.6 at 37°C, using 6 substrate concentrations that varied over an 11-fold range with at least one concentration above and below the K_m value (final concentration 1.25 mM - 0.088 mM BAPA). Release of ρ-nitroanaline was monitored at $A_{400\text{-}410}$ using an absorption coefficient (ϵ) of 9300 $M^{-1}cm^{-1}$ (Stone *et al.*, 1991), which was found to be constant over the pH range of 3.7-8.6. Substrate concentrations were determined at 342 nm using the absorption coefficient of 8270 $M^{-1}cm^{-1}$ for BAPA (Lottenberg and Jackson, 1983).

Theory and Data Analysis

The reaction catalysed by trypsin can be represented by Scheme I, where E is the enzyme, A is the substrate, EA is the Michaelis complex and P_1 and P_2 are the hydrolysis products (ρ-nitroanaline and peptide respectively).

Scheme I

$$E + A \underset{k_{-1}}{\overset{k_1}{\rightleftharpoons}} EA \xrightarrow{k_{cat}} E + P_1 + P_2$$

Under steady-state conditions, the dependence of reaction velocity (v) on substrate concentration can be described by the Michaelis-Menten equation:

$$v = \frac{V\,[A]}{K_m + [A]} \qquad 1$$

where V is the limiting velocity and K_m is the Michaelis constant (the substrate concentration at which a particular enzyme yields one-half its limiting velocity).

pH Effect on the trypsin-BAPA reaction

pH profiles of V and V/K_m for ρ-nitroanalide substrates by serine proteases are usually bell-shaped between pH 4 and 10 (Stone *et al.*, 1991; Guizani *et al.*, 1992). As the uncatalysed hydrolysis of BAPA above pH 9 was too great to permit accurate

estimates of initial velocity (also observed by Stone *et al.*, 1991), kinetic constants for *T. orientalis* trypsin with BAPA were obtained between pH 3.7 - 8.6. Initial velocity data for BAPA obtained at each of 16 pH values were fitted by non-linear regression to the hyperbolic curve of initial velocity versus substrate concentration described by equation 1 using "Regression" version M1.23 Blackwell Scientific (1990) (MacIntosh), to obtain estimates for V, V/K_m and K_m. Velocity data was weighted, according to 1/v. This was particularly important for calculating K_m as it was greatly affected by inaccuracy at low substrate concentrations. The equations for a half-bell-shaped profile are as follows:

$$\frac{V}{K_m} = \frac{(V/K_m)(opt)}{1 + [H]/K_a} \qquad 2$$

$$V = \frac{V(opt)}{1 + [H]/K_a} \qquad 3$$

where V/K_m(opt) and V(opt) are the pH independent values of V/K_m and V respectively, and K_a is the acid dissociation constant. The logarithms of these equations (4 and 5 below) were used to fit the data by non-linear regression (no weighting used) to obtain values of V(opt), V/K_m(opt) and K_a from which pK_a were calculated.

$$\log V = \log V(opt) - \log(1 + [H]/K_a) \qquad 4$$

$$\log\frac{V}{K_m} = \log\frac{V}{K_m}(opt) - \log(1 + [H]/K_a) \qquad 5$$

The catalytic constant, k_{cat}, is a measure of the rate of substrate hydrolysis and is directly proportional to V by the relationship:

$$k_{cat} = \frac{V}{[E_o]} \qquad 6$$

where $[E_o]$ is the concentration of active enzyme (trypsin) per reaction (μmol mg^{-1}) determined using the chromogenic inhibitor ρ-nitrophenyl-ρ-guanidinobenzoate (pNp'GB), following the method of Chase and Shaw (1970). pNp'GB is a substrate

analogue of trypsin whereby its guanidine group binds to the primary specificity pocket in a similar manner to that of the guanidinium group of arginine. The ρ-nitrophenol group is cleaved off simultaneously but the guanidinium group remains bound to the trypsin. In this way only one molecule of ρ-nitrophenol is released per molecule of trypsin so the number of moles of ρ-nitrophenol released by trypsin is equal to the number of moles of active trypsin present. Optimal values of V and V/K_m calculated in this study were converted to k_{cat} and k_{cat}/K_m using equation 6.

Implications of The Kinetic Constants, k_{cat}, K_m and k_{cat}/K_m.

The Michaelis constant, K_m, is often associated with the strength of binding of substrate to enzyme. In other words, it is a measure of the affinity of an enzyme for its particular substrate. This is certainly true in the Michaelis-Menten limiting case, where k_{cat} is very small. Under these circumstances a large K_m means that k_{-1} is much greater than k_1 (refer Scheme 1), and the enzyme binds substrate very weakly (low affinity) (Mathews and van Holde, 1990). The opposite is true for a small K_m which indicates a strong binding to substrate (high affinity).

The second constant, k_{cat}, is a direct measure of the catalytic production of product. The larger k_{cat} is, the faster the rate of catalysis. Specifically, k_{cat} measures the number of substrate molecules turned over per enzyme molecule per second (units are s^{-1}). Thus it is often called the "turnover number".

Further insight into the meaning of these parameters can be gained by considering the situation at very low substrate concentrations. Under these circumstances, [A] << K_m, and most of the enzyme is free, so $[E]_t \approx [E]$. Then equation 1 becomes:

$$V = \frac{k_{cat}}{K_m}[E][A] \qquad 7$$

Under these circumstances the ratio k_{cat}/K_m behaves as a second order rate constant for the reaction between substrate and free enzyme. This ratio, otherwise known as the specificity constant, is important as it provides a direct measure of enzyme efficiency and specificity - it shows what the enzyme and substrate can accomplish when abundant enzyme sites are available. An upper limit exists for these rates, determined by

the frequency with which enzyme and substrate molecules can collide. If every collision results in the formation of an enzyme-substrate complex, diffusion theory predicts that k_1 will have a value of approximately 10^8 - 10^9 $M^{-1}s^{-1}$. Therefore an enzyme that approaches maximum possible efficiency in every respect will have a value of k_{cat}/K_m in this range (Mathews and van Holde, 1990). In other words, the greater the proportion of collisions that are effective, the greater the rate of catalysis.

7.3 RESULTS

7.3.1 Trypsin Purification

Trypsin from *T. orientalis* was successfully purified by ion exchange chromatography and gel filtration. A summary of purification data is presented in Table 7.1 and elution patterns for each step are illustrated in Fig. 7.4; 7.5A,B. Pure trypsin had a specific activity of 0.375 units mg^{-1} representing a 45-fold increase in amidase activity over that of the crude extract. Although specific activity did not increase after Superose 12, gel filtration was necessary to eliminate a small impurity still present in the Econo-Pac Q eluate. The enzyme eluted as a single peak (Fig. 7.4; 7.5A,B) and was shown to migrate as a single band by SDS-PAGE indicating its high degree of purity (Fig. 7.6). Ability to visualise the band of trypsin within the crude extract is consistent with its 45-fold purification.

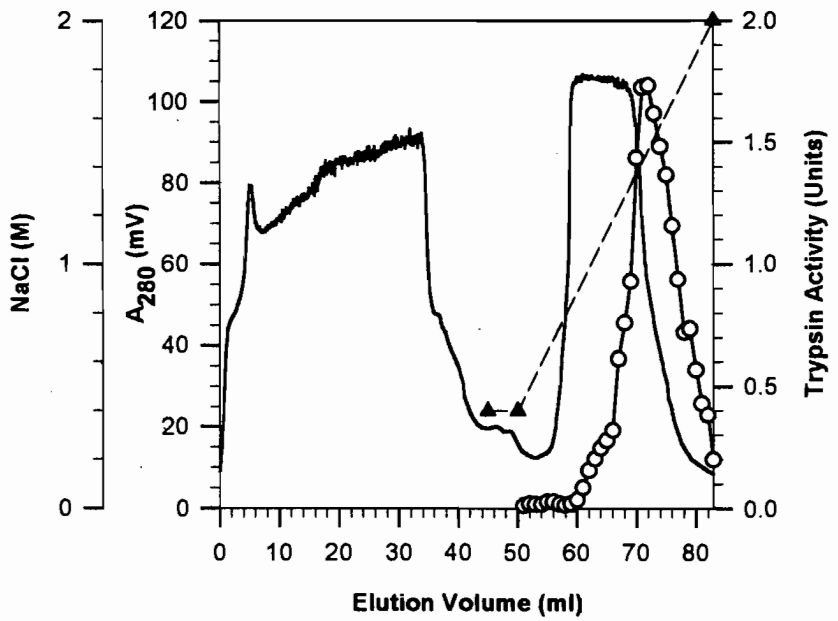

Figure 7.4. Elution profile of trypsin from a crude digestive gland extract of *T. orientalis* on a DE-52 anion exchange column using FPLC. The column was equilibrated with 20 mM Tris-HCl 400 mM NaCl pH 7.3 and protein eluted with a 0.4-2 M NaCl gradient (- ▲ -). Protein concentration was monitored at A_{280} (—) and fractions assayed for trypsin activity (- ○ -). Units are measured in μmol ρ-nitroanalide s^{-1} at 37°C pH 7.5.

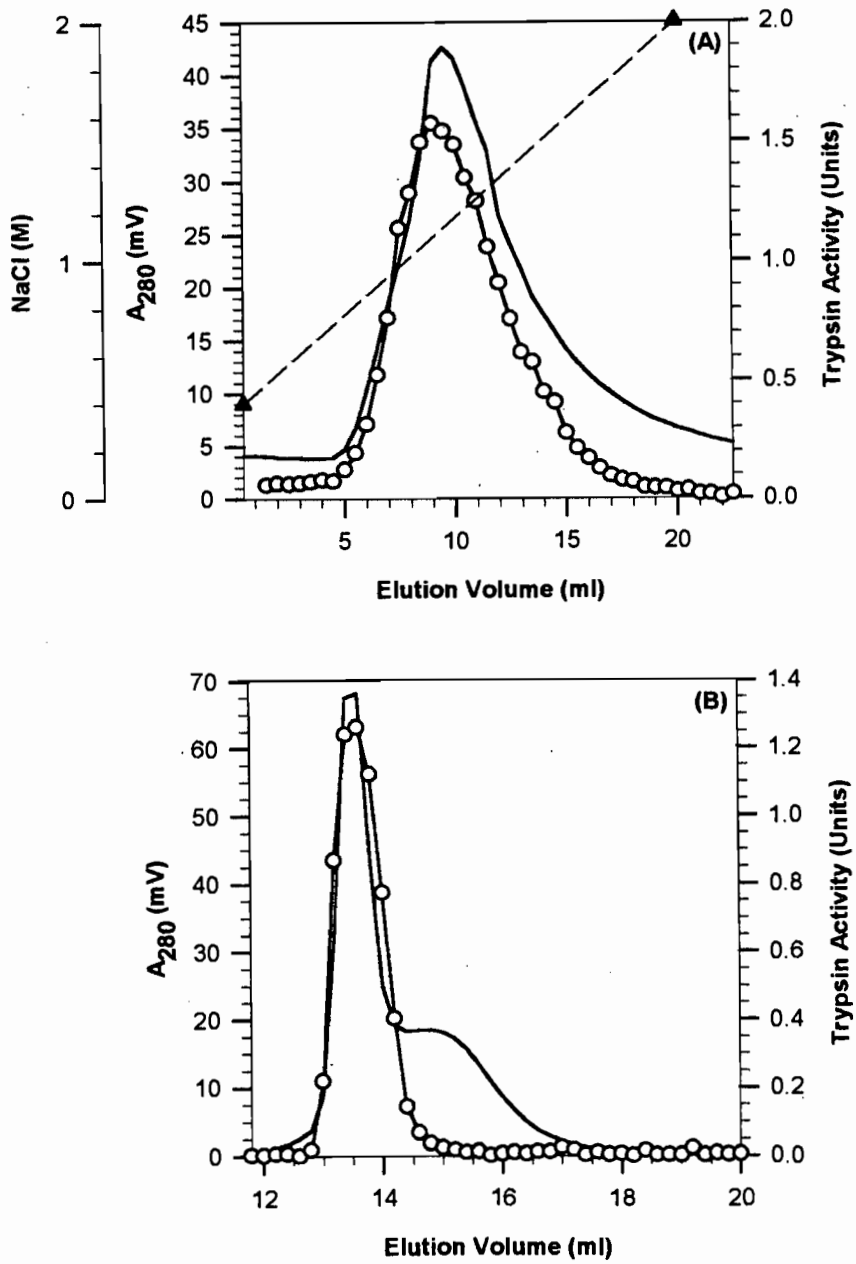

Figure 7.5. A. Elution profile of trypsin from partially purified digestive gland extract of *T. orientalis* on an Econo-Pac Q anion exchange column using FPLC. The column was equilibrated with 20 mM Tris-HCl 400 mM NaCl pH 7.3 and protein eluted with a 0.4-2 M NaCl gradient (- ▲ -). Protein concentration was monitored at A_{280} (—) and fractions assayed for trypsin activity (- O -).

B. Elution profile of trypsin from partially purified digestive gland extract of *T. orientalis* on a Superose 12 gel filtration column using FPLC. The column was equilibrated with 20 mM Tris-HCl 100 mM NaCl pH 7.3. Protein concentration was monitored at A_{280} (—) and fractions assayed for trypsin activity (- O -).Units are measured in μmol ρ-nitroanalide s^{-1} at 37°C pH 7.5.

Table 7.1. Purification of trypsin from crude digestive gland extract of *Thenus orientalis*. [a] Trypsin activity was measured using BAPA as substrate. Units are measured in μmol ρ-nitroanalide s^{-1} at 37°C pH 7.5.

Purification Step	Volume (ml)	Protein (mg)	Total Activity (Units[a])	Specific Activity (Units mg^{-1})	Yield (%)	Purification (-fold)
Crude Extract	130	183.1	1.52	0.009	100	-
DE-52	38	10.6	0.65	0.062	43.1	7.25
Econo-Pac Q	11.5	0.8	0.31	0.377	20.2	46.5
Superose 12	7.8	0.58	0.21	0.375	14.4	45.4

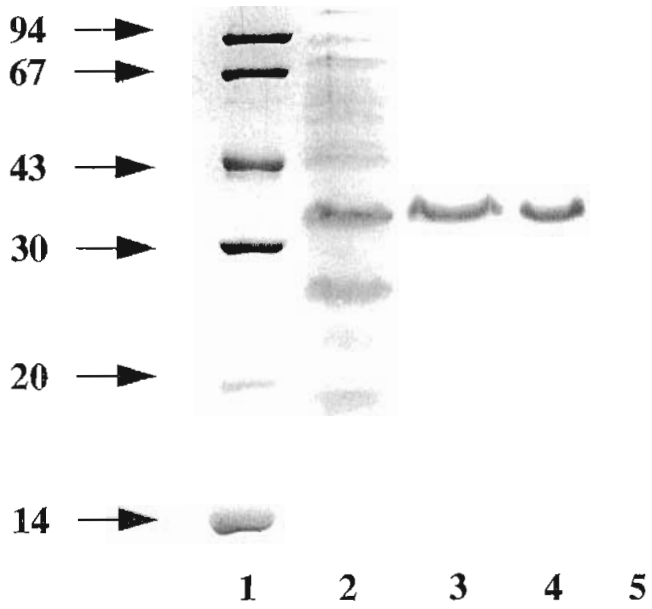

Figure 7.6. SDS-PAGE summarising the purification of *T. orientalis* trypsin. Electrophoresis was performed on a 12% polyacrylamide gel using a Tris-glycine anode-cathode buffer system. The gel was run at 180 mV for 1 h and stained with Coomassie brilliant blue. Lane 1, molecular weight standards (see Ch 7.2.2); lane 2, crude digestive gland extract (3 μg); lane 3, active fraction from DE-52 (3 μg); lane 4, active fraction from Econo-Pac Q (3 μg); lane 5, active fraction from Superose 12 (2.5 μg). Molecular weight (kDa) of the standards is indicated.

7.3.2 Molecular Weight

Comparison of purified trypsin R_f with those of known molecular weight standards on SDS-PAGE indicated a subunit molecular weight of approximately 36 kDa (Fig. 7.6). This was in close correlation with the native molecular weight of 34.6 kDa determined by gel filtration using the standard curve illustrated in Fig. 7.7.

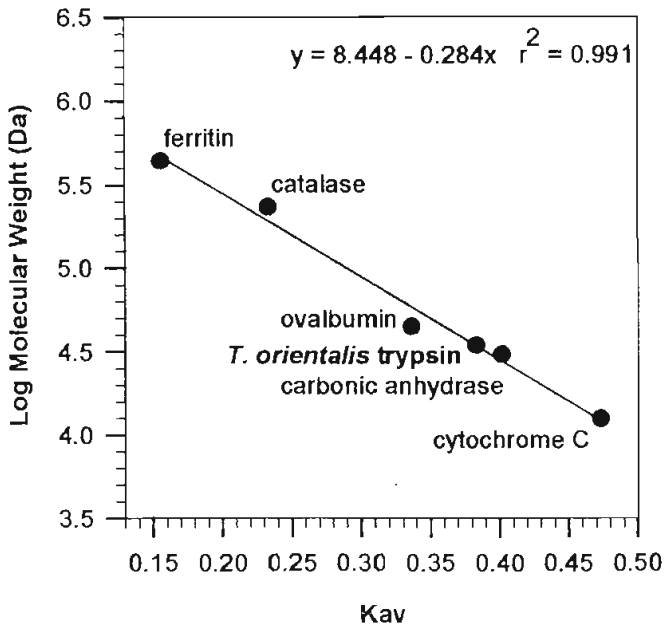

Figure 7.7. Molecular weight determination of *T. orientalis* trypsin by Superose 12 gel filtration. Molecular weight standards and trypsin were eluted with 20 mM This-HCl 200 mM NaCl pH 7.3 at 0.5 ml min^{-1}. Log molecular weight was calculated using the equation of the standard curve indicated, where x = elution volume. K_{av} was calculated in the usual way.

7.3.3 Glycosylation

The purified protein gave a positive reaction with PAS indicating that trypsin from *T. orientalis* is glycosylated (Fig. 7.8, lane 3). Both positive (tridacnin lectin) and negative (BSA) controls reacted as predicted with the PAS reagent. A stronger reaction occurred with tridacnin lectin than *T. orientalis* trypsin as it is a known glycoprotein with a considerable number of carbohydrate sidechains.

No difference in molecular weight occurred when *T. orientalis* trypsin was incubated with N-glycanase indicating the carbohydrate sidechain could not be removed by this enzyme (Fig. 7.9). This suggests that *T. orientalis* trypsin is an O-linked glycoprotein. However, the glycan chains do not contain mannose as a negative reaction was obtained when the blot was probed with Concanavalin A conjugated to HRP (Fig. 7.10A,B).

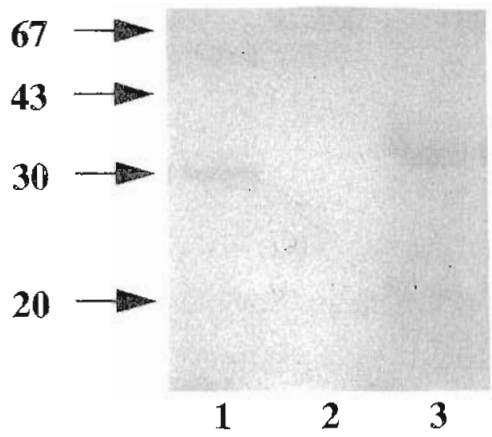

Figure 7.8. Glycoprotein stain (PAS) of an SDS polyacrylamide gel of pure *T. orientalis* trypsin. Electrophoresis was performed on a 12% gel using a Tris-glycine buffer system and run at 180 mV for 1 h. The gel was stained in 0.2% periodic acid for 1 h followed by Schiffs reagent for 4 h and destained in 7.5% acetic acid. The samples were: lane 1, tridacnin lectin (7.5 μg) positive control; lane 2, BSA (3 μg) negative control; lane 3, *T. orientalis* trypsin (15 μg). The molecular weight (kDa) of the standards is indicated.

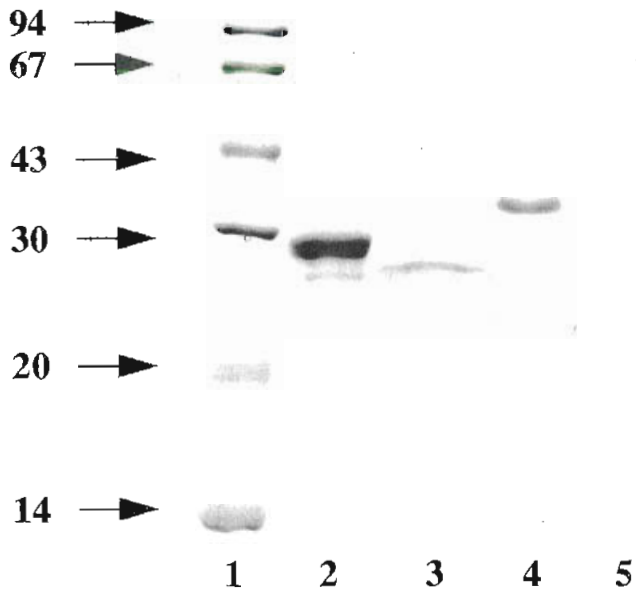

Figure 7.9. SDS-PAGE of N-glycanase digest for determination of N-glycosidic linkages within pure *T. orientalis* trypsin. Electrophoresis was performed on a 12% polyacrylamide gel using a Tris-glycine buffer system and run at 180 mV for 1 h and stained with Coomassie brilliant blue. Tridacnin lectin (positive control) and *T. orientalis* trypsin were incubated for 18 h at 37°C with 0.6 U N-glycanase prior to running the gel (Ch 7.2.5). Lane 1, molecular weight standards; lane 2, tridacnin lectin (2.5 μg) positive control; lane 3, tridacnin lectin and N-glycanase digest (1 μg); lane 4, *T. orientalis* trypsin (2 μg); lane 5, *T. orientalis* trypsin and N-glycanase digest (1 μg). The molecular weight (kDa) of the standards is indicated.

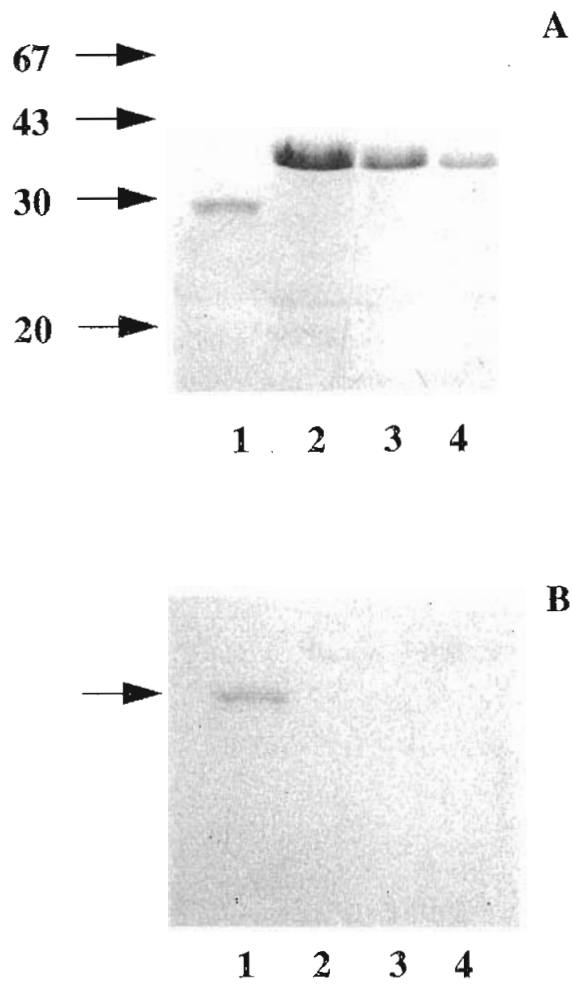

Figure 7.10. Determination of mannose residues within pure *T. orientalis* trypsin using Concanavalin A.
A. SDS-PAGE performed on a 12% polyacrylamide gel using a Tris-glycine buffer system and run at 180 mV for 1 h and stained with Coomassie brilliant blue. Lane 1, tridacnin lectin positive control (4 μg), lanes 2,3,4, *T. orientalis* trypsin (15, 10, 5 μg, respectively). Molecular weight (kDa) of the standards is indicated.
B. Western Blot of the SDS gel probed with Concanavalin A. The blot was developed using 4-chloro-1-naphthol (Kijimoto-Ochiai *et al* ., 1985). Lanes are the same as A. Arrow indicates tridacnin lectin.

Figure 7.11. N-terminal amino acid sequences of crustacean and bovine trypsin and chymotrypsin. The amino acid sequence of crustacean trypsin-like enzymes is numbered from the N-terminus, while the universal numbering system based on bovine chymotrypsinogen (Hartley and Shotton, 1971) for serine proteases is also provided. Amino acid residues identical with that of *T. orientalis* trypsin are enclosed. Amino acid sequences were taken from *A. fluviatilis*, bovine trypsin (Titani *et al.*, 1983), *A. leptodactylus* (Zwilling *et al.*, 1975), *P. monodon* (Lu *et al.*, 1990), *U. pugilator* (Grant *et al.*, 1980) and bovine chymotrypsin (Swiss-Prot protein sequence data bank).

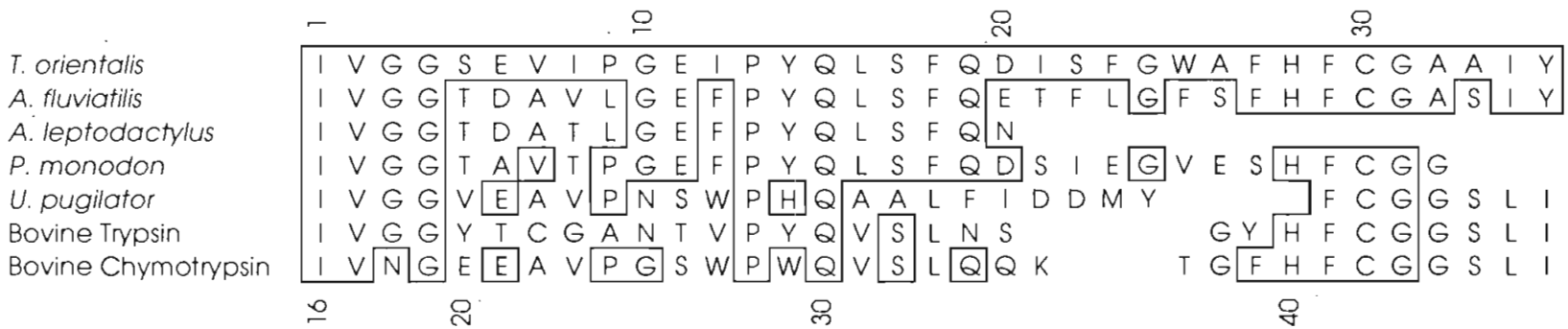

7.3.4 N-Terminal Amino Acid Sequence

The N-terminal amino acid sequence of *T. orientalis* trypsin exhibits considerable homology with serine proteases. In particular, it possesses the highly conserved residues Gly19, Pro28 and Gly43, as well as the less conserved residues Gln30, Ser32, His40 and Phe41 of serine proteases, according to the universal bovine chymotrypsinogen numbering system (Hartley and Shotton, 1971) (Fig. 7.11). Closest homology was with the sequence of trypsin from other crustaceans: *Astacus leptodactylus, Astacus fluviatilis* (crayfish) and *Penaeus monodon* (prawn), with large regions of the sequence (residues 16-19, 28-34 and 40-43) in common. All the crustacean trypsins have an insertion of approximately 3 amino acids between residues 36-37, which is absent from bovine trypsin and chymotrypsin.

7.3.5 Antibody Studies

T. orientalis anti-trypsin serum was highly specific for trypsin, binding primarily to the trypsin band within the crude digestive gland extract but no other proteins (Fig. 7.12B). A high titre was achieved as a 1:5000 dilution of the antibody was sufficient to visualise the trypsin band with DAB.

Close sequence homology between *T. orientalis* and other crustacean trypsins is also reflected in the western blot analysis of a range of serine proteases using the antiserum to *T. orientalis* trypsin. Both crayfish (*C. quadricarinatus*) and prawn (*P. merguiensis*) trypsins reacted strongly with the antiserum while the barnacle (*T. squamosa*) enzyme showed only a weak reaction (Fig. 7.12B, lanes 3,4,6). This suggests crayfish and prawn trypsin are antigenetically similar to *T. orientalis* trypsin. Bands of lower molecular weight which were poorly recognised are proteolytic fragments of the parent trypsin and were not evident on SDS-PAGE (Fig. 7.12A). Commercial porcine trypsin and bovine chymotrypsin did not cross-react with the antiserum suggesting that they are not antigenically similar to *T. orientalis* trypsin (Fig. 7.12B, lanes 7,8).

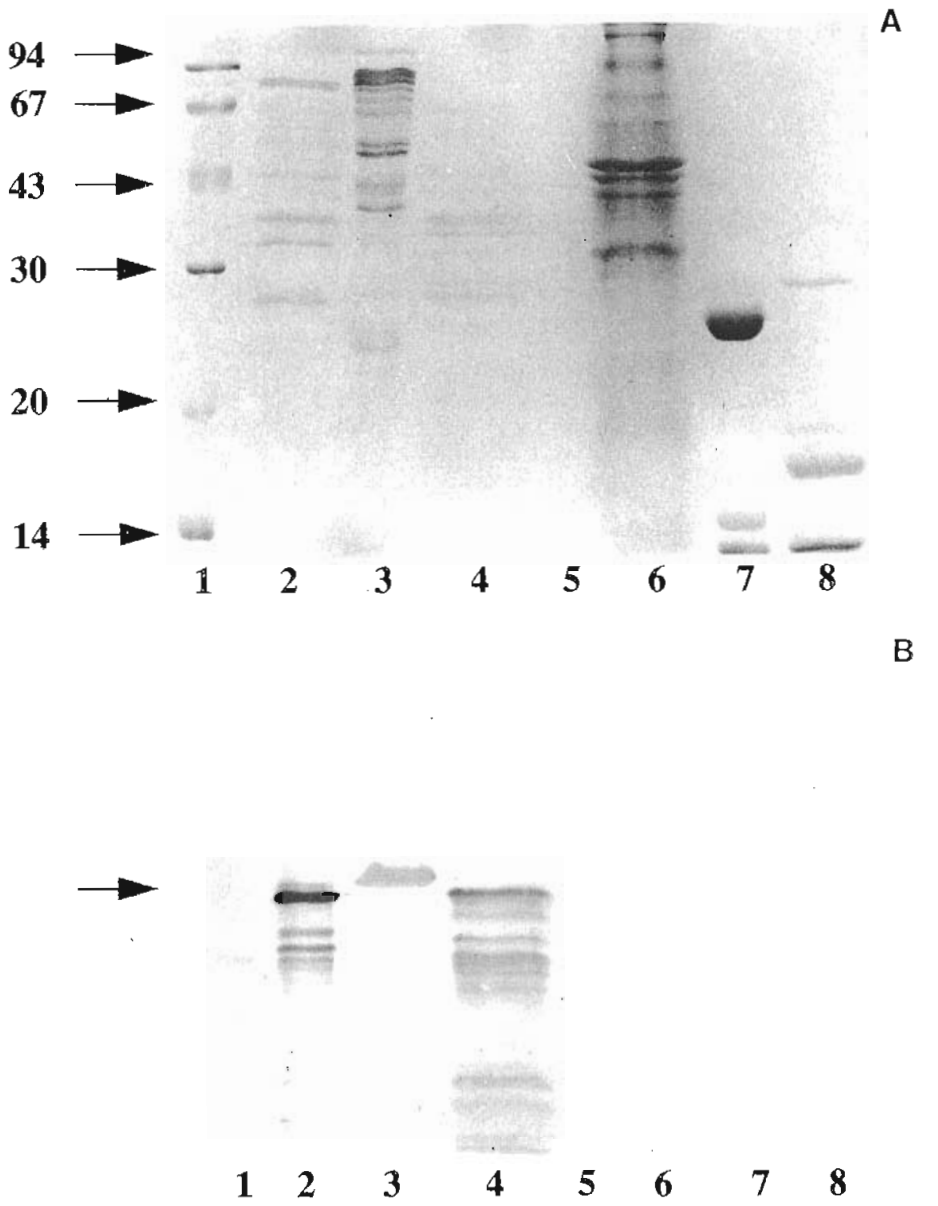

Figure 7.12. Antigenic comparison between *T. orientalis* trypsin and other serine proteases.
A. SDS-PAGE performed on a 12% polyacrylamide gel using a Tris-glycine buffer system and run at 180 mV for 1 h and stained with Coomassie brilliant blue. Lane 1, molecular weight standards, lane 2, *T. orientalis* digestive gland extract (3 μg); lane 3, *C. quadricarinatus* digestive gland extract (6 μg); lane 4, *P. merguiensis* digestive gland extract (6 μg); lane 6, *T. squamosa* digestive gland extract (15 μg); lane 7, porcine pancreas trypsin (2 μg); lane 8, bovine pancreas chymotrypsin (3 μg). The molecular weight (kDa) of the standards is indicated.
B. Western Blot analysis of various serine proteases against *T. orientalis* anti-trypsin polyclonal antibodies. Lane 2, *T. orientalis* digestive gland extract (20 μg), lane 3; *C. quadricarinatus* digestive gland extract (28 μg); lane 4, *P. merguiensis* digestive gland extract (13 μg); lane 6, *T. squamosa* digestive gland extract (25 μg); lane 7, porcine pancreas trypsin (10 μg); lane 8, bovine pancreas chymotrypsin (10 μg). The *T. orientalis* trypsin is identified (arrow). Bands of lower molecular weight in lanes 2 and 4 are proteolytic fragments of the parent trypsin and are not evident on the SDS-PAGE gel (A). The blot was developed using 3 mM DAB and H_2O_2.

7.3.6 Inhibitor Studies

Substantial inhibition of *T. orientalis* trypsin amidase activity against BAPA occurred by PMSF and TLCK, indicating the enzyme has a serine and histidine residue, respectively, at the active site involved in catalysis (Table 7.2). Hence, *T. orientalis* trypsin belongs to the family of serine proteases. Inhibition by SBTI reveals the enzyme purified from crude digestive gland extract is indeed trypsin.

Table 7.2. Effect of protease inhibitors on the specific activity of *T. orientalis* trypsin. Inhibitors (1 mM) were incubated for 30 min at 37 °C with enzyme prior to assay. Units are in μmol s^{-1} ± standard errors. Variation in trypsin specific activity between inhibitors is attributed to the use of different extracts.

	Specific Activity (Units mg^{-1})		
Inhibitor	**Inhibitor Absent**	**Inhibitor Present**	**% Inhibition**
PMSF	0.17 ± 0.014	0.004 ± 0.0003	97
TLCK	0.30 ± 0.02	0.03 ± 0.006	90
SBTI	0.48 ± 0.05	0.04 ± 0.005	92

7.3.7 Kinetics

Calculation of kinetic constants, V and K_m, at each pH value by non-linear regression to equation 1 was accurate as indicated by the good fit of the hyperbolic curve to the data (Fig. 7.13A). pH profiles of K_m, log$V$, and log (V/K_m) over the pH range 3.7-8.6 were obtained (Fig. 7.13B; 7.14A,B) with nonlog data profiles for V and V/K_m provided in Appendix 2. K_m exhibits a marked increase at acid pH below pH 4.5 and decreases to an optimal value of 0.094 mM between pH 6-8 (Fig. 7.13B). pH profiles of log$V$ and log (V/K_m) are half bell-shaped with pK_a values derived from non-linear regression of the data of 4.67 and 5.7, respectively (Fig. 7.14A,B; Table 7.3). Optimal catalytic activity occurs between pH 6.5-8.0 and corresponds to V(opt) of 0.04 μmol s^{-1} mg^{-1} (Fig. 7.14A; Table 7.3). Optimal enzyme specificity and efficiency is exhibited between pH 7.5-8.6 and corresponds to V/K_m(opt) of 0.44 $mg^{-1}ml^{-1}s^{-1}$ (Fig. 7.14B; Table 7.3). A comparison of kinetic parameters k_{cat}, k_{cat}/K_m and K_m of *T. orientalis* trypsin with literature values for other crustacean and mammalian trypsin-like enzymes is presented in Table 7.4.

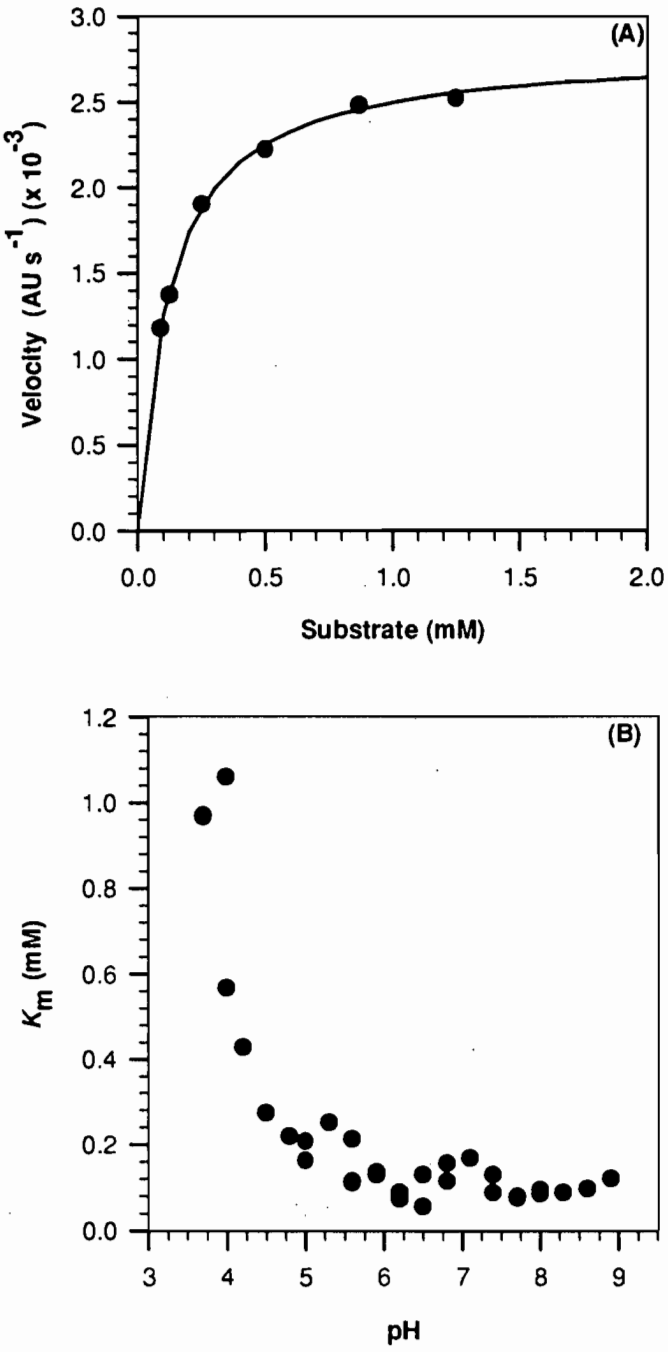

Figure 7. 13. A. Initial rate of hydrolysis by *T. orientalis* trypsin at varying concentrations of substrate (BAPA) at pH 6.5. Kinetic constants (V and K_m) were calculated by non-linear regression to the hyperbolic curve described by equation 1 using "Regression" M1.23 (Macintosh) (see Ch 7.2.9).
B. Variation of K_m with pH for BAPA hydrolysis by *T. orientalis* trypsin. K_m values at each pH were calculated by nonlinear regression to equation 1, an example of which is given in A.

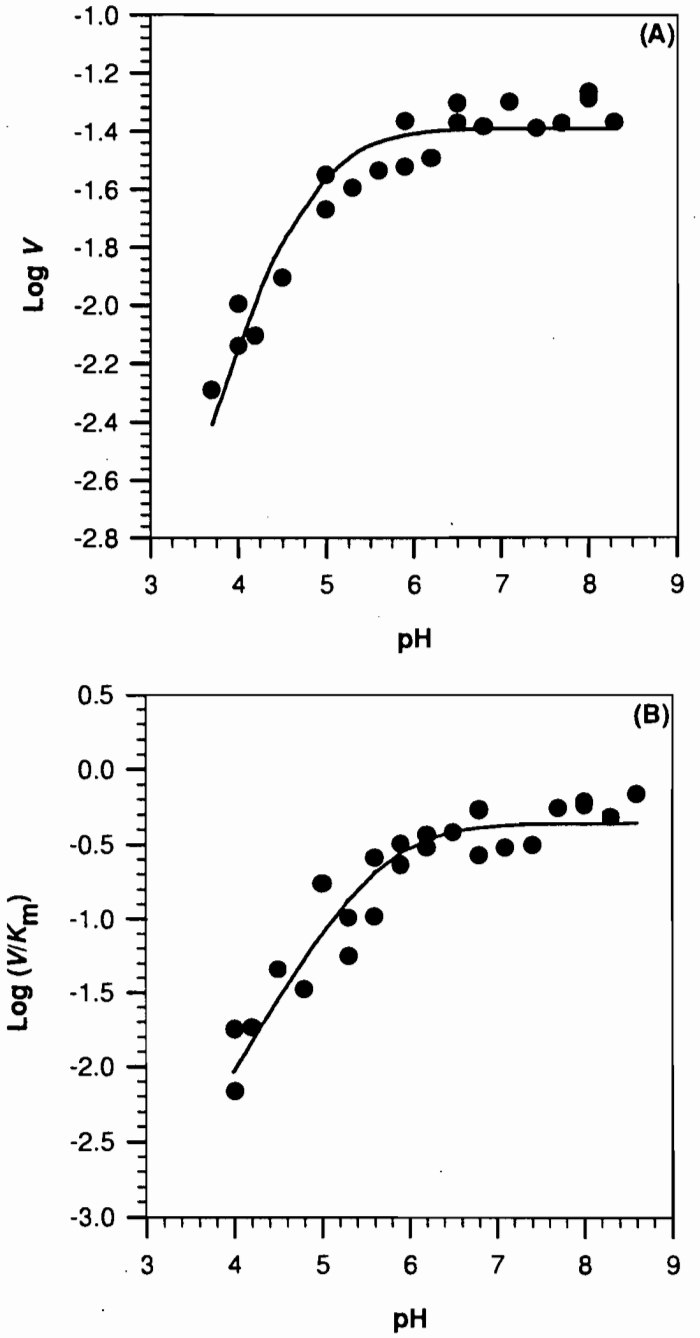

Figure 7.14. Variation of **A.** log V and **B.** log (V/K_m) with pH for BAPA hydrolysis by *T. orientalis* trypsin. V and K_m values at each pH were calculated by nonlinear regression to equation 1, an example of which is given in Fig. 7.13A. Units of V and (V/K_m) are μmol $s^{-1}mg^{-1}$ and $mg^{-1}ml$ s^{-1}, respectively. The curves represent the fit of the data to equation 4 (A) and 5 (B) (Ch 7.2.9).

Table 7.3. Optimum V and V/K_m and their respective pK_a values for *T. orientalis* trypsin with the substrate BAPA. Estimates for V and V/K_m were determined between pH 3.7-8.6 as described Ch 7.2.9. The logarithm of these values was fitted by non-linear regression to equation 4 and 5 to obtain estimates of their optimum values and respective K_a, pK_a and standard errors. V (opt) and V/K_m (opt) are measured in units of μmol s^{-1} mg^{-1} and mg^{-1} ml s^{-1}, respectively.

Parameter	Value	K_a	pK_a
V (opt)	0.04 ± 0.002	$2.1 \pm 0.3 \times 10^{-5}$	4.67 ± 0.06
V/K_m (opt)	0.44 ± 0.06	$2.2 \pm 0.5 \times 10^{-6}$	5.7 ± 0.1

Table 7.4. Comparison of kinetic parameters of trypsin-like enzymes with the substrate BAPA. V (opt) and V/K_m (opt) values were converted to k_{cat} and k_{cat}/K_m using data obtained from the pNp'GB study outlined in Kinetic Theory (Ch 7.2.9). Kinetic data were extracted from the literature; [a]Osnes & Mohr (1985) enzyme II,III represent serine endopeptidases with trypsin-like specificity; [b],Grant *et al.* (1983) protease II represents a collagenolytic trypsin-like protease; [c],Lu *et al.* (1990); [d],Honjo *et al.* (1990); [e],Lottenberg *et al.* (1981).

Species	k_{cat} (s^{-1})	k_{cat}/K_m (M^{-1} s^{-1})	K_m (mM)
T. orientalis	0.908	9.7×10^3	0.093
Euphausia superba[a] (Antarctic krill)			
enzyme II	0.74	-	0.04
enzyme III	0.45	-	0.04
Uca pugilator[b] (fiddler crab) protease II	2.0	2.9×10^5	0.0069
Penaeus monodon[c] (prawn)	-	2.04×10^4	-
Penaeus indicus[d] (prawn)	-	-	0.249
Mammalian trypsin[e] pH8.0	2.7	2.3×10^3	1.2

7.4 DISCUSSION

This study is the first to document the purification and characterisation of a digestive enzyme, trypsin, from a scyllarid species. This particular protease was examined as it is functionally important in *T. orientalis* based on the correlation between its high concentration and the large proportion of protein ingested by this scyllarid (refer Ch 6). Although several decapod trypsins have now been partially characterised, it is the only study which comprehensively examines the structure and catalytic mechanism of this protease in a crustacean, by combining several biochemical and structural techniques with detailed kinetic analysis. This has enabled comparisons with other crustacean and mammalian serine proteases to be made and conclusively demonstrates its classification into this protein family.

T. orientalis trypsin was successfully purified from crude digestive gland extract by ion exchange chromatography and gel filtration. It had a specific activity of 0.375 units mg^{-1} representing a 45-fold increase in amidase activity over that of the crude extract (Table 7.1; Fig. 7.4; 7.5A,B). The *T. orientalis* trypsin isolated was pure as judged by SDS-PAGE (Fig. 7.6) and has a molecular weight of 34-36 kDa as determined from SDS-PAGE and gel filtration (Fig. 7.7). This molecular weight is notably higher than most other crustacean and mammalian trypsin-like enzymes, the majority of which are between 20-28 kDa; for example the crustaceans, *Penaeus japonicus* and *P. kerathurus* - 25 kDa (Galgani *et al.*, 1984; 1985) and *Panulirus japonicus* and *P. setiferus* - 24 kDa (Gates and Travis, 1969; Galgani and Nagayama, 1987). Only three studies have reported higher molecular weights similar to *T. orientalis* trypsin: *P. indicus* - 36 kDa (Honjo *et al.*, 1990), *C. sapidus* - 33.5 kDa (Dendinger and O'Connor 1990) and *P. clarkii* - 33.6 kDa (Guizani *et al.*, 1992). Although these authors acknowledged the higher than normal molecular weight, no explanations regarding the structure of these enzymes were given. Hence, further investigation into the higher molecular weight of *T. orientalis* trypsin was conducted.

Given that the N-terminal sequence for *T. orientalis* trypsin is similar to that of other trypsins (Fig. 7.11), there are two possible reasons for increased molecular weight of this protein. These are: an extended polypeptide chain, either through a large number of insertion loops in the amino acid sequence or an extended C-terminus (additional domain), or glycosylation of the protein backbone (carbohydrate sidechains). Without the

complete amino acid sequence it is not possible to determine whether an extended polypeptide chain contributes to this increased molecular weight. However, of the serine protease sequences available, only acrosin has been shown to possess a C-terminal domain (Kraut, 1977). Consequently, the possiblility of glycosylation was examined.

A positive reaction with PAS, which recognises 1,2-diol groups of glycoproteins in polyacrylamide gels, revealed that *T. orientalis* trypsin is in fact a glycoprotein (Fig. 7.8). The glycan side-chains may be O-linked, rather than N-linked, as trypsin was not deglycosylated by N-glycanase as revealed by its unchanged molecular weight on the gel (Fig. 7.9). Furthermore, the negative reaction with Concanavalin A indicates the glycan chains do not contain mannose residues which are often indicative of N-glycosylation (Fig. 7.10A,B). Thus the higher molecular weight can be accounted for, at least in part, by glycosylation of this trypsin. This appears to be highly unusual for serine proteases as there are no reports in the literature for their glycosylation. Nevertheless, although the functional significance of this modification in structure is not clear, it is unlikely to alter the catalytic mechanism of *T. orientalis* trypsin from that of other serine proteases. Glycosylation is, however, known to increase the stability of some proteins. This would be beneficial for *T. orientalis* trypsin which is transported from its site of synthesis within the F-cells of the digestive gland to the cardiac stomach where it facilitates initial proteolysis in an acidic environment (gut fluid pH 5.9). Further investigation on the functional implications of glycosylation in scyllarid proteolysis is, however, necessary.

The N-terminal amino acid sequence reveals considerable homology between *T. orientalis* trypsin and other serine proteases. This supports kinetic and inhibition data verifying that it belongs to this family of enzyme. In particular, *T. orientalis* trypsin possesses some of the most highly conserved residues of serine proteases at the N-terminus such as Gly19, Pro28, and Gly43; along with Gln30, Ser32, His40 and Phe41 which are also common to most serine proteases but are not as highly conserved (Kraut, 1977) (Fig. 7.11). The N-terminus of *T. orientalis* trypsin also begins with the peptide sequence, Ile-Val-Gly-Gly-, common to most other trypsins and serine proteases.

Greatest sequence homology at the N-terminus is exhibited between the trypsin of *T. orientalis* and the crustaceans *A. leptodactylus*, *A. fluviatilis* (crayfish) and *P. monodon* (prawn). This is reflected in their identities of 63%, 63% and 68%,

respectively, with the scyllarid. In particular, three regions are identical: Ile16-Gly19, Pro28-Gln34 and Phe39-Ala44. Where the sequence is not identical, the substitutions are structurally and hence functionally conservative. For example, Ser20 (*T. orientalis*) and Thr20 (crayfish and prawn) or Tyr37 (*T. orientalis*) and Phe37 (crayfish).

Markedly less homology exists between *T. orientalis* and bovine trypsin (40% identity) with only the highly conserved regions of serine proteases being identical. This might be expected given the evolutionary separation between mammals and crustaceans. However, the serine protease (collagenolytic) from the fiddler crab *Uca pugilator* (Grant *et al.*, 1980) has even less homology (35% identity). This suggests that although a crustacean enzyme, crab collagenase is a separate serine protease with only the essential structural characteristics of this protease family in common with *T. orientalis* trypsin.

Additional information on the relatedness of *T. orientalis* trypsin with other crustacean and mammalian trypsins is provided by antibody studies. This is based upon the knowledge that antibodies against a pure protein from one species will recognise a structurally similar protein from another species if they possess common epitopes. Hence, the cross-reaction of antibodies to *T. orientalis* trypsin with crayfish (*C. quadricarinatus*) and prawn (*P. merguiensis*) trypsins (Fig. 7.12) corroborates the strong homology between N-terminal amino acid sequences of crayfish and prawn trypsin with the slipper lobster protease (60-70%). Markedly less cross-reaction was exhibited against barnacle trypsin presumably reflecting a lower level of homology consistent with a more distant evolutionary relationship to *T. orientalis* than the crayfish and prawn. Lack of cross-reaction with mammalian trypsin and chymotrypsin, despite 40% sequence homology, indicates that crustacean trypsins differ markedly in antigenicity to mammalian trypsins and chymotrypsins.

Inhibitors play an important role in determining the catalytic mechanism of an enzyme as they interact with and therefore identify amino acid residues at the active site and/or substrate binding site. Hence an enzyme can be assigned to a particular family in which the amino acid residues involved in catalysis are known. Inhibition of *T. orientalis* trypsin by PMSF and TLCK indicates that this enzyme possesses residues equivalent to Ser195 and His57, respectively, at the active site. This feature is common to all serine proteases (Powers and Harper, 1986) providing conclusive evidence that this enzyme

belongs to this protein family. SBTI alters the primary specificity pocket of trypsin in such a way that arginine and lysine residues are no longer able to bind with the active site of this enzyme. Hence, inhibition of *T. orientalis* by SBTI confirms that this serine protease is trypsin.

Analysis of the effects of pH on kinetic parameters determined for an enzyme also provides valuable information on its catalytic mechanism. In particular, the characteristic ionisation constants (pK_a) of amino acid side chain groups calculated from pH data (refer Fig. 7.14A,B; Ch 7.2.9) has led to the use of such studies in identifying the amino acids involved in catalysis (Tipton and Dixon, 1979). This is possible as it is only the protonation and deprotonation of amino acids involved in catalysis that can be detected by measurement of enzyme activity (Tipton and Dixon, 1979). This approach is considered the most important function of pH studies and was applied in the present examination of *T. orientalis* trypsin.

The variation of V and V/K_m with pH often gives a bell-shaped curve which can be interpreted as the enzyme containing only two amino acids that are essential for activity. The pH range in this study was restricted to pH 3.7-8.6, due to uncatalysed hydrolysis of BAPA above pH 9. Hence the variation in V and V/K_m with pH gave a half-bell shaped curve (Fig. 7.14A,B). Consequently, only one of the two amino acids essential for *T. orientalis* trypsin activity could be determined.

The plot of log V/K_m against pH gives a pK_a value of 5.7, which corresponds with the pK_a value of a catalytic residue in the free uncomplexed enzyme, whereas the plot of log$V$ against pH gives a pK_a value for this residue in the Michaelis complex of 4.7 (Tipton and Dixon, 1979). The difference in these pK_a values of 1 pH unit indicates that binding of the free enzyme to the substrate (BAPA) causes significant changes in conformation of the active site. Comparison of these values with those of amino acid residues known to be involved in catalysis of other serine proteases, reveals they are consistent with the active site histidine (pK_a value 6.0). This is consistent with the histidine identified from inhibition studies with TLCK. Based on the presence of His57 at the active site of *T. orientalis* trypsin, its catalytic mechanism is probably similar to that of all other serine proteases involving protonation of His57 prior to formation of the acyl enzyme complex (Powers and Harper, 1986).

BAPA hydrolysis by *T. orientalis* trypsin is characterised by optimal catalytic activity (V), substrate specificity (V/K_m) and affinity (K_m) between pH 6 and 8 (Fig. 7.13B; 7.14A,B). In contrast, pH profiles indicate these parameters are optimal between pH 7 and 9 for the trypsin-like enzyme of the crayfish *P. clarkii* (Guizani *et al.*, 1992). However, no values for these parameters were published in this latter study, so accurate comparison of enzyme activity is difficult. A similar K_m profile was however exhibited, in which K_m increased at acid pH. This indicates that acid pH substantially reduces the affinity of this enzyme for its substrate (BAPA) in both crustaceans. This is consistent with the poor catalytic activity exhibited by *T. orientalis* trypsin below pH 4.5 (Fig. 7.14A).

T. orientalis trypsin has an optimal catalytic constant, k_{cat}, (rate of BAPA hydrolysis) of 0.908 s^{-1}. This is intermediate between that documented for trypsin-like enzymes of other crustaceans and mammals, the values of which vary 8-fold (Table 7.4). The specificity constant (V/K_m) is 2-fold and 30-fold less than the enzymes from *P. monodon* and *U. pugilator*, respectively, although it is 4-fold higher than mammalian trypsin. K_m values for *T. orientalis* trypsin and BAPA are 13-fold higher than the *U. pugilator* enzyme which reflects its markedly lower specificity compared with the crab. However, the enzyme from *P. indicus* appears to have a lower affinity for BAPA than *T. orientalis*, the reported K_m being 2.5 times greater. In summary, the affinity and specificity of *T. orientalis* trypsin for BAPA is considerably greater than mammalian trypsin despite the latters exhibition of a greater rate of catalysis. In contrast, substrate specificity is much lower than that of other crustacean proteases although their affinity and rate of catalysis is more variable (Table 7.4).

Although such comparisons of kinetic parameters are possible with the crustacean and mammalian trypsins documented, the sparse amount of kinetic data available on Crustacea makes it difficult to make broad evolutionary conclusions on the nature of substrate hydrolysis and catalytic mechanism between crustacean and mammalian (vertebrate) trypsins. In particular, existing studies are often incomplete with many providing data on "trypsin-like proteases" which may or may not be structurally or functionally similar to the purified trypsin from *T. orientalis* and that of mammalian and other vertebrate trypsins.

Data on this scyllarid provides the most comprehensive investigation to date on the structure and catalytic mechanism of a crustacean trypsin-like enzyme, enabling its classification with the well characterised family of serine proteases. As such it contributes significantly to the developing knowlege of crustacean digestion, in particular, the important process of proteolysis and provides the basis for future studies on other crustacean proteases.

Zymogens

The absence of a higher molecular weight protein band additional to the purified trypsin on SDS-PAGE suggests a zymogen form of this enzyme does not exist in *T. orientalis*. This is based upon the knowlege that zymogens possess an additional peptide sequence which is cleaved to form the active enzyme and confirms suggestions by other workers that a zymogen form does not exist in crustaceans (Gates and Travis, 1969; Brockerhoff *et al.* 1970). Nevertheless, this evidence remains inconclusive as enzyme extraction during this study involved the homogenisation of digestive gland tissue which effectively breaks up cell membranes and organelles. During this process, zymogens, if present in the crude extract, may be activated by enzymes released from elsewhere in the cell ie. autocatalysis may have occurred. Hence, detection by visualisation on a gel is unlikely.

Zymogen granules were not observed in the F-cell cytoplasm of the digestive gland of *T. orientalis* using cytological methods (see Ch 5), which supports the findings of many other workers (Dall and Moriarty, 1983; Caceci *et al.*, 1988; Vogt *et al.*, 1989). It is also consistent with the aforementioned biochemical evidence. However, the entire F-cell was not surveyed in this study and it is possible the shortness of their cellular phase, reported to be less than 90 min in *P. semisulcatus* (Al-Mohanna *et al.*, 1985b), prevented detection. Therefore the absence of zymogens from the F-cells and digestive gland extract of *T. orientalis* remains inconclusive based on insufficient cytological and biochemical evidence.

Nevertheless, the fact that *T. orientalis* trypsin is a glycoprotein, a feature known to increase the stability of a protein, as well as the optimal activity of *T. orientalis* carbohydrases at acid pH, found in this and the majority of crustacean guts (van Weel, 1970), indicates these enzymes are well adapted for extracellular digestion. Therefore,

digestive enzymes of *T. orientalis* are unlikely to be stored intracellularly in the form of zymogens, as proposed by Vogt *et al.* (1989), despite the inconclusive biochemical and cytological evidence.

In future, studies aimed at identifying zymogens biochemically must involve homogenisation of digestive gland tissue in the presence of protease (trypsin) inhibitors to prevent activation of zymogens by cleavage of the polypeptide. Crude extract would then be run on SDS-PAGE and blotted with *T. orientalis* anti-trypsin antisera which would recognise trypsin and its zymogen trypsinogen if present (two bands would appear). If no zymogen exists only trypsin would be recognised by the antisera (one band). If a zymogen form was found it would need to be purified and its characteristics (amino acid sequence, molecular weight) and DNA sequence determined to fully understand its role in protease digestion.

Correlation of Enzyme Secretion with Feeding

It is also difficult to determine whether *T. orientalis* produces enzymes on demand, that is, enzyme production is correlated with feeding, or whether enzymes are released continually. This is because the F-cells of decapods are known to secrete enzymes via merocrine secretion which does not involve an obvious cytological change in the cell shape. This process would be hard to detect cytologically for use as an index of secretion, unless obvious zymogen granules were present. In contrast apocrine secretion by barnacles such as *T. squamosa* (Johnston *et al.*,1993) is easily detected and could be used to determine whether secretion had occurred in response to feeding. As scyllarids are nocturnal scavengers, hiding from predators during the day in shelters (Spanier *et al.*, 1988; Spanier and Almog-Shtayer, 1992), it is likely they only produce enzymes in response to feeding as continual production throughout the day would be energetically wasteful. Enzyme production and secretion is almost instantaneous after feeding in penaeids, which supports this hypothesis (Al-Mohanna *et al.*, 1985b).

Chapter 8. General Conclusions

T. orientalis is a carnivorous scavenger, efficient in the location, manipulation and opening of bivalve molluscs. Structural characteristics of its mouthparts and proventriculus, as well as the high concentration of proteases produced by the digestive glands, reflect the predominantly soft flesh diet of this scyllarid and two ingestion modes allow efficient ingestion of a range of food types and sizes. Structural specialisations of the feeding appendages and cardiac stomach for ingestion and storage of large items, are consistent with its scavenging lifestyle. The digestive gland is central to all digestive processes and is the primary site of digestive enzyme synthesis and secretion in the alimentary tract. Digestion is primarily extracellular with enzymes optimally active in the acid conditions of the gut. Trypsin plays an important role in proteolysis. Its catalytic mechanism is similar to other serine proteases based on their analogy in structure and active site amino acids.

T. orientalis uses a flexible search pattern to locate food, involving either probing or digging, depending on prey density. This is advantageous to the survival of scavengers as it allows them to feed on prey of varying density and distribution thus maximising energy intake in minimal time. *T. orientalis* is a specialised predator of bivalves, which they dig from the substratum and open by the process of wedging. Both diet and opening technique are consistent with other scyllarid genera which prey on bivalves (Lau, 1987; Spanier, 1988). However, *T. orientalis* cannot feed on large bivalves like scallops because the force applied by the slender pereiopod dactyli is insufficient to prise the shell valves apart. This suggests that, in the absence of small bivalves like *Drosinia* and *Mactra* spp., *T. orientalis* probably relies on small benthic crustaceans, polychaetes or other flesh items like dead fish and squid (see Suthers and Anderson, 1981; Lau, 1988). An indication of dietary variation is given by the two ingestion modes and the production of high concentrations of N-acetyl-glucosaminidase, which hydrolyses chito-oligosaccharides, the base unit of the structural polysaccharide chitin, a major component of crustacean exoskeletons.

The importance of soft flesh and muscle in the diet of *T. orientalis* is supported by the structural characteristics of the mouthparts and proventriculus and the types and

concentrations of digestive enzymes produced. Compared with other macrophagous decapods, the crista dentata and mandibles are much reduced. Gripping of soft material is facilitated by simple stout setae on the dactylus and propus of the third maxillipeds, which are adapted for piercing and impaling flesh. The mandibles masticate food only slightly during ingestion with tearing of large items between them and third maxillipeds aided by the simple stout setae on the second maxilliped dactyls. Physical degradation is primarily carried out by the gastric mill, the teeth of which are well adapted for tearing and cutting flesh, particularly the sharp serrated masticating edges of the lateral teeth chitinous plates.

Two distinct ingestion modes allow *T. orientalis* to consume a range of food types and sizes that would otherwise be unavailable and by specialising in a particular size range, ingestion efficiency is maximised. This is indicated by the particularly fast rate of ingestion, resulting from the highly co-ordinated and functionally integrated action of the mouthparts as well as the minimal amount of mandibular chewing. The membranous lobe also facilitates the quick and efficient ingestion of large items, as retraction of its anterior lip, concurrent with the labrum, dilates the preoral cavity and oesophagus allowing them to be swallowed easily. Lubrication with copious amounts of mucus secreted from tegumental glands in the paragnaths, membranous lobe and oesophagus, together with expansion of the oesophageal walls via its four longitudinal folds further facilitates the ingestion of large food items. Furthermore, the reduced ossicle framework and calcification of the cardiac stomach together with extensive folding of its walls enable considerable expansion for storage of large food items.

These specialisations in ingestion mechanisms and proventricular structure maximise the survival of scavengers which must quickly ingest and store a variety of food types and sizes. They are also adaptations to the successful exploitation of a macrophagous diet by a slow moving benthic crustacean. Other proventricular features consistent with the macrophagous diet of *T. orientalis* include the absence of complex ventral filtration channels and setation characteristic of particulate feeders that exhibit considerable mouthpart processing.

During physical and chemical degradation in the cardiac stomach, partially

digested food is filtered in the pyloric filter press prior to entry into the digestive glands. Fluid movement into and out of the gland is aided by peristaltic contractions of the circular and longitudinal muscles of the primary ducts, a feature not previously reported. The digestive gland is central to all digestive processes in *T. orientalis*. Information derived from the present study has resolved some of the existing controversy surrounding cell function. R-cells are involved in the storage of lipid for metabolic purposes and the detoxification of metals by their storage in an insoluble form in residual bodies for mobilisation or excretion. Calcium and magnesium are stored for the calcification and hardening of the exoskeleton, whereas aluminium and chromium are accumulated for waste removal. An absorptive role of B-cells is evident although the unknown nature of material absorbed and accumulated prevents their role in intracellular digestion (Al-Mohanna and Nott, 1986; 1989), or lysosomal degradation and excretion (Vogt, 1993), being conclusively determined. Immunohistochemical localisation of trypsin conclusively verified that F-cells are responsible for the production and secretion of digestive enzymes. This supports the findings of Vogt *et al.*, (1989) who used similar techniques on *A. astacus*. Based on the absence of trypsin in tissues of the oral region, proventriculus and hindgut, it is evident that the digestive glands are the primary site of enzyme synthesis and secretion in the alimentary tract of *T. orientalis*. This has been verified by biochemical studies which, compared with all other regions of the tract, have identified the digestive glands as the site of greatest enzyme activity (Tsai *et al.*, 1986a; McClintock *et al.*, 1991).

Digestive enzymes are secreted by the F-cells into the digestive gland lumen and eventually into the cardiac stomach where the majority of extracellular digestion takes place. *T. orientalis* digestive enzymes are well adapted for extracellular digestion as they are optimally active within the acid conditions of the gut (pH 5.9). This is consistent with glycosylation of typsin, a feature which confers structural stability to the enzyme.

The range and concentration of digestive enzymes produced reflects the carnivorous diet of *T. orientalis*, with the proteases trypsin and chymotrypsin produced in high concentrations. Furthermore, detection of α-amylase, α-glucosidase and maltase indicates that *T. orientalis* is capable of hydrolysing glycogen, the major storage polysaccharide in muscle, to its component glucose units. These features indicate a

digestive capability specialised for the hydrolysis of flesh. Negligible cellulase, cellobiase and laminarinase activity indicates little ability to hydrolyse cellulose and laminarin, which is consistent with the minimal amount of plant and algal tissue ingested by scyllarids (Suthers and Anderson, 1981; Lau, 1988; Spanier, 1988). In contrast, considerable N-acetyl-glucosaminidase activity reveals that *T. orientalis* is capable of hydrolysing chito-oligosaccharides and strongly suggests it can digest chitin from crustacean exoskeletons, that have also been found in the diet of other scyllarids. The concentrations and pH optima of *T. orientalis* enzymes are similar to those of other decapods with comparable diets, indicating that they are conservative in their suite of enzymes produced and ability to hydrolyse their dietary components.

Trypsin plays a major role in proteolysis. It belongs to the family of serine proteases based on structural characteristics in common with this family including, homology in N-terminal amino acid sequence and the presence of serine 195 and histidine 57 at the active site. Kinetic analysis verified histidine 57 as one of the amino acids which participates in catalysis. Therefore its catalytic mechanism is similar to that of other serine proteases involving protonation of histidine and the formation of an acyl-enzyme complex. Considerable structural and antigenic similarity exists between *T. orientalis* trypsin and that of other crustaceans (60-70% sequence homology with lobster and prawn), indicating the structure of crustacean trypsins is highly conserved. Reduced sequence homology and considerable antigenic differences with bovine (mammalian) trypsin are consistent with their greater evolutionary separation. Despite these structural differences, on account of identical amino acid residues involved in the catalytic mechanism, the basis of scyllarid proteolysis is similar to all other groups possessing serine proteases.

Following degradation, indigestible material passes into the dorsal chamber of the pyloric stomach and is guided through the posterior pyloric sector and into the hindgut via the dorsal and lateral sheaths. The ventral sheaths prevent the entry of large particles into the digestive gland primary ducts. Passage of the bolus is aided by mucus secreted from the dorsal caecum epithelium. Processing of material into a faecal pellet occurs in the posterior pyloric sector with acidophilic and proteinaceous secretions from granular cells probably contributing to the peritrophic membrane. The pellet is extruded from the

hindgut by peristaltic contractions of its muscular walls.

This comprehensive study is the first to examine food procurement and processing in a scyllarid by integrating three important biological processes: food acquisition, ingestion and digestion. It has provided a valuable insight into the mechanisms by which *T. orientalis* is adapted to a scavenging macrophagous lifestyle. The application of specialised biological and biochemical techniques to investigate mechanical and chemical degradation has considerably improved the understanding of digestive processes. This has contributed significantly to the knowledge of decapod digestion, and by focusing on structural and catalytic aspects of trypsin a unique insight into crustacean proteolysis has been provided. This is one of the few studies to investigate all three biological processes in one decapod species and therefore forms the basis for comparisons with other scyllarid and decapod species. Consequently it highlights the importance of an integrated study in achieving a comprehensive understanding of the biology of an animal.

Future Research

Areas requiring further research have been identified throughout the study. These include a comprehensive dietary analysis to identify items, other than bivalve molluscs, ingested by *T. orientalis*. Based on the adoption of two ingestion modes allowing *T. orientalis* to ingest a range of food types and sizes and the considerable N-acetyl-glucosaminidase activity detected, it is likely that small crustaceans and other benthic organisms are preyed upon in the absence of their preferred food source. Structural specialisations of the mouthparts and proventriculus suggest that soft fleshy food remains a principal dietary component.

Despite the detailed investigation of digestive gland structure and function, the controversy over B-cell function remains and requires further investigation. In particular, research is needed on the origin and status of activity of trypsin found in the central vacuole as well as the identification of active glucosidases and peptidases to verify their role in intracellular digestion. Alternatively, characteristic lysosomal enzymes such as acid phosphatase must be identified using histochemical techniques to determine whether

the subapical vacuole and central vacuole are indeed lysosomes. Only then can the hypothesis proposed by Vogt (1993) be supported or refuted. The role of the primary duct in facilitating fluid movement into and out of the gland must also be verified by *in situ* observations of peristaltic contractions of the duct musculature. The driving force behind fluid flow has been a contentious issue in digestion for decades and the identification of duct musculature in *T. orientalis* is the first clue to an accessory process to those previously proposed (see Ch 4).

The apparently unique possession of the posterior pyloric sector by *T. orientalis* invites detailed examination of its structure and role in digestion. In particular, cytological features of the granular cells as well as histochemical identification of their secretions are needed to verify their role in peritrophic membrane production. Only then can the origin of the peritrophic membrane, a subject of much contention in all decapods, be conclusively determined.

Despite information on the kinetic parameters of *T. orientalis* trypsin provided by this study, the sparse amount of kinetic data available on crustaceans makes it difficult to make broad evolutionary conclusions on the nature of substrate hydrolysis and catalytic mechanism between crustacean and mammalian trypsins. Only the nature of proteolysis has been determined with the catalytic mechanism of other important enzymes such as α-amylase remaining unknown. Hence future research must concentrate upon biochemical aspects of a range of digestive enzymes, in particular kinetics, before a comprehensive understanding of crustacean digestion is achieved, allowing comparison with other invertebrate and vertebrate groups.

Absorption is the process by which digested nutrients are taken up by tissues for metabolic purposes and is the next step in the investigation of digestive processes. In particular, the mobilisation of dietary components to body tissues should be traced to ascertain the final destination and role of the various dietary components in metabolism and the maintenance of other body systems. This contribution of dietary components places food consumption and digestion into a broader whole organism context.

Implications for Aquaculture

T. orientalis is an important component of Australian fisheries and contributes significantly to the incidental catch of otter trawlers which fish for penaeid prawns and scallops (Jones, 1984; 1988; 1993). Information on food consumption and digestive capabilities provided by the present study can now be applied in assessing and improving growth and production in wild and cultivated populations. In particular, this research has direct relevance for the promotion of its commercial viability in aquaculture systems where a knowledge of ingestive and digestive capabilities is central to their successful cultivation.

Adaptations in mouthpart and proventricular structure as well as ingestive mechanisms for the efficient ingestion and storage of large food items implies that the small pelletised diets manufactured for penaeids are unsuitable for scyllarids. In addition, the absence of a complex arrangement of longitudinal channels and setation in much of the cardiac stomach suggests it would be incapable of extensive filtration required for the successful processing and utilisation of particulate materials. Instead, provision of large and ideally, fleshy, items would be most suitable as they can be ingested and macerated by the gastric mill with little wastage. The marked selectivity of *T. orientalis* for bivalves does however indicate caution is needed in the nature of flesh to be provided. Manufacture may require the incorporation of a palatable extract perhaps derived from bivalve tissue as provision of bivalves themselves would be too expensive.

Knowledge of digestive capabilities is also fundamental to the formulation of commercial diets to achieve maximal efficiency in digestive assimilation. The high concentrations of proteases produced by *T. orientalis* further support the need for a flesh diet in which protein is the primary constituent. Based on the production of α-amylase, α-glucosidase and maltose, α-linked carbohydrates must also be incorporated, such as glycogen and maltose, for nutritional purposes. The considerable amount of N-acetyl-glucosaminidase also suggests chito-oligosaccharides should be included although provision of the hardened structural polysaccharide chitin should be minimised.

Although these important aspects promote the aquacultural viability of adult scyllarids, additional information is needed on the dietary requirements of their larval

stages, an issue which has prevented their successful cultivation in the past. Growth rates must also be examined to provide the optimal size and age for economical harvesting. Combined with future studies targeting these problems, this study has highlighted the importance and potential success of *T. orientalis* in aquaculture.

References

Ache, B. W., 1982. Chemoreception and thermoreception. In, Atwood, H. L. and Sanderman, D. C. (eds.): *Neurobiology: Structure and Function. The Biology of Crustacea, vol. 3.* 369-398. New York, Academic Press.

Ahearn, G. A., 1974. Kinetic characteristics of glycine transport by the isolated midgut of the marine shrimp, *Penaeus marginatus. J. Exp. Biol.*, **61**, 677-696.

Ahearn, G. A. and Clay, L. P., 1987. Membrane-potential-sensitive, Na-independent lysine transport by lobster hepatopancreatic brush border membrane vesicles. *J. Exp. Biol.*, **127**, 373-387.

Aiken, D. E. and Waddy, S. L., 1982. Cement gland development, ovary maturation, and reproductive cycles in the American lobster *Homarus americanus. J. Crust. Biol.*, **2**, 315-327.

Al-Mohanna, S. Y. and Nott, J. A., 1986. B-cells and digestion in the hepatopancreas of *Penaeus semisulcatus* (Crustacea: Decapoda). *J. Mar. Biol. Ass. (U.K.)*, **66**, 403-414.

Al-Mohanna, S. Y. and Nott, J. A., 1987. R-cells and the digestive cycle in *Penaeus semisulcatus* Crustacea: Decapoda). *Mar. Biol.*, **95**, 129-137.

Al-Mohanna, S. Y. and Nott, J. A., 1989. Functional cytology of the hepatopancreas of *Penaeus semisulcatus* (Crustacea: Decapoda) during the moult cycle. *Mar. Biol.*, **101**, 535-544.

Al-Mohanna, S. Y., Nott, J. A. and Lane, D. J. W., 1985 a. M-"Midget" cells in the hepatopancreas of the shrimp, *Penaeus semisulcatus* De Haan, 1844 (Decapoda, Natantia). *Crustaceana*, **48**, 260-268.

Al-Mohanna, S. Y., Nott, J. A. and Lane, D. J. W., 1985 b. Mitotic E- and secretory F-cells in the hepatopancreas of the shrimp *Penaeus semisulcatus* (Crustacea: Decapoda). *J. Mar. Biol. Ass. (U.K.)*, **65**, 901-910.

Alexander, C. G., 1988. The paragnaths of some intertidal crustaceans. *J. Mar. Biol. Ass. (U.K.)*, **68**, 581-591.

Alexander, C. G., 1989. Tegumental glands in the paragnaths of *Palaemon serratus* (Crustacea:Natantia). *J. Mar. Biol. Ass. (U.K.)*, **69**, 53-63.

Alexander, C. G. and Hindley, J. P. R., 1985. The mechanism of food ingestion by the banana prawn, *Penaeus merguiensis. Mar. Behav. Physiol.*, **12**, 33-46.

Alexander, C. G., Hindley, J. P. R. and Jones, S. G., 1980. Structure and function of the third maxillipeds of the banana prawn, *Penaeus merguiensis. Mar. Biol.*, **58**, 245-249.

Altner, H. and Prillinger, L., 1980. Ultrastructure of invertebrate chemo-, thermo- and hygroreceptors and its functional significance. *Int. Rev. Cytol.*, **67**, 69-139.

Arnaud, J., Brunet, M. and Mazza, J., 1984. Cytochemical detection of phosphatase and arylsulphatase activities in the midgut of *Centropages typicus* (Copepod, Calanoid). *Basic Appl. Histochem.*, **28**, 399-412.

Arsenault, A. L., Clattenburg, R. E. and Aiken, D. E., 1979. The morphology and secretory-transport mechanism of the tegumental glands of the lobster (*Homarus americanus*) as related to the moult cycle. *J. Submicrosc. Cytol.*, **11**, 193-207.

Babu, D. E., Shyamusundari, K. and Hanumantha Rao, K., 1982. Studies on the digestive system of the crab *Menippe rumphii* (Fabricius) (Crustacea:Brachyura). *J. Exp. Mar. Biol. Ecol.*, **58**, 175-191.

Bancroft, J. D. and Stevens, A., (eds.). 1982. *Theory and Practice of Histological Techniques*. New York, Churchill Livingston.

Barker, P. L. and Gibson, R., 1977. Observations on the feeding mechanism, structure of the gut and digestive physiology of the European lobster *Homarus gammarus* (L.) (Decapoda:Nephropidae). *J. Exp. Mar. Biol. Ecol.*, **26**, 297-324.

Barker, P. L. and Gibson, R., 1978. Observations on the structure of the mouthparts, histology and alimentary tract, and digestive physiology of the mud crab *Scylla serrata* (Forskal) (Decapoda:Portunidae). *J. Exp. Mar. Biol. Ecol.*, **32**, 177-196.

Bärlocher, F. and Porter, C. W., 1986. Digestive enzymes and feeding strategies of three stream invertebrates. *J. N. Am. Benthol. Soc.*, **5**, 58-66.

Barnett, B. M., 1989. Final-stage phyllosoma larvae of Scyllarus species (Crustacea:Decapoda:Scyllaridae) from shelf waters of the Great Barrier Reef (Australia). *Invertebr. Taxon.*, **3**, 123-134.

Barnett, B. M., Hartwick, R. F. and Milward, N. E., 1984. Phyllosoma and nisto stage of the Moreton Bay bug, *Thenus orientalis* (Lund) (Crustacea:Decapoda:Scyllaridae), from the shelf waters of the Great Barrier Reef. *Aust. J. Mar. Freshw. Res.*, **35**, 143-152.

Barnett, B. M., Hartwick, R. F. and Milward, N. E., 1986. Descriptions of the nisto stage of *Scyllarus demani* Holthuis, two unidentified *Scyllarus* species, and the juvenile of *Scyllarus martensii* Pfeffer (Crustacea:Decapoda:Scyllaridae), reared in the laboratory; and behavioural observations of the nistos of *S. demani, S. martensii* and *Thenus orientalis* (Lund). *Aust. J. Mar. Freshw. Res.*, **37**, 595-608.

Bauer, R. T., 1989. Decapod crustacean grooming: functional morphology, adaptive value, and phylogenetic significance. In, Felgenhauer, B. E., Watling, L. and Thistle, A. B. (eds.): *Functional Morphology of Feeding and Grooming in Crustacea. Crustacean Issues, vol. 6.* 49-73. Rotterdam, A.A. Balkema.

Bergmeyer, H. U., Bernt, E., Schmidt, F. and Stork, H., 1984. D-glucose. In, Bergmeyer, H. U. (ed.): *Metabolites: Carbohydrates. Methods in Enzymatic Analysis, vol. 4.* 3rd. edn. 1196-1201. New York, Verlag Chemie, Academic Press.

Blandamer, A. and Beechy, R. B., 1964. The identification of an α-amylase in aqueous extracts of the hepatopancreas of *Carcinus maenas*, the common shore crab. *Comp. Biochem. Physiol.*, **13B**, 97-105.

Bode, W., Mayr, I., Baumann, U., Huber, R., Stone, S. R. and Hofsteenge, J., 1989. The refined 1.9 Å crystal structure of human α-thrombin: interaction with D-Phe-Pro-Arg chloromethylketone and significance of the tyr-pro-pro-trp insertion segment. *EMBO J.*, **8**, 3467-3475.

Borradaile, L. A., 1917. On the structure and function of the mouthparts of the palaemonid prawns. *Proc. Zool. Soc.*, **19**, 31-71.

Boxshall, G. A., 1982. On the anatomy of the misophrioid copepods, with special reference to *Benthomisophria palliata* Sars. *Phil. Trans. R. Soc. Lond., B.*, **297**, 125-181.

Boxshall, G. A., 1985. The comparative anatomy of two copepods, a predatory calanoid and a particle-feeding mormonilloid. *Phil. Trans. R. Soc. Lond., B.*, **311**, 303-377.

Bradford, M. M., 1977. A rapid and sensitive method for the quantitation of microgram quantities of proteins utilising the principle of protein dye binding. *Analyt. Biochem.*, **72**, 248-254.

Branford, J. R., 1980. Notes on the scyllarid lobster *Thenus orientalis* (Lund, 1793) off the Tokar Delta (Red Sea). *Crustaceana*, **38**, 221-224.

Brimacombe, J. S. and Webber, J. M., 1964. *Mucopolysaccharides: Chemical structure, distribution and isolation.* London, Elsevier.

Brockerhoff, H., Hoyle, R. J. and Hwang, P. C., 1970. Digestive enzymes of the American lobster (*Homarus americanus*). *J. Fish. Res. Bd. Can.*, **27**, 1357-1370.

Brun, G. L. and Wojtowicz, M. B., 1976. A comparative study of the digestive enzymes in the hepatopancreas of jonah crab (*Cancer borealis*) and rock crab (*Cancer irroratus*). *Comp. Biochem. Physiol.*, **53B**, 387-391.

Brunet, M., Arnaud, J. and Mazza, J., 1994. Gut structure and digestive cellular processes in marine crustacea. *Oceanogr. Mar. Biol. Annu. Rev.*, **32**, 335-376.

Bunt, A. H., 1968. An ultrastructural study of the hepatopancreas of *Procambarus clarkii* (Girard) (Decapoda, Astacidea). *Crustaceana,* **15**, 282-288.

Caceci, T., Neck, K. F., Lewis, D. H. and Sis, R. F., 1988. Ultrastructure of the hepatopancreas of the Pacific White shrimp, *Penaeus vannemei* (Crustacea: Decapoda). *J. Mar. Biol. Ass. (U.K.),* **68**, 323-337.

Caine, E. A., 1975 a. Feeding and masticatory structures of selected Anomura (Crustacea). *J. Exp. Mar. Biol. Ecol.,* **18**, 277-301.

Caine, E. A., 1975 b. Feeding and masticatory structures of six species of the crayfish genus *Procambarus* (Decapoda, Astacidae). *forma et functio,* **8**, 49-66.

Caine, E. A., 1976. Relationship between diet and the gland filter of the gastric mill in hermit crabs (Decapoda, Paguridae). *Crustaceana,* **31**, 312-313.

Cannon, H. G. and Manton, S. M., 1927. On the feeding mechanism of a mysid crustacean, *Hemimysis lamornae. Trans. Roy. Soc. Edin.,* **55**, 219-253.

Chan, T.-Y. and Yu, H.-P., 1992. *Scyllarus formosanus*, a new slipper lobster (Decapoda, Scyllaridae) from Taiwan. *Crustaceana,* **62**, 121-127.

Chandramahon, D. and Thomas, I., 1984. *Studies on chitinase activity and chitinoclastic bacteria in sediments, fishes and prawns.* Proceedings on the Symposium of Coastal Aquaculture, Cochin, India.

Chapman, R. F., 1982. *The Insects: Structure and Function.* Cambridge, Harvard University Press.

Chase, T. and Shaw, E., 1970. Titration of trypsin, plasmin, and thrombin with ρ-Nitrophenyl ρ'-Guanidinobenzoate HCl. *Methods Enzymol.,* **19**, 20-27.

Chong, V. C. and Sasekumar, A., 1981. Food and feeding habits of the White Prawn *Penaeus merguiensis. Mar. Ecol. Prog. Ser.,* **5**, 185-191.

Chuang, N-N., Huang, J. D. and Lin, K-S., 1992 b. Comparative study of free and membrane-bound acidic β-D-glucosidase from the hepatopancreas of the shrimp *Penaeus japonicus* (Crustacea: Decapoda). *Comp. Biochem. Physiol.,* **102B**, 279-283.

Chuang, N-N., Lin, K-S. and Yang, B-C., 1992 a. Purification and characterisation of an α-glucosidase from the hepatopancreas of the shrimp *Penaeus japonicus* (Crustacea:Decapoda). *Comp. Biochem. Physiol.,* **102B**, 273-277.

Clark, D. J., Lawrence, A. L. and Swakon, D. H. D., 1993. Apparent chitin digestibility in penaeid shrimp. *Aquaculture,* **109**, 51-57.

Clark, J., Quayle, K. A., MacDonald, N. L. and Stark, J. R., 1988. Metabolism in marine flatfish. V. Chitinolytic activities in Dover sole, *Solea solea* (L.). *Comp. Biochem. Physiol.,* **90B**, 379-384.

Cook, H. C., 1972. *Human Tissue Mucins*. London, Butterworths.

Cook, H. C., 1974. *Manual of Histochemical Demonstration Techniques*. Brisbane, Butterworths.

Coombs, E. F. and Allen, J. A., 1978. The functional morphology of the feeding appendages and gut of *Hippolyte varians* (Crustacea:Natantia). *Zool. J. Linn. Soc.*, **64**, 261-282.

Creswell, P. D. and Marsden, I. D., 1990. Morphology of the feeding apparatus of *Cancer novaezelandiae* in relation to diet and predatory behaviour. *Pacific Sci.*, **44**, 384-400.

Dall, W., 1967. The functional anatomy of the digestive tract of a shrimp *Metapenaeus bennettae* (Racek and Dall) (Crustacea: Decapoda: Penaeidae). *Aust. J. Zool.*, **15**, 699-714.

Dall, W. and Moriarty, J. W., 1983. Functional aspects of nutrition and digestion. In, Mantal, L. H. (ed.): *Internal Anatomy and Physiological Regulation. The Biology of Crustacea, vol. 5*. 215-251. New York, Academic Press.

Danulet, E. and Kausch, H., 1984. Chitinase activity in the digestive tract of the cod, *Gadus morhua*. *J. Fish. Biol.*, **24**, 125-133.

Davidson, R. J., 1986. Mussel selection by the paddle crab *Ovalipes catharus* (White): evidence of flexible foraging behaviour. *J. Exp. Mar. Biol. Ecol.*, **102**, 281-299.

Dempsey, A. C. and Kitting, C. L., 1987. Characteristics of bacteria isolated from penaeid shrimp. *Crustaceana*, **52**, 90-94.

Dendinger, J. E., 1987. Digestive proteases in the midgut gland of the Atlantic blue crab, *Callinectes sapidus*. *Comp. Biochem. Physiol.*, **88B**, 503-506.

Dendinger, J. E. and O'Connor, K. L., 1990. Purification and characterisation of a trypsin-like enzyme from the midgut gland of the Atlantic blue crab, *Callinectes sapidus*. *Comp. Biochem. Physiol.*, **95B**, 525-530.

Derby, C. D., 1982. Structure and function of cuticular sensilla of the lobster *Homarus americanus*. *J. Crust. Biol.*, **2**, 1-21.

Derby, C. D. and Atema, J., 1982. The function of chemo- and mechanoreceptors in lobster (*Homarus americanus*) feeding behaviour. *J. Exp. Biol.*, **98**, 317-327.

DeVillez, E. J. and Fyler, D. J., 1986. Isolation of hepatopancreatic cell types and enzymatic activities in B-cells of the crayfish *Orconectes rusticus*. *Can. J. Zool.*, **64**, 81-83.

Doughtie, D. G. and Rao, K. R., 1982. Rosette glands in the gills of the grass shrimp, *Palaemonetes pugio*. I. Comparative morphology, cyclical activity, and innervation. *J. Morph.*, **171**, 41-67.

Du Preez, H. H., 1984. Molluscan predation by *Ovalipes punctatus* (De Haan) (Crustacea: Brachyura: Portunidae). *J. Exp. mar. Biol. Ecol.*, **84**, 55-71.

Dubray, G. and Bezard, G., 1982. A highly sensitive periodic acid-silver stain for 1,2-diol groups of glycoproteins and polysaccharides in polyacrylamide gels. *Analyt. Biochem.*, **119**, 325-329.

Eisen, A. Z., Henderson, K. O., Jeffrey, J. J. and Bradshaw, R. A., 1973. A collagenolytic protease from the hepatopancreas of the fiddler crab, *Uca pugilator*. Purification and properties. *Biochem.*, **12**, 1814-1822.

Ellis, K. J. and Morrison, J. F., 1982. Buffers of constant ionic strength for studying pH-dependant processes. *Methods Enzymol.*, **87**, 405-426.

Eloffson, R., Myhrberg, H., Aramant, R., Lindvall, O. and Falck, B., 1978. Catecholaminergic salivary glands in *Gammarus pulex* (Crustacea:Amphipoda): an electron microscopic and microfluorometric study. *J. Ultrastruct. Res.*, **64**, 14-22.

Elyakova, L. A., 1972. Distribution of cellulases and chitinases in marine invertebrates. *Comp. Biochem. Physiol.*, **43B**, 67-70.

Erlanger, B. F., Kokowsky, N. and Cohen, W., 1961. The preparation and properties of two chromogenic substrates of trypsin. *Arch. Biochem. Biophys.*, **95**, 271-278.

Erri Babu, D., Shymusandari, K. and Hanumantha Rao, K., 1979. The structure and histochemistry of the oesophageal glands in the crab *Menippe rumphii* (Fabricius) (Crustacea:Brachyura). *Proc. Indian Acad. Sci.*, **88B**, 277-285.

Erri Babu, D., Shyamasundari, K. and Hanumantha Rao, K., 1982. Studies on the digestive system of the crab *Menippe rumphii* (Fabricius) (Crustacea:Brachyura). *J. Exp. Mar. Biol. Ecol.*, **58**, 175-191.

Essaiassen, M., Myrnes, B. and Olsen, R., 1992. Purification and some properties of two β-N-acetylhexosaminidases from the hepatopancreas of northern shrimp, *Pandalus borealis*. *Comp. Biochem. Physiol.*, **101B**, 513-517.

Factor, J. R., 1978. Morphology of the mouthparts of larval lobsters, *Homarus americanus* (Decapoda: Nephropidae), with special emphasis on their setae. *Biol. Bull.*, **154**, 383-408.

Factor, J. R. and Naar, M., 1985. The digestive system of the lobster, *Homarus americanus*: 1. Connective tissue of the digestive gland. *J. Morph.*, **184**, 311-321.

Farmer, A. S., 1974. The functional morphology of the mouthparts and pereiopods of *Nephrops norvegicus* (L.) (Decapoda: Nephropidae). *J. Nat. Hist.*, **8**, 121-142.

Fawcett, D. W., 1994. The Cell. *A Textbook of Histology*. 12th edn. 26-28. New York, Chapman and Hall.

Felder, D. L. and Felgenhauer, B. E., 1993. Morphology of the midgut-hindgut juncture in the Ghost shrimp *Lepidophthalmus louisianensis* (Schmitt) (Crustacea: Decapoda: Thalassinidea). *Acta Zool.*, **74**, 263-276.

Felgenhauer, B. E., 1987. Techniques for preparing crustaceans for scanning electron microscopy. *J. Crust. Biol.*, **7**, 71-76.

Felgenhauer, B. E. and Abele, L. G., 1983. Ultrastructure and functional morphology of feeding and associated appendages in the tropical freshwater shrimp *Atya innocous* (Herbst) with notes on its ecology. *J. Crust. Biol.*, **3**,336-363.

Felgenhauer, B. E. and Abele, L. G., 1985. Feeding structures of two Atyid shrimps, with comments on Caridean phylogeny. *J. Crust. Biol.*, **5**, 397-419.

Felgenhauer, B. E. and Abele, L. G., 1989. Evolution of the foregut in the lower Decapoda. In, Felgenhauer, B.E., Watling, L. and Thistle, A.B. (eds.): *Functional Morphology of Feeding and Grooming in Crustacea. Crustacean Issues, vol. 6.* 205-219. Rotterdam, A.A. Balkema.

Fersht, A. R., 1985. *Enzyme Structure and Mechanism.* New York, Freeman.

Foster, R., 1988. An overview of immunohistochemistry. In, Burgess, G.W. (ed.) *ELISA Technology in Diagnosis and Research.* 152-167. Townsville, James Cook University of North Queensland.

Fox, C. J., 1993. The effect of dietary chitin on the growth, survival and chitinase levels in the digestive gland of juvenile *Penaeus monodon* (Fab.). *Aquaculture,* **109**, 39-49.

Fryer, G., 1977. Studies on the functional morphology and ecology of the atyid prawns of Dominica. *Phil. Trans. R. Soc. Lond., B.*, **277**, 57-129.

Galgani, F. and Nagayama, F., 1987. Digestive proteinases in the Japanese spiny lobster *Panulirus japonicus. Comp. Biochem. Physiol.*, **87B**, 889-893.

Galgani, F. G., Benyamin, Y. and Ceccaldi, H. J., 1984. Identification of digestive proteinases of *Penaeus kerathurus* (Forskål): a comparison with *Penaeus japonicus* Bate. *Comp. Biochem. Physiol.*, **78B**, 355-361.

Galgani, F. G., Benyamin, Y. and Van Wormhoudt, A., 1985. Purification, properties and immunoassay of trypsin from the shrimp *Penaeus japonicus. Comp. Biochem. Physiol.*, **81B**, 447-452.

Gates, B. J. and Travis, J., 1969. Isolation and comparative properties of shrimp trypsin. *Biochem.*, **8**, 4483-4489.

Gates, B. J. and Travis, J., 1973. Purification and characterisation of carboxypeptidases A and B from the white shrimp (*Penaeus setiferus*). *Biochem.*, **12**, 1867-1874.

George, R. W. and Griffen, D. J. G., 1972. The shovel nosed lobsters of Australia. *Aust. Nat. Hist.*, **17**, 227-231.

George, R. W. and Griffen, D. J. G., 1973. Two shovel-nosed lobsters of the genus *Scyllarides* (Decapoda, Scyllaridae) new to Australia. *Crustaceana*, **24**, 144-146.

Ghiradella, H. T., Case, J. F. and Cronshaw, J., 1968. Structure of aesthetascs in selected marine and terrestrial decapods: chemoreceptor morphology and environment. *Am. Zool.*, **8**, 603-621.

Gibson, R. and Barker, P. L., 1979. The decapod hepatopancreas. *Oceanogr. Mar. Biol.*, **17**, 285-346.

Glass, H. J. and Stark, J. R., 1995. Carbohydrate digestion in the European lobster *Homarus gammarus* (L.). *J. Crust. Biol.*, **15**, 424-433.

Gorvett, H., 1946. The tegumental glands in the land Isopoda. A. The rosette glands. *Quart. J. Microsc. Sci.*, **87**, 209-235.

Grant, G. A. and Eisen, A. Z., 1980. Substrate specificity of the collagenolytic serine protease from *Uca pugilator*: studies with noncollagenous substrates. *Biochem.*, **19**, 6089-6093

Grant, G. A., Henderson, K. O., Eisen, A. Z. and Bradshaw, R. A., 1980. Amino acid sequence of a collagenolytic protease from the hepatopancreas of the fiddler crab, *Uca pugilator*. *Biochem.*, **19**, 4653-4659.

Grant, G. A., Sacchettini, J. C. and Welgus, H. G., 1983. A collagenolytic serine protease with trypsin-like specificity from the fiddler crab *Uca pugilator*. *Biochem.*, **22**, 354-358.

Greenwood, J. G., 1972. The mouthparts and behaviour of two species of hermit crabs. *J. Nat. Hist.*, **6**, 325-337.

Growns, I. O. and Richardson, M. M., 1990. A comparison of the gastric mills of nine species of Parastacid crayfish from a range of habitats, using multivariate morphometrics (Decapoda, Astacoidea). *Crustaceana*, **58**, 33-43.

Guizani, N., Marshall, M. R. and Wei, C. I., 1992. Purification and characterisation of a trypsin-like enzyme from the hepatopancreas of crayfish (*Procambarus clarkii*). *Comp. Biochem. Physiol.*, **103B**, 809-815.

Hamner, W. M., 1988. Biomechanics of filter feeding in the Antarctic krill *Euphausia superba*: review of past work and new observations. *J. Crust. Biol.*, **8**, 149-163.

Harada, E., 1962. On the genus *Scyllarus* (Crustacea Decapoda: Reptantia) from Japan. *Publ. Seto Mar. Biol. Lab.*, **11**, 109-139.

Harlow, E. and Lane, D., 1988. *Antibodies: A Laboratory Handbook.* New York, Cold Spring Harbour.

Hartley, B. S. and Shotton, D. M., 1971. *The Enzymes.* 323-373. New York, Academic Press.

Hazlett, B. A., 1971. Chemical and chemotactic stimulation of feeding behaviour in the hermit crab *Petrochirus diogenes. Comp. Biochem. Physiol.*, **39A**, 665-670.

Heinzel, H. G., 1988. Gastric mill activity in the lobster. I. Spontaneous modes of chewing. *J. Neurophysiol.*, **59**, 528-550.

Hestrin, S., Feingold, D. S. and Schram, M., 1957. Hexoside Hydrolases: iii) β galactosidase (lactase) from *Escherichia coli. Methods Enzymol.*, **1**, 241-248.

Hindley, J. P. R., 1975. The detection, location and recognition of food by juvenile banana prawns, *Penaeus merguiensis* de Man. *Mar. Behav. Physiol.*, **3**, 193-210.

Hindley, J. P. R. and Alexander, C. G., 1978. Structure and function of the chelate pereiopods of the banana prawn *Penaeus merguiensis. Mar. Biol.*, **48**, 153-160.

Hirsch, G. C. and Jacobs, W., 1928. Der arbeitrhythmus der mitteldarmdrüse von *Astacus leptodactylus*. I. Methodik und technick: Der beweis der periodizität. *Z. Vergl. Physiol.*, **8**, 102-144.

Hirsch, G. C. and Jacobs, W., 1930. Der arbeitrhythmus der mitteldarmdrüse von *Astacus leptodactylus*. II. Wachstumals primärer faktor des rhythmus eines polyphasischen organischen sekretionssystems. *Z. Vergl. Physiol.*, **12**, 524-528.

Holliday, C. W., Mykles, D. L., Terwilliger, R. C. and Dangott, L. J., 1980. Fluid secretion by the midgut caecae of the crab, *Cancer magister. Comp. Biochem. Physiol.*, **67A**, 259-263.

Holthuis, L. B., 1968. The Palinuridae and Scyllaridae of the Red Sea. *Zool. Meded. (Leiden)*, **42**, 281-301.

Holthuis, L. B., 1977. Two new species of scyllarid lobsters (Crustacea Decapoda, Palinuridea) from Australia and the Kermadec Islands, New Zealand. *Zool. Meded. (Leiden)*, **52**, 191-200.

Holthuis, L. B., 1985. A revision of the family Scyllaridae (Crustacea Decapoda Macrura). I. Subfamily Ibacinae. *Zool. Verh.*, **218**, 3-129.

Honjo, I., Kimura, S. and Nonaka, M., 1990. Purification and characterisation of trypsin-like enzyme from shrimp *Penaeus indicus. Jap. Soc. Sci. Fish. Bull.*, **56**, 1627-1634.

Hood, M. A. and Meyers, S. P., 1973. *Microbial aspects of penaeid shrimp digestion.* Proceedings of the Gulf of Caribean Fisheries Institute 26th Annual Session, New Orleans.

Hopkin, S. P. and Nott, J., 1979. Some observations on concentrically structured, intracellular granules in the hepatopancreas of the shore crab *Carcinus maenas* (L.). *J. Mar. Biol. Ass. (U.K.)*, **59**, 867-877.

Hopkin, S. P. and Nott, J., 1980. Studies on the digestive cycle of the shore crab *Carcinus maenas* (L.), with special reference to the B-cells in the hepatopancreas. *J. Mar. Biol. Ass. (U.K.)*, **60**, 891-907.

Hossain, M. A., 1979. On the fecundity of the sand lobster, *Thenus orientalis* from the Bay of Bengal. *Bangladesh J. Sci. Res.*, **2**, 25-32.

Hughes, R. N., 1980. Optimal foraging theory in the marine context. *Oceanogr. Mar. Biol. Annu. Rev.*, **18**, 423-481.

Hughes, R. N. and Seed, R., 1981. Size selection of mussels by the blue crab *Callinectes sapidus*: energy maximiser or time minimiser? *Mar. Ecol. Prog. Ser.*, **6**, 83-89.

Hunt, M. J., Winsor, H. and Alexander, C. G., 1992. Feeding by penaeid prawns: the role of the anterior mouthparts. *J. Exp. Mar. Biol. Ecol.*, **160**, 33-47.

Icely, J. D. and Nott, J., 1985. Feeding and digestion in *Corophium volutator* (Crustacea: Amphipoda). *Mar. Biol.*, **89**, 183-195.

Icely, J. D. and Nott, J. A., 1980. Accumulation of copper within the "hepatopancreatic" caeca of *Corophium volutator* (Crustacea: Amphipoda). *Mar. Biol.*, **57**, 193-199.

Icely, J. D. and Nott, J. A., 1992. Digestion and absorption: digestive system and associated organs. In, Harrison, F. W. and Humes, A. G. (eds.): *Decapod Crustacea. Microscopic Anatomy of Invertebrates, vol 10.* 147-201. New York, Wiley-Liss.

Ito, M. and Lucas, J. S., 1990. The complete larval development of the scyllarid lobster, *Scyllarus demani* Holthuis, 1946 (Decapoda, Scyllaridae), in the laboratory. *Crustaceana*, **58**, 144-167.

Jacklyn, P. M. and Ritz, D. A., 1986. Hydrodynamics of swimming in scyllarid lobsters. *J. Exp. mar. Biol. Ecol.*, **101**, 85-99.

Jacobs, W., 1928. Untersuchungen über die cytologie der sekretbildung in der mitteldarmdrüse von *Astacus leptodactylus*. *Z. Zellforsch. Mikrosk. Anat.*, **8**, 1-62.

Jacques, F., 1989. The setal system of crustaceans: types of setae, groupings, and functional morphology. In, Felgenhauer, B. E., Watling, L. and Thistle, A. B. (eds.): *Functional Morphology of Feeding and Grooming in Crustacea. Crustacean Issues, vol. 6.* 1-13. Rotterdam, A.A. Balkema.

Jeuniaux, C., 1966. Chitinases. *Methods Enzymol.*, **8**, 644-650.

Johnson, B. and Talbot, P., 1987. Ultrastructural analysis of the pleopod tegumental glands in male and female lobsters, *Homarus americanus. J. Crust. Biol.*, **7**, 288-301.

Johnston, D. J., Alexander, C. G. and Yellowlees, D., 1993. Histology, histochemistry, and enzyme biochemistry of the digestive glands in the tropical surf barnacle *Tetraclita squamosa. J. Mar. Biol. Ass. (U.K.)*, **73**, 1-14.

Jones, C. M., 1984. Development of the bay lobster fishery in Queensland. *Aust. Fish.*, **43**, 19-21.

Jones, C. M., 1988. The biology and behaviour bay lobsters, *Thenus* spp. (Decapoda:Scyllaridae), in northern Queensland, Australia. PhD. Thesis, University of Queensland, Australia.

Jones, C. M., 1990. Morphological characteristics of bay lobsters, *Thenus* Leach species, (Decapoda;Scyllaridae), from north-eastern Australia. *Crustaceana*, **59**, 265-275.

Jones, C. M., 1993. Population structure of *Thenus orientalis* and *T. indicus* (Decapoda:Scyllaridae) in northeastern Australia. *Mar. Ecol. Prog. Ser.*, **97**, 143-155.

Kaleemur Rahman, M. and Subramoniam, T., 1989. Molting and its control in the female sand lobster *Thenus orientalis. J. Exp. Mar. Biol. Ecol.*, **128**, 105-115.

Kanneworff, E. and Nicolaisen, W., 1969. The stomach (foregut) of the amphipod *Bathyporeia sarsi* Watkin. *Ophelia*, **6**, 211-229.

Kiernan, J. A., 1990. *Histological and Histochemical Methods: Theory and Practice.* Oxford, Pergamon Press.

Kijimoto-Ochiai, S., Katagiri, Y. V. and Ochiai, H., 1985. Analysis of N-linked oligosaccharide chains of glycoproteins on nitocellulose sheets using lectin-peroxidase reagents. *Analyt. Biochem.*, **147**, 222.

Kimoto, K., Yokoi, T. and Murakami, K., 1985. Purification and characterisation of chymotrypsin-like proteinase from *Euphausia superba. Agric. Biol. Chem.*, **49**, 1599-1603.

King, R. A., 1991. Comparative functional morphology of the decapod proventriculus. Honours Thesis, James Cook University of North Queensland, Australia.

King, R. A. and Alexander, C. G., 1994. Fluid extraction and circulation in the proventriculus of the banana prawn *Penaeus merguiensis* De Man. *J. Crust. Biol.*, **14**, 497-507.

Koga, D., Mizuki, K., Ide, A., Kono, M., Matsui, T. and Shimizu, C., 1990. Kinetics of a chitinase from a prawn, *Penaeus japonicus*. *Agric. Biol. Chem.*, **54**, 2505-2512.

Koga, D., Nakashima, M., Matsukara, T., Kimura, S. and Ide, A., 1986. Purification and properties of β-N-acetylglucosaminidase from alimentary canal of the silkworm, *Bombyx mori*. *Agric. Biol. Chem.*, **50**,2357-2368.

Kono, M., Matsui, T., Shimizu, C. and Koga, D., 1990. Purifications and some properties of chitinase from the liver of a prawn, *Penaeus japonicus*. *Agric. Biol. Chem.*, **54**, 2145-2147.

Kramer, K. J. and Aoki, H., 1987. Chitinolytic enzymes from pupae of the red flour beetle, *Tribolium castaneum*. *Comp. Biochem. Physiol.*, **86B**, 613-621.

Kraut, J., 1977. Serine proteases: structure and mechanism of catalysis. *Ann. Rev. Biochem.*, **46**, 331-358.

Kristensen, J. H., 1972. Carbohydrases of some marine invertebrates with notes on their food and on the natural occurrence of the carbohydrates studied. *Mar. Biol.*, **14**, 130-142.

Kumari, C., Hanumantha Rao, K. and Shyamusandari, K., 1983. Histology and histochemistry of the tegumental glands in *Ligia exotica* Roux (Crustacea:Isopoda). *Proc. Indian Acad. Sci.*, **92**, 207-214.

Kunze, J. and Anderson, D. T., 1979. Functional morphology of the mouthparts and gastric mill in the hermit crabs *Clibanarius taeniatus* (Milne Edwards), *Clibanarius virescens* (Krauss), *Paguristes squamosus* (McCullogh), *Dardanus setifer* (Milne Edwards), (Anomura:Paguridae). *Aust. J. Mar. Freshw. Res.*, **30**, 683-722.

Laemmli, U. K., 1970. Cleavage of structural proteins during the assembly of the head of bacteriophage T4. *Nature*, **227**, 680-685.

Lau, C. J., 1987. Feeding behaviour of the Hawaiian slipper lobster, *Scyllarides squamosus*, with a review of decapod crustacean feeding tactics on molluscan prey. *Bull. Mar. Sci.*, **41**, 378-391.

Lau, C. J., 1988. *Dietary comparison of two slow-moving crustacean (Decapoda:Scyllaridae) predators by a modified index of relative importance.* Proceedings of the 6th International Coral Reef Symposium, Australia.

Lavalli, K. L. and Factor, J. R., 1992. Functional morphology of the mouthparts of juvenile lobsters, *Homarus americanus* (Decapoda: Nephropidae), and comparison with the larval stages. *J. Crust. Biol.*, **12**, 467-510.

Lee, P. G., Blake, N. J. and Rodrick, G. E., 1980. A quantitative analysis of digestive enzymes for the freshwater prawn *Macrobrachium rosenbergii*. *Proc. World Maricult. Soc.*, **11**, 392-402.

Lee, P. G., Smith, L. L. and Lawrence, A. L., 1984. Digestive proteases of *Penaeus vannamei* Boone: relationship between enzyme activity, size and diet. *Aquaculture*, **42**, 225-239.

Lillie, R. D. and Fullmer, H. M., 1976. *Histopathologic Technique and Practical Histochemistry*. New York, McGraw-Hill Book Company.

Lindsay, G. J. H., 1987. Seasonal activities of chitinase and chitobiase in the digestive tract and serum of cod, *Gadus morhua* (L.). *J. Fish. Biol.*, **30**, 495-500.

Loizzi, R. F., 1971. Interpretation of crayfish hepatopancreatic function based on fine structural analysis of epithelial cell lines and muscle network. *Z. Zellforsch.*, **113**, 420-440.

Loizzi, R. F. and Peterson, D. R., 1971. Lipolytic sites in crayfish hepatopancreas and correlation with fine structure. *Comp. Biochem. Physiol.*, **39B**, 227-236.

Loret, S. M. and Devos, P. E., 1992. Structure and possible functions of the calcospherite-rich cells (R^* cells) in the digestive gland of the shore crab *Carcinus maenas*. *Cell Tissue Res.*, **267**, 105-111.

Lottenberg, R., Christensen, U., Jackson, C. M. and Coleman, P. L., 1981. Assay of coagulation proteases using peptide chromogenic and fluorogenic substrates. *Methods Enzymol.*, **80**,341-361.

Lottenberg, R. and Jackson, C. M., 1983. Solution composition dependant variation in extinction coefficients for ρ-nitroanaline. *Biochim. Biophys. Acta*, **742**,558-564.

Lovett, D. L. and Felder, D. L., 1989. Ontogeny of gut morphology in the white shrimp *Penaeus setiferus* (Decapoda, Penaeidae). *J. Morph.*, **201**, 253-272.

Lovett, D. L. and Felder, D. L., 1990 a. Ontogeny of kinematics in the gut of the white shrimp *Penaeus setiferus* (Decapoda:Penaeidae). *J. Crust. Biol.*, **10**, 53-68.

Lovett, D. L. and Felder, D. L., 1990 b. Ontogenetic change in digestive enzyme activity of larval and postlarval white shrimp *Penaeus setiferus* (Crustacea, Decapoda, Penaeidae). *Biol. Bull.*, **178**, 144-159.

Lu, P-J., Liu, H-C. and Tsai, I-H., 1990. The midgut trypsins of shrimp (*Penaeus monodon*). High efficiency toward native protein substrates including collagens. *Biol. Chem.*, **371**, 851-859.

Lynn, I., 1990. Chitinases and chitobiases from the American lobster (*Homarus americanus*). *Comp. Biochem. Physiol.*, **96B**, 761-766.

Lyon, R. and Simkiss, K., 1984. The ultrastructure and metal-containing inclusions of mature cell types in the hepatopancreas of a crayfish. *Tissue and Cell*, **16**, 805-817.

Lyons, W. G., 1970. Scyllarid lobsters (Crustacea, Decapoda). *Mem. Hourglass Cruises*, **1**, 1-74.

Lyons, W. G., 1980. The postlarval stages of scyllaridean lobsters. *Fisheries*, **5**, 47-49.

Maitland, D. P., 1990. Feeding and mouthpart morphology in the semaphore crab *Heloecius cordiformis* (Decapoda: Brachyura: Ocypodidae). *Mar. Biol.*, **105**, 287-296.

Manjulatha, C. and Babu, D. E., 1991. Functional organisation of mouthparts, and filter feeding, in *Clibanarius longitarsus* (Crustacea: Anomura). *Mar. Biol.*, **109**, 121-127.

Martins, H. R., 1985. Biological studies of the exploited stock of the Mediterranean locust lobster *Scyllarides latus* (Latreille, 1803) (Decapoda:Scyllaridae) in the Azores. *J. Crust. Biol.*, **5**, 294-305.

Mathews, C. K. and van Holde, K. E., 1990. *Biochemistry*. Redwood City, The Benjamin/Cummings Publishing Company, Inc.

Maynard, D. M. and Dando, M. R., 1974. The structure of the stomatogastric neuromuscular system in *Callinectes sapidus, Homarus americanus* and *Panulirus argus* (Decapoda Crustacea). *Phil. Trans. R. Soc. Lond., B.*, **268**, 161-220.

McClintock, J. B., Klinger, T. S., Marion, K. and Hseuh, P., 1991. Digestive carbohydrases of the blue crab *Callinectes sapidus* (Rathbun): implications in utilization of plant-derived detritus as a trophic resource. *J. Exp. Mar. Biol. Ecol.*, **148**, 233-239.

McIver, S. B., 1975. Structure of cuticular mechanoreceptors of arthropods. *Ann. Rev. Entomol.*, **20**, 381-397.

McKenzie, L. J. and Alexander, C. G., 1989. Mucus-secreting glands in the paragnaths and second maxillipeds of the banana prawn, *Penaeus merguiensis* de Man. *Aust. J. Mar. Freshw. Res.*, **40**, 669-677.

McLaughlin, P. A., 1982. Comparative morphology of crustacean appendages. In, Abele, L. G. (ed.): *Embryology, morphology and genetics. The Biology of Crustacea, vol. 2*. 197-233. Sydney, Academic Press.

Meiss, D. E. and Norman, R. S., 1977. Comparative study of the stomatogastric system of several decapod crustacea. I. Skeleton. *J. Morph.*, **152**, 21-54.

Mikami, S. and Takashima, F., 1993. Development of the proventriculus in larvae of the slipper lobster, *Ibacus ciliatus* (Decapoda: Scyllaridae). *Aquaculture*, **116**, 199-217.

Mocquard, F., 1883. Recherces anatomiques sur l'estomac des crustaces podophthalmaires. *Ann. Sc. Nat. Zool.*, **16**, 1-311.

Momin, M. A. and Rangneker, P. V., 1975. Histochemical patterns of lipolytic enzymes of the hepatopancreas of *Scylla serrata* and their possible relation to eyestalk factor(s). *Zool. J. Linn. Soc.*, **57**, 75-84.

Mykles, D. L., 1977. The ultrastructure of the posterior midgut caecum of *Pachygrapsus crassipes* (Decapoda: Brachyura) adapted to low salinity. *Tissue and Cell*, **9**,681-691.

Mykles, D. L., 1980. The mechanism of fluid absorption at ecdysis in the American lobster, *Homarus americanus*. *J. Exp. Biol.*, **84**, 89-101.

Mykles, D. L. and Ahearn, G. A., 1978. Changes in fluid transport across the perfused midgut of the freshwater prawn *Macrobrachium rosenbergii*, during the moulting cycle. *Comp. Biochem. Physiol.*, **61A**, 643-645.

New, M. B., 1976. A review of dietary studies with shrimp and prawns. *Aquaculture*, **9**,101-144.

Ngoc-Ho, N., 1984. The functional anatomy of the foregut of *Porcellana platycheles* and a comparison with *Galathea squamifera* and *Upogebia deltaura* (Crustacea:Decapoda). *J. Zool.*, **203**, 511-535.

Nicol, E. A. T., 1932. The feeding habits of the Galatheidea. *J. Mar. Biol. Ass. (U.K.)*, **18**, 87-106.

Ogura, K., 1959. Midgut gland cells accumulating iron or copper in the crayfish, *Procambarus clarkii*. *Annot. Zool. Jap.*, **32**, 133-142.

Osnes, K. K. and Mohr, V., 1985. On the purification and characterisation of three anionic, serine-type peptide hydrolases from Antarctic krill, *Euphausia superba*. *Comp. Biochem. Physiol.*, **82B**, 607-619.

Oxley, D. and Bacic, A., 1995. Microheterogeneity of N-glycosylation on a stylar self-incompatability glycoprotein of *Nicotiana alata*. *Glycobiology*, **In Press**.

Patwardan, S. S., 1935 a. On the structure and mechanism of the gastric mill in Decapoda. 2. The structure of the gastric mill in Brachyura. *Proc. Indian Acad. Sci.,B*, **1**, 359-375.

Patwardan, S. S., 1935 b. On the structure and mechanism of the gastric mill in Decapods. 3. Structure of the gastric mill in Anomura. *Proc. Indian Acad. Sci.,B*, **1**, 405-413.

Patwardan, S. S., 1935 c. On the structure and mechanism of the gastric mill in Decapoda. 4. The structure of the gastric mill in Reptantous Macura. *Proc. Indian Acad. Sci.,B*, **1**, 414-422.

Patwardan, S. S., 1935 d. On the structure and mechanism of the gastric mill in Decapoda. 5. The structure of the gastric mill in Natantous Macrura-Caridea. *Proc. Indian Acad. Sci.,B*, **1**, 693-704.

Percival, E., 1970. Algal polysaccharides. In, Pigman, W. and Horton, D. (eds.): *The Carbohydrates 2B*. 537-565. New York, Academic Press.

Phillips, B. F., Cobb, J. S. and George, R. W., 1980. General biology. In, Cobb, J. S. and Phillips, B. F. (eds.): *Physiology and Behaviour. The Biology and Management of Lobsters, vol. 4*. 1-82. New York, Academic Press.

Phillips, B. F. and McWilliam, P. S., 1986. Phyllosoma and nisto stages of *Scyllarus martensii* Pfeffer (Decapoda, Scyllaridae) from the Gulf of Carpentaria, Australia. *Crustaceana*, **51**, 133-153.

Pohle, G. and Telford, M., 1981. Morphology and classification of decapod crustacean larval setae: a scanning electron microscope study of *Dissodactylus crinitichelis* Moreira, 1901 (Brachyura: Pinnotheridae). *Bull. Mar. Sci.*, **31**, 736-752.

Pollock, D. E., 1979. Predator-prey relationships between the rock lobster *Jasus lalandii* and the mussel *Aulacomya ater* at Robben Island on the Cape West Coast of Africa. *Mar. Biol.*, **52**,347-356.

Powell, R. R., 1974. The functional morphology of the fore-guts of the Thalassinid crustaceans, *Callianassa californiensis* and *Upogebia pugettensis*. *Univ. Calif. Publ. Zool.*, **102**, 1-41.

Powers, J. C. and Harper, J. W., 1986. Inhibitors of serine proteinases. In, Barrett and Salveson (eds.): *Proteinase Inhibitors*. 55-152. Cambridge, Elsevier Science Publishers (Biomedical Division).

Price, R. B. and Ache, B. W., 1977. Peripheral modification of chemosensory information in the spiny lobster. *Comp. Biochem. Physiol.*, **57A**, 249-253.

Puanglarp, N., Oxley, D., Currie, G., Bacic, A., Craik, D. J. and Yellowlees, D., 1995. Oligosaccharides from tridacnin, a lectin found in the haemolymph of the giant clam *Hippopus hippopus*. *Eur. J. Biochem.*, **In Press**.

Pugh, J., 1962. A contribution toward a knowledge of the hindgut of fiddler crabs (Decapoda, Grapsidae). *Trans. Am. Microsc. Soc.*, **81**,309-320.

Rainbow, P. S. and Walker, G., 1977. Functional morphology of the alimentary canal of barnacles (Cirripedia:Thoracica). *J. Exp. Mar. Biol. Ecol.*, **28**, 183-206.

Reddy, A. R., 1935. The gastric armature of some South Indian Decapod Crustacea. *J. Annamalai Univ.*, **4**, 82-118.

Reynold, E. R., 1963. The use of lead citrate at high pH as an electron-opaque stain in electron microscopy. *J. Cell Biol.*, **17**, 208-212.

Richards, O. W. and Davies, R. G., 1977. *Imms' General Textbook of Entomolgy. I. Structure, physiology and development.* New York, John Wiley and Sons.

Robertson, R. M. and Laverack, M. S., 1979. The structure and function of the labrum in the lobster *Homarus gammarus* (L.). *Proc. Roy. Soc. Lond. B.*, **206**, 209-233.

Rodriguez, A., Le Vay, L., Mourente, G. and Jones, D. A., 1994. Biochemical composition and digestive enzyme activity in larvae and postlarvae of *Penaeus japonicus* during herbivorous and carnivorous feeding. *Mar. Biol.*, **118**, 45-51.

Sather, B. T., 1969. A comparative study of amylases and proteinases in some decapod crustacea. *Comp. Biochem. Physiol.*, **28**, 371-379.

Schaefer, N., 1970. The functional morphology of the foregut of three species of decapod crustacea: *Cyclograpsus punctatus* Milne-Edwards, *Diogenes brevirostris* Stimpson, and *Upogebia africana* (Ortmann). *Zool. Afr.*, **5**, 309-326.

Schmitt, B. C. and Ache, B. W., 1979. Olfaction: responses of a decapod crustacean are enhanced by flicking. *Science*, **205**, 204-206.

Shelton, R. G. J. and Laverack, M. S., 1970. Receptor hair structure and function in the lobster *Homarus gammarus* (L.). *J. Exp. Mar. Biol. Ecol.*, **4**, 201-210.

Shyamasundari, K., 1979. Studies on the alimentary canal of amphipods: histochemistry of cephalic mucous glands in *Talorchestia martensii* (Weber) (Crustacea: Amphipoda). *Z. Zellforsch.*, **93**, 417-424.

Shyamasundari, K. and Hanumantha Rao, K., 1977. Studies on the alimentary canal of amphipods: morphology and histology of cephalic mucus glands. *Crustaceana*, **33**, 149-153.

Shyamasundari, K. and Hanumantha Rao, K., 1978. Studies on the Indian sand lobster *Thenus orientalis* (Lund): Mucopolysaccharides of the tegumental glands. *Folia Histochem. Cytochem.*, **16**, 247-254.

Skilleter, G. A. and Anderson, D. T., 1986. Functional morphology of the chelipeds, mouthparts and gastric mill of *Ozius truncatus* (Milne Edwards) (Xanthidae) and *Leptograpsus variegatus* (Fabricius) (Grapsidae) (Brachyura). *Aust. J. Mar. Freshw. Res.*, **37**, 67-79.

Smith, R. I., 1978. The midgut caeca and the limits of the hindgut of Brachyura: a clarification. *Crustaceana*, **35**, 195-205.

Snodgrass, R. E., 1951. *Comparative Studies on the Head of Mandibulate Arthropods.* New York, Comstock Publishing Company, Inc.

Snow, P. J., 1973. The antennular activities of the hermit crab, *Pagurus alaskensis* (Benedict). *J. Exp. Biol.*, **58**, 745-765.

Sova, V. V., Elyakova, L. A. and Vaskovsky, V. E., 1970. The distribution of laminarinases in marine invertebrates. *Comp. Biochem. Physiol.*, **32**, 459-464.

Spanier, E., 1987. Mollusca as food for the slipper lobster (*Scyllarides latus*) in the coastal waters of Isreal. *Levantina*, **68**, 713-716.

Spanier, E. and Almog-Shtayer, G., 1992. Shelter preferences in the Mediterranean slipper lobster: effects of physical properties. *J. Exp. Mar. Biol. Ecol.*, **164**, 103-116.

Spanier, E., Tom, M., Pisanty, S. and Almog, G., 1988. Seasonality and shelter selection by the slipper lobster *Scyllarides latus* in the southeastern Mediterranean. *Mar. Ecol. Prog. Ser.*, **42**, 247-255.

Spanier, E., Weihs, D. and Almog-Shtayer, G., 1991. Swimming in the Mediterranean slipper lobster. *J. Exp. Mar. Biol. Ecol.*, **145**, 15-31.

Spindler, K. D. and Buchholz, F., 1988. Partial characterisation of chitin degrading enzymes from Euphausids, *Euphausia superba* and *Meganyctiphanes norvegica*. *Polar Biol.*, **9**, 115-122.

Spindler-Barth, M., Van Wormhoudt, A. and Spindler, K.-D., 1990. Chitinolytic enzymes in the integument and midgut-gland of the shrimp *Palaemon serratus* during the moulting cycle. *Mar. Biol.*, **106**, 49-52.

Spurr, A. R., 1969. A low viscosity epoxy resin embedding medium for electron microscopy. *J. Ultrastruct. Res.*, **26**, 31-43.

Stevenson, J. R. and Murphy, J. C., 1967. Mucopolysaccharide glands in the isopod crustacean *Armadillium vulgare*. *Trans. Am. Microsc. Soc.*, **86**, 50-57.

Stone, S. T., Betz, A. and Hofsteenge, J., 1991. Mechanistic studies on thrombin catalysis. *Biochem.*, **30**, 9841-9848.

Stryer, L., 1988. *Biochemistry*. New York, W.H. Freeman and Company.

Suthers, I. M., 1984. Functional morphology of the mouthparts and gastric mill in *Penaeus plebejus* (Decapoda:Penaeidae). *Aust. J. Mar. Freshw. Res.*, **35**, 785-792.

Suthers, I. M. and Anderson, D. T., 1981. Functional morphology of mouthparts and gastric mill of *Ibacus peronii* (Leach) (Palinura:Scyllaridae). *Aust. J. Mar. Freshw. Res.*, **32**, 931-944.

Talbot, P. and Zao, P., 1991. Secretion at molting by the pleopod tegumental glands of the lobster *Homarus americanus* (Milne Edwards). *J. Crust. Biol.*, **11**, 1-9.

Telford, M., 1970. Comparative carbohydrase activities of some crustacean tissue and whole animal homogenates. *Comp. Biochem. Physiol.*, **34**, 81-90.

Thomas, W. J., 1970. The setae of *Austropotamobius pallipes* (Crustacea:Astacidae). *J. Zool.*, **160**, 91-142.

Thomas, W. J., 1979. Setal relationships and their significance in *A. pallipes*. *Experimentia*, **35**, 1309-1311.

Thomas, W. J., 1984. The paragnaths of Austropotamobius pallipes. In, Brink, P. (ed.): *Freshwater Crayfish 6. Papers from the 6th International Symposium of Astacology*. 42-47. Lund, Sweden.

Tipton, K. F. and Dixon, H. B. F., 1979. Effects of pH on enzymes. *Methods Enzymol.*, **63**, 183-227.

Titani, K., Sasagawa, T., Woodbury, R. G., Ericsson, L. H., Dorsam, H., Kraemer, M., Neurath, H. and Zwilling, R., 1983. Amino acid sequence of crayfish (*Astacus fluviatilis*) trypsin I_f. *Biochem.*, **22**, 1459-1465.

Toullec, J. Y., Chikhi, M. and Van Wormhoudt, A., 1992. In vitro protein synthesis and α-amylase activity in F-cells from hepatopancreas of *Palaemon serratus* (Crustacea: Decapoda). *Experimentia*, **48**, 272-277.

Tsai, I-H., Chuang, K-L. and Chuang, J. L., 1986 a. Chymotrypsins in digestive tracts of crustacean decapods (shrimps). *Comp. Biochem. Physiol.*, **85B**, 235-239.

Tsai, I-H., Liu, H-C. and Chuang, K-L., 1986 b. Properties of two chymotrypsins from the digestive gland of prawn *Penaeus monodon*. *FEBS Lett.*, **203**, 257-261.

Tsai, I-H., Lu, P-J. and Chuang, J-L., 1991. The midgut chymotrypsins of shrimps (*Penaeus monodon, Penaeus japonicus* and *Penaeus penicillatus*). *Biochim. Biophys. Acta*, **1080**, 59-67.

Tyagi, A. P. and Kaushik, S., 1970. Role of mandibular gland in the digestion of the crab, *Pontamon martensi*. *J. Mar. Biol. Ass. (India)*, **12**, 220-221.

van Weel, P. B., 1970. Digestion in Crustacea. In, Florkin, M. B. and Scheer, B. T. (eds.): *Chemical Zoology, vol. 5*. 97-115. New York, Academic Press.

Van Wormhoudt, A., Chevalier, P. L. and Sellos, D., 1992. Purification, biochemical characterisation and N-terminal sequence of a serine protease with chymotryptic and collagenolytic activities in a tropical shrimp, *Penaeus vannamei* (Crustacea, Decapoda). *Comp. Biochem. Physiol.*, **103B**, 675-680.

Vega-Villasante, F., Nolasco, H. and Civera, R., 1993. The digestive enzymes of the Pacific brown shrimp *Penaeus californiensis*. I - Properties of amylase activity in the digestive tract. *Comp. Biochem. Physiol.*, **106B**, 547-550.

Vogt, G., 1985. Histologie und cytologie der mitteldarmdrüse von *Penaeus monodon* (Decapoda). *Zool. Anz.*, **215**, 61-80.

Vogt, G., 1987. Monitoring of environmental pollutants such as pesticides in prawn aquaculture by histological diagnosis. *Aquaculture*, **67**, 157-164.

Vogt, G., 1993. Differentiation of B-cells in the hepatopancreas of the prawn *Penaeus monodon*. *Acta Zool.*, **74**, 51-60.

Vogt, G., Stocker, W., Storch, V. and Zwilling, R., 1989. Biosynthesis of *Astacus* protease, a digestive enzyme from crayfish. *Histochemistry*, **91**, 373-381.

Walsh, K. A. and Wilcox, P. E., 1970. Serine proteases. *Methods Enzymol.*, **19**, 31-112.

Watling, L., 1989. A classification system for crustacean setae based on the homology concept. In, Felgenhauer, B. E., Watling, L. and Thistle, A. B. (eds.): *Functional Morphology of Feeding and Grooming in Crustacea. Crustacean Issues, vol. 6*. 15-26. Rotterdam, A.A. Balkema.

Weiss, L., 1983. The Structure of the Cell. In, *Histology. Cell and Tissue Biology*. 5th edn. 56-60. New York, The Macmillan Press.

Welsch, U. and Storch, V., 1975. *Comparative Animal Cytology and Histology*. London, Sidgwick and Jackson.

Winsor, L., 1984. *Manual of Basic Zoological Microtechniques for Light Microscopy*. Townsville, James Cook University of North Queensland, Australia.

Wojtowicz, M. B. and Brockerhoff, H., 1972. Isolation and some properties of the digestive amylase of the American lobster (*Homarus americanus*). *Comp. Biochem. Physiol.*, **42B**, 295-302.

Yokoe, Y. and Yasumasu, I., 1964. The distribution of cellulase in invertebrates. *Comp. Biochem. Physiol.*, **13**, 323-338.

Yonge, C. M., 1924. Studies on the comparative physiology of digestion. II. The mechanism of feeding, digestion and assimilation in *Nephrops norvegicus*. *J. Exp. Biol.*, **1**, 343-389.

Yonge, C. M., 1932. On the nature and permeability of chitin. I. - The chitin lining the foregut of Decapod Crustacea and the function of the tegumental glands. *Proc. Roy. Soc. Lond. B.*, **3**, 298-327.

Zwilling, R., Jakob, F., Bauer, H., Neurath, H. and Enfield, D. L., 1979. Crayfish carboxypeptidase. Affinity chromatography, characterisation and amino-terminal sequence. *Eur. J. Biochem.*, **94**, 223-229.

Zwilling, R. and Neurath, H., 1981. Invertebrate proteases. *Methods Enzymol.*, **80**, 633-664.

Zwilling, R., Neurath, H., Ericsson, L. H. and Enfield, D. L., 1975. The amino-terminal sequence of an invertebrate trypsin (crayfish *Astacus leptodactylus*): homology with other serine proteases. *FEBS Lett.*, **60**, 247-249.

Zwilling, R., Pfleiderer, G., Sonneborn, H-H., Kraft, V. and Stucky, I., 1969. The evolution of endopeptidases-V. Common and different traits of bovine and crayfish trypsin. *Comp. Biochem. Physiol.*, **28**, 1275-1287.

Appendix 1. General Histological Techniques

1. Processing

Method: automatic

70% alcohol	held
90% alcohol	45 min
100% alcohol(1)	45 min
100% alcohol(2)	45 min
toluene(1)	45 min
toluene(2)	45 min
paraffin wax(1)	45 min
paraffin wax(2)	45 min
paraffin wax(pure)	45 min
vacuum infiltration	

Embedding medium: paraffin wax

2. Staining

A. Dewaxing

1. Sections into xylene(1) for 5 min	
2. Immerse in xylene(2)	20 dips
3. Immerse in xylene/absolute alcohol	20 dips

B. Hydration

1. Into absolute alcohol(1)	20 dips
2. Into absolute alcohol(2)	20 dips
3. Into 70% alcohol	20 dips
4. Wash well in running tap water	

C. Appropriate staining procedure

HAEMATOXYLIN and EOSIN (Winsor, 1984)

1. Stain in Mayer's haematoxylin for 5 min
2. Transfer to water
3. Immerse in Scott's Tap Water for 2 min

4. Wash well in running water
5. Stain in Younge's eosin for 2 minutes
6. Rapidly rinse in running water

MALLORY-HEIDENHAIN (Winsor, 1984)

1. Immerse sections in Mallory Mordant for 30 min at 60°C
2. Wash well in running water
3. Immerse in Mallory-Heidenhain stain for 5 min
4. Quickly rinse in running water to remove excess stain

D. Dehydration

1. Into 70% alcohol	20 dips
2. Into absolute alcohol(1)	20 dips
3. Into absolute alcohol(2)	20 dips

E. Clearing and mounting

1. Into absolute alcohol/xylene	20 dips
2. Into xylene(1)	20 dips
3. Into xylene(2)	20 dips

4. Mount from xylene into DePeX.

Appendix 2. Raw kinetics data for *T. orientalis* trypsin.

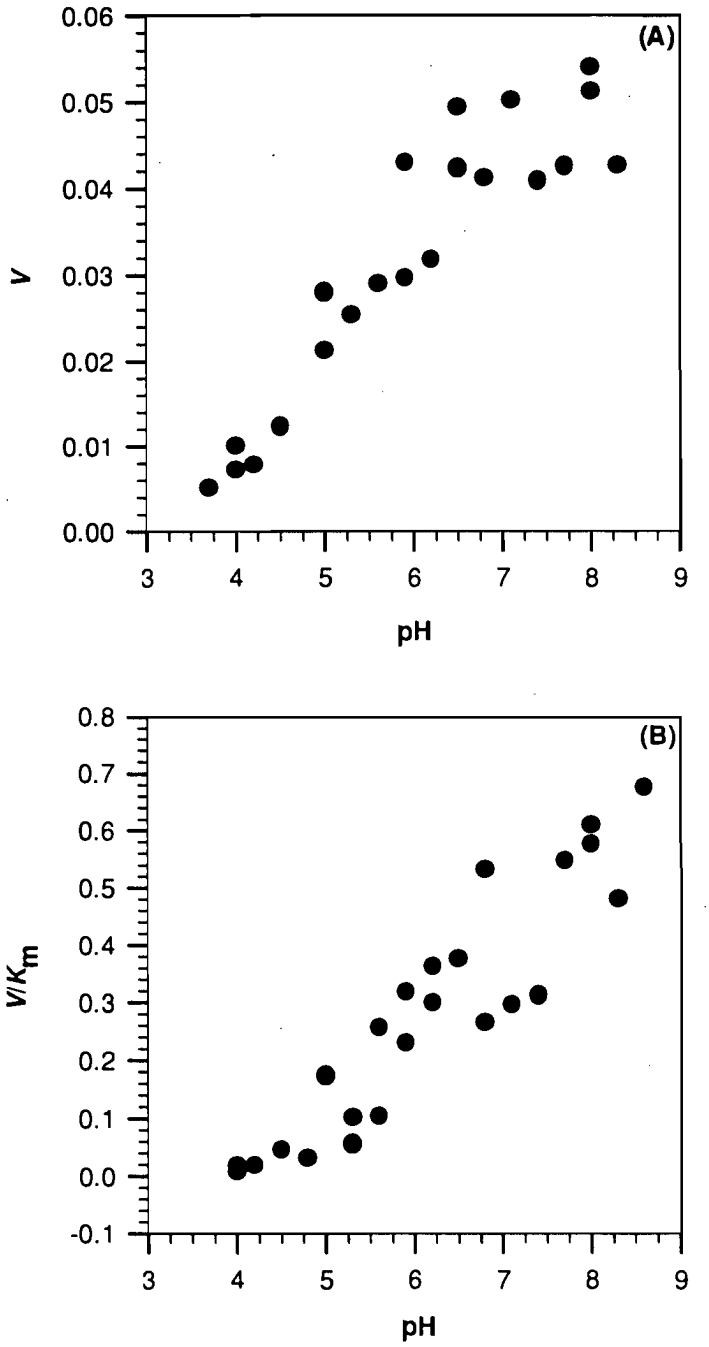

Figure 1. Variation of **A.** V and **B.** V/K_m with pH for BAPA hydrolysis by *T. orientalis* trypsin. V and K_m values at each pH were calculated by nonlinear regression to equation 1 (Ch 7.2.9), an example of which is given in Fig. 7.13A. Units of V and (V/K_m) are μmol $s^{-1}mg^{-1}$ and $mg^{-1}ml\ s^{-1}$, respectively.

Appendix 3. Publication reprint: Johnston, 1994

(reprint for Johnston *et al.*, 1995 not yet available)

Johnston, D. J., 1994. Functional morphology of the membranous lobe within the preoral cavity of Thenus orientalis (Crustacea: Scyllaridae). J. Mar. Biol. Ass. (U.K.), 74, 787- 800.